THE UNIVERSITY OF QUEENSLAND

AUSTRALIA

Bacteriostatic and bactericidal effects of free nitrous acid on model microbes in wastewater treatment

Shuhong Gao

Master of Science

Harbin Institute of Technology, Harbin, China

A thesis submitted for the degree of Doctor of Philosophy at

The University of Queensland in 2016

School of Chemical Engineering

Advanced Water Management Centre

Abstract

There is great potential to use free nitrous acid (FNA), the protonated form of nitrite (HNO_2), as an antimicrobial agent due to its bacteriostatic and bactericidal effects on a range of microorganisms. However, the antimicrobial mechanism of FNA is largely unknown. The overall objective of this thesis is to elucidate the responses of two model bacteria, namely *Psuedomonas aeruginosa* PAO1 and *Desulfovibrio vulgaris* Hildenborough, in wastewater treatment in terms of microbial susceptibility, tolerance and resistance to FNA exposure.

The effects of FNA on the opportunistic pathogen *P. aeruginosa* PAO1, a well-studied denitrifier capable of nitrate/nitrite reduction through anaerobic respiration, were determined. It was revealed that the antimicrobial effect of FNA is concentration-determined and population-specific. By applying different levels of FNA, it was seen that 0.1 to 0.2 mg N/L FNA exerted a temporary inhibitory effect on *P. aeruginosa* PAO1 growth, while complete respiratory growth inhibition was not detected until an FNA concentration of 1.0 mg N/L was applied. The FNA concentration of 5.0 mg N/L caused complete cell killing and likely cell lysis. Differential killing by FNA in the *P. aeruginosa* PAO1 subpopulations was detected, suggesting intra-strain heterogeneity. A delayed recovery from FNA treatment suggested that FNA caused cell damage which required repair prior to *P. aeruginosa* PAO1 showing cell growth.

To further understand the inhibitory mechanisms of FNA on the model denitrifier *P. aeruginosa* PAO1 in wastewater treatment, genome-wide transcriptome analyses, coupled with a suite of physiological detections were conducted. The responses of *P. aeruginosa* PAO1 were detected in the absence and presence of an inhibitory level of FNA (0.1 mg N/L) under anaerobic denitrifying conditions. Respiration was likely inhibited as denitrification activity was severely depleted in terms of decreased transcript levels of most denitrification genes. As a consequence, the tricarboxylic acid (TCA) cycle was inhibited due to the lowered cellular redox state in FNA exposed cultures. Meanwhile *P. aeruginosa* PAO1 rerouted its carbon metabolic pathway from the TCA cycle to pyruvate fermentation with acetate as the end product to survive the FNA stress. Moreover, protein synthesis was significantly decreased while ribosomes were preserved. These findings improved our understanding of *P. aeruginosa* PAO1 in response to FNA.

Hydrogen sulfide produced by sulfate reducing bacteria (SRB) in sewers causes odor problems and asset deterioration due to the sulfide induced concrete corrosion. FNA was recently demonstrated as a promising antimicrobial agent to alleviate hydrogen sulfide production in sewers. However, knowledge of the antimicrobial mechanisms of FNA are largely unknown. Here we report the

multiple-targeted antimicrobial effects of FNA on the SRB *Desulfovibrio vulgaris* Hildenborough by determining growth, physiological and gene expression responses to FNA exposure. The activities of growth, respiration and ATP generation were inhibited when exposed to FNA. These changes were reflected in corresponding transcript levels detected during exposure. Removal of FNA was evident by nitrite reduction that likely involved nitrite reductase and the poorly characterised hybrid cluster protein since the genes coding for these proteins were highly expressed. During FNA exposure lowered ribosome activity and protein production were detected. Additionally, conditions within the cells were more oxidising and there was evidence of oxidative stress.

A sequential window acquisition of all theoretical mass spectra (SWATH-MS) quantitative proteomics investigation was performed to gain a comprehensive and systematic understanding of the antimicrobial mechanisms of FNA on *D. vulgaris* Hildenborough. Protein expression dynamics were determined when *D. vulgaris* Hildenborough was exposed to FNA concentrations of 0, 1.0, 4.0, and 8.0 μg/L for periods of 2, 8 and 12 h. Based on the interpretation of the measured protein changes the responses of *D. vulgaris* Hildenborough to different FNA levels over incubation time were revealed. During exposure to 1.0 μg N/L FNA, only the proteins involved in nitrite reduction (nitrite reductase and the poorly characterized hybrid cluster protein) showed obvious increased expression levels. In the presence of 4.0 and 8.0 μg N/L FNA, an increase of proteins levels for nitrite reduction was also evident. The abundance of proteins involved in the sulfate reduction pathway (from sulfite to hydrogen sulfide) and lactate oxidation pathway (from pyruvate to acetate) were firstly lowered by FNA at 8 h incubation, and then recovered at 12 h incubation. During FNA exposure, lowered ribosomal protein levels were detected while the total protein levels for viable cells remained constant. Additionally, there was evidence that proteins corresponding to the genes DVU0772 and DVU3212 play a critical role in defending oxidative stress caused by FNA.

The outcomes of this thesis advance our understanding of *P. aeruginosa* PAO1 and *D. vulgaris* Hildenborough in response to FNA, and contribute towards the potential application of this environmentally sustainable antimicrobial agent for improving wastewater treatment technologies, such as sewer corrosion control and odor elimination in wastewater treatment.

Declaration by author

This thesis **is composed of my original work, and contains** no material previously published or written by another person except where due reference has been made in the text. I have clearly stated the contribution by others to jointly-authored works that I have included in my thesis.

I have clearly stated the contribution of others to my thesis as a whole, including statistical assistance, survey design, data analysis, significant technical procedures, professional editorial advice, and any other original research work used or reported in my thesis. The content of my thesis is the result of work I have carried out since the commencement of my research higher degree candidature and does not include a substantial part of work that has been submitted **to qualify for the award of any** other degree or diploma in any university or other tertiary institution. I have clearly stated which parts of my thesis, if any, have been submitted to qualify for another award.

I acknowledge that an electronic copy of my thesis must be lodged with the University Library and, subject to the policy and procedures of The University of Queensland, the thesis be made available for research and study in accordance with the Copyright Act 1968 unless a period of embargo has been approved by the Dean of the Graduate School.

I acknowledge that copyright of all material contained in my thesis resides with the copyright holder(s) of that material. Where appropriate I have obtained copyright permission from the copyright holder to reproduce material in this thesis.

Publications during candidature

Peer-reviewed journal papers

- **Gao S.,** Fan L., Yuan Z., Bond P.L. (2015). The concentration-determined and population-specific antimicrobial effects of free nitrous acid on *Pseudomonas aeruginosa* PAO1. Applied Microbiology and Biotechnology, 99:2305-2312.
- **Gao S.,** Fan L., Peng L., Guo J., Agulló-Barceló M., Yuan Z., Bond P.L. (2016). Determining multiple responses of *Pseudomonas aeruginosa* PAO1 to an antimicrobial agent, free nitrous acid. Environmental Science & Technology, 50:5305-5312.
- **Gao S.,** Ho J., Fan L., Yuan Z., Bond P.L. (2016). Antimicrobial effects of free nitrous acid on *Desulfovibrio vulgaris*: implications for sulfide induced concrete corrosion. Applied and Environmental Microbiology, doi:10.1128/AEM.01655-16.

Conference presentations

- **Gao S.,** Fan L., Peng L., Guo J., Yuan Z., Bond P.L. (2015). Global transcriptome response to the antimicrobial agent free nitrous acid (FNA) by *Pseudomonas aeruginosa* PAO1 via RNA sequencing. Poster presentation at 6th Congress of European Microbiologists (FEMS 2015), Maastricht, The Netherlands, 7-11th June, 2015.

- **Gao S.,** Fan L., Peng L., Guo J., Yuan Z., Bond P.L. (2015). Determining growth inhibition mechanisms of the antimicrobial agent free nitrous acid (FNA) on *Pseudomonas aeruginosa* PAO1. Poster presentation at 115th general meeting of American Society for Microbiology (ASM 2015), New Orleans, Louisiana, United States, May 30th – 2nd June, 2015.

- **Gao S.,** Fan L., Yuan Z., Bond P.L. (2015). The concentration-determined and population-specific antimicrobial effects of free nitrous acid on *Pseudomonas aeruginosa* PAO1. Best Journal paper (Advanced Water Management Centre) at Faculty of Engineering, Architecture and Information Technology (EAIT) postgraduate conference 2015, Brisbane, Australia. 10th June, 2015.

Publications included in this thesis

Gao S., Fan L., Yuan Z., Bond P.L. (2014), The concentration-determined and population-specific antimicrobial effects of free nitrous acid on *Pseudomonas aeruginosa* PAO1. Applied Microbiology and Biotechnology, 99:2305-2312. –Incorporated as Appendix A.

Contributor	Statement of contribution
Author Gao S. (Candidate)	Gao S. established the research methodology, conducted all the experiments, and composed the content of the manuscript from initial draft to final submission. (65%)
Author Fan L.	Fan L. participated in the discussion of research methodology, helped to conduct part of the experiment, and shared comments on the manuscript. (10%)
Author Yuan Z.	Yuan Z. participated in the discussion of research methodology and advised on experimental design. (10%).
Author Bond P.L.	Bond P.L. advised on experimental design, and critically reviewed the paper. (15%)

Gao S., Fan L., Peng L., Guo J., Agulló-Barceló M., Yuan Z., Bond P.L. (2016), Determining multiple responses of *Pseudomonas aeruginosa* PAO1 to an antimicrobial agent, free nitrous acid. Environmental Science & Technology, 50:5305-5312. –Incorporated as Appendix B.

Contributor	Statement of contribution
Author Gao S. (Candidate)	Gao S. established the research methodology, conducted all experiments, completed RNA sequencing data analysis and composed the content of manuscript from initial draft to final submission. (50%)
Author Fan L.	Fan L. participated in the discussion of research methodology, analysing the RNA sequencing data, and made comments on the manuscript. (10%)
Author Peng L.	Peng L. participated in conducting the experiment and discussing the research methodology. (5%)
Author Guo J.	Guo J. participated in analysing RNA sequencing data. (5%)
Author Agulló-Barceló M.	Agulló-Barceló M. participated in conducting the experiment. (5%)
Author Yuan, Z.	Yuan Z. participated in the discussion of research methodology and advised on experimental design. (5%)
Author Bond P.L.	Bond P.L advised on experimental design, results interpretation, and critically reviewed the paper. (20%)

Gao S., Ho J., Fan L., Yuan Z., Bond P.L. (2016), Antimicrobial effects of free nitrous acid on *Desulfovibrio vulgaris*: implications for sulfide induced concrete corrosion. Applied and Environmental Microbiology. doi:10.1128/AEM.01655-16 –Incorporated as Appendix C.

Contributor	Statement of contribution
Author Gao S. (Candidate)	Gao S. established the research methodology, conducted all experiments, completed RNA extraction and sequencing data analysis and composed the content of manuscript from initial draft to final submission. (60%)
Author Ho J.	Ho J. participated in discussing the research methodology, conducting the experiment and analysing the data. (15%)
Author Fan L.	Fan L. participated in analysing the RNA sequencing data, and made comments on the manuscript. (5%)
Author Yuan, Z.	Yuan Z. participated in the discussion of research methodology and advised on experimental design. (5%)
Author Bond P.L.	Bond P.L advised on experimental design, results interpretation, and critically reviewed the paper. (20%)

Contributions by others to the thesis

This thesis includes contributions made by others, particularly in the chemical analysis of pure culture biological samples. These contributions are acknowledged as follows:

- Dr. Beatrice Keller-Lehmann, Jianguang Li and Nathan Clayton operated the ion chromatography (IC), gas chromatography (GC), high performance liquid chromatography (HPLC) and Flow Injection Analyzer (FIA) to analyse dissolved sulfur species, nitrous oxide, organic acids and dissolved nitrogen species.
- Dr. Michael Nefedov, from the School of Chemistry and Molecular Biosciences (SCMB, UQ) helped with the BD FACS AriaII flow cytometer and data analysis.
- Dr. Amanda Nouwens, from the School of Chemical and Molecular Biosciences (SCMB, UQ) assisted with proteomic procedures, performed the operation of the mass spectrometer, as well as initial interpretation of proteomic spectra.
- Prof. Jizhong Zhou and Dr Aifen Zhou, from the Department of Microbiology and Plant Biology, University of Oklahoma, generously provided pure culture *D. vulgaris* Hildenborough, shared medium recipe and kindly helped with the cultivation of this strictly anaerobic culture.

Statement of parts of the thesis submitted to qualify for the award of another degree

None.

Acknowledgements

My PhD has been a rewarding and memorable journey and one that could never be completed on my own. First and foremost, I owe my principal advisor Dr. Phil Bond my deepest gratitude and respect. No matter what the problem or question, I could always come knocking and be greeted with a smile. I thank you greatly for your time, your incredible patience and the continual encouragement and support through both the ups and downs of my PhD. I learned a lot from you not only your profound knowledge but also your personality over the past three years and nine months which will definitely benefit my future life.

I would like to extend my sincere gratitude to my co-advisor, Prof. Zhiguo Yuan, for your valued advice, knowledge and insightful suggestions. I thank you sincerely for your support and kind help during my application to access the opportunity joining this great team to pursue my PhD. Your enthusiasm and passion towards research deeply impress me. I would like to extend my special gratitude to my co-advisor, Dr Lu Fan, who teaches me lab skills, being more organised, developing the scientific thinking and writing on research, and accompanied me when conducting experiments late at night and early morning as the good friend.

Thank you to the ASL team, in particular Beatrice for your rigorous attitude and analytical expertise. My sincere thanks also goes to Dr Lai Peng, Dr Yiwen Liu, Dr Guojun Xie, Dr Bing-Jie Ni, Dr Jianhua Guo, Jun Yuan Ho, Andrew Laloo, Dr Christy Grobbler, Robert Hoelzle, Dr Amanda Nouwens, Dr Qilin Wang, Dr Jing Sun, Dr Ying Shi for helping me considerably during my PhD.

I am grateful to the AWMC academics, researchers, laboratory staff, administrative staff, and students who gave their support and kindness. Thanks to them for making the centre an enjoyable and fun place to work. I thank all my friends in Australia and China. Their continued friendship and love have made my life full of happiness. I am grateful to the financial support from China Scholarship Council. I also thank Advanced Water Management Centre for topping up the scholarship. This study was funded by the Australian Research Council and The University of Queensland.

The biggest heartfelt thanks go to my parents, my brother, my sister-in-law and my little adorable nephew. Thank you all for believing in me, for your never-ending support and encouragement and sticking by me. Last but not least, I would like to thank Huailong as the excellent partner for your consistent unconditional love and support.

Keywords

free nitrous acid, antimicrobial effects, mechanism, wastewater treatment, *Pseudomonas aeruginosa* PAO1, *Desulfovibrio vulgaris* Hildenbourough, transcriptomics, proteomics

Australian and New Zealand standard research classifications (ANZSRC)

ANZSRC code: 060501Bacteriology, 30%

ANZSRC code: 060405 Gene Expression (incl. Microarray and other genome-wide approaches), 50%

ANZSRC code: 090703 Environmental Technologies, 20%

Fields of research (FoR) classification

FoR code: 0605, Microbiology, 80%

FoR code: 0907 Environmental Engineering, 20%

Table of Contents

List of Figures & Tables

AckA: acetate kinase; CS: citrate synthase; ACN: aconitase; IDH: isocitrate dehydrogenase; malS: malate synthase; malDH: probable L-malate dehydrogenase; ICL: isocitrate lyase; OGDC: 2-oxoglutarate dehydrogenase; SCS: succinyl-coA decarboxylase; SDH: succinate dehydrogenase; fumH: fumarate hydratase.

Figure 10. Respiration pathways of lactate oxidation, sulfate reduction and nitrite reduction in *D. vulgaris* (Haveman et al. 2004). Enzyme abbreviations: Sat, sulfate adenylyltransferase; PpaC, pyrophosphatase; ApsBA, adenosine phosphosulfate reductase; DsrAB, dissimilatory sulfite reductase; QmoABC, quinone-interacting membrane-bound oxidoreductase; DsrMKJOP, triheme cytochrome c-containing membrane-bound oxidoreductase; Ldh, lactate dehydrogenase; Por, pyruvate:ferredoxin oxidoreductase; Pta, phosphate transacetylase; Ack, acetate kinase; c3 network, network of periplasmic, tetrahemic c-type cytochromes; APS, adenosine phosphosulfate.

Figure 11. Growth profiles of *D. vulgaris* Hildenborough batch cultures in the presence of different levels of FNA (μg N/L). FNA was added after 26 hours incubation, at time 0 h. The control culture has no FNA addition. Error bars were calculated based on the growth of the triplicate cultures. The figure key shows the FNA starting concentrations in the different cultures.

Figure 12. Levels of nitrite (A), FNA (B), lactate (C), acetate (D), sulfate (E), sulfide (F), sulfite (G), and thiosulfate (H) in *D. vulgaris* Hildenborough batch cultures grown on lactate and sulfate. The batch cultures were exposed to different levels of FNA which was added at time 0 h, which was 26 hours after inoculation. No FNA was added to the control cultures. Error bars represent the standard deviation of analyses performed from triplicate batch cultures. The figure key shows the FNA starting concentrations.

Figure 13. Physiological features of *D. vulgaris* Hildenborough measured during the batch culture incubations in the presence of different levels of FNA and when no FNA was added (control). The percentage of live cells (A), cellular thiol levels (B), intracellular redox levels, where higher fluorescence indicates lower redox potential (C), and cellular ATP levels (D). FNA was added at time 0 h.

Figure 14. Proposed antimicrobial effects of FNA (4.0 μg N/L) on *D. vulgaris* Hildenborough based on interpretations of measured physiological activities and the transcriptional responses. The colored boxes indicate activities or events where the associated gene expression was primarily increased (green) or decreased (red) in response to FNA exposure.

Figure 15. Total protein levels per microliter of *D. vulgaris* Hildenborough culture in the presence of different FNA levels (control, 1.0, 4.0 and 8.0 μg/L) at different incubation time period (2, 8 and 12h) (A), and cellular protein levels per live cells of *D. vulgaris* Hildenborough when exposed to

different levels of FNA (control, 1.0, 4.0 and 8.0 μg/L) with different treatment time period (2, 8 and 12h) (B).

Table 1. Summary of main literature findings on the bacteriostatic and bactericidal effects of FNA in wastewater treatment.

Table 2. Proteins with roles in tolerance to NO and nitrosative stress in bacteria.

Table 3. Proteins expression dynamics in the presence of different FNA concentrations relevant to metabolism.

Table 4. Proteins expression dynamics in the presence of different FNA concentrations relevant to protein synthesis and amino acid metabolism.

Table 5. Proteins expression dynamics in the presence of different FNA concentrations relevant to oxidative stress

Table 6. Proteins expression dynamics differences in the presence of four different FNA concentrations at different treatment time.

List of Abbreviations used in the thesis

AckA	Acetate kinase
ACN	Aconitase
AMO	Ammonia mono-oxygenase
AOB	Ammonium oxidising bacteria
APS	Adenosine phosphosulfate
ATP	Adenosine triphosphate
BOD	Biochemical oxygen demand
CS	Citrate synthase
DNA	Deoxyribonucleic acid
DsrAB	Dissimilatory sulfite reductase
DsrMKJOP	Triheme cytochrome c-containing membrane-bound oxidoreductase
EBPR	Enhanced biological phosphorus removal
ED pathway	Entner–Doudoroff pathway
EMP pathway	Embden-Meyerhof-Parnas pathway
FDR	False discovery rate
FIA	Flow injection analyzer
FNA	Free nitrous acid
fumH	Fumarate hydratase
Fur	Ferric uptake regulator
GAOs	Glycogen-accumulating organisms
GC	Gas chromatography
GK	Glycerol kinase
GLYM9	Glycerol modified M9
GSH	Glutathione
HC	Homocysteine
HPLC	High performance liquid chromatography
IC	Ion chromatography
ICL	Isocitrate lyase
IDA	Information dependent acquisition
IDH	Isocitrate dehydrogenase
LDH	Lactate dehydrogenase
LFC	Log2 fold-change
malDH	L-malate dehydrogenase

malS	Malate synthase
NADH	Nicotinamide adenine dinucleotide
NADPH	Nicotinamide adenine dinucleotide phosphate
NH_2	Amine
NIR	Nitrite reductase
NO	Nitric oxide
NO•	Nitric oxide radical
NO^+	Nitrosonium cation
NO_2	Nitrogen dioxide
NOB	Nitrite oxidising bacteria
NrfA	Cytochrome c nitrite reductase
OGDC	2-oxoglutarate dehydrogenase
QmoABC	Quinone-interacting membrane-bound oxidoreductase
$ONOO^-$	Peroxynitrite
OxyR	Hydrogen peroxide-inducible genes activator
PAOs	Polyphosphate-accumulating organisms
PDH	Pyruvate dehydrogenase
PGK	Phosphoglycerate kinase
PKA	Pyruvate kinase II
PKF	Pyruvate kinase I
pmf	Proton motive force
Por	Pyruvate ferredoxin oxidoreductase
PpaC	Pyrophosphatase
PTA	Phosphotransacetylase
RNIs	Reactive nitrogen intermediates
RNS	Reactive nitrogen species
ROS	Reactive oxygen species
RSNO	S-nitrosothiols
SAOB	Sulfide anti-oxidant buffer
Sat	Sulfate adenylyltransferase
SCS	Succinyl-coA decarboxylase
SDH	Succinate dehydrogenase
SoxR	Redox-sensitive transcriptional activator
SRB	Sulfate reducing bacteria
SWATH-MS	Sequential window acquisition of all theoretical mass spectra

TCA	Tricarboxylic acid
UV	Ultraviolet
WAS	Waste activated sludge

Chapter 1 Introduction

1.1 Background

The antimicrobial properties of nitrite have been known for a long time and nitrite has been used as a food preservative for centuries. Evidence has been accumulating that increased levels of nitrite is shown to inhibit the metabolism of numerous key microbes involved in wastewater treatment processes (Vadivelu et al. 2007). However, recent studies provide compelling evidence that it is in fact FNA, the protonated form of nitrite (HNO_2), instead of nitrite that causes the bacteriostatic and bactericidal effect (Jiang et al. 2011; Vadivelu et al. 2006b; Zhou et al. 2007). It is shown that parts per billion (ppb, equal to 1.0 μg N/L) levels of FNA are bacteriostatic (Pijuan et al. 2010; Vadivelu et al. 2006b; Zhou et al. 2008) while parts per million (ppm, equal to 1.0 mg N/L) levels of FNA are bactericidal (Jiang et al. 2011; Wang et al. 2013a). There are a number of findings relating to the inhibitory and bactericidal effects of FNA in studies of wastewater treatment applications. For example, it is reported that FNA inhibits the anabolic processes of nitrite oxidizing bacteria (NOB) *Nitrobacter* at approximately 0.01 mg N/L (Vadivelu et al. 2006b). In comparison, inhibition of growth of the ammonium oxidizing bacteria (AOB) *Nitrosomonas* occurs at higher concentrations of approximately 0.1 mg N/L FNA (Vadivelu et al. 2006a). Sewer biofilms consisting of sulfate reducing bacteria (SRB) and methanogenic bacteria were destroyed at a FNA concentration of 0.2 mg N/L (Jiang et al. 2011). This is significant as it greatly reduces the production of sulfide, which will considerably lower sewer corrosion (Jiang et al. 2013). In another application, FNA at 2.13 ppm caused lysis of activated sludge cells and this improves the biodegradability of the sludge and enhances methane production during its anaerobic digestion (Wang et al. 2013a). These findings highlight tolerance differences among bacteria towards FNA and highlight the needs for research on other bacteria relevant to wastewater treatment for its better application.

Since there are many potential applications of FNA for control and manipulation of microbial growth, it is of great necessity and interest to better understand the antimicrobial mechanisms of FNA on bacteria. This includes knowledge of how microbes may respond to and tolerate exposure to FNA and whether adapted resistance may occur. In the past few decades, many studies attempted to determine how nitrite produced antimicrobial effects and various mechanisms have been proposed. For example, it is supposed that nitrite might directly inhibit the activity of certain enzymes, such as those involved in denitrification process (Schulthess et al. 1995; Zhou et al. 2008). The nature of this inactivation is unknown, while suggested causes include nitric oxides forming

nitrosyl groups with catalytic metal or haem groups to deactivate respiratory enzymes (Morita et al. 2004). FNA *per se* and the reactive nitrogen intermediates (RNIs) derived directly from FNA or by reactions of FNA with other cellular molecules are thought to cause oxidative damage in microbial cells (Yoon et al. 2006; Zahrt and Deretic 2002). These oxidants could have general deleterious effects such as reacting with sulfhydryl groups to inactivate proteins, or cause oxidative damage to lipids or DNA (Zhou et al. 2010b). A further suggestion is that FNA could directly cross the cell membranes, and then the intracellular dissociation of the weak acid uncouples the membrane proton motive force (pmf), resulting in the termination of ATP synthesis and finally causing energetically damage to bacteria cells (Fang 2004; Sijbesma et al. 1996). In a pure culture study, nitric oxide (NO), which can be produced through the reduction of nitrite, was shown to be able to cause dispersal of *P. aeruginosa* biofilm, and it is suggested that the dispersing cells were energetically activated (Barraud et al. 2009). In contrast, a gene expression analysis indicates that planktonic cells of *P. aeruginosa* are energetically compromised after exposure to nitrite (Platt et al. 2008). While these findings are not conclusive and even contradictory, there still lacks a clear and systematic elucidation of the fundamental mechanisms of the antimicrobial effects of FNA on bacteria and also the responses of bacteria to FNA in wastewater treatment.

1.2 Thesis Objectives

The aim of this PhD thesis is to obtain a fundamental understanding of essential mechanisms of the bacteriostatic and bactericidal effects of FNA on two model microbes (*P. aeruginosa* PAO1 and *D. vulgaris* Hildenborough) in wastewater treatment. This project is expected to provide an improved understanding of this environmentally sustainable antimicrobial agent and to offer the underpinning knowledge for developing the innovative strategies for bacterial growth and biofilm control in wastewater treatment.

1.3 Thesis Organization

This thesis contains four chapters and four appendices.

Chapter 1 gives a general introduction to the background, objectives, and organization of this thesis.

Chapter 2 presents a comprehensive literature review. Firstly, roles of microbes in the environment especially in wastewater treatment are briefly reviewed. Secondly, the antimicrobial effects of FNA in wastewater treatment are introduced. The current investigation outcomes on the inhibitory and bactericidal effects of FNA on microbes especially in wastewater treatment are summarised. Lastly, the

hypothesised different antimicrobial mechanisms of FNA on microbes and the possible responses of microbes towards FNA are reviewed.

Chapter 3 consists of three sections, namely Research Objectives, Research Methods, and Results and Discussion. Sections within this chapter are summaries and descriptions of the detailed investigations described in the papers/manuscripts presented as Appendix A to D. It provides an overview of the research undertaken as part of this thesis.

Chapter 4 summarises the significant conclusions and promising prospects achieved from this project, and the recommendations for future research.

The four appendices are papers and manuscripts that include the detailed experimental studies for the distinct research objectives outlined and summarised in Chapter 3. Appendix A reports the concentration-determined and population-specific antimicrobial effects of FNA on the environmentally relevant denitrifier *P. aeruginosa* PAO1. Appendix B presents the antimicrobial mechanisms of FNA to *P. aeruginosa* PAO1 is multi-targeted via analysing global transcriptome expression changes and detecting a suite of physiological assays. Appendix C elucidates the antimicrobial mechanisms of FNA to a model microorganism in sewers *D. vulgaris* Hildenborough and reveals its responses to FNA stress by applying genome wide transcriptome analysis and substrate transformations as well as selected physiological detections. Appendix D unravels the responses comparison of *D. vulgaris* Hildenborough to different levels of FNA and different treatment time period after FNA addition based on proteomics study.

Chapter 2 Literature review

The literature review below summarises findings of previous studies that are highly relevant to the thesis topic. In section 2.1, roles of microbes in the environment especially in wastewater treatment are briefly reviewed. Section 2.2 describes the antimicrobial effects of FNA in wastewater treatment. This is followed by the investigation regarding the bacteriostatic and bactericidal effects of FNA on various bacteria in wastewater treatment as previously reported. In section 2.4, the current findings on the hypotheses of inhibitory and bactericidal effects of FNA on microbes are summarised. Section 2.5 reviews the possible responses of microbes towards FNA and RNIs.

2.1 Roles of microbes in wastewater treatment

Wastewater treatment practice began at an industrial scale at the beginning of 20th century. Afterwards, many biological wastewater treatment approaches have been developed based on microbial activities for the removal of undesired components within wastewater. Microbes in wastewater treatment can decompose waste organic matter and have essential roles for removing carbonaceous biochemical oxygen demand (BOD), coagulating non-settable colloidal solids, stabilizing organic matter, and detoxifying pollutants. Specifically, they mainly function for BOD and chemical oxygen demand reduction and for the removal of nutrients, carbon, nitrogen and phosphate, such that the effluent produced following the wastewater treatment can be discharged with minimal impact on natural waters (Metcalf 2003).

One of the most well used wastewater treatment systems is activated sludge treatment, which is a biological treatment process that uses a suspended growth of microbes. It is of great significance for the microbes in activated sludge to form flocs with the density that enables the separation of the biomass from the treated wastewater. The activated sludge treatment removes organic carbon by biomass growth and by conversion of organic carbon to carbon dioxide; nitrogen removal is achieved by conversion of organic or inorganic nitrogen to nitrogen gas, and phosphate removal by conversion to intracellular polyphosphate (Metcalf 2003). In addition, some bacteria are capable of cleaning up troublesome environmental pollutants (namely bioremediation). For example, the obligate hydrocarbonoclastic bacteria are able to remove petroleum hydrocarbons from polluted marine waters (Yakimov et al. 2007). Bacteria in the genus *Shewanella* are capable of digesting toxic waste such as hexavalent chromium in the wastewater (Xafenias et al. 2013).

2.2 Microbial control in wastewater treatment

While many bacteria in wastewater treatment play beneficial roles in the treatment processes, others may have detrimental effects. Therefore, control of microbial growth and activities is required in many practical situations. For instance, since the activated sludge wastewater treatment process is aerobic, biomass production occurs, resulting in the drawbacks of excess sludge production that needs to be tackled (Wei et al. 2003). Treatment and disposal of sewage sludge from wastewater treatment accounts for about half, even up to 60%, of the total cost of wastewater treatment (Davis and Hall 1997) and effective control of sludge production has potential cost advantages. Another representative example is the development of unwanted biofilms on the surfaces of wastewater infrastructure and facilities. Sewer biofilms produce hydrogen sulfide, which causes odor nuisance and rapid asset deterioration (Jiang et al. 2010). Similarly, biofilms growing on membranes used for wastewater treatment cause biofouling. This hampers the performance of membrane bioreactors and dealing with the biofouling can use around 60% of the total operational and maintenance cost (Drews 2010; Hwang et al. 2008). Therefore, the ability to inhibit the performance of detrimental bacteria is essential in the wastewater industry.

2.3 FNA as a bacteriostatic and bactericidal agent in wastewater treatment

2.3.1 Antimicrobial agents used for microbial control in wastewater treatment

Antimicrobial agents can be classed as those that have a killing effect, called bactericidal, and those that do not kill but only inhibit the growth of the bacteria, termed bacteriostatic. Chlorine, as an oxidising agent, is widely applied for disinfection in the drinking water industry and for reduction of excess activated sludge production in wastewater treatment (Saby et al. 2002). Other oxidising agents including ozone and hydrogen peroxide are used as disinfectants as well (Glaze et al. 1987). Odour control in sewers may use aeration/air, UV, metal salts and alkali to curb the growth of SRB (Chandler; Jiang et al. 2011). However, the traditional dosing strategies involve constant addition of chemicals which require large chemical consumption and high operational costs. Additionally, the use of these can be constrained due to the effect not having the required specificity or the agent may have further unwanted effect. For example, it may be difficult to adopt them on a large scale or because they are extremely costly (Glaze et al. 1987). Many antibiotics are used to control microbial communities when required in the clinical area. The discovery of penicillin isolated from *Penicillium notatum* by Alexander Fleming in the early 1940s, provides the basis for the era of modern antimicrobial therapy of bacterial infection. However, antibiotics are generally not used for microbial control in wastewater treatment due to the possible release of microbes to the environment with enhanced resistance to antibiotics (Kim and Aga 2007). Furthermore, many

antibiotics, such as penicillin and tetracycline, show high susceptibility to hydrolysis and become ineffective through binding to free irons or sediments in wastewater treatment (Heberer 2002; Hirsch et al. 1999).

2.3.2 Bacteriostatic and bactericidal effects of FNA on microbes

The antimicrobial properties of nitrite have been known for a long time. It has been used as a food preservative for centuries to inhibit the growth of food spoilage bacteria. For example, nitrite can inhibit growth of *Clostridium botulinum* which is a producer of one of the most lethal natural toxins known (Pierson and Smoot 1982). Nitrite is also well documented in medical research. For example, it is reported that salivary nitrite could serve as a useful host defence mechanism against swallowed pathogens via the formation of bactericidal compounds in the stomach (Benjamin et al. 1994). In an *in vitro* study, Rao et al. (2006) showed that normal stomach acidity in combination with physiological concentrations of nitrite can kill *Clostridium difficile* spores (Rao et al. 2006). Phillips et al. (2004) achieved approximately 100% killing of *Mycobacterium ulcerans* at FNA concentration of 4.3 mg N/L over a 10 min exposure time (Phillips et al. 2004). They further proved that the killing was due to the action of FNA rather than nitrite. Later, Yoon et al. (2006) claimed that mucoid, mucA mutants of *P. aeruginosa* could be completely killed at FNA level of around 0.17 mg N /L in 2 days (Yoon et al. 2006). Such findings are aimed for eradicating mucoid *P. aeruginosa* from the cystic fibrosis airways (Yoon et al. 2006).

However, recently there is accumulating evidence demonstrating that FNA, the protonated form of nitrite (HNO_2), is the true metabolic inhibitor behind the often observed “nitrite inhibition” to a broad range of microbes at ppb levels and a strong bactericidal agent at ppm levels under both aerobic and anaerobic conditions in wastewater treatment (Jiang et al. 2011; Vadivelu et al. 2006b; Wang et al. 2013a; Zhou et al. 2008). Therefore, there is an opportunity to apply FNA as a bacteriostatic or bactericidal agent to control the growth and activities of microbes important to wastewater treatment. Some of the research outcomes based on bacteriostatic and bactericidal effects from recent experiments are summarised in (Table 1).

Table 1 - Summary of main literature findings on the bacteriostatic and bactericidal effects of FNA in wastewater treatment

Types of microbes	Culture/System/Organism	FNA (mg N/L)	Remarks (bacteriostatic or bactericidal)	References
Summary of studies based on the bacteriostatic effect of FNA in wastewater treatment				
NOB	Activated sludge treating municipal wastewater	0.22-2.8	Threshold for inhibitory initiation	(Anthonisen et al. 1976)
NOB	Enriched *Nitrabacter* culture (73%)	0.011	Threshold for anabolic process inhibition	(Vadivelu et al. 2006a)
		0.023	100% inhibition on biosynthesis	
		0.05	No inhibition on catabolism	
AOB	*Nitrosomonas europaea*	1.72	50% inhibition on ammonia monooxygenase activity	(Stein et al. 1998)
AOB	AOB enrichment	0.16	20%-25% inhibition	(Fux et al. 2003)
AOB	Enriched *Nitrosomonas* culture (82%)	0.10	Inhibition threshold for anabolism	(Vadivelu et al. 2006b)
		0.40	100% inhibition on anabolism	
		0.50-0.63	50% inhibition on catabolism	
AOB	SHARON	0.21	50% inhibition	(VanHulle et al. 2007)
AOB	Enriched AOB culture	0.0013	50% inhibition	(Jiménez et al. 2012)
AOB and NOB	Urban landfill leachate	0.004-0.68	Stable nitration was triggered since NOB was completely inhibted	(Sun et al. 2013)
Denitrifier	Activated sludge receiving high-strength ammonium wastewater	0.039	Threshold for inhibition	(Abeling et al.1992)
Denitrifier	Pure culture: *Pseudomonas fluorescens*	0.066	Inhibition threshold for cell growth, but not for nitrate and nitrite reduction, and carbon source consumption	(Almeida et al. 1995)
Denitrifier	Activated sludge	0.02	Threshold for inhibition	(Glass et al. 1997)
Denitrifier	Activated sludge	0.01-0.025	40% inhibition on nitrate reduction	(Ma et al. 2010a)
		0.2	100% inhibition on nitrate reduction	
PAOs	Enriched *Accumulibacter* culture (86%)	0.02	100% inhibition on P-uptake, 40% inhibition on denitrification	(Zhou et al. 2007)
PAOs	Denitrifying P-removal culture	0.0007-0.001	50% inhibition on N_2O reduction	(Zhou et al. 2008)
PAOs	Denitrifying P-removal culture;	0.01	50% inhibition on P-uptake	
	Accumulibacter accounts for 40%	0.037	100% inhibition on P-uptake	

		0.02	60% inhibition on glycogen production	(Zhou et al. 2010a)
		0.02-0.07	40% inhibition on PHA degradation	
PAOs	Enriched *Accumulibacter* culture (90%)	0.0005	50% inhibition on anabolism	(Pijuan et al. 2010)
		0.006	100% inhibition on anabolism	
		0.002-0.01	50%-60% inhibition on catabolism	
PAOs	FNA adapted PAOs	0.01	100% growth inhibition	(Zhou et al. 2012a)
GAOs	Enriched *Competibacter* culture (90%)	0.0015	50% inhibition on cell growth	(Ye et al. 2010)
PAOs and GAOs	EBPR system	0.0022 (Maximum)	A stronger inhibitory effect of FNA on the anaerobic metabolism of PAOs than GAOs.	(Ye et al. 2013)
Sludge	Biological nutrient removal sludge	0.01-0.025	Nitrate reduction inhibition initiated	(Ma el al. 2010a)
		0.2	Threshold for complete nitrate reduction inhibition	
Summary of studies and technologies based on the bactericidal effect of FNA in wastewater treatment				
Sewer biofilm	Lab scale sewer biofilm system	0.2	Viable cell percentage dropped from 80% to around 5-15% after 6-24 h	(Jiang et al. 2011)
Sewer biofilm	Lab scale sewer biofilm system fed with real wastewater	0.26	Reduce average sulfide production by >80% dosed with FNA for 12h every 5 days	(Jiang et al. 2011a)
		0.09	Inhibition threshold for the methane generation after 6h exposure	
Sewer biofilm	Anaerobic wastewater system	0.2-0.3	Cause 90% biofilm inactivation with an exposure time longer than 6h	(Jiang et al. 2013)
Sewer biofilm	Sewers systems in field trials	0.26	Gaseous hydrogen sulfide production reduced by over 95% immediately after applying FNA for 6 or 24 h	(Jiang et al. 2013a)
Secondary sludge	Lab scale bioreactors	2.02	Viable cells decreased to 20% and biodegradability of secondary sludge enhanced after 48 h exposure	(Pijuan et al. 2012)
		≥0.2	Cause 2-log (99%) biofilm inactivation with hydrogen peroxide at 30 mg/L and exposure time more than 6h	
WAS	Sludge collected from wastewater treatment plant	2.13	Methane production from activated sludge enhanced six times after 24 h pretreatment compared with sludge without FNA treatment	(Wang et al. 2013c)
WAS	Sequencing batch reactors	2.0	Reduced 20% sludge production without affecting treatment performance and sludge properties	(Wang et al. 2013b)

WAS	Sludge collected from wastewater treatment plant	0.52-1.11	Biochemical methane potential of the pre-treated WAS was increased 17-26% and hydrolysis was improved by 20-25% combined with heat pretreatment	(Wang et al. 2014a)
Algae	Lab cultured microalgae	2.19	Lipid extraction was enhanced with FNA preteatment	(Bai et al. 2014)

PAOs: polyphosphate-accumulating organisms
GAOs: glycogen-accumulating organisms
WAS: waste activated sludge

The results summarised in Table 1 show that the anabolism of AOB, NOB and PAOs is more sensitive to FNA than their catabolism. For instance, FNA initiated inhibition of the anabolic processes of *Nitrobacter* (NOB) at approximately 0.011 mg N/L and completely stopped biomass synthesis at a concentration of approximately 0.023 mg N/L, while up to 0.05 mg N/L did not show any inhibitory effect on the catabolic processes (Vadivelu et al. 2006b). The inhibitory effect on the anabolic processes towards PAOs was much stronger than that on the catabolic processes since 50% inhibition on all anabolic processes occurred at approximately 0.5 μg N/L while 50%-60% inhibition on catabolic process occurred at 2-10 μg N/L (Pijuan et al. 2010). Additionally, AOB are more tolerant to FNA than NOB (Table 1). This characteristic can be potentially used to selectively remove NOB from the system during N removal in activated sludge in wastewater treatment. Recent studies showed that side-stream sludge treatment using FNA could indeed selectively eliminate NOB and achieve the nitrite pathway for a more efficient wastewater treatment nitrogen removal process (Wang et al. 2014b). In addition, FNA has a significantly stronger inhibitory effect on the aerobic metabolism of PAOs than that of GAOs (Table 1), which potentially provides a selective advantage for GAOs to outcompete PAOs in enhanced biological phosphorus removal (EBPR) plants.

Based on the antimicrobial capabilities, availability and cost-effectiveness, FNA is strongly considered for biological control and increasing FNA-based technologies in wastewater treatment were developed (Table 1). For instance, experiments have also been conducted to assess the capability of FNA to improve the biodegradability of secondary sludge (Pijuan et al. 2012). In this study, 90% of the FNA treated biomass was consumed during 14-day digestion compared to 41% achieved with the untreated biomass. Following on from that, a novel strategy based on FNA treatment was verified to achieve sludge reduction (Wang et al. 2013b). In the experimental system, 2.0 mg N/L FNA was exposed to 50% of the excess sludge for 24-42 h in an FNA treatment unit and then returned to the parent reactor. The sludge production in the experimental system was 28% lower compared to the control without negatively affecting the reactor performance and sludge properties. Furthermore, FNA treatment on waste activated sludge (WAS) was observed to enhance the methane production (Wang et al. 2014a). The biochemical methane potential of WAS treated with 0.52-1.53 mg N/L at 25 ºC was 12-16% higher than that of control, and the hydrolysis rate was improved by 15-25%.

In addition, FNA dosing for the control of sulfide and sewer corrosion was investigated (Table 1). It was demonstrated that intermittent FNA dosing for the control of sulfide and methane production in sewers is more cost-effective compared to the addition of other widely used chemicals and the estimated cost of FNA dosing to achieve 80% control of sulfide production is about $2.10/kg-S (Jiang et al. 2011), much less than that of $2.736-10.368/kg-S using other chemicals including oxygen, hydrogen peroxide, NaClO, $FeCl_3$ and $FeSO_4$ as well as other possible biological sulfide control in sewers (Zhang et al. 2008). In recent treatment of sewer biofilms it was seen that application of FNA for 6-24 hours at 0.2-0.3 mg N/L decreased the live cell percentage from about 80% to 5-15% (Jiang et al. 2011). Since then FNA has been applied in sewer field trials for the control of sulfide production in real sewers in Australia with FNA dosing at 0.26 mg N/L for 8-24 hours every four weeks (Jiang et al. 2013). The application of FNA for control of sewer sulfide levels is highly feasible. Moreover, a novel and simple treatment for control of sulfide induced sewer concrete corrosion by FNA spray was developed as a very cheap and effective strategy (Sun et al. 2015). In this study, the H_2S uptake rates of two concrete coupons with active corrosion activity with surface pH 3.8±0.3 and 2.7±0.2 respectively were reduced by 84% -92% 15 days after spraying 5 mL 8.3 g $NaNO_2$-N/L. No obvious recovery of the H_2S uptake rate was observed during the entire experiment period up to 12 months after the spray, indicating that the FNA treatment in controlling the activity of the corrosion-causing biofilms is effective long-term. In addition, FNA is also reported to be feasible for biofouling and scaling control of reverse osmosis membrane in one-step as a low cost bactericidal agent (Filloux et al. 2015).

All these research discoveries strongly support FNA, as a potential antimicrobial agent, is a promising antimicrobial agent to be implemented in the wastewater treatment to control the undesired microbes. However, at this stage the details of these bacteriostatic and bactericidal mechanisms of FNA are not known.

2.4 Proposed antimicrobial mechanism of FNA on microbes

Despite there have been numerous evidences of the antimicrobial nature of FNA/nitrite and prevalent applications of it in clinical treatments and bioengineering are emerging, up to date, the detailed mechanisms of FNA-induced effects to the microbes are not yet clearly elucidated. Experimental data has shown FNA can possibly cause oxidative stress to microbes and affect numerous metabolic processes, including the active transport of substrates across the cell membrane,

oxygen uptake, as well as oxidative phosphorylation. These studies and the proposed hypotheses so far are introduced below.

2.4.1 Biochemistry of FNA

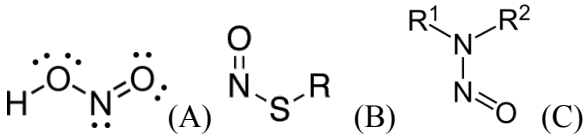

Figure 1 Chemical structures of FNA (A), S-nitrosothiol (B) and nitrosomine (C)

FNA (Figure 1), protonated form of nitrite, is a weak monobasic acid (pKa 3.3) known only in solution and mostly stable at pH $\geq$ 5. FNA is thought to decompose following the subsequent equations 1-4 in which nitrosonium cation (NO^+), dinitrogen trioxide (N_2O_3), nitric oxide radical (NO•) and nitrogen dioxide (NO_2) are generated in acidic aqueous solution (Oldreive and Rice-Evans 2001; Takahama U. & Hirota S., 2012) .

Equation 1: $NO_2^- + H^+ \Leftrightarrow HONO$ (pKa=3.3)

Equation 2: $HONO + H^+ \Leftrightarrow H_2NO_2^+ \Leftrightarrow H_2O + NO^+$

Equation 3: $2HONO \Leftrightarrow N_2O_3 + H_2O$

Equation 4: $N_2O_3 \Leftrightarrow NO\bullet + NO_2$

Based on the biochemistry of FNA, it is thought that a variety of reactive nitrogen intermediates (RNIs) that have cytotoxic properties may be generated in biological conditions (Takahama U. & Hirota S., 2012). The potential physiological effects of these molecules are introduced below.

1) Peroxynitrite ($ONOO^-$)

Under aerobic conditions, the more reactive species, peroxynitrite ($ONOO^-$) can be formed from the reaction of NO with superoxide or nitrosyl ion with oxygen (Maraj et al. 1995). Although $ONOO^-$ is unreactive, it can be transformed to NO_2• and OH• radicals as well as nitrate, thereby introducing oxidative stress by itself and by producing NO_2• and OH• radicals. $ONOO^-$ is a powerful oxidant that causes microbial cell death through oxidation of protein thiols, iron-sulfur centers, DNA, and membrane phospholipids (Zaki et al. 2005).

2) NO-derived nitrosyl complexes

NO reacts directly with haem and metal centres of proteins, forming nitrosyl complexes (Fang 2004). Molecular targets of NO encompass haem/nonhaem iron cofactors, iron-sulfur clusters, and other redox metal sites, all forming metal-nitrosyl complexes (Fang 2004). Therefore, NO can cause the inactivation of metal-containing enzymes such as glyceraldehyde-3-phosphate dehydrogenase (Hinze and Holzer 1986).

In addition, NO can interact with proteins with the reduced thiol on surface in the presence of eletron acceptor, forming S- nitrosothiols (Gow et al. 1997). S-nitrosothiols are organic compounds or functional groups containing a nitroso group attached to the sulfur atom of a thiol.

4) N-nitroso compounds formed by nitrosylation

N-nitorso compounds are easily formed by interaction of a secondary amino compound with a nitrosating agent such as NO^{+}(Lijinsky 1999). For example, nitrosamine can be formed by the reaction of NO^{+} with an amine, thereby modifying proteins and potentially altering function (Kulshrestha et al. 2010).

2.4.2 FNA alters intracellular pH

FNA is able to diffuse across the membrane, be trapped inside the cells in its anionic form due to the normal neutral intracellular pH inside the cells, release the protons within the cells, thus decreasing the intracellular pH and interfering with the trans-membrane pH gradient required for ATP synthesis (Anthonisen et al. 1976; Zhou et al. 2011). To counteract the acidification effect of the weak inorganic acid FNA, cell will pump out protons through energy-requiring plasma H^{+}-ATPase, leading to the uncoupling of energy generation from growth (Zhou et al. 2011) and finally causing the bacteriostatic or bactericidal effect. The intracellular pH of *Salmonella enterica* Serovar Typhimurium was observed to decrease upon the addition of FNA (Mühlig et al. 2014). However, there are also other studies that do not support this view. For example, there is no significant uncoupling effect occurring in *Paracoccus denitrificans* with FNA exposure (Alefounder et al. 1983). And although the growth was inhibited severely, the energy generation capacity of *Nitobacter* was not affected (Vadivelu et al. 2006b). These findings implicate that this mechanism of bactericidal effect of FNA may not occur in all microbes.

2.4.3 FNA acts as a protonophore to uncouple the proton motive force (pmf) and inhibit intracellular ATP generation

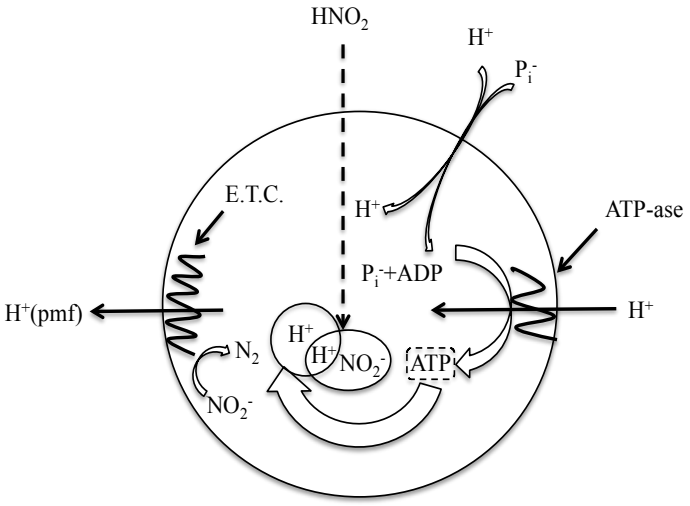

Figure 2 Illustration of ATP production and proton transportation in a denitrifying bacterial cell. The electron transport chain generates the protein motive force (pmf), pmf crosses the cell membrane, which is then used to generate ATP by the ATP-ase (Zhou et al. 2011).

It is generally believed that FNA may passively pass through the bacterial cytoplasmic membrane, increase the proton permeability of membranes and lead to dissipation of transmembrane electrochemical proton motive force (pmf) (Sijbesma et al. 1996; Zhou et al. 2010b). FNA could be transported into the cells by passive diffusion as the protonophore shuttling protons between the two membrane sides without generating energy (Maeda et al. 1998; Wu and Stewart 1998). This will cause the collapse of pmf required for ATP synthesis (Almeida et al. 1995; Anthonisen et al. 1976; Sijbesma et al. 1996), thereby inhibiting the ATP synthesis and affecting various exchange reactions catalysed by ATPase, which is energetically damaging to the cell (Sijbesma et al. 1996). The decreased bacterial growth even death could be due to the expenditure of energy depletion to pump protons out of the cells after FNA has diffused through the cell membrane (Almeida et al. 1995; Anthonisen et al. 1976; Sijbesma et al. 1996). The intracellular ATP levels of *Accumulibacter* were seen to decrease with increasing levels of FNA (Zhou et al. 2010b; Zhou et al. 2007). Besides, in *Escherichia coli* O157:H7 cells, the addition of FNA inhibited the synthesis of ATP (O'Leary and Solberg 1976). In the yeast *Saccharomyces cerevisiae*, the intracellular ATP level was also found to decrease immediately after FNA addition (Hinze and Holzer 1985).

However, it is assumed that in the presence of FNA, if pmf were collapsed, denitrifying- EBPR sludge would increase their respiration rate to pump out more protons, and would lead to a higher N_2O reduction rate, which contradicted the experimental data shown (Zhou et al. 2008). This

suggested FNA may not inhibit ATP generation metabolism of all microbes or the FNA uncoupling effect alone may not be the sole mechanism of FNA inhibition.

2.4.4 FNA inactivates many cell enzymes

FNA was reported to interact with enzymes that contain thiols, heme groups, iron sulfur clusters, phenolic or aromatic amino acid residues, tyrosyl radicals, or amines and inactivate them (Fang 1997). Sulfhydryl (SH)-containing enzymes are key regulators in the tricarboxylic acid (TCA) cycle, and the activities of those enzymes could be suppressed by FNA, which would negatively impact the energy generation process of cells (Figure 3) (O'Leary and Solberg 1976; Park 1993). FNA could also inhibit the oxidising of the cytochrome component of ferrous iron to ferric iron in *P. aeruginosa*, thereby hindering the normal functionality of the electron transport chain and leading to the inhibitory and bactericidal effect (Rowe et al. 1979). Glyceraldehyde-3-phosphate dehydrogenase, an enzyme involved in both glycolysis and gluconeogenesis (Hinze and Holzer 1986) was demonstrated to be inactivated by FNA (Hinze and Holzer 1986; O'Leary and Solberg 1976), which coincides with the findings of Zhou et.al (2010a) where both glycogen generation (i.e. through gluconeogenesis) and degradation (i.e. through glycolysis) were severely inhibited under anoxic conditions with FNA concentrations of 0.01 mg N/L (Zhou et al. 2010b).

The enzymes involved in denitrificaiton were reported to be another target of FNA. Various levels of FNA was evidenced to have a strong inhibitory effect on nitrite reductase (NIR) and inhibit the NsrR gene, in which the expression of the NIR is regulated (Beaumont et al. 2004). NIR genes were induced with FNA exposure, while the enzymes could not be detected. This is possibly because the translation of the NIR was inhibited or NIR was trans-located and folded improperly, or the conformational structure of synthesised NIR was changed and inactivated by FNA (Baumann et al. 1997). FNA was also observed to suppress the NO reductase in denitrifying sludge, resulting in the NO accumulation (Schulthess and Gujer 1996), which will further impede the activity of N_2O reductase (Schulthess and Gujer 1996). N_2O reductase contains two metal centers, a binuclear copper center, CuA, which serves to receive electrons from soluble donors, and another tetranuclear copper-sulfide center, CuZ, at the active site. FNA could bind to the active sites of copper-containing enzymes, causing competitive inhibition to N_2O reduction (Zhou et al. 2008).

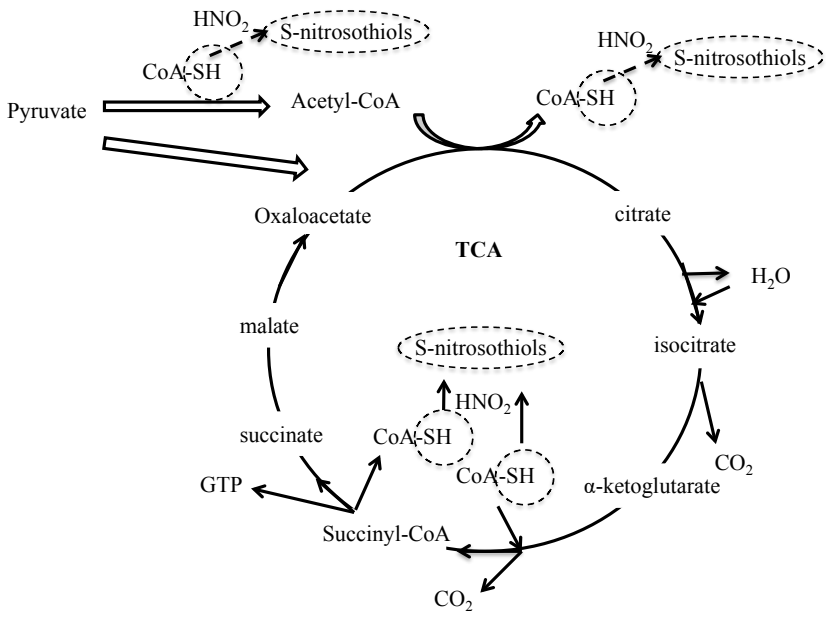

Figure 3 FNA reacting with thiol groups to form S-nitrosothiols, resulting in the decrease of free thiol groups in the liquid phase (Zhou et al. 2011).

2.4.5 FNA causes other cellular damage

As an extremely reactive molecule, FNA is capable of interacting with a broad range of substrates and inducing mutagenic effects (Fang 2004). For example, FNA can cause oxidative deamination of the amine (NH_2) group of adenine or cytosine to an ether group (Malling 2004). It can also convert adenine to hypoxanthine, cytosine to uracil and guanine to xanthine. By altering a DNA base pair directly to a "miscoding" form and the change of DNA base paring (mutagenesis), FNA is lethal to microbes (Malling 2004). FNA was also reported to be able to suppress one or more steps of the carbon transformation performed by nitrifiers and maybe the carbon transformation of other microbes was affected as well (Almeida et al. 1995; Vadivelu et al. 2006b).

2.4.6 RNIs introduce damage to bacterial cells

Based on the biochemistry of FNA, a variety of RNIs can be generated in biological conditions, including NO, N_2O_3, NO_2, $ONOO^-$ in the presence of oxygen, NO-derived metal nitrosyl complexes, S-nitrosothiols (RSNO) and N-nitroso compounds formed by nitrosylation with cell components (Fang 2004; Oldreive and Rice-Evans 2001). These RNIs can readily diffuse across cell membrane and are cytotoxic to bacteria (Fang 2004) (Figure 4). RNIs can damage DNA (Woodmansee and Imlay 2003) and modify protein micromoities including Fe-S clusters (Soum and Drapier 2003), heme (Mayburd and Kassner 2002) and sulfhydryl groups (Spallarossa et al. 2003) by nitrosalytion, and also cause damage to the tyrosine residues et.al (Schopfer et al. 2003).

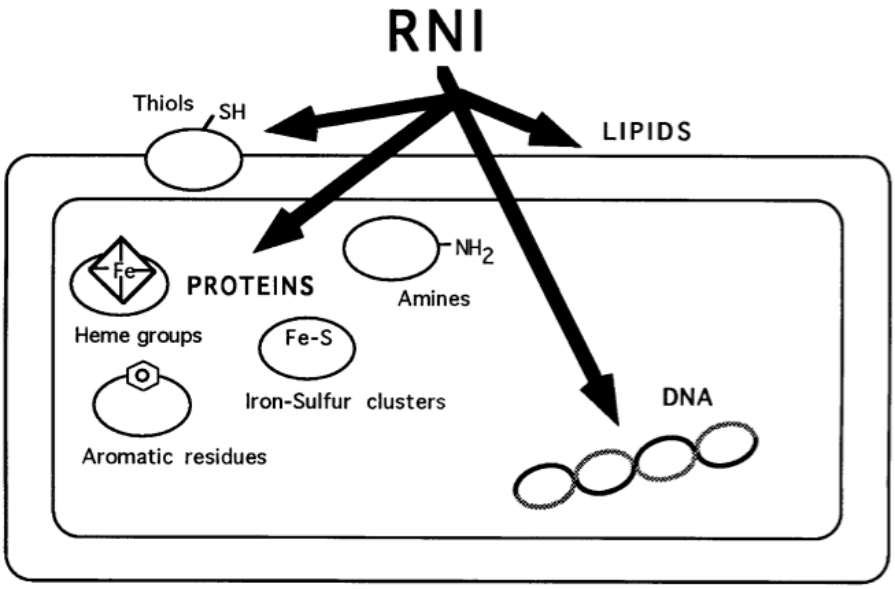

Figure 4. Microbial cellular targets of RNIs (Fang 1997).

Cellular damage caused by NO

Nitrosyl complexes, formed by the reaction of NO with cellular heme, thiols and metal centre of proteins (118), inactivate enzymes containing these groups. For example, the nitrosylation has been seen for ribonucleotide reductase and ubiquinone reductase (respiratory enzyme), resulting in the DNA replication inhibition and respiration chain disruption respectively (Nakaki et al. 1990; Phillips et al. 2004; Woods and Wood 1982; Woods et al. 1981).

Thiol is the most important target of NO, and nitrosylation of thiols may modify protein function per se, facilitate subsequent modification such as ADP-ribosylation, or accelerate disulfide formation between vicinal thiols (Fang 2004), and finally disable the enzymes containing thiol groups. The reaction of NO with cysteine sulfhydryl can result in the S-nitrosylation and disulfide-bond formation, which will inactivate certain enzymes requiring functional cysteine and cause detrimental effects to bacterial cells (Nathan and Shiloh 2000). Moreover, NO or S-nitrosothiols was reported to reversibly inhibit bacterial DNA replication through a mechanism that involves zinc mobilization from metalloproteins (Schapiro et al. 2003). However, up to date, the real mechanism underlying the bacteriostatic and bactericidal effect of nitrosothiols was not clearly elucidated.

Metal-nitrosyl complexes, formed by the reaction of NO with cellular heme/noneheme iron or iron-sulphur centres, may inactivate enzymes. This has been seen for ribonucleotide reductase and ubiquinone reductase containing Fe-S clusters (e.g. aconitase, NADH dehydrogenase, succinate

dehydrogenase), resulting in the DNA replication inhibition and respiration chain disruption respectively (Nakaki et al. 1990; Phillips et al. 2004). NO can also nitrosylate iron-containing heme proteins such as guanylyl cyclase in physiological signal transduction and this nitrosylation can result in the inactivation of other heme proteins as well, such as catalase and cytochrome systems (Fang 2004). Moreover, intriguingly in contrast to the reaction of NO with heme iron, which is reversible, the reaction of NO with iron-sulfur clusters often results in destruction of the cluster (Butler et al. 1995). This may be the nature of the cytotoxic action of NO to several key enzymes, such as aconitase, NADH-ubiquinone oxidoreductase and NADH-succinate oxidoreductase, containing iron-sulfur clusters. Additionally, it is thought that the formation and efflux of iron-nitrosyl complex or direct release of iron from metalloenzymes by NO could promote iron depletion, leading to the inactivation of iron dependent enzymes (Drapier et al. 1991). Furthermore, NO at millimole (mM) range in several bacteria is reported to inactivate the ferric uptake regulator (Fur) and depress iron acquisition (D'Autreaux et al. 2002; Moore et al. 2004). All in all, it is possible that metal-nitrosyl complex may either exert its cytotoxic effect by inactivating various cell essential enzymes through destruction of the iron-sulfur center or via iron depletion within the cells. However, as with nitrosothiols, details of the effect on the cell resulting from the NO-metal interaction still needs to be clarified.

The interactions between NO and tyrosyl radicals accounts for the inhibiton of ribonucleotide reductase by RNIs, which limits the availability of precursors for the synthesis and repair of DNA (Lepoivre et al. 1991). Bacteriophage genes were activated with NO exposure, and it was speculated that phage could mediate the cell lysis and lead to the cell death in *P. aeruginosa* (Platt et al. 2008).

Cell damage caused by other RNIs

N_2O_3 was proven to be a strong nitrosating intermediate and is capable of modifying the function of certain proteins (Yoon et al. 2006) and proposed to cause the DNA mutation through base conversions (e.g. G: C→ A: T transitions). Changes may also involve $ONOO^-$ and NO_2, since both of them can cause oxidative damage to DNA, resulting in termination sites, strand breaks, and a variety of other DNA alterations (Juedes and Wogan 1996). It is seen that bacteria deficient in DNA recombinational repair is hypersusceptible to inhibition or killing by S-nitrosotiols and peroxynitrite, this further indicating the interactions between RNIs, DNA and DNA repair systems.

Compared with FNA itself, $ONOO^-$ is a far more potent antimicrobial agent. $ONOO^-$ can pass through cell membrane probably in terms of peroxynitrous acid and was reported to be responsible for the candidacidal activity of murine macrophages (Fang 2004). $ONOO^-$ and NO_2 was also demonstrated to mediate the lipid peroxidation, which results in cell membrane damage (Halliwell et al. 1992; Rubbo et al. 1994) and can also nonspecifically oxidize proteins at a variety of sites (Ischiropoulos and Al-Mehdi 1995). As a powerful oxidant, $ONOO^-$ could also cause microbial cell death through oxidation of protein thiol cell components, DNA and membrane phospholipids as well as inhibition of the electron transport chain (Zaki et al. 2005).

2.5 Proposed responses of microbes against FNA

Although direct investigation of bacterial resistance to FNA is scarce, there are investigations of bacterial adaptation to RNIs that may be derived from FNA (Poole 2005). It is discovered that bacteria use various mechanisms for coping with the toxic effects exerted by RNIs (Rogstam et al. 2007) including activating genes that encode proteins involved in detoxification, repair, and maintenance of homeostasis (Poole 2005).

2.5.1 Detoxification enzymes

It is stated that microbes have evolved a number of mechanisms for coping with nitrosative stress, in which detoxification enzymes play a pivotal role. Considerable research in this area indicates proteins with roles in tolerance to NO and nitrosative stress (Table 2). Globins and reductases are the two main types of proteins involved in this tolerance. Globins function under nitrosating stress either through converting NO into nitrate or directly consuming NO to alleviate the potential toxicity. Reductases are reported to participate in the detoxification process through reducing NO or controlling the cellular levels of NO-derived complexes such as S-nitrosothiols.

Table 2. Proteins with roles in tolerance to NO and nitrosative stress in bacteria

Class	Protein	Organism(s)	Function/reactions catalyzed	Comments	References
Globins	Flavohaemoglobin	*E.coli, Salmonella,* many others	Enzymatic detoxification of NO by conversion into nitrate	Hmp expression up-regulated by NO and nitrosating agents	(Poole and Hughes 2000)
	Truncated globin (HbN)	*Mycobacterium bovis*	Conversion of NO into nitrate	NO inducible NO uptake, mechanism unknown	(Ouellet et al. 2002)
	Vitreoscila globin (Vgb)	*Vitreoscillo sp.*	NO consumption	Mechanism unknown	(Frey et al. 2002)
	Single-domain globin	*Compylobacter jejuni Campylobacter coli*	Confers enhanced resistance to NO and nitrosating agents	Mechanism unknown	(Elvers et al. 2004)
Reductase	Flavorubredoxin (NorVW)	*E. coli*	NO reduction and detoxification	Up-regulated in response to NO and nitroprusside	(Gardner et al. 2002)
	Cytochrome c nitrite reductase (NrfA)	*E. coli*	NO reduction and detoxification	Nrf $^-$ strains show higher NO sensitivity	(Poock et al. 2002)
	GSH-dependent formaldehyde dehydrogenase	*E. coli,*yeast	S-nitrosoglutathione (GSNO) reductase	Control cellular levels of S-nitrosothiols and S-nitrosylated proteins	(Liu et al. 2001)
	Cytochrome bd	Bacteria	NO reduction at Cu_B	Activity maybe restricted to oxidase in haem-Cu_B family	(Borisov et al. 2004)
Others	Hybrid cluster protein	*E. coli*	Hydroxylamine reductase?	Up-regulated by nitrosating agents	(Filenko et al. 2005; Wolfe et al. 2002)
	Cytochrome c	*Rhodobacter capsulatus*	NO reductase, forming N_2O	CycP mutants are hypersensitive to nitrosothiols and NO	(Cross et al. 2001)

	AhpC (peroxiredoxins)	*Salmonella, Mycobacterium tuberculosis*	Confers enhanced resistance to peroxynitrite and nitrosating agents	Mechanism unknown	(Chen et al. 1998; Master et al. 2002)

Note: Nrf$^-$ strains mean strains that do not have cytochrome c nitrite reductase activity.

2.5.2 Scavenger molecules

Low molecular weight thiols such as glutathione (GSH) and homocysteine (HC) have important scavenging roles in microbes to remove free radicals. Mutant *Salmonella* strains incapable of synthesising GSH and HC are hypersusceptible to inhibition by S-nitrosothiols, peroxynitirte and NO (De Groote et al. 1996). It is also reported that alginate, produced by the mucoid *P. aeruginosa*, might favour the survival of mucoid forms of *P. aeruginosa* by scavenging the free radicals (Simpson et al. 1989).

2.5.3 Sequestration of iron

Iron sequestration is another important mechanism to resist RNIs stress. Free iron can interact with NO• to form iron complexes, which might potentiate nitrosative stress (Lobysheva et al. 1999). Several studies demonstrate that bacteria would avoid toxic RNIs by compartmentalizing their iron stores as well as by controlling the availability of iron uptake. Ferritin and DNA-binding proteins from starved cells can sequester iron atoms to prevent their participation in the formation of iron-dependent toxic reactive oxygen species (Zhao et al. 2002).

2.5.4 Regulators in antioxidant defence

Microbial resistance to RNIs overlaps considerably with cellular antioxidant defence. There are many regulators that are reported to be involved in cellular responses to reactive oxygen species (ROS). For example, redox-sensitive transcriptional activator (SoxR) and hydrogen peroxide-inducible gene activator (OxyR) in *E. coli* are implicated to confer resistance to NO-related antimicrobial activity in bacterial cells. SoxR, which consists of *zwf* (glucose-6-phosphate dehydrogenase), *sodA* (manganese superoxide dismutase) and *nfo* (endonuclease IV) genes, may contribute to antinitrosative defences by generating reducing equivalents, reducing intracellular peroxynitrite formation and repairing DNA damage respectively (Fang 1997). OxyR is supposed to confer resistance to S-nitrosothiols in *E. coli* (Hausladen et al. 1996). However, *S. typhimurium* carrying mutations in *soxS* or *oxyR* retains virulence in mice, suggesting that other important regulators conferring NO resistance are yet to be identified.

2.5.5 DNA repair systems in bacteria

Cellular DNA repair systems that repair oxidative injury appear to be similarly involved in repairing nitrosative injury. RecBCD exonuclease, required for most homologous recombinational DNA repair confers resistance to both hydrogen peroxide (Buchmeier et al. 1993) and NO donor

compounds (De Groote and Fang 1995). Glucose-6-phosphate dehydrogenase, a major source of reducing equivalents (NADPH), regenerates thiols and other antioxidants in defence against both reactive oxygen and nitrogen species (Nunoshiba et al. 1995). Cu, Zn-superoxide dismutase may protect against both oxidative and nitrosative stress by removing periplasmic superoxide and limiting peroxynitrite formation (De Groote et al. 1997).

Salmonella can develop resistance to S-nitrosothiols by acquiring mutations which inactivate specific peptide transport systems (De Groote and Fang 1995) However, it is quite difficult to establish whether such systems are involved in resistance in vivo because the specific S-nitrosothiol responsible for antimicrobial activity are unknown. Pyocyanin, a phenazine pigment produced by *P. aeruginosa*, is reported to be nitrosylated by NO in vitro, but the pathophysiological significance of this action is uncertain (Warren et al. 1990). In summary, RNIs may have broad cell targets and cause multiple diverse resistant effects. Therefore there must be multiple cell resistance pathways. All these can afford us the fundamental understanding of possible bacterial resistance towards FNA.

Chapter 3 Thesis Overview

This chapter provides an overview of the research work undertaken in this thesis. First, the research objectives are discussed. Then the key research methods and analytical techniques are briefly described. Finally, the major outcomes and key results are outlined and discussed.

3.1 Research objectives

3.1.1 Examining the antimicrobial effects of FNA on pure culture *Pseudomonas aeruginosa* PAO1

Recently, FNA is demonstrated to be the true metabolic inhibitor behind the often observed "nitrite inhibition" (Vadivelu et al. 2006b). The antimicrobial effects of FNA are found to be concentration-related and different microbial populations have the differential tolerance to FNA. This is not only observed between bacterial species (Vadivelu et al. 2006a; Vadivelu et al. 2006b) but also in intraspecies strains (Rhoades and Orme 1997). However, it is currently unknown whether there is a clear concentration threshold that determines the bacteriostatic or bactericidal effects, in terms of metabolic activity and cell viability, of FNA on microbes.

This study investigates the potential concentration-related effects of FNA on *P. aeruginosa* PAO1 under denitrifying anaerobic conditions. Anaerobic respiratory growth conditions were chosen to detect the antimicrobial effects of FNA on *P. aeruginosa* PAO1, as these conditions are relevant to the organisms in various natural environments. To this end, FNA concentrations of 0.01, 0.05, 0.1, 0.15, 0.2, 1.0, and 5.0 mg N/L was added to the planktonic *P. aeruginosa* PAO1 cultures grown in serum bottles when they were in early log phase. During the incubation, the culture optical density at 600 nm (OD_{600}), medium pH value, the levels of glycerol, nitrate, and nitrite were determined. The viable cells before and after FNA treatment were examined to assess the bactericidal effect of FNA on *P. aeruginosa* PAO1. The regrowth of cultures following the removal of FNA was studied to detect the possible carryover of detrimental effects on cell activities.

3.1.2 Determining the responses of *Pseudomonas aeruginosa* PAO1 to inhibitory levels of FNA

FNA has recently been demonstrated as an antimicrobial agent on a range of microorganisms, especially in wastewater treatment systems. Consequently, there is a great potential to use FNA to control the growth and activities of unwanted microbes in various industrial and medical applications (Wang et al. 2013a; Wang et al. 2013b; Weller et al. 2001). However, the antimicrobial mechanism of FNA is largely unknown.

In order to better apply FNA as an antimicrobial agent in wastewater treatment, a systematic understanding of the whole picture regarding the fundamental mechanisms of susceptibility, tolerance, and resistance to exposure inhibitory level of FNA (0.1 mg N/L) on *P. aeruginosa* PAO1 cultures, a model denitrifier in wastewater treatment, under anaerobic denitrifying conditions was examined. The global up and down regulated gene profiles were detected by whole genome RNA sequencing. Selected physiological responses including viable cell percentages, cellular redox status, intracellular ATP levels, and cellular thiols were examined to further reveal the mechanism of antimicrobial effect of FNA. The responses of *P. aeruginosa* PAO1 to FNA was achieved by combining the global activated and suppressed gene profiles and selected physiological responses.

3.1.3 Unravelling the antimicrobial effect of FNA on *Desulfovibrio vulgaris* Hildenborough

Hydrogen sulfide produced by SRB in sewers results in serious deterioration of sewer assets that requires very costly and demanding rehabilitation efforts (Jiang et al. 2011; Pikaar et al. 2014). Consequently there is great interest to efficiently control SRB and minimise hydrogen sulfide production in sewers. FNA was recently demonstrated as a promising antimicrobial agent to alleviate hydrogen sulfide production in sewers. However, knowledge of the antimicrobial mechanisms of FNA is largely unknown. *Desulfovibrio* species are reported to be prevalent SRB in sewers (Sun et al. 2014) and are likely important for H_2S production in sewage. Therefore, *D. vulgaris* Hildenbogough was selected in this study.

This study aims to achieve a comprehensive and systematic understanding of the mechanism of the antimicrobial effect of FNA on *D. vulgaris* Hildenborough in order to better guide the application of FNA in sewers to control the activity of SRB. *D. vulgaris* Hildenborough utilizes sulfate as the electron acceptor and lactate as the electron donor with sulfide and acetate as the end products respectively (Heidelberg et al. 2004). The substrate (lactate and sulfate) transformation and product production (hydrogen sulfide and acetate) were monitored in the presence of four different FNA concentrations (0, 1, 4, and 8 μg N/L) to examine the antimicrobial effect of FNA on *D. vulgaris* Hildenborough in terms of growth metabolic activities. Four physiological assays (live cell percentage, cellular thiol levels, cellular redox status and cellular ATP levels in the presence and absence of FNA) were conducted in four different FNA levels to further uncover the FNA effect on the cellular physiology of *D. vulgaris* Hildenborough. Additionally, whole genome RNA sequencing was carried out on *D. vulgaris* Hildenborough cultures in the presence or absence of

inhibitory levels of FNA (4.0 μg N/L). The antimicrobial effect of FNA on *D. vulgairs* Hildenborough and the culture responses to FNA was achieved by combining examinations of growth, physiological and gene expression responses.

3.1.4 Comparative proteomic analysis of *Desulfovibrio vulgaris* Hildenborough in response to sustainable antimicrobial agent FNA in wastewater treatment

While the above transcriptome analysis allows us to examine the changing caused by FNA in the RNA level (Wang et al. 2009), not all the differentially expressed transcripts end up in functional proteins due to post-transcriptional modification. Quantitative proteomics can explore the metabolic and physiological details of microbes in response to antimicrobial agents at functional protein levels. Sequential window acquisition of all theoretical mass spectra (SWATH-MS) is a recently developed approach that provides extensive label-free quantitation of the measurable peptide ions in a sample (Vowinckel et al. 2013), which makes the quantitative proteomics possible.

The objective of this research question is to uncover the responses of *D. vulgaris* Hildenborough to different levels of FNA over different incubation time periods by quantitative proteomics analysis. The proteome of *D. vulgaris* Hildenborough in the presence of different levels of FNA (0, 1, 4 and 8 μg N/L) with different treatment time periods (2, 8, and 12 hours after FNA addition) was compared to detect protein expression differences, thereby further detecting the protein dynamics and assessing the key determinant in response to FNA.

3.2 Research methods

3.2.1 Culturing and media

Culturing Pseudomonas aeruginosa PAO1

P. aeruginosa PAO1 (DSM No: 22644) was obtained from the Deutsche Sammlung von Mikroorganismen und Zellkulturen GmbH (DSMZ), Germany. Glycerol modified M9 (GLYM9) medium was established and used to cultivate the bacterium in anaerobic conditions (Webb et al. 2003). This medium contained 0.2 M phosphate buffer, 9 mM NaCl, 38 mM NH_4Cl, 2 mM $MgSO_4 \cdot 3H_2O$, 100 μM $CaCl_2 \cdot 2H_2O$, 10 g/L glycerol, 0.2 g/L yeast extract and 30 mM of $NaNO_3$ with the pH adjusted to 6.3±0.3. *P. aeruginosa* PAO1 was activated according to the supplier (DSMZ) and grown on tryptic soy agar plates at 30 ºC for 26 hours. One colony was then selected and transferred to tryptic soy broth medium and incubated shaken at 150 rpm at 30 ºC for another 26 hours. Afterwards, 5 mL of bacterial suspension was transferred into the serum bottles

containing 150 mL of sterile anaerobic GLYM9 medium in an anaerobic chamber. The anaerobic GLYM9 medium was made by aerating each serum bottle with nitrogen gas for 30 minutes before capping with a butyl rubber stopper. After 26 hours' incubation, OD_{600} was measured and then adjusted to 0.5. 10 mL of this inoculum standard was transferred into 150 mL of sterile anaerobic GLYM9 medium in serum bottles in an anaerobic chamber to finally achieve the anaerobic condition. *P. aeruginosa* PAO1 cultures were then incubated at 30 ˚C while shaken at 150 rpm for the use of batch experiments.

Culturing Desulfovibrio vulgaris Hildenborough

D. vulgaris Hildenborough (ATCC 29579) was generously provided by Professor Jizhong Zhou and Dr Aifen Zhou from Institute for Environmental Genomics, University of Oklahoma. For all the performed experiments, a defined lactate sulfate medium (LS4D medium) (Zhou et al. 2010a) was used to cultivate the culture. The anaerobic LS4D medium was prepared by aerating each serum bottle with nitrogen gas for 30 min before capping with butyl rubber stopper for autoclave. 1.5 mL culture glycerol stock was inoculated as the inoculum to the serum bottles containing 140 mL medium and cultivated at 37°C for 48 h to achieve the early stationary phase of growth (OD_{600} 0.9 to 1.0). OD_{600} of the culture was then adjusted to 0.5 before 10 mL of this culture (standard inoculum) was transferred into 140 mL of autoclaved anaerobic LS4D medium in serum bottles inside the anaerobic chamber. The cultures were then incubated at 30°C without shaking for the use of batch experiment.

Since *D. vulgaris* cultures prepared and inoculated for experiments are not from a single colony as described in the Material & Methods part in the thesis, thus sanger sequencing was performed during the batch experimental period to make sure that the cultures were not contaminated. Sequences of the 16S rRNA genes matched the reference genes of *P. aeruginosa* PAO1 and *D. vulgaris* Hildenborough and confirmed the purity of the cultures."

3.2.2 Batch experimental setup

FNA treatment on Pseudomonas aeruginosa PAO1

When the *P. aeruginosa* PAO1 cultures were in early log phase of growth, 11h after inoculation, different amounts of nitrite were added to achieve the different FNA ($\mathrm{FNA\,(as\,HNO_2 - N)} = \frac{\mathrm{NO_2{-}N}}{\mathrm{K_a \times 10^{pH}}}$, $\mathrm{K_a} = \mathrm{e}^{-2300/(270+\mathrm{T(^{\circ}C)})}$) starting concentrations. Control cultures (no added FNA) had the

same volume of sterilized Milli-Q water added. Experiments for the control and FNA treated cultures were conducted in triplicates.

FNA treatment of Desulfovibrio vulgaris Hildenborough

Twenty-six h after the standard inoculation at 30°C when the culture was in early log phase (OD_{600} around 0.3), nitrite was added to serum bottles to achieve the starting FNA concentrations of 0, 1.0, 4.0, and 8.0 μg N/L. Each FNA concentration was performed in triplicate.

3.2.3 Chemical analysis

OD_{600}, pH

Cultures OD_{600} and pH were monitored with a Cary 50 bio UV visible spectrophotometer (Varian, Australia) and a labCHEM-pH Benchtop pH - mV - Temperature Meter, respectively.

Ammonia, nitrate, nitrite

Liquid samples were filtered through disposable Millipore filter units (0.22 μm pore size) after being taken from the serum bottles. The ammonia, nitrate, and nitrite concentrations were analysed using a Lachat QuikChem8000 Flow Injection Analyzer (Lachat Instrument, Milwaukee) (FIA).

Glycerol, lactate, volatile fatty acids (VFAs)

Glycerol levels were determined in filtered samples using an external standard by high-performance liquid chromatography (HPLC). This was a Shimadzu LC equipped with a Phenomenex Rezex ROA column (300×7.8 nm), specialized for organic acid analysis, and a Shimadzu refractive index detector (RID-10A). For the analysis of lactate and VFAs such as acetate, lactate, formic acid, glucose, 1, 3-propanediol, ethanol and pyruvate, 1.0 mL sample was filtered (0.22 μm, Merck Millipore, USA) and applied to a HPLC unit fitted with an Agilent Hi-Plex H 300 mm × 7.8 mm column. High purity helium was used as carrier gas at a constant pressure of 103 kPa. For both analyses, the mobile phase was 0.008 N H_2SO_4 with a flow rate of 0.4 mL/min.

Sulfide, sulfite, thiosulfate, and sulfate

The concentrations of sulfur species (sulfide, sulfite, thiosulfate, and sulfate) were determined in culture samples by ion chromatography (IC). For this 1.5 mL samples were filtered (0.22 μm, Merck Millipore, USA) into 2 mL vials containing 0.5 mL of sulfide anti-oxidant buffer (SAOB), a

solution to preserve the samples against sulfide oxidation (73). Samples were then analysed within 24 h using IC (Dionex ICS-2000).

3.2.4 Physiological assays detection

Various assays were conducted on *P. aeruginosa* PAO1 and *D. vulgaris* Hildenborough cultures taken at different times of growth in the absence and presence of FNA.LIVE/DEAD staining was conducted on the cells as described in the manufacturers instructions (BacLight Bacterial Viability Kit, Molecular Probes, L7012). The LIVE/DEAD ratio of cells was then quantified by applying 500 µL of the stained samples to a FACSAria™ II (BD Biosciences, San Jose, USA) flow cytometer. To determine the cellular redox status 500 µL samples of cultured cells were stained using the RedoxSensor™ Green reagent provided in the BacLight RedoxSensor Green Vitality Kit (Life Technologies, B34954) as per the manufacturers instructions. The fluorescence signal of the stained cultures was quantified using the FACSAria™ II type flow cytometer and as described in the manufacturers protocol. Cellular ATP levels were measured in 500 µL samples using the BacTiter-Glo™ Microbial Cell Viability Assay (Promega Corporation, G8231) as described by the manufacturers instructions. Intracellular pH was determined using the fluorescent probes cFSE (Molecular Probes, C1157) as previously described (D et al. 1998). Cellular thiol levels were determined on 200 µL samples using the Thiol and Sulfide Quantitation Kit (Molecular Probes, T-6060) as instructed by the manufacturer.

3.2.5 Transcriptomic analysis

RNA extraction and sequencing

Samples were taken for RNA extraction from the triplicate cultures of *P. aeruginosa* PAO1 and *D. vulgaris* Hildenborough after 13h incubation, that is 2h after FNA addition. 5 mL of the bacterial suspension from each serum bottle was centrifuged at 13,000 x g for 2 minutes, the supernatant was discarded and the pellets were immediately frozen in liquid nitrogen before storing at -80ºC for later RNA extraction. Total RNA extraction was performed using the QIAGEN miRNeasy Mini Kit (Catalog number: 217004) according to the manufacturer's instructions except adding an extra bead-beating step to ensure the complete lysis of the bacterial cells. Strand-specific cDNA library construction and Illumina paired-end sequencing (HiSeq 2000, Illumina Inc., San Diego, CA, USA) was performed on the extracted RNA (Macrogen, Seoul, Korea).

RNA-seq data processing and differentially expressed gene analysis

The raw sequence reads were obtained for the triplicate cultures and the sequences were progressively trimmed at the 3'-ends until a quality value ≥ 20 was reached. The ambiguous characters (Ns/Xs) and poly-As/Ts longer than six bases at either end of the reads were then removed. Reads containing at least 85% bases with quality value > 20 were kept. The 3'-end residual adapter and primer sequences were removed and then one base from the 5'-end and three from the 3'-end were trimmed. The NGS QC Toolkit (v2.3.3) (Patel and Jain 2012) was used for all these sequence-modifying processes. The resulting clean reads no shorter than 75 bp were used for downstream analyses.

The cleaned sequence reads for each sample were aligned to the *P. aeruginosa* PAO1 reference genome (NC_002516) and *D. vulgaris* Hildenborough reference genome (NC_002937) using SeqAlto (version 0.5) (Mu et al. 2012). Strand-specific coverage for each gene was calculated and differential expression analysis was conducted using the cuffdiff command in Cufflinks (version 2.2.1) on the triplicate samples (Trapnell et al. 2012). Statistical analyses and visualization were conducted using the cummeRbund package in R (http://compbio.mit.edu/cummeRbund/). Gene expression was calculated as reads per kilobase of a gene per million mapped reads (RPKM), a normalized value derived from the frequency of detection and the length of a given gene (Trapnell et al. 2012). For *P. aeruginosa* PAO1, differences in fold-change values were calculated between control and FNA-treated samples (0.1 mg N/L) by determining the $\log_2$ fold-change (LFC) of the averaged RPKM values determined from the replicate experiments run on two separate occasions. Genes with LFC of ≥2.5 and ≤-2.5 with q value less than 0.01 were defined as the "highly" differentially expressed genes. Genes with LFC of <2.5 but ≥1.0 and ≤-1.0 but >-2.5 with q value less than 0.01 were defined as the "moderately" differentially expressed genes. For *D. vulgaris* Hildenborough, differences in fold-change values were also calculated between control and FNA-treated samples (4.0 μg N/L) by determining LFC of the averaged RPKM values of two triplicate experiments. A stringency cut-off of LFC ≥ 1 or ≤ -1 with q value less than 0.05 was used to identify the significantly differentially expressed genes. All other genes are considered as no change in response to FNA. The q value is the allowed false discovery rate (FDR) such that for q<0.01 there is less than one false positive in a total of one hundred significantly expressed gene transcripts. This value is determined by the characteristics of the transcriptional profile of the samples. Annotation of the differentially expressed genes was based on the online-curated pathway tools genome database PseudoCyc (http://www.pseudomonas.com). The program Circos was used to visualize expression and determine the RPKM values for each gene (Krzywinski et al. 2009).

3.2.6 Proteomic analysis

Protein extraction and digestion

Ten mL of the *D. vulgaris* Hildenborough suspension was taken from the cultures and centrifuged at 12,000 rpm for 5 minutes, the supernatant was discarded and the cell pellets were immediately frozen in liquid nitrogen before storing at -80ºC prior to total protein extraction. Protein extractions were performed on these cell pellets. Each sample was dissolved in 1 mL extraction buffer (77 mg dithiothreitol & 1 tablet of complete Protease Inhibitor (Roche) into 10 ml B-PER II Bacterial Protein Extraction Reagent (Thermo Scientific, 78260)) and subjected to three freeze/thaw cycles by placing samples into liquid nitrogen and thawing at 4 ˚C. Cell debris was removed by centrifugation at 14,000 rpm for 15 min at 4 ˚C. Proteins were precipitated by adding trichloroacetic acid (13% v/v final concentration) and incubated overnight at 4 ˚C. Then proteins were collected through centrifugation at 14,000 rpm for 15 min at 4 ˚C before washing in cold 80% acetone twice, dried for no more than 5 minutes and resuspended in suspension buffer (8 mM Urea, 50mM ammonium bicarbonate). Total resuspended protein was then quantified by 2D Quant (GE Healthcare).

The extracted protein samples were then reduced and alkylated by adding dithiothreitol (5 mM final concentration) for 30 min at 56 ˚C, cooled to room temperature, then treated with iodoacetamide (25 mM final concentration) and incubated at room temperate in the dark for 30 min. The same volume of dithiolthreitol was added again to quench the excess iodoacetamide. Protein samples were diluted with 50 mM ammonium bicarbonate buffer to reduce urea concentration to less than 2 M, and digested 6 hours with trypsin (Promega) at an enzyme to protein ratio of 1:100 at 37˚C. Following on this, the protein samples were digested overnight again with trypsin using the same enzyme to protein ratio at 37˚C. C18 Zip-tip (Millipore) clean-up was performed on the digested proteins (Kappler and Nouwens 2013). Amount of protein sample was normalised to 1 µg for each and used for SWATH-MS analysis in triplicate. In addition, 5 µg aliquots of each triplicate samples were taken and pooled for mass spectrometry analysis, which was performed in duplicate.

Mass spectrometry analysis

Peptides were directly analysed on a Triple-Tof 5600 instrument (ABSciex) equipped with a Nanospray III interface. Gas 1 was set to 10 psi, curtain gas to 30 psi, ion spray floating voltage 2700 V. Samples were scanned across m/z 350-1800 for 0.5 sec followed by the information

dependent acquisition (IDA) on high sensitivity mode of 20 peptides with intensity greater than 100 counts across m/z 40-1800 for 0.05 sec. Collision energy was set to 40 +/- 15 V. SWATH analyses were scanned across m/z 350-1800 for 0.5 sec followed by high sensitivity IDA mode, using 26 Da (1 Da for window overlap) isolation windows for 0.1 sec, across m/z 400-1250. Collision energy for SWATH samples was automatically assigned based on m/z mass windows by Analyst software. Mass spectrometry (MS) data from IDA were combined and searched using ProteinPilot software (ABSciex, Forster City CA). The search setting for enzyme digestion was set to Trypsin and alkylation was set to iodoacetamide. The searched databases were *D. vugaris* (received from NCBI on the 28th of January 2016) with the search effort set to thorough and cut off applied > 0.05 (10%). The false detection rate was determined using proteomics system performance evaluation pipeline software (PSPEP), an add-on to ProteinPilot, which uses a decoy database constructed by reversing all the protein sequences in the searched database.

SWATH-MS data analysis

The library acquired by IDA library and SWATH-MS data were loaded into PeakView (version 1.2) software for processing using the SWATH micro processing script using a confidence level of 99, the number of peptides set at 5 and the number of transitions used set at 3. A minimum of 2 peptide and 3 transitions was used for quantitative analysis. The R- based program MSstats (Choi et al. 2014) was used for statistical analysis of the spectral data. The "ion" data file exported from the Peakview software was loaded into MSstats as a .csv file using the following command:

FNADvHWhole.superhirn <- read.csv("LabelFree_LCMS_Proteins_Raw_whole.csv")

The data file was then "pre-processed" were $\log_2$ transformation and normalisation are applied using the command:

FNADvHWhole.TMP <- dataProcess (raw=FNADvHWhole.superhirn, fillIncompleteRows = TRUE, normalization = "equalizeMedians", summaryMethod = "TMP", censoredInt = "NA", cutoffCensored = "minFeatureNRun", MBimpute = TRUE)

A comparison matrix was then created using the command:

(With different incubation time period, the following pair wise comparison was done for *D. vulgaris* Hildenborough as an expample)

comparison1<- matrix(c(1, 0, 0, 0, 0, 0, 0, 0, 0, -1, 0, 0), nrow=1)

comparison2<- matrix(c(0, 0, 0, 1, 0, 0, 0, 0, 0, -1, 0, 0), nrow=1)

comparison3<- matrix(c(0, 0, 0, 0, 0, 0, 1, 0, 0, -1, 0, 0), nrow=1)

comparison_12h<-rbind(comparison1,comparison2, comparison3)

row.names(comparison) <- c("1ug_12h-C_12h", "4ug_12h-C_12h","8ug_12h-C_12h")

comparison_12h

(With different FNA concentration added, the following pair wise comparison was done for *D. vulgaris* Hildenborough as an expample)

comparison10<- matrix(c(1, -1, 0, 0, 0, 0, 0, 0, 0, 0, 0, 0), nrow=1)

comparison11<- matrix(c(0, -1, 1, 0, 0, 0, 0, 0, 0, 0, 0, 0), nrow=1)

comparison_1µg <- rbind(comparison10,comparison11)

row.names(comparison) <- c("1ug_12h-1ug_2h", "1ug_8h-1ug_2h")

comparison_1µg

The comparison was then performed using the command:

FNADvHWhole.comparisons12h <- groupComparison(contrast.matrix = comparison, data = FNADvHWhole.TMP)

FNADvHWhole_1ug <- groupComparison(contrast.matrix = comparison, data = FNADvHWhole.TMP)

The final result was displayed and written using the command:

SignificantProteins <- with (FNADvHWhole.comparisons12h, ComparisonResult[ComparisonResult$adj.pvalue < 0.05,])

write.table(FNADvHWhole.comparisons12h$ComparisonResult, 'diff_protein.12h.txt', sep = '\t', row.names = F, col.names = T, quote = F)

SignificantProteins <- with (FNADvHWhole _1ug, ComparisonResult[ComparisonResult$adj.pvalue < 0.05,])

write.table(FNADvHWhole _1ug$ComparisonResult, 'diff_protein_1ug.txt', sep = '\t', row.names = F, col.names = T, quote = F)

Pathway Tools (Karp et al. 2010) was used for metabolic pathway reconstruction of the identified proteins. A stringency cut-off of LFC $\geqslant$ 1 or $\leqslant$ -1 with q value less than 0.001 was used to identify the significantly differentially expressed proteins. The mass spectrometry proteomics data have been deposited to the ProteomeXchange Consortium (http://proteomecentral.proteomexchange.org) via the PRIDE partner repository (Vizcaíno et al. 2013) with the dataset identifier (PXD004475).

3.3 Results and Discussion

3.3.1 Antimicrobial effects of FNA on *Pseudomonas aeruginosa* PAO1 is concentration-determined and population-specific

This section summarises the findings of the work described in Appendix A which is published in Applied Microbiology and Biotechnolgy.

There is opportunity to use FNA as a bacteriostatic or bactericidal agent to control the growth and activities of microbes for various industrial and medical applications (Wang et al. 2013a; Wang et al. 2013b; Weller et al. 2001). However, it is currently unknown whether there is a clear concentration threshold that determines the bacteriostatic or bactericidal effects, in terms of metabolic activity and cell viability, of FNA on microbes. P*seudomonas aeruginosa* is an important model organism with respect to its significant roles in the environment as a ubiquitous denitrifier (Morita et al. 2014; Stover et al. 2000). It is a facultative anaerobic bacterium that forms biofilms, which are essential for its persistence and resistance to various antimicrobial agents (Filiatrault et al. 2006; Schurek K.N. et al., 2012). This study demonstrates the antimicrobial effect of FNA on *P. aeruginosa* PAO1 is concentration-determined and population-specific under anaerobic denitrifying conditions.

1) Concentration-determined antimicrobial effects of FNA on cell growth and population differential disruption of cell membrane integrity by FNA

The growth of *P. aeruginosa* PAO1 in batch cultures treated with different levels of FNA (mg N/L) was determined (Figure 5). During the 64 hours incubation, similar growth patterns were observed for *P. aeruginosa* PAO1 in the control cultures (no FNA addition) and in the cultures exposed to low

starting FNA concentrations of 0.01 and 0.05 mg N/L (Figure 5). FNA induced inhibition of growth was evident at FNA concentrations higher than 0.05 mg N/L. The length of the inhibition time period, before the culture regrowth was detected, increased with increasing starting concentrations from 0.05 to 1.0 mg N/L. The higher the starting FNA concentration applied, the longer the inhibition time lasted (Figure 5). After the inhibition period and within the total 64 hours incubation, cultures treated with 0.15 mg N/L or lower FNA starting concentrations eventually grew to reach cell levels similar to the control cultures (Figure 5).

To determine whether there is a clear concentration threshold to distinguish bacteriostatic and bactericidal effects of FNA upon *P. aeruginosa* PAO1, cell viability was measured in different FNA levels by LIVE/DEAD staining using flow cytometer as detailed in appendix A. Prior to FNA treatment the *P. aeruginosa* PAO1 cultures consistently contained around 90% viable cells (Figure 6). The control cultures (no FNA addition) maintained this level up to the end of the exponential growth. In contrast, there were substantial decreases in the proportion of live cells immediately upon the addition of FNA (Figure 6). *P. aeruginosa* PAO1 cultures were almost completely killed with FNA concentration of 5.0 mg N/L (Figure 6). This result does not support the previous assumption that there is a clear concentration threshold between the bacteriostatic and bactericidal effects of FNA (Jiang et al. 2011; Pijuan et al. 2010; Vadivelu et al. 2006a; Vadivelu et al. 2006b; Ye et al. 2010b; Zhou et al. 2007; Zhou et al. 2008). In contrast, we show here that, from low to high FNA levels, cell killing occurred in a subpopulation of *P. aeruginosa* PAO1 cells, while another subpopulation was inhibited in growth but still active in respiration (Figure 6).

In this experiment, the surviving subpopulations of *P. aeruginosa* may be explained by either phenotypic or genotypic variations in the presence of FNA. However, the nature of mode of action of FNA on bacteria which is multi-targeted, makes it hard for the bacteria to form adaptation by mutation. Therefore, this needs further investigation since we have no evidence of genotype variation.

2) FNA inhibition on culture growth recoverability

The recoverability of *P. aeruginosa* PAO1 after being treated with different levels of FNA was determined (Figure 7). To study this cultures were exposed to FNA and during growth inhibition periods the FNA was removed and the extent of regrowth was then detected in fresh media. The experimental details of culture growth recovery after FNA treatment can be found in Appendix A. It

was seen that with the higher FNA starting concentrations, slower culture regrowth occurred (Figure 7a). At relatively low starting FNA concentrations of 0.05 and 0.1 mg HNO_2- N/L, the regrowth was comparable to that of the control. However, in starting FNA concentration of 1.0 mg N/L, culture regrowth was delayed by 53 hours (Figure 7a). No recovery was observed for the culture with starting FNA concentration of 5.0 mg N/L, suggesting complete killing of the cells at this high level of FNA occurred (Figure 6). Therefore, it was evident that the recovery times of the cultures with high FNA concentrations were much greater than those of the untreated cells, even though these had equivalent levels of live cells (Figure 7b). These extended recovery times were about 10 hours for a starting FNA concentration of 0.1 mg N/L and about 60 hours for a starting FNA concentration of 1.0 mg N/L (Figure 7b).

3) Discussion

A significantly lower FNA threshold concentration for cell growth (anabolism) inhibition was detected in comparison to catabolic inhibition (i.e. 0.1 versus 1.0 mg N/L). This is consistent with previous studies upon FNA treatment of enriched cultures (Vadivelu et al. 2006a; Vadivelu et al. 2006b) and cultures of P*seudomonas fluorescens* (Almeida et al. 1995). For instance, Vadivelu et al. (2006a) reported that FNA initiated inhibition of the anabolic processes of *Nitrobacter* (NOB) at approximately 0.011 mg N/L and completely stopped biomass synthesis at a concentration of approximately 0.023 mg N/L, while up to 0.05 mg N/L did not show any inhibitory effect on the catabolic processes. In this study, an immediate bactericidal effect on *P. aeruginosa* PAO1 cells was detected even at low FNA concentrations. At the FNA concentration of 0.05 mg N/L, the live cell percentage decreased from 90% to about 70% during the inhibitory period (Figure 6). In contrast, 30% of the cells were still alive after 53 hours exposure to 1.0 mg N/L FNA. This not only indicates the high tolerance of *P. aeruginosa* PAO1 to FNA but this also contradicts the existence of a uniform bactericidal threshold of FNA within a specific bacterial strain. The results aforementioned reveal the concentration-related and population-specific antimicrobial effects of FNA to *P. aeruginosa* PAO1 culture.

Heterogeneity could either be phenotypic or genetic based on whether the bacterial genome was mutated when exposed to antimicrobial agents. Bacterial heterogeneity formation is often controlled by non-mutational epigenetic mechanisms that generate distinct morphological and physiological properties by differing gene expression without altering the DNA sequence (Casadesús and Low 2013). However, the underlying mechanisms are diverse, ranging from relatively simple feedback

loops such as stochastic events to complex self-perpetuating DNA methylation patterns (Casadesús and Low 2013). Relevant examples of phenotypic heterogeneity in natural environments are the formation of "persisters", which are dormant bacterial cells resistant to antibiotics/antimicrobial agents. "Persisters" are considered as the old cells, and they are seen neither grow nor die in the presence of antimicrobial agents, and thus exhibit tolerance (Keren et al. 2004). "Persisters" may also be explained by genotypic variations in the presence of FNA. However, the nature of mode of action of FNA on bacteria which is multi-targeted, makes it hard for the bacteria to develop genetic based changes although this still needs further investigation. In summary, heterogeneity could be age related, and the aged cells could exhibit ability to survive killing by antimicrobial agents (Avery 2006).

It would be better to confirm the cell lysis by microscopy. However, the cell lysis has already been measured to some degree by Live/Dead Staining in which cells with compromised membrane was determined as the dead cells. Phage detection in the presence of FNA was conducted as well, however no positive results were detected and no constructive conclusion was generated from the experiment.

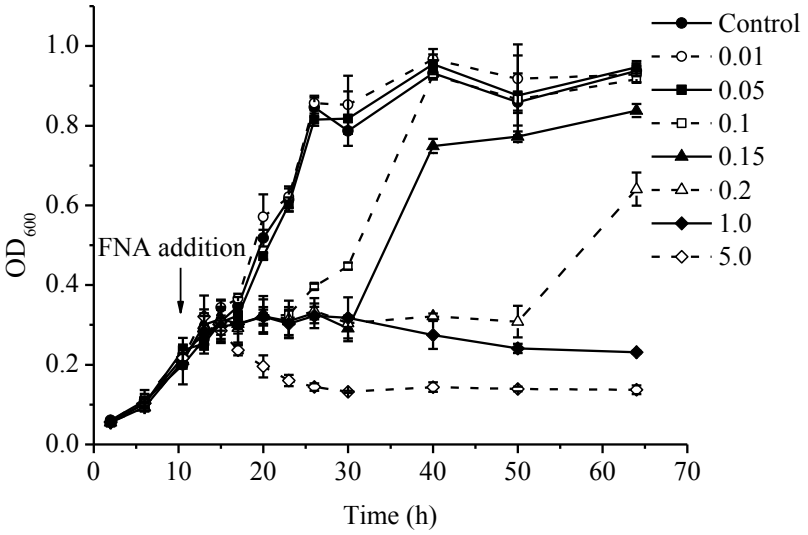

Figure 5. Growth profiles of *P. aeruginosa* PAO1 batch cultures treated with different levels of FNA (mg N/L). FNA was added 11 hours into the incubation period. The control culture had no FNA addition. Error bars show the standard deviation of the triplicate control samples.

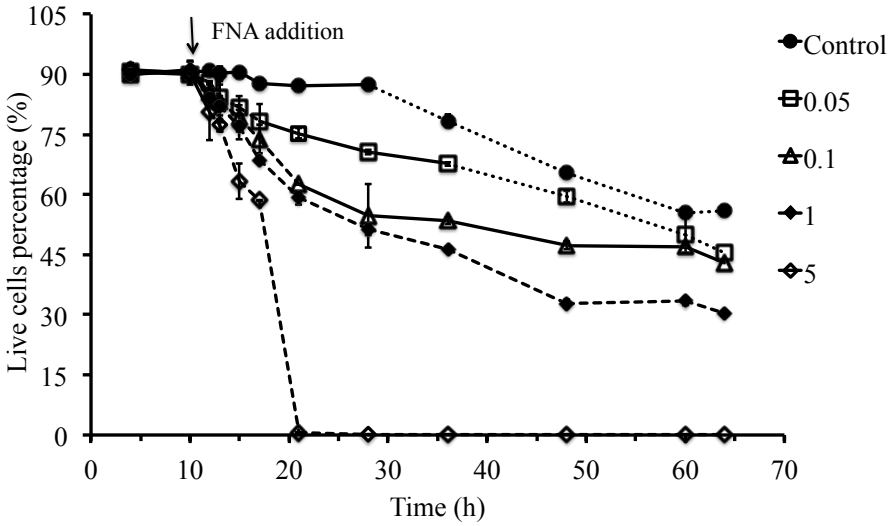

Figure 6. Cell viability of *P. aeruginosa* PAO1 cultures treated with different levels of FNA (mg N/L) as determined by the LIVE/DEAD BacLight stain. Dashed lines represent periods when the culture growth was inhibited by FNA. Solid lines after FNA addition represent the period of exponential growth. Dot lines represent the stationary growth phase after adding FNA. Error bars were determined for all samples and show the standard deviation of triplicate analyses.

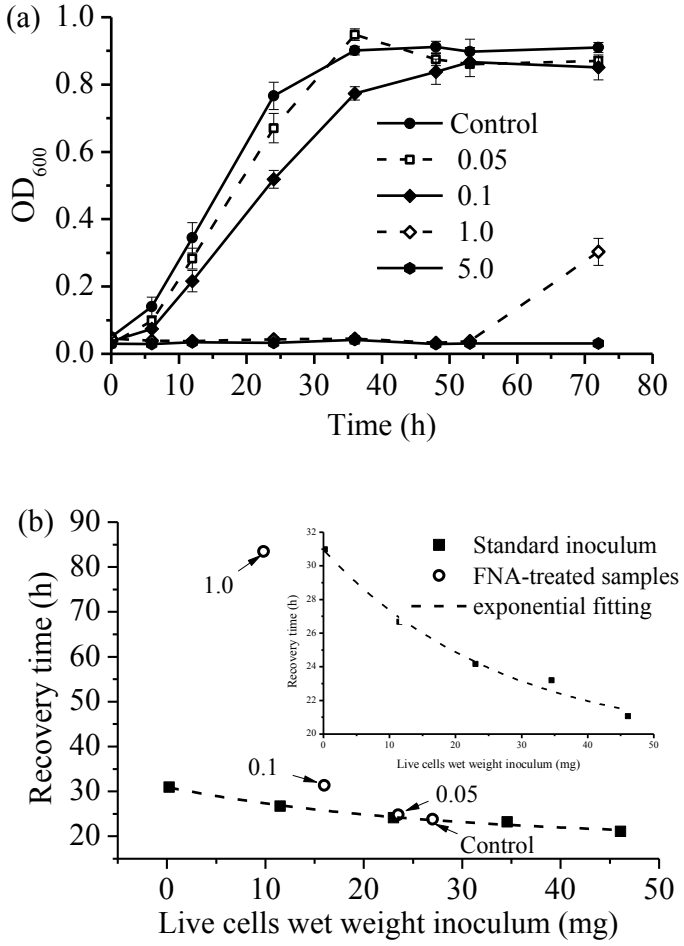

Figure 7. FNA effects on growth recoverability of *P. aeruginosa* PAO1 cultures. (a) Growth recovery of cultures after being treated with different FNA starting levels shown in the key (mg N/L). Error bars indicate the standard deviation of the triplicate samples. (b) The carryover effects of FNA on the growth recoverability of live cells. The embedded graph shows the standard inoculum curve over a smaller time scale. Recovery time is the time needed for cultures to achieve OD_{600} 0.5. Number with arrows is the FNA concentration.

3.3.2 Determining multiple responses of *Pseudomonas aeruginosa* PAO1 to antimicrobial agent FNA

This section summarises the findings of the work described in Appendix B which is published in Environmental Science & Technology.

There is strong potential to apply FNA, the protonated form of nitrite (HNO_2), as an antimicrobial agent. Recently, while using nitrite as an antimicrobial agent, FNA was discovered to be the true metabolic inhibitor (Vadivelu et al. 2006b). Currently, there are many potential applications of FNA for control and manipulation of microbial growth, thus it is of great necessity and interest to better understand the antimicrobial action of FNA. Consequently, there lacks a clear and systematic understanding of the fundamental mechanisms of microbial tolerance and resistance to exposure of FNA on *P. aeruginosa* PAO1 cultures under anaerobic denitrifying conditions. This study focused on the inhibitory mechanisms of FNA towards *P. aeruginosa* PAO1 and performed genome-wide RNA sequencing (RNA-Seq) analysis on *P. aeruginosa* in the absence and presence of a bacteriostatic-level of FNA (0.1 mg N/L) (Gao et al. 2015) in anaerobic denitrifying conditions. By combining gene expression profiles with selected measured physiological responses, the microbial response to FNA exposure was detected and potential multi-targeted mechanisms of FNA on this environmentally and medically important bacterium was revealed. The key findings from this research are illustrated below.

1) Cell growth and activity of P. aeruginosa detected during exposure to FNA

During the early growth phase of *P. aeruginosa* PAO1 we added FNA at a starting concentration of 0.1 mg N/L and the observed growth profile (Figure 8A) was similar to that previously reported in section 3.3.1. Cellular ATP levels of *P. aeruginosa* PAO1 decreased from 0.6 fmol per cell to

around 0.4 fmol per cell after 6 h exposure to FNA (Figure 8B). The percentage of live cells after this exposure showed only a slight decrease, from near 90% (no FNA addition) to about 80% (Figure 8C). The intracellular pH of *P. aeruginosa* PAO1 decreased from 7.5 to 7.2 at one hour after FNA exposure and dropped further to 6.4 after 6 h exposure (Figure 8D). This drop in intracellular pH is consistent with other studies of bacteria exposed to nitrite (Mühlig et al. 2014). In the *P. aeruginosa* PAO1 culture cellular thiol levels were seen to rise after 2 h of FNA exposure and then return to pre-FNA added levels 6 h after the FNA addition (Figure 8E). Protein thiol groups are reported to be altered by FNA exposure, this resulting in an antimicrobial effect (Fang 2004). FNA is also reported to cause oxidative stress to bacterial cells (Poole 2005). Thus, the intracellular redox of *P. aeruginosa* PAO1 was measured and during the 6 h incubation period it was seen that in general the cells became more oxidised over time (Figure 1F). However, in the cultures exposed to FNA the intracellular redox was always lower than the control cells.

2) FNA inhibited anaerobic respiration and energy production

Genes involved in denitrification processes were down regulated in the presence of FNA including the genes for nitrate reductase, nitrite reductase, N_2O reductase, NADH dehydrogenase, and ATP synthase (Appendix B, Table S2). Typically respiratory denitrification would contribute to formation of cellular proton motive force and facilitate ATP generation in *P. aeruginosa* PAO1 through the membrane-bound ATPase (Richardson et al. 2009). Decreased ATP level in *P. aeruginosa* PAO1 following FNA exposure coincides with the decreased abundance of transcripts coding for ATP synthesis (Figure 8). Together, these events of lowered ATP production (Figure 8), lowered intracellular redox potential (Figure 8), and decreased expression of denitrification genes and ATP synthase genes (Appendix B Table S2), all strongly support the notion that FNA had an impairing effect on the denitrification pathway and respiration of *P. aeruginosa* PAO1.

3) FNA caused altered carbon flux pathways

Typically, glycerol would firstly be transformed to glyceraldehyde-3-phosphate and then to pyruvate, via the Embden-Meyerhof-Parnas (EMP) pathway, before being utilized in the TCA cycle for energy generation. Most of the genes (*pgk, pykA* and *eno*) coding for enzymes of the EMP had decreased transcript levels (Appendix B, Table S2 and Figure 2). In contrast a number of genes involved in the Entner-Duoforoff (ED) pathway (PA3181, *zwf*, and *edd*) showed either no change or increased transcript levels in the presence of FNA (Appendix B Table S2 and Figure 2). The EMP pathway to pyruvate produces NADH, while the ED pathway, an alternative route for pyruvate

production, produces NADPH. During exposure to FNA it is possible the ED pathway was favoured, this brought about by lowered intracellular redox (NADH) levels causing altered gene expression (Chavarría et al. 2013). Genes encoding enzymes involved in the TCA cycle (*sdhABCD, sucABCD, ipdG*) (Appendix B Table S2 and Figure 2) were down regulated, suggesting this cycle was less active during FNA exposure.

However, transcripts of genes coding pyruvate dehydrogenase (PA3416 and PA3417) and dihydrolipoamide acetyltransferase (PA3415) displayed the greatest increases in transcription after FNA treatment (Appendix B, Table S2). These enzymes produce acetyl-CoA, which would normally feed into the TCA cycle when respiration is active. However, in FNA exposure, respiration and the TCA cycle were inhibited. The genes coding the pyruvate fermentation pathway and specifically required stress proteins (aceF, *pta, ackA,* PA1753, PA3017, PA3309, PA4352) all showed increased abundance after FNA exposure (Schreiber et al. 2006) (Appendix B, Table S2). In the presence of FNA there was a 37-fold increase in acetic acid levels in comparison to cells not exposed to added FNA (Appendix B, Table S7). It seems in response to FNA, unable to produce ATP through respiration, *P. aeruginosa* PAO1 converted the produced acetyl-CoA to acetate through pyruvate fermentation to generate ATP. Potentially, this could provide a possible survival mechanism for *P. aeruginosa* PAO1 in the presence of FNA, and possibly enable the organism faster recovery following the removal of the inhibitor (Schreiber et al. 2006).

4) FNA disrupted DNA replication, transcription and translation

Genes coding key enzymes involved in DNA replication (i.e. DNA polymerase, ATP-dependent DNA helicase), transcription (DNA-directed RNA polymerase), and protein synthesis including ribosomal RNA processing proteins, various amino acid transfer RNA synthases (32 tRNA modification genes), the small and large ribosome structural proteins et.al were all down regulated (Appendix B, Table S3). It was evident that FNA caused decreased activity of protein synthesis, DNA replication, and transcription in *P. aeruginosa* PAO1.

Interestingly, genes coding for the ribosome modulation factor (RMF) and the hibernation-promoting factor (HPF) were up regulated in response to FNA exposure (Appendix B, Table S3). These factors function to preserve active 70S ribosome units into inactive units in stressful conditions. Once the stress disappears, the inactive ribosomes are liberated from the RMF and the HPF to become active again in translation (Kato et al. 2010; Polikanov et al. 2012). It is likely that

for coping with FNA stress, *P. aeruginosa* PAO1 ceases production of ribosomes and conserves the existing ones. This implies that the ribosome itself is not the direct target of FNA mediated damage, but that ribosome inactivation is caused by altered regulation of its production and by its storage.

5) Detoxification of FNA and P. aeruginosa recovery from FNA damage

In contrast to the denitrification genes mentioned above, genes encoding NO reductase and those of the operon *nir*QOP showed higher expression in the presence of FNA (Appendix B, Table S2). NO reductase activity is reported to be essential for nitric oxide detoxification (Wang et al. 2011). It is likely that while other denitrification steps of *P. aeruginosa* PAO1 were inhibited by FNA, NO reductase levels were raised as a response to reduce toxic levels of NO derived from the added FNA. Additionally, it is known that flavohaemoglobin is an important detoxifying oxidoreductase that converts toxic NO to non-toxic nitrate in the presence of N_2O in P*seudomonas* (Fang 2004). Our transciptome analysis revealed increased expression of the *fhp* gene encoding flavohaemoglobin during FNA addition (Table S6). Thus, there is evidence here of a strategy by *P. aeruginosa* PAO1 through the increased activities of NO reductase and flavohaemoglobin for the removal of the toxic NO derived from FNA.

The *isc* operon (*iscRSUA, hscBA*, *fdx2*, and PA3808) and the gene *nfuA* coding for the synthesis of Fe-S clusters in *P. aeruginosa* PAO1 showed increased transcripts levels (Appendix B, Table S5), suggesting that FNA affected *P. aeruginosa* PAO1 was attempting to assemble new Fe-S clusters to replace damaged components. It seems that FNA and its derivatives are damaging Fe-S clusters in *P. aeruginosa* PAO1 and the organism is responding to that by repair and assembly of new clusters. Interestingly, genes encoding several proteolysis enzymes had increased expression during FNA exposure. This includes an ATP-binding protease component ClpA (PA2620), periplasmic serine protease (PA1832) and an ATP dependent Lon protease (PA1803) (Appendix B, Table S5). It is speculated that ClpA degrades abnormal and damaged proteins and the Lon protease cleaves multiple peptide bonds. Consequently, it appears that FNA and/or the RNIs are causing damage to proteins, and then this induced activity is enabling recycling of peptides and amino acids.

6) The multifaceted response of P. aeruginosa PAO1 to FNA exposure

A proposed model was compiled to describe the effects of FNA and the multiple responses that enable *P. aeruginosa* PAO1 to withstand this bacteriostatic level of FNA exposure (Figure 9). In this model, during exposure to FNA, most of the denitrification pathway is less active. As a result,

NADH consumption and ATP generation coupled with denitrification is suppressed leading to energy starvation in *P. aeruginosa* PAO1 cultures. In contrast, the respiratory enzyme NO reductase shows increased activity to detoxify the NO that is derived from FNA. The lowered requirement of NADH further restrains the carbon utilization, in which normal glycerol metabolism and TCA cycle activities are impeded. Consequently, *P. aeruginosa* PAO1 alters its normal glycerol utilization from the Embden-Meyerhof-Parnas pathway (EMP pathway) to the Entner–Doudoroff pathway (ED pathway) to generate pyruvate. The pyruvate, no longer utilized through the TCA cycle, is then fermented to acetate for energy generation and to provide a survival mechanism to the stress imposed by FNA. Meanwhile, in response to the lowered cell metabolism, *P. aeruginosa* PAO1 shuts down protein synthesis, ceases nucleic acid replication and the ribosome units are preserved in a dormant state. Additionally, in response to damaged proteins *P. aeruginosa* PAO1 produces new Fe-S clusters and degrades abnormal proteins for recycling of the amino acids.

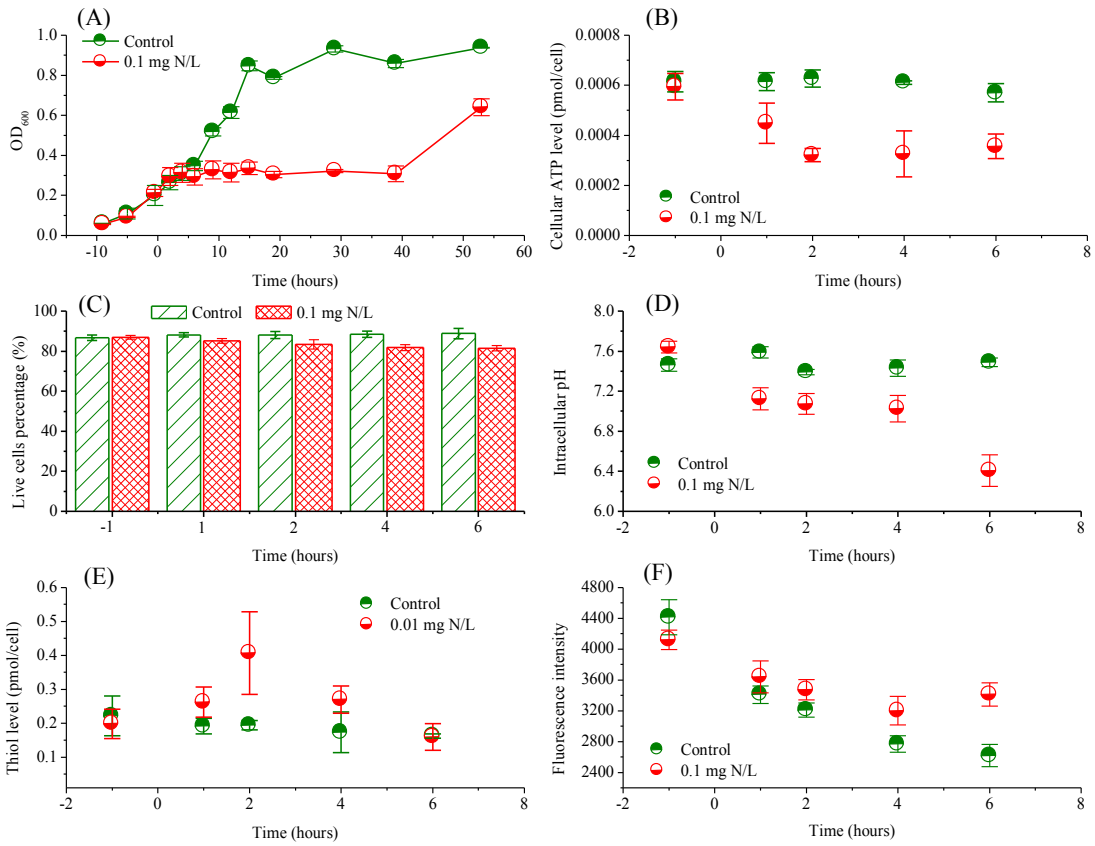

Figure 8. Different physiological features of *P. aeruginosa* PAO1 growth measured in the presence and absence (Control) of 0.1 mg N/L FNA. Growth profiles in terms of OD_{600} (A), cellular ATP levels (B), the precents of live cells (C), intracellular pH (D), cellular thiol levels (E), and intracellular redox levels (F, higher fluorescence indicates lower redox potential). FNA was added at time 0 hour. Error bars indicate the standard deviations of the triplicate samples.

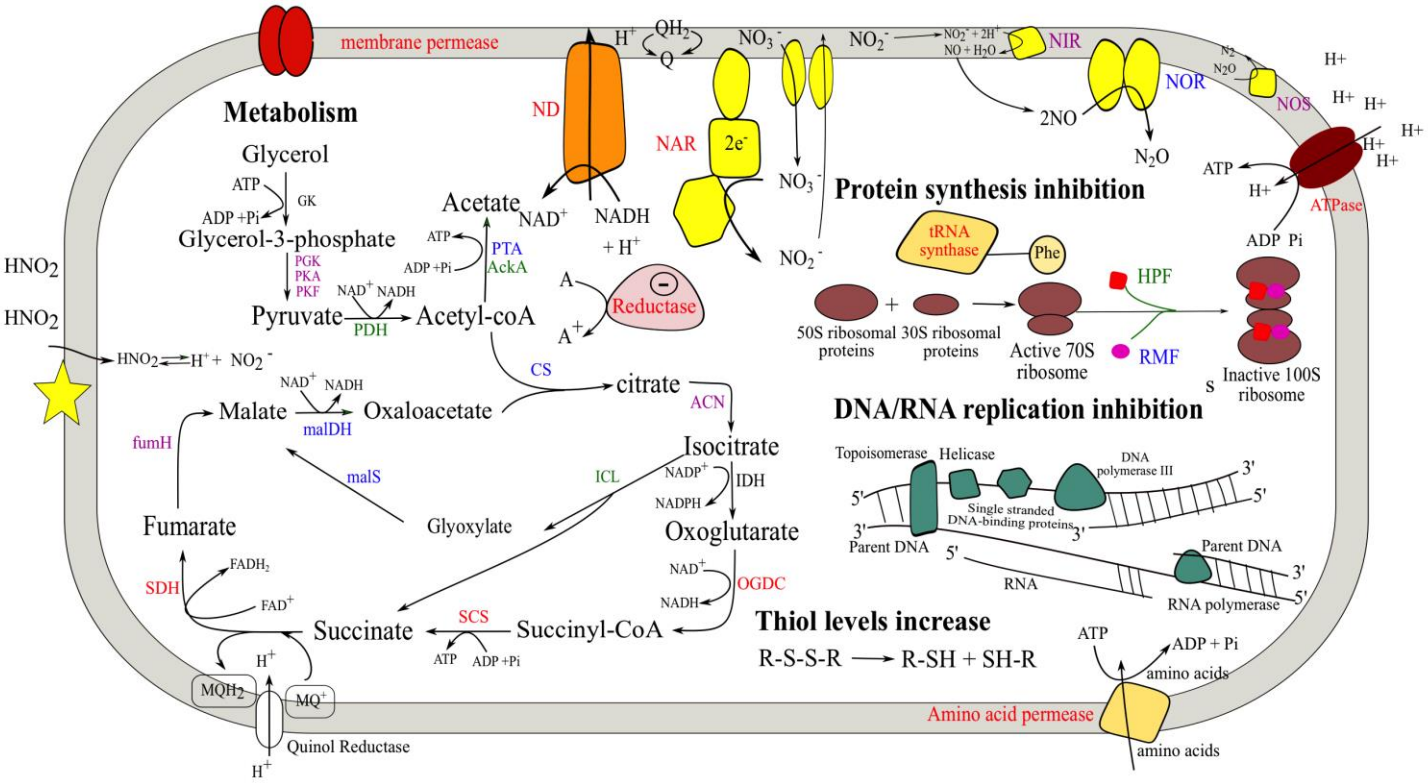

Figure 9. A proposed model for the response of *P. aeruginosa* PAO1 to FNA stress and its survival strategies. The enzymes/proteins in red and green represent the encoding genes "highly" up or down regulated respectively, enzymes/proteins in blue and purple represent the encoding genes "moderately" up or down regulated respectively, and enzymes/proteins in black stand for encoding genes with no change with FNA treatment. GK: Glycerol kinase; PGK: phosphoglycerate kinase; PKA: pyruvate kinase II; PKF: pyruvate kinase I; PDH: pyruvate dehydrogenase; PTA: phosphotransacetylase; AckA: acetate kinase; CS: citrate synthase; ACN: aconitase; IDH: isocitrate dehydrogenase; malS: malate synthase; malDH: probable L-malate dehydrogenase; ICL: isocitrate lyase; OGDC: 2-oxoglutarate dehydrogenase; SCS: succinyl-coA decarboxylase; SDH: succinate dehydrogenase; fumH: fumarate hydratase.

3.3.3 Unravelling multiple responses of *Desulfovibrio vulgaris* Hildenborough to antimicrobial agent FNA

This section summarises the findings of the work described in Appendix C which is published in Applied and Environmental Microbiology.

Hydrogen sulfide produced by SRB in sewers causes odor problems and results in serious deterioration of sewer assets that requires very costly and demanding rehabilitation efforts. There is current interest in the application of the antimicrobial agent FNA to inhibit growth of SRB and sulfide production in sewers. To improve the application of FNA as an antimicrobial agent in sewers, it is of great importance to determine details of the antimicrobial effects of FNA on SRB. *Desulfovibrio* species can be prevalent SRB in sewers (Sun et al. 2014) and *D. vulgaris* Hildenborough is a well studied sulfate reducer with lactate as the eletron donor in sewers (Figure 10) which is demonstrated to have a periplasmic cytochrome c nitrite reductase (NrfA) for the conversion of nitrite to ammonium with the possible production of intermediate hydroxylamine as a detoxifying mechanism to FNA stress (Heidelberg et al. 2004). To date, the antimicrobial effects of FNA on bacteria in general are believed to be multi-targeted (Fang 2004) and there have been some transcriptional investigations, based on macroarray and microarray analyses, to examine the effects of nitrite on *D. vulgaris* Hildenborough (Haveman et al. 2004; He et al. 2006). These studies implicate that nitrite stress could inhibit sulfate reduction and cause possible oxidative stress, as well as disrupt iron homeostasis. However, all the conclusions and hypotheses drawn from those investigations are based only on the transcriptional responses. A comprehensive and systematic understanding of the antimicrobial mechanisms of FNA on *D. vulgaris* Hildenborough is still lacking, which could be achieved by combining the transcriptional response with detection of cell activities and physiological changes.

In this study, substrate transformations and physiological changes were detected in response to different levels of FNA (0, 1.0, 4.0, 8.0 μg N/L). In addition, whole genome messenger RNA sequencing (RNA-seq) analysis was also conducted on *D. vuglaris* Hildenborough cultures in the presence and absence of a sub-bactericidal level of FNA (4.0 μg N/L). The global transcriptome response was combined with analyses of substrate transformations and physiological responses to test the hypotheses mentioned above. From this a more comprehensive understanding of the effects

of FNA was obtained to verify the key determinants of FNA stress in this model sewer hydrogen sulfide producing bacterium as described below.

1) Concentration-dependent effects of FNA on D. vulgairs Hildenborough growth and respiratory activities

Growth profiles of *D. vulgaris* Hildenborough batch cultures in the presence of different levels of FNA were determined (Figure 11). *D. vulgaris* Hildenborough cultures exposed to the lowest starting FNA concentration of 1.0 μg N/L showed only slight growth inhibition during the 48 h incubation (Figure 11). Inhibition of growth increased with the increased levels of FNA and the growth almost stopped completely with FNA at 8.0 μg N/L. Substrate transformation in *D. vulgaris* Hildenborough batch cultures grown on lactate and sulfate in the presence of different levels of FNA was detected (Figure 12). Levels of lactate oxidation and sulfate reduction with FNA level 1.0 μg N/L were slightly less than that of the control culture (no FNA addition) (Figure 12C, E) and this coincided with the observed slight decreased growth (Figure 11), indicating FNA was having only a slight inhibitory effect on the organism at this level. During the incubation 1.0 μg N/L FNA was completely reduced within 8 h after addition (Figure 12A, B). In comparison, much lower lactate oxidation levels were detected in cultures with starting FNA concentrations of 4.0 and 8.0 μg N/L (Figure 12C). Therefore, in these cultures there would be limited electrons available for sulfate reduction, which was severely diminished (Figure 12E), and this coincided with the reductions in growth levels detected (Figure 11). In contrast, in the batch cultures nitrite reduction occurred with limited electron supply from lactate oxidation (Figure 12 A, B) after FNA addition, which is a logical response and is in agreement with previous observations of *D. vulgaris* Hildenborough to nitrite exposure (Haveman et al. 2004; He et al. 2006). This was evident at all FNA concentrations and was likely due to nitrite reductase activity of *D. vulgaris* Hildenborough.

The absolute ratios of lactate consumed, sulfate used and acetate produced were calculated from the concentrations detected during the 48 h incubations of *D. vulgaris* Hildenborough at the different FNA levels. The ratios were compared to the theoretical ratio determined when acetate is considered as the product of the lactate oxidation (Appendix C, Table 1). For the control culture not exposed to FNA, these values are reasonably close to the stoichiometric ratios for the lactate oxidation (Appendix C, Table 1). However, the ratios of lactate used and acetate produced were raised, at the higher level of applied FNA. This could be explained if there was increased competition for electrons during FNA exposure, which may likely have resulted from increased

nitrite reduction activity. Sulfite and thiosulfate levels were detected during the batch incubations (Figure 12G, H). There were no obvious differences in the levels of sulfite that correlated with the different FNA levels while thiosulfate was only detected in the cultures that were exposed to FNA levels of 4 and 8 μg N/L (Figure 12H).

2) Changes in specific cell activities during FNA exposure

LIVE/DEAD staining was performed on the *D. vulgaris* batch cultures to evaluate the effect of FNA on cell viability. At early log phase prior to FNA addition, the viable cell numbers in the cultures were around 85%-90% (Figure 13A). When no FNA was added, the live cell percentage stayed at this level until 24 h incubation before dropping to around 65% at 48 h incubation (Figure 13A). This drop in live cells could have resulted from changes in the culture conditions, such as lactate depletion (Figure 12C). In comparison, the viable cell numbers for the FNA concentration of 1.0 μg N/L decreased quickly to around 60% when the incubation time was 7 h and this remained near that level through the incubation period (Figure 13A). Substantial decreases in the percentage of live cells were detected immediately upon the addition of FNA at 4.0 μg N/L FNA, and at 8.0 μg N/L, such that near 95% killing of the *D. vulgairs* Hildenborough cultures occurred within 12 h incubation (Figure 13A). These results support the suggestion that the bacteriostatic and bactericidal effects of FNA are concentration-determined and population-specific as previously detected in *P. aeruginosa* PAO1 (Gao et al. 2015).

Cellular thiol levels of *D. vulgaris* Hildenborough increased with the addition of FNA (Figure 13B). At FNA starting concentrations of 1.0 and 4.0 μg N/L N/L, a small increase in cellular thiol levels was detected at 12 and 24 h incubation (Figure 13B). However, cellular thiol levels increased markedly throughout the incubation period when the cells were exposed to 8.0 μg N/L FNA (Figure 13B). It is thought that FNA could nitrosylate thiol groups, such as those on proteins, which could change the activity or function of those (Fang 2004). There is also a hypothesis that FNA imposes oxidative stress on bacterial cells (Poole 2005). Thus in these batch cultures the cell redox status was determined and it was observed that with increasing levels of FNA the cells were more oxidised (Figure 13C). Cellular ATP levels of the *D. vulgaris* Hildenborough batch cultures (normalised to per live cell) decreased with the increase of added FNA concentrations (Figure 13D). This supports the idea that FNA acts as a protonophore, to decouple the proton motive force across cell membranes and thereby inhibiting ATP synthesis (Zhou et al. 2011).

3) Evidence of oxidative stress and detoxification of FNA by D. vulgaris Hildenborough

In FNA-added cultures (4.0 μg N/L) the gene coding for NrfA (DVU0625) exhibited considerable up regulation (Appendix B, Table 2), implying its detoxifying role by the reduction of nitrite (and proportional reduction of FNA). This observation agrees with the decreasing nitrite levels detected in the batch cultures (Figure 12A). Additionally, the gene, DVU2543, which codes for what is known as the hybrid cluster protein (HCP), was the most up-regulated gene detected when exposed to FNA (Appendix C, Table 2). The HCP is proposed to have hydroxylamine reductase activity (Wolfe et al. 2002), and was possibly acting to remove hydroxylamine as part of the detoxification of nitrite. High expression of this gene in *D. vulgaris* Hildenborough has been reported previously in response to nitrite exposure (Haveman et al. 2004; He et al. 2006). The enzyme is thought to be either for reduction of RNS (the hyrdroxylamine reductase activity) or for reduction of reactive oxygen species (Aragao et al. 2008). There is strong possibility here that hydroxylamine or other RNS accumulate during FNA exposure, possibly through incomplete reduction of nitrite by NrfA (Bykov and Neese 2015). Characterisation of the HCP from *E. coli* shows reduction of hydroxylamine with production of ammonium (Wolfe et al. 2002). While the enzyme has not been characterised in *D. vulgaris* Hildenborough, one suggestion is that the HCP is acting similarly or in conjunction with NrfA to detoxify the high levels of nitrite.

Additionally, various genes coding for response to oxidative stress displayed highly increased transcript levels in the FNA-added cultures (e.g. DVU0772 and *ahpC* (DVU2247), Appendix C, Table 2). This implies that FNA caused oxidising conditions, which is what was detected by the cellular redox measurement in FNA-added cultures (Figure 13C). The genes *msrA* (DVU1984) and *msrB* (DVU0576), coding for reductases, that reduce methionine sulfoxides as an antioxidant response, were observed to have increased transcript levels in FNA-added cultures. There is possibility that HCP is acting to relieve oxidative stress (Aragao et al. 2008). Considering these detected events, oxidative stress is suggested as an important antimicrobial effect caused by FNA in *D. vulgaris*. While it is currently not known, it is possible that oxidative damage to the cell components was caused by RNS (Fang 2004).

4) FNA inhibited anaerobic respiration and energy generation of D. vulgaris Hildenborough

In the presence of FNA, various genes coding for enzymes involved in lactate oxidation and sulfate reduction processes were down regulated. This included the genes DVU0849-50 and DVU1286-90 that code for the quinone-interacting membrane-bound oxidoreductase complex (Qmo) and the

sulfite reductase complex (DsrAB) respectively (Appendix C, Table 3) (Figure 10). It is proposed that Qmo transfers electrons from lactate oxidation directly to adenosine-5'-phosphosulfate reductase while DsrAB transfers electrons to the sulfite reductase (Heidelberg et al. 2004). This down regulated gene expression is observed in previous studies of nitrite exposure to *D. vulgaris* Hildenborough (Haveman et al. 2004; He et al. 2006) , and would be an appropriate action in cells that experienced diminished electron flow from lactate oxidation. Interestingly, thiosulfate, the intermediary product of the sulfate reduction by the trithionate-reducing pathway (Kim and Akagi 1985), was found to accumulate in FNA treated samples while sulfite did not (Fig 12G and H). Previous studies demonstrate two possible pathways of sulfite reduction to sulfide in *D. vulgaris* Hildenborough, one is by direct reduction without intermediates and the other is via the trithionate pathway with thiosulfate and sulfite as the intermediates (Rabus R. et al., 2006). The observed accumulation of thiosulfate supports the inhibitory effect of nitrite on DsrAB and suggests that the trithionate-reducing pathway is the mechanism of sulfite reduction in *D. vulgaris* Hildenborough under these conditions.

Genes in *luo* (for lactate utilization operon) operon including DVU3026 for lactate permease, DVU3027-28 and DVU3032-33 for lactate dehydrogenase subunits, DVU3025 for pyruvate-ferredoxin oxidoreductase, DVU3030 for acetate kinase, and DVU3029 for phosphate acetyltransferase were demonstrated to involve lactate oxidation in *D. vulgaris* Hildenborough and showed down regulation in the presence of FNA (Appendix C, Table 3). Down regulation of most genes in the *luo* operon were detected when exposed to FNA (Appendix C, Table 3) and importantly these genes had high expression values when lactate and sulfate utilisation, and when acetate and sulfide production, were active (Appendix C, Table 3) (Figure 12C, D, E, and F). This down regulation of the *luo* operon genes during FNA exposure is logical when the cells respiratory activities were lowered, as observed. Additionally, these findings further support the involvement of the recently described *luo* operon in lactate oxidation (Vita et al. 2015).

Down regulation of these genes, involved in lactate oxidation and transfer of electrons for sulfate reduction, correlated with reductions of lactate and sulfate utilisation (Figure 12C, E) and lowered acetate and sulfide production (Figure 12D, F) when *D. vulgaris* Hildenborough was exposed to FNA. Additionally, the transcripts of genes DVU0774-80, and DVU0918 coding for ATP synthase were all markedly down regulated (Appendix C, Table 3). This coincided with the lowered ATP

level detected in the cells. All together, it seems the cells were shutting down the main energy conserving reactions when exposed to FNA.

5) FNA disrupts DNA replication, transcription and translation of D. vulgaris Hildenborough

Genes encoding for critical enzymes involved in DNA replication (e.g. chromosomal replication initiator protein DnaA, DNA polymerase, DNA gyrase, DNA topoisomerase) and transcription (DNA-directed RNA polymerase) exhibited down regulation after FNA exposure for 1 h (Appendix C, Table 4). As well, the genes coding for 30S and 50S ribosomal structure proteins (Appendix C, Table 4) and a variety of amino acid transfer RNA synthetases showed significantly decreased transcripts. It is apparent that FNA could be causing decreased cell activities of DNA replication, transcription and protein biosynthesis in *D. vulgaris* Hildenborough. The gene *yfi* (DVU1629) coding for the ribosomal subunit interface protein displayed 14.4 fold up regulation (Appendix C, Table 4). This factor is demonstrated to stabilise ribosomes and stop translation in stressful conditions (Agafonov et al. 2001). Possibly *D. vulgaris* Hildenborough is ceasing translation, and inactivates, and conserves the existing ribosomes in the presence of FNA as we observed in *P. aeruginosa*.

6) The multifaceted response of D. vulgaris Hildenborough to FNA exposure

Based on the substrate consumption, physiological assays detection combined with transcriptome analysis, a conceptual model was proposed that summarises the antimicrobial effects of FNA on *D. vulgaris* (Figure 14). During exposure to FNA, *D. vulgaris* Hildenborough switched from a status of prolific growth to a phase of severely inhibited growth. When exposed to FNA at 4.0 μg N/L sulfate reduction and lactate oxidation coupled with ATP generation were suppressed, leading to energy starvation in the FNA-added cultures. Expression of genes coding for lactate oxidation and sulfate reduction were subsequently lowered. In response to energy starvation, *D. vulgaris* Hildenborough stabilised its existing ribosomes and ceased translation of proteins. In addition, FNA caused more oxidative conditions in *D. vulgaris* Hildenborough and there was transcriptional evidence of attempts to alleviate the oxidative stress. The findings of this study not only provide insight and fundamental understanding of the antimicrobial mechanism of FNA, but also can assist in the application of FNA in real sewers for control of sulfide production and corrosion.

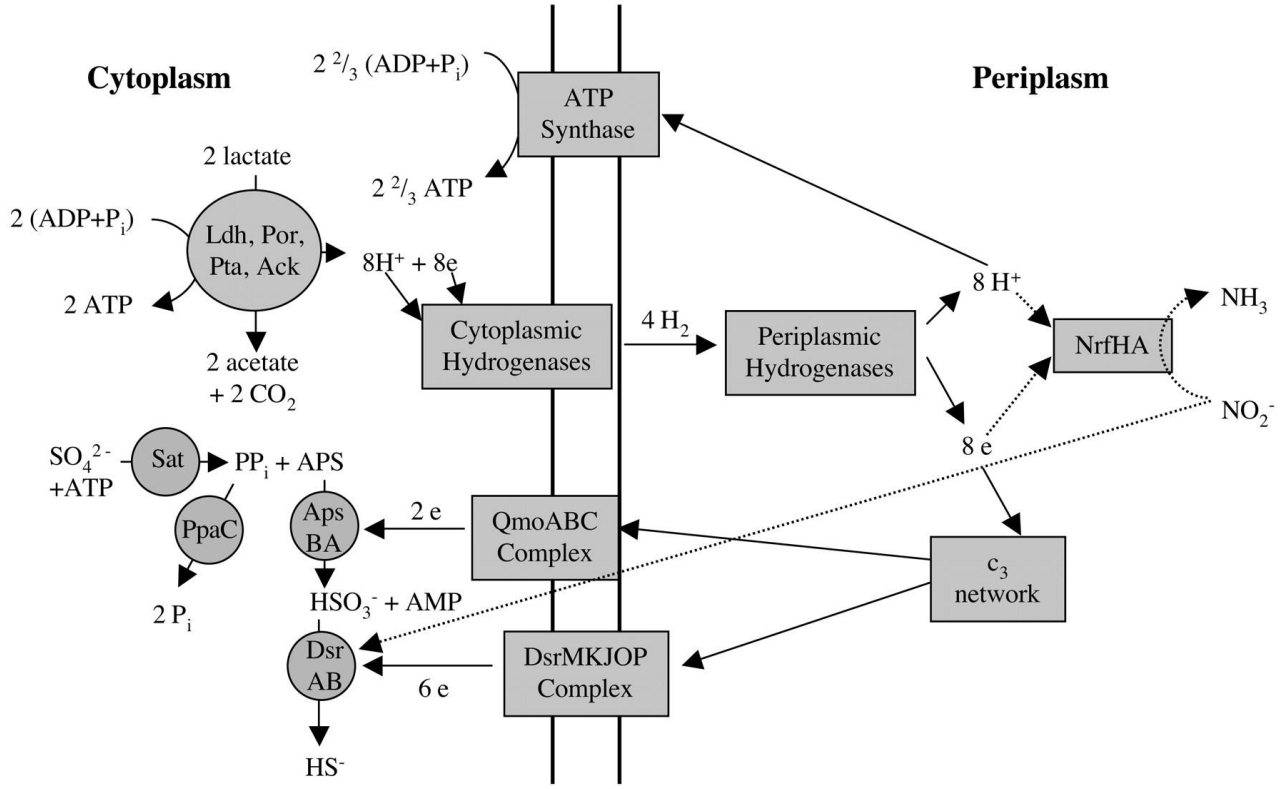

Figure 10. Respiration pathways of lactate oxidation, sulfate reduction and nitrite reduction in *D. vulgaris* Hildenborough (Haveman et al. 2004). Enzyme abbreviations: Sat, sulfate adenylyltransferase; PpaC, pyrophosphatase; ApsBA, adenosine phosphosulfate reductase; DsrAB, dissimilatory sulfite reductase; QmoABC, quinone-interacting membrane-bound oxidoreductase; DsrMKJOP, triheme cytochrome c-containing membrane-bound oxidoreductase; Ldh, lactate dehydrogenase; Por, pyruvate:ferredoxin oxidoreductase; Pta, phosphate transacetylase; Ack, acetate kinase; c3 network, network of periplasmic, tetrahemic c-type cytochromes. APS, adenosine phosphosulfate.

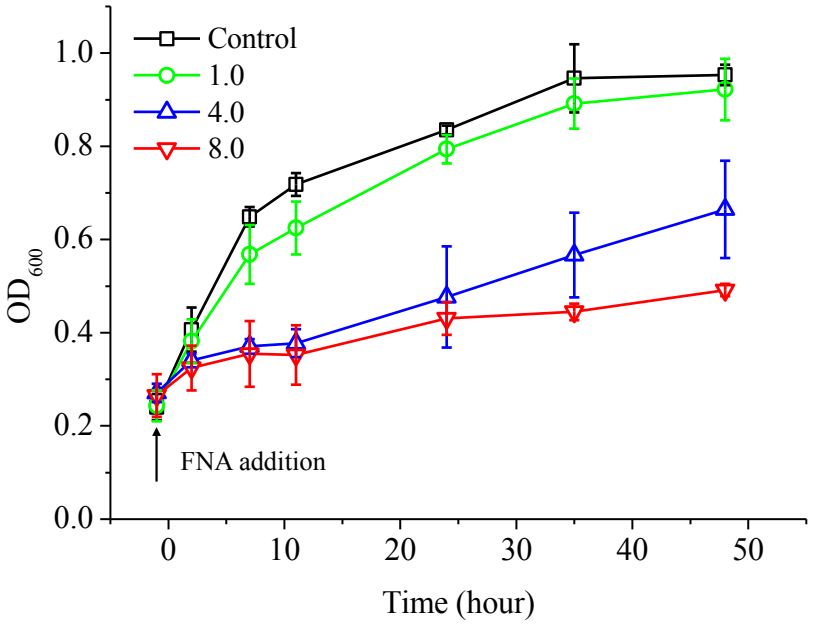

Figure 11. Growth profiles of *D. vulgaris* Hildenborough batch cultures in the presence of different levels of FNA (µg N/L). FNA was added after 26 hours incubation, at time 0 h. The control culture has no FNA addition. Error bars were calculated based on the growth of the triplicate cultures. The figure key shows the FNA starting concentrations in the different cultures.

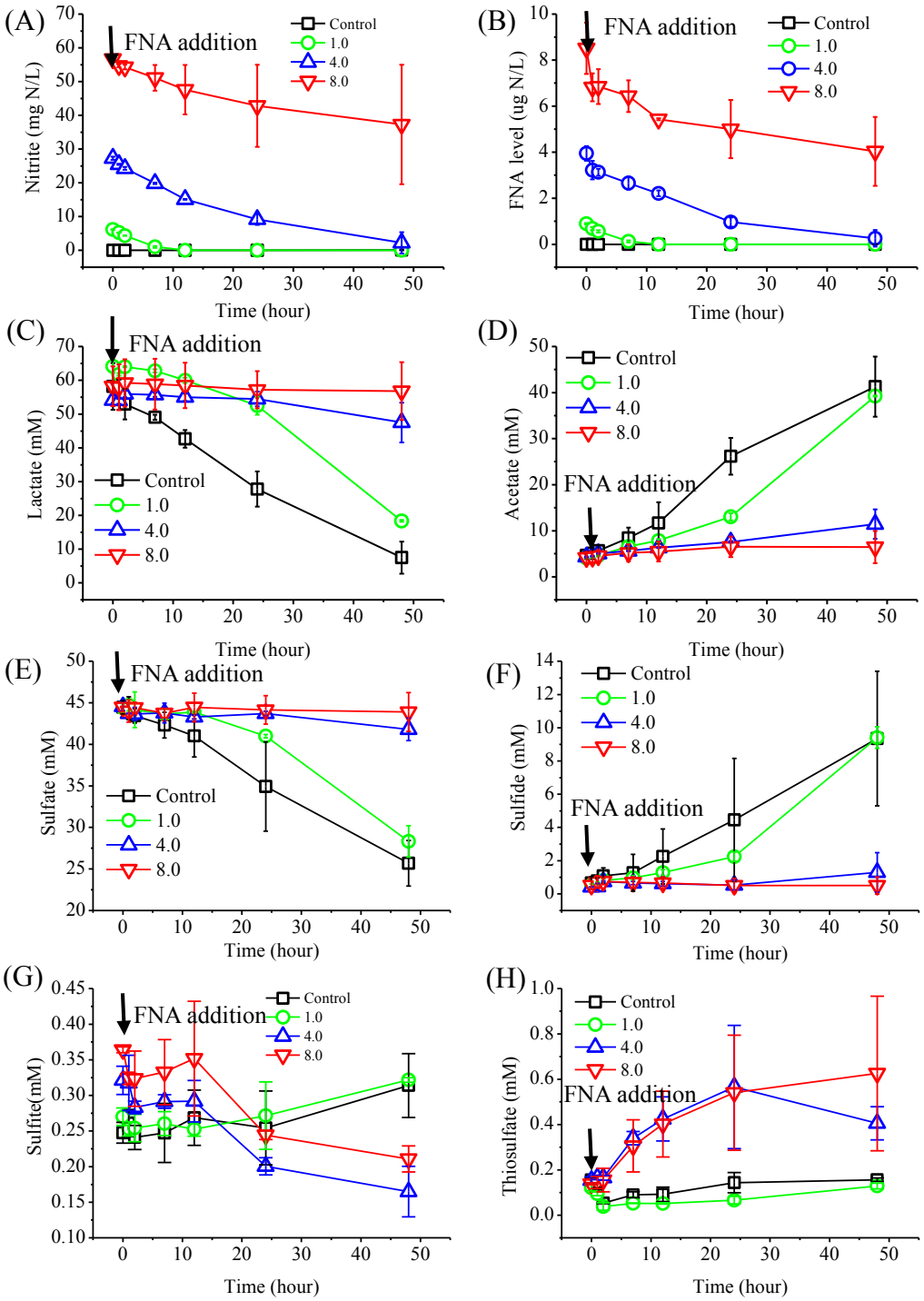

Figure 12. Levels of nitrite (A), FNA (B), lactate (C), acetate (D), sulfate (E), sulfide (F), sulfite (G), and thiosulfate (H) in *D. vulgaris* Hildenborough batch cultures grown on lactate and sulfate. The batch cultures were exposed to different levels of FNA which was added at time 0 h, which was 26 hours after inoculation. No FNA was added to the control cultures. Error bars represent the standard deviation of analyses performed from triplicate batch cultures. The figure key shows the FNA starting concentrations.

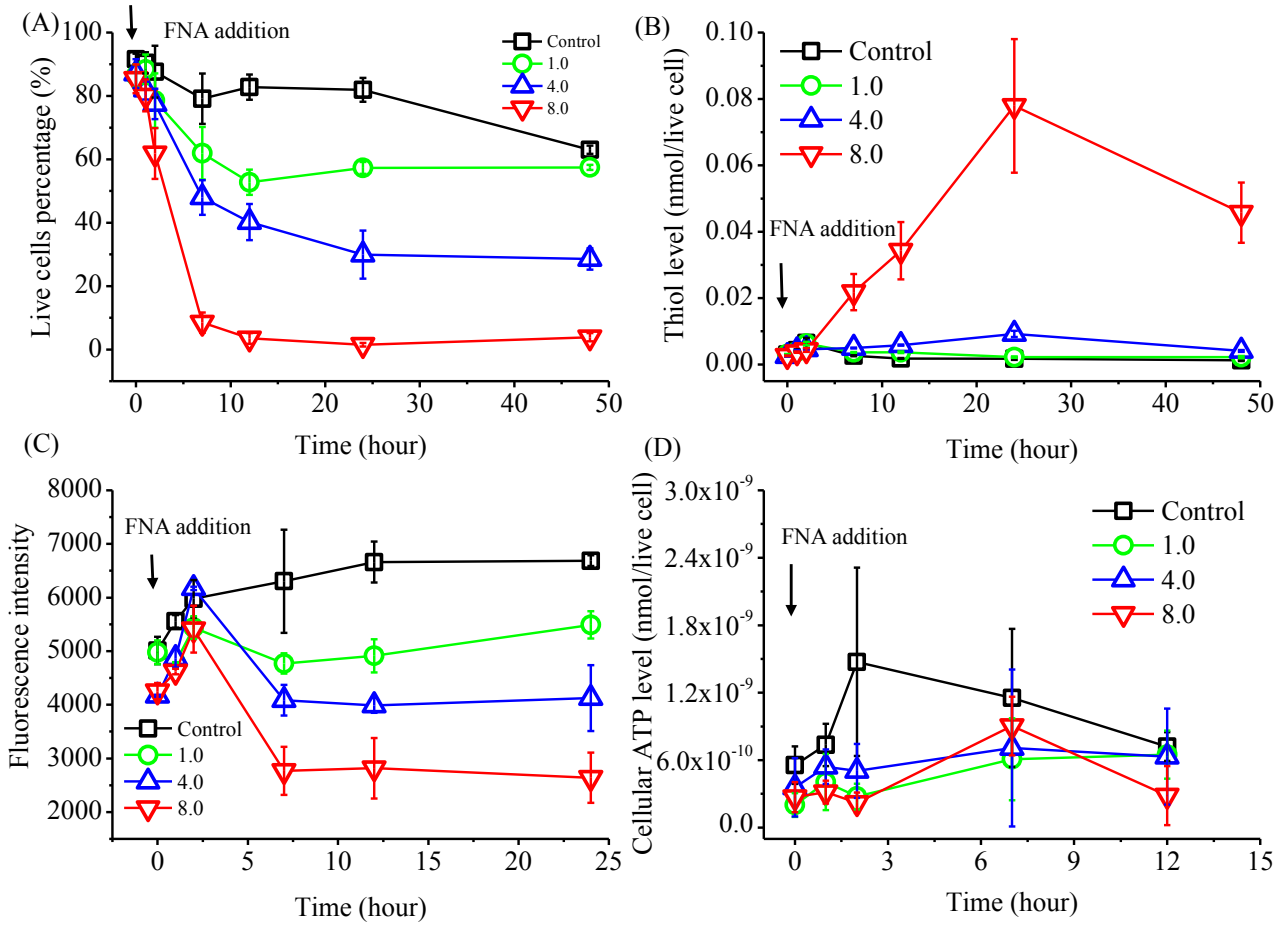

Figure 13. Physiological features of *D. vulgaris* Hildenborough measured during the batch culture incubations in the presence of different levels of FNA and when no FNA was added (control). The percentage of live cells (A), cellular thiol levels (B), intracellular redox levels, where higher fluorescence indicates lower redox potential (C), and cellular ATP levels (D). FNA was added at time 0 h.

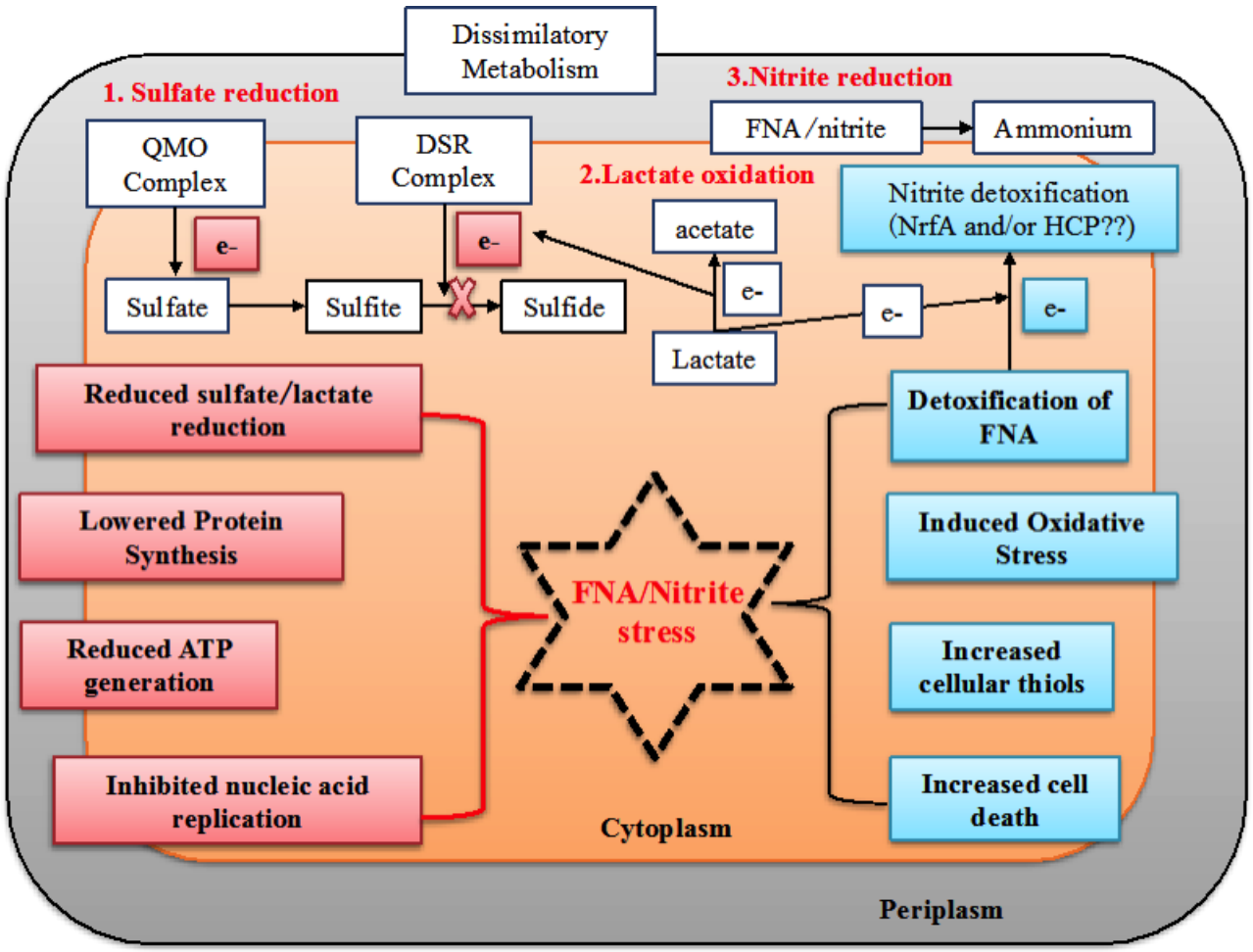

Figure 14. Proposed antimicrobial effects of FNA (4.0 µg N/L) on *D. vulgaris* Hildenborough based on interpretations of measured physiological activities and the transcriptional responses. The colored boxes indicate activities or events where the associated gene expression was primarily increased (blue) or decreased (red) in response to FNA exposure.

3.3.4 Determining the response of *Desulfovibrio vulgaris* Hildenborough through comparative proteomic analysis to the antimicrobial agent FNA

This section summarises the findings of the work described in Appendix D which is to be submitted to Journal of proteomics.

Complementary to the previous study in section 3.3.3 that examined the gene expression response to FNA, this study determines the protein expression dynamics with different FNA levels (0, 1.0, 4.0, and 8.0 µg N/L) over different treatment time (2, 8, and 12 h) on *D. vulgaris* Hildenborough.

While the transcriptome analysis in section 3.3.3 allows us to examine the changing messenger RNA level caused by FNA (Wang et al. 2009), not all the differentially expressed transcripts end up in functional proteins due to post-transcriptional modification. Quantitative proteomics can explore the metabolic and physiological details of microbes in response to antimicrobial agents at functional protein levels. In addition, the proteomics analysis in this study could further explain and verify the transcriptomics responses detected in section 3.3.3.

Previous to the transcriptome analysis reported in section 3.3.3, there have been some transcriptional investigations, based on macroarray and microarray analyses, to examine the effects of nitrite on *D. vulgaris* Hildenborough (Haveman et al. 2004; He et al. 2006; Gao et al. 2016a). These studies suggest that nitrite stress could inhibit sulfate reduction and cause possible oxidative stress, as well as disrupt iron homeostasis in a short time after FNA/nitrite addition. However, all the conclusions and hypotheses drawn from those investigations are based only on either physiological responses or the transcriptional responses (Haveman et al. 2004; He et al. 2006; Gao et al. 2016a).

This study detected the whole cell protein content and protein expression dynamics of *D. vulgaris* Hildenborough using the quantitative proteomics approach of SWATH-MS. SWATH-MS is a recently developed approach that provides extensive label-free quantitation of the measurable peptide ions in a sample (Vowinckel et al. 2013). This approach rapidly acquires high resolution Q-TOF mass spectrometer data through repeated analysis of sequential isolation windows (swaths) throughout the chromatographic elution range (Gillet et al. 2012). The cultures were exposed to FNA concentrations of 0, 1.0,4.0, and 8.0 μg/L and sampled at three incubation periods after FNA addition of 2, 8 and 12 h. Differential expressed proteins in FNA-added cultures were compared to those in the control cultures (no FNA addition) to test the hypotheses of FNA toxicity and its duration. From this a more comprehensive understanding of the FNA effects on *D. vulgaris* Hildenborough was obtained and the key determinants for withstanding FNA over incubation were verified in this sewer corrosion relevant strain.

1) FNA effect on protein levels of D. vulgaris Hildenborough

The amount of protein produced by *D. vulgaris* Hildenborough in the presence of different FNA levels was detected during incubation (Figure 15). Similar protein levels (amount per microliter culture) were observed for *D. vulgaris* Hildenborough in the control cultures (no FNA addition) and

in the cultures exposed to 1 µg N/L, and for *D. vulgaris* Hildenborough in the presence of 4 and 8 µg N/L (Figure 15A). The protein levels at 8 and 12 h after FNA addition decreased with the increased levels of FNA except for FNA level of 8 µg/L (Figure 15A). In comparison, there is a slight increase of protein production with 1 µg N/L FNA exposure in terms of cellular protein level, suggesting the cultures are active and experienced protein synthesis to cope with FNA stress (Figure 15B). This is also coincided with the fact that this level of FNA only slightly inhibited the growth of *D. vulgaris* Hildenborough (Figure 11). Meanwhile, cellular protein levels in the presence of 4 µg N/L FNA were lower than that of control cultures due to the inhibition of culture growth (Figure 15B). However, an unexpected high cellular protein level (4 pg/cell) was detected when exposed to a FNA level of 8 µg N/L for 8 h and this protein level decreased to about 2 pg/cell at 12 h (Figure 15B). Extremely low levels of live cells and characteristics of protein stability could account for these outlier cellular protein values at 8 h and 12 h treatment with 8 µg N/L. Data from this study suggest that total protein levels per live cell kept stable (Figure 15B), indicating the possibility that viable cells have the somewhat constant amounts of protein, regardless of the protein types.

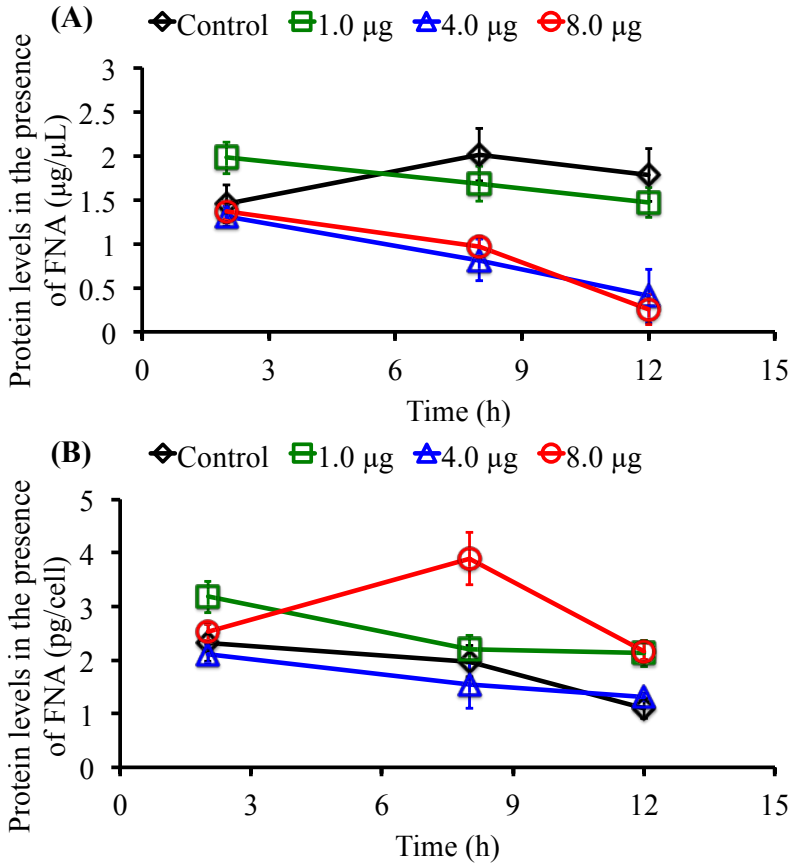

Figure 15. Total protein levels per microliter of *D. vulgaris* Hildenborough culture in the presence of different FNA levels (control, 1.0, 4.0 and 8.0 µg/L) at different incubation time periods of 2, 8 and 12 h (A), and cellular protein levels per live cells of *D. vulgaris* Hildenborough when exposed

to different levels of FNA (control, 1.0, 4.0 and 8.0 μg/L) with different treatment time periods of 2, 8 and 12 h (B).

2) Proteomics analysis of D. vulgaris Hildenborough responses to different levels of FNA exposure

A total of 863 unique proteins were identified within the library acquired by IDA with a false detection rate of 0.01 calculated with a Paragon method within the ProteinPilot software. The number of significantly different (adjust p value < 0.001) expressed proteins was determined between pairwise comparisons of the *D. vulgaris* cultures treatment with different FNA levels at different treatment time. There were 7/4/4, 4/43/43 and 4/21/64 differentially abundant proteins between the comparison of control cultures to cultures exposed to 1.0, 4.0 and 8.0 μg/L FNA at 2/8/12 h incubation respectively ($log_2FC > 0.5$, adjusted p value < 0.001).

3) Proteins differentially expressed relevant to culture metabolism

Proteins differentially expressed relevant to metabolism in the presence of FNA was determined (Table 3). In the presence of 1.0 μg N/L FNA at all incubation time points and 2 h after different FNA concentrations applied, all of the proteins detected relevant to lactate oxidation and sulfate reduction showed no change. In contrast, proteins involved in nitrite reduction showed highly increased expression levels at 2, 8, and 12 h incubation. These include cytochrome c nitrite reductase (DVU0625), HCP (DVU2543), and iron-sulfur cluster-binding protein (DVU2544) (Table 3), in which HCP is one of the highest expressed proteins in FNA-treated cultures. This strongly coincides with transcriptomics data and implicates the important role played by HCP in defense to FNA stress. Additionally, proteins involved in sulfate reduction and lactate oxidation pathways (Table 3) showed no change compared to control cultures, implying that 1.0 μg N/L FNA would not affect sulfate reduction and lactate oxidation pathways, which can be also reflected from the fact that this level of FNA caused no obvious inhibition effect on cell growth as previously reported (Figure 11). Proteins involved in nitrite reduction showed increased expression levels at all three incubation periods in the presence of all FNA concentrations (Table 3).

In comparison, many proteins involved in metabolism including sulfate reduction and lactate oxidation were differentially expressed with FNA concentrations of 4.0 and 8.0 μg N/L. Adenylyl-sulfate reductase (DVU0846) and sulfate adenylyltransferase (DVU1295) for sulfate reduction (Figure 10) showed stable increased expression at either 8 h and/or 12 h incubations with FNA

levels 4.0 and 8.0 μg N/L (Table 3). This can be explained by the fact that the culture growth started to recover at 8 h incubation after adding 4.0 μg N/L FNA. For FNA concentrations 8.0 μg N/L, it is possibly because DVU0846 and DVU1295 were expressed by the remaining viable cultures to prepare for the sulfate reduction at 12 h incubation after FNA addition. In comparison, with the addition of starting FNA level 4.0 μg N/L heterodisulfide reductase (DVU0850) for sulfite reduction largely reduced its expression at 8 h and no change was observed at 12 h when FNA concentration reduced to around 2.0 μg N/L (Table 3). This demonstrates that heterodisulfide reductase (DVU0850) expression was inhibited by FNA and the approximate inhibition threshold is around 2.0 μg N/L. These observations also indicate that FNA does not inhibit the expression of DVU0846 and DVU1295 but DVU0850 in *D. vulgaris* Hildenborough, and the energy generation by sulfate reduction was down regulated as long as 12 h incubation in the presence of 4 and 8 μg/L.

In agreement with sulfate reduction, several proteins involved in lactate oxidation in the presence of 4.0 and 8.0 μg N/L showed different expressions. These proteins include pyruvate ferredoxin oxidoreductase (DVU1569), alcohol dehydrogenase (DVU2201), formate dehydrogenase (DVU2482), and part of the *luo* operon uncharacterized protein (DVU3032) and iron-sulfur cluster-binding protein (DVU3033) (Table 3). DVU1569 and DVU2201 showed decreased expression at 8 h incubation while DVU3032 and DVU3033 increased their expression at 8 h and 12h after FNA addition. *Luo* operon was reported to function in lactate oxidation in *D. vulgaris* Hildenborough, and DVU3032 and DVU3033 are part of *luo* operon (Vita et al. 2015). All these obervations suggest that sulfate reduction pathway (from sulfite to hydrogen sulfide) and lactate oxidation pathway (from pyruvate to acetate) were the target of FNA contributing for the growth inhibition and cell death. Additionally, ATP synthesis protein (DVU0775) and electron transfer protein HMC (DVU0535) (Table 3) also showed increased expression level at 8 h and/or 12 h with FNA level 4.0 and/or 8.0 μg N/L, indicating the metabolic activity recovery of *D. vulgaris* Hildenborough cultures which coincides with the protein expression dynamics in sulfate reduction and lactate oxidation. In comparison, transcriptomics results described in section 3.3.3 demonstrated the down regulation of all the genes involved in sulfate and lactate reduction, which could be explained by the fact that it only showed the results at 1 h after 4.0 μg N/L FNA addition and/or quick response of the cultures to resist FNA stress before growth recovery.

In addition, more proteins involved in carbon metabolism, including glyceroldehyde-3-phosphate dehydrogenase (DVU0565), sugar dehydratase (DVU0448), 2-oxoglutarate oxidoreductase

(DVU3348), and pyruvate flavodoxin-ferredoxin oxidoreductase (DVU3349) (Table 3) exhibited decreased protein abundance in the presence of 4.0 μg N/L at 8 h incubation. This suggests that the carbon metabolism was severely inhibited by 4.0 μg N/L after FNA addition. However, the abundance of DVU3349 protein showed no change in a study investigating the responses of *D. vulgaris* Hildenborough under salt stress (He et al. 2010). Moreover, the expression of protein DVU0263 for acidic cytochrome c3 and DVU0266 for uncharacterized protein which are proposed as a respiratory complex in the cell membrane of *D. vulgaris* (Walian et al. 2012), was down regulated in the presence of 4.0 and 8.0 μg N/L FNA over incubation, further supporting that FNA inhibited the respiration activity of *D. vulgaris* Hildenborough.

4) Proteins differentially expressed relevant to protein synthesis

As is the same case we observed in proteins relevant to metabolism, the levels of proteins involved in protein synthesis showed no significant changes in the presence of 1.0 μg N/L FNA and at 2 h incubation for all the other FNA concentrations (4.0 and 8.0 μg N/L) (Table 4). Of total 53 proteins identified, 5 of them showed increased expression at 8 h and/or 12 h incubation in the presence of 4.0 and 8.0 μg N/L. These proteins include 50S ribosomal protein L15 (DVU1322), 50S protein ribosomal protein L17 (DVU1330), 50S ribosomal protein L32 (DVU1209), 30S ribosomal protein S2, and 30S ribosomal protein S6 (Table 4). Increased expression in these proteins coincided with the increased protein abundance in sulfate reduction and lactate oxidation in the presence of 4.0 and 8.0 μg N/L FNA at 8 and 12 h treatment. In comparison, the severe down regulation of the genes involved in protein synthesis was observed as illustrated in section 3.3.3. This discrepancy between transcriptomics and proteomics could possibly be explained by the fact that the ribosomes are probably preserved in an inactive state as suggested by the transcriptomics data while the inactive state ribosomes can still be detected by the LC- MS/MS and/or the initial down regulation of the protein synthesis genes was alleviated over incubation with nitrite reduction, especially at 8 and 12 h when the culture regrowth was evidenced. Additionally, it can be inferred that proteins involved in protein synthesis and the protein synthesis pathway could be the corresponding response to decrease in lactate oxidation and sulfate reduction rather than the direct effect of FNA. This result is consistent with what we observed in previous studies in *P. aeruginosa* PAO1 and *D. vulgaris* Hildenborough by using whole genome transcriptome analysis demonstrating that proteins involved in protein synthesis are not the direct targets of FNA (Gao et al. 2016a; Gao et al. 2016b).

5) Differential protein expression in the presence of FNA response to oxidative stress

FNA was proposed to exert the oxidative stress to *D. vulgaris* Hildenborough and this was confirmed by cellular redox measurement in the presence of different FNA levels compared to control cultures (no FNA addition) (Figure 12). Surprisingly, this study revealed that in the presence of FNA, only two proteins that are proposed to be involved in oxidative stress are more expressed than control cultures with FNA concentrations 4.0 and 8.0 μg N/L. These two proteins are DVU0772 annotated as uncharacterised protein which is part of the PerR regulon (peroxide-sensing regulator) and DVU3212 for pyridine nucleotide-disulfide oxidoreductase (Table 5). PerR regulon is predicted to be involved in oxidative stress (Mukhopadhyay et al. 2007). Of 5 PerR regulon members we detected by SWATH-MS quantitative analysis (DVU0772 for conserved hypothetical protein, DVU2247 for alkyl hydroperoxide reductase subunit C-like protein, DVU3094 for rubrerythrin, DVU3093 for rubredoxin-type Fe(Cys)4 protein, and DVU2318 for rubrerythrin), only protein DVU0772 significantly increased its expression in the presence of high levels of FNA at 8 h and 12 h incubation while other proteins either showed decreased expression or no change (Table 5). This indicates that DVU0772 plays a critical role in resisting oxidative stress caused by FNA. In addition to PerR regulon members, rubredoxin including DVU3183 for desulfoferrodoxin, DVU3184 for rubredoxin, DVU3185 for rubredoxin-oxygen oxidoreductase, and DVU3212 for pyridine nucleotide-disulfide oxidoreductase have been suggested to be involved in the oxygen defence mechanism of *D. vulgaris (Chhabra et al. 2011)*. A recent mutant study demonstrated that DVU3183 and DVU3185 play an important role under aerobic and anaerobic conditions respectively (Wildschut et al. 2006). DVU3212 is suggested to have a flavin monoculeotide (FMN) cofactor that reduces oxygen to hydrogen peroxide and transfers electrons to adenylylphophosulfate (APS) reductase from NADH, indicating DVU3212 plays a role in both oxygen defence and sulfate reduction (Chen et al. 1994). However, under normal conditions DVU3212 was not found to interact with energy metabolism proteins to a significant degree and DVU3212 is isolated from the energy metabolism network of *D. vulgaris*. All these evidence infer that defending oxidative stress in *D. vulgaris* culture is the primary function of DVU3212 (Chhabra et al. 2011). In our study, protein DVU3184 was not detected by SWATH-MS analysis. We observed increased protein levels for DVU3212 in the presence of 4.0 and 8.0 μg N/L at 8 h and 12 h incubation while decreased protein levels/no change for DVU3183 and DVU3185 in the presence of FNA. These results suggest that DVU3212 is critical to resist the oxidative stress caused by FNA/RNS rather than DVU3183 and DVU3185. It should be noted that DVU1228 for thiol peroxidase which accounts for the peroxidase activity in vivo (Brioukhanov et al. 2010; Redding et al. 2006) showed decreased protein levels in the presence of FNA, in agreement with the fact that FNA increased the cellular

thiol levels with FNA stress as previously described in *P. aeruginosa* PAO1 and *D. vulgaris* Hildenborough (Gao et al. 2016a; Gao et al. 2016b) (Figure 12). Additionally, the protein levels of DVU1568 for ferritin and DVU3276 for ferredoxin I decreased in the presence of FNA with unknown reasons which needs further explanation.

6) Protein expression dynamics comparison in the presence of four different FNA concentrations relevant to other aspects

Apart from the proteins aforementioned in three main aspects (metabolism, protein synthesis and oxidative stress), many other proteins showed different expression levels in the presence of different FNA levels. In the presence of 1.0 μg N/L at 2 h incubation rather than 8 h and 12 h, DVU0004 for DNA gyrase subunit A, DVU0042 for RNA methyltransferase, DVU3199 for nucleoid-associated protein, DVU0132 for CRISPR-associated protein, and DVU0146 for uncharacterized protein were observed to have significant higher expression (Table 6) than control cultures and other cultures exposed to 4.0 and 8.0 μg N/L. Proteins DVU0004, DVU0042 and DVU3199 are involved in DNA and RNA biosynthesis, indicating that *D. vulgaris* Hildenborough enhanced its DNA and RNA replication with 1.0 μg N/L. DVU2929 for DNA-directed RNA polymerase subunit beta displayed decreased expression levels with 4.0 μg N/L FNA over incubation, suggesting the inhibition of RNA biosynthesis which coincided with the results from previous studies in *P. aeruginosa* and *D. vulgaris* Hildenborough when exposed to FNA (Gao et al. 2016a; Gao et al. 2016b) .

DVU2108 belongs to the Orange Protein (ORP) family and DVU2105 for an uncharacterized protein in *D. vulgaris* (Neca et al. 2016) exhibited declined protein levels only in the presence of 8.0 μg N/L at 12 h incubation. This complex has been proposed to be involved in the cell division of this organism. In *D. vuglaris*, there are two ORP gene clusters including DVU2103-DVU2104-DVU2105 (orp2) and DVU2107-DVU2108-DVU2109 (orp1) which encodes a protein complex in vivo, the absence of which induced aberrant cellular morphology. Down regulation of protein DVU2108 and DVU2105 imply that high FNA levels could cause cell morphology changes. However, there is no experimental evidence until now to support this. Protein DVU2569 for peptidyl-prolyl cis-trans isomerase which involves in cell wall biosynthesis (Stolyar et al. 2007) was found to be down regulated in the presence of 4.0 and 8.0 μg N/L FNA at 8 h and 12 h incubation. This may implicate a pause in cell growth in cell wall composition to the stress, in agreement with the observation of *D. vulgaris* with alkaline stress (Stolyar et al. 2007). Up regulation of several proteins involved in periplasmic binding, transport, and excretion such as DVU1260 for outer

membrane protein P1, DVU1343 for cation ABC transporter, and DVU1612 for ACT domain protein occurred in cultures when exposed to 4.0 and 8.0 μg N/L FNA.

Several universal stress proteins (DVU0261, DVU0423, and DVU1030) in *D. vulgaris* Hildenborough had different expression levels with FNA stress, in which DVU0261 showed decreased expression levels with the increased FNA concentration and incubation time, DVU0423 showed almost no change while DVU1030 exhibited increased expression levels with FNA stress (Table 6). There is a study reporting that DVU1030 is a stasis induced protein (Clark et al. 2006), indicating FNA changed the cultures from active status to stationary phase. It can be inferred that DVU0423 and DVU1030 contribute to the FNA stress response in *D. vulgaris* Hildenborough. DVU2441 for heat shock protein increased its protein levels in the presence of 4.0 and 8.0 μg N/L FNA. The response to heat shock represents a protective and homeostatic response which assist folding nascent proteins and repairing damaged proteins (Chhabra et al. 2006), indicating protein damage to the cultures occurred in the presence of FNA. In comparison, another heat shock protein DVU0811 for chaperone protein DnaK (Chhabra et al. 2006) showed decreased abundance at 12 h in the presence of 8.0 μg N/L FNA with no change at other FNA concentrations and incubation time.

In addition, many uncharacterized and hypothetical proteins (DVU0410, DVU0671, DVU1176, DVU1241, DVU2105, DVU2427, DVU4006, and DVUA202) displayed changed expression levels when exposed to FNA (Table 6). However, the detailed function of these proteins in response to FNA stress is not clear and needs further investigations, especially DVU1241 possibly encoding the homology cupin family protein which exhibited the highest increased protein expression levels in all FNA concentrations.

7) Discussion and comparison between transcriptomics and proteomics results

In summary, the proteomic results reveal that *D. vulgaris* Hildenborough initiates a coordination of differential protein expression allowing the alleviation of nitrite stress by nitrite reduction. The proteomics response dynamics to increasing FNA levels is in a logical way. Firstly, proteins involved in nitrite reduction especially HCP (DVU2543) were highly expressed with all FNA concentrations at all treatment time; Secondly, FNA concentration 4 and 8 μg N/L initially led to sulfate reduction (from sulfite to hydrogen sulfide) and lactate oxidation (from pyruvate to acetate) inhibition, then these inhibitions were evidenced to release in terms of increased protein levels involved in sulfate reduction and lactate oxidation at 8 and 12 h treatment when exposed to 4 and 8

μg N/L. Lastly, the levels of proteins involved in protein synthesis do not change much and could possibly be explained by the probable preservation of ribosomes by cultures as suggested by the previous transcriptomic data which can still be detected by SWATH-MS.

Proteomics results in this study are in good agreement with the transcriptomics results presented in section 3.3.3 in terms of three main parts including initially culture metabolism inhibition, protein synthesis inhibition before culture regrowth occurrence, and oxidative stress caused by FNA stress. More importantly, proteomics analysis with different FNA level over different treatment time provides more important insight on how FNA affects *D. vulgaris* Hildenborough and also how *D. vulgaris* Hildenborough responds to FNA stress. By using these two complementary analysis tools, a comprehensive and systematic understanding of the antimicrobial mechanisms of FNA on *D. vulgaris* Hildenborough was obtained.

Table 3. Proteins expression dynamics in the presence of different FNA concentrations relevant to metabolism

Gene ID	Gene name	1 µg vs Control			4 µg vs Control			8 µg vs Control		
		2h_LFC	8h_LFC	12h_LFC	2h_LFC	8h_LFC	12h_LFC	2h_LFC	8h_LFC	12h_LFC
Nitrite reduction										
DVU0625	Cytochrome c-552 nitrite reductase	0.39	0.99	0.68	0.09	-0.22	-0.37	0.14	-0.14	-0.29
DVU2543	Hybrid cluster protein	-0.22	5.37	4.05	2.94	4.51	3.81	1.73	3.72	3.09
DVU2544	Iron-sulfur cluster-binding protein	-0.23	4.6	3.93	2.43	3.2	3.66	1.35	1.93	2.61
Sulfate reduction										
DVU0263	Acidic cytochrome c3	0.84	0.58	0.28	-0.03	0.23	-0.45	0.23	-0.14	-0.9
DVU0266	Uncharacterized protein	0.81	-0.21	-0.3	-0.03	-0.5	-0.68	0.07	-0.38	-0.7
DVU0402	Sulfite reductase, dissimilatory-type subunit alpha	0.56	0.27	0.04	-0.04	0.19	0.14	-0.08	0.07	0.16
DVU0403	Sulfite reductase, dissimilatory-type subunit beta	0.56	0.02	0.03	0.05	-0.11	0.01	0.02	-0.05	-0.16
DVU0847	Adenylylsulphate reductase beta-subunit	0.21	0.27	-0.03	0.31	0.89	0.41	0.27	0.58	0.46
DVU0846	Adenylyl-sulphate reductase, alpha subunit	0.21	0.17	0.15	0	0.55	0.5	-0.05	0.39	0.49
DVU0848	Heterodisulfide reductase, putative	0.21	-0.09	0.01	-0.12	0.13	0.22	0.01	0.13	0.2
DVU0849	Heterodisulfide reductase, iron-sulfur-binding subunit, putative	0.21	-0.13	0.04	0.25	0.24	0.51	0.11	-0.06	0.55
DVU0850	Heterodisulfide reductase, transmembrane subunit, putative	0.2	-0.35	0.1	-0.36	-1.65	-0.54	0.34	-0.8	-0.98
DVU1287	Reductase, iron-sulfur binding subunit, putative	0.09	0.22	-1.61	-0.56	NA	0.31	-0.73	-0.21	0.78
DVU1295	Sulfate adenylyltransferase	0.09	0.2	0.11	-0.09	0.44	0.63	-0.23	0.38	0.55
DVU1597	Sulfite reductase, assimilatory-type	0	0.12	-0.05	-0.19	0	0.06	0.1	-0.14	-0.28
Lactate oxidation										
DVU0448	GDP-mannose 4,6-dehydratase	0.53	-0.25	-0.09	-0.2	-0.62	-0.41	-0.37	-0.31	-0.08
DVU0565	Glyceraldehyde-3-phosphate dehydrogenase	0.43	-0.27	-0.22	0.14	-0.78	-1.06	0.34	-0.55	-0.73
DVU0587	Formate dehydrogenase, alpha subunit, selenocysteine-containing	0.42	-0.13	0.27	0.21	-0.26	-0.08	0.47	0.05	0.22
DVU0588	Formate dehydrogenase, beta subunit, putative	0.41	0.08	0.25	0.19	-0.19	-0.09	0.32	-0.08	-0.07
DVU0589	Molybdopterin-guanine dinucleotide biosynthesis protein B, putative	0.41	-0.41	-0.19	-0.66	-1.62	-0.96	-0.14	-1.1	-1.24
DVU1569	Pyruvate ferredoxin oxidoreductase, alpha subunit	0.01	-0.28	0.03	0.15	-1.34	-0.53	0.34	-0.57	-0.67
DVU1570	Pyruvate ferredoxin oxidoreductase, beta subunit	0.01	0.11	0.08	0.15	-0.79	-0.89	0.22	-0.63	-0.77
DVU2201	Alcohol dehydrogenase, iron-containing	-0.1	-0.18	-0.21	0.3	-0.53	-0.67	0.51	-0.44	-0.78

DVU2451	L-lactate permease family protein	-0.17	0.05	-0.67	-0.01	0.02	-0.63	-0.06	-0.01	-0.45
DVU2482	Formate dehydrogenase, alpha subunit, selenocysteine-containing	-0.18	-0.06	-0.11	0.34	-0.52	-0.64	0.44	-0.31	-0.43
DVU3026	L-lactate permease family protein	-0.4	0.45	-0.1	-0.03	0.18	0.36	0.24	-0.26	0.26
DVU3028	Glycolate oxidase iron-sulfur subunit	-0.41	-0.43	-0.24	0.43	-0.42	-0.17	1.21	-0.49	-0.23
DVU3027	Glycolate oxidase, subunit GlcD	-0.41	-0.03	-0.1	0.24	-0.04	-0.05	-0.76	-0.43	-0.22
DVU3025	Pyruvate-ferredoxin oxidoreductase	-0.4	0.06	-0.11	0.11	0.12	-0.16	0.17	0.17	-0.18
DVU3029	Phosphate acetyltransferase	-0.41	0.22	-0.67	0.35	0.34	0.02	0.69	0.49	1.16
DVU3030	Acetate kinase	-0.42	-0.01	-0.13	-0.03	0.09	0.13	-0.15	0.1	0.26
DVU3032	Uncharacterized protein	-0.42	0.24	0.07	0.24	0.64	0.46	0.19	0.64	0.7
DVU3033	Iron-sulfur cluster-binding protein	-0.46	0.21	0.14	0.64	0.87	0.86	0.79	0.75	0.8
DVU3348	2-oxoglutarate/2-oxoacid ferredoxin oxidoreductase, subunit beta	-1.37	-0.24	-0.23	-0.18	-2.14	-0.72	-0.08	-0.74	-0.38
DVU3349	Pyruvate flavodoxin/ferredoxin oxidoreductase, thiamine diP-binding domain protein	-1.46	-0.26	-0.25	-0.34	-0.57	-0.3	-0.23	-0.43	-0.2
ATP synthesis										
DVU0777	ATP synthase subunit alpha	0.27	0.1	0.13	0.16	0.37	0.44	0.01	0.41	0.46
DVU0774	ATP synthase epsilon chain	0.28	-0.75	-1.38	-1.06	-0.4	-1.22	-0.65	-0.01	0.46
DVU0775	ATP synthase subunit beta	0.28	0.14	0.13	0.37	0.5	0.51	0.2	0.5	0.57
DVU0776	ATP synthase gamma chain	0.28	-0.14	0.14	0.28	-0.41	-0.18	0.37	-0.21	0.01
Electron transfer										
DVU0431	Ech hydrogenase, subunit EchD, putative	0.53	-0.37	-0.57	0.06	-0.87	NA	-0.27	-0.03	0.14
DVU0535	Protein DVU0535 (HMC operon ORF 2)	0.43	0.31	-0.2	0.93	0.85	1.68	0.22	0.97	2.3
DVU0536	High-molecular-weight cytochrome c	0.43	0.27	0.3	-0.42	-0.4	0.04	-0.8	-0.93	-0.99
DVU2792	Electron transport complex protein RnfC, putative	-0.27	-0.68	-0.23	-0.16	-1.02	-1.1	-0.61	-1.25	-0.7
Hydrogenases										
DVU1769	Periplasmic [Fe] hydrogenase large subunit	-0.02	0.09	-0.05	0.11	0.71	-0.01	0.28	-0.43	0.11
DVU1917	Periplasmic [NiFeSe] hydrogenase, small subunit	-0.05	0.13	-0.05	0.11	-0.08	-0.16	0.04	0.07	-0.11
DVU1918	Periplasmic [NiFeSe] hydrogenase, large subunit, selenocysteine-containing	-0.05	0.23	0.29	-0.01	0.05	0.19	0	0.06	0.03
DVU1921	Periplasmic [NiFe] hydrogenase small subunit 1	-0.06	0.08	-0.62	NA	0.27	-0.16	NA	NA	NA
DUV1922	Periplasmic [NiFe] hydrogenase, large subunit, isozyme 1	-0.06	0.43	0.05	-0.53	0.28	-0.4	-1.54	-1.49	-1.58
DVU2329	Hydrogenase accessory protein HypB	-0.13	-0.3	-0.3	-0.22	-0.4	-0.57	-0.64	-0.28	-0.34

Note: LFC of the detected proteins with adjusted q value less than 0.001 is shown in red in which proteins with LFC ≥0.5 or ≤-0.5 are defined as the differential expressed proteins in the presence of FNA, while LFC of the detected proteins with q value value less than 0.05 but larger than 0.001 is shown in blue. All others are the proteins with q value larger than 0.05.

Table 4. Proteins expression dynamics in the presence of different FNA concentrations relevant to protein synthesis and amino acid metabolism

Gene ID	Gene name	1 μg vs Control			4 μg vs Control			8 μg vs Control		
		2h_LFC	8h_LFC	12h_LFC	2h_LFC	8h_LFC	12h_LFC	2h_LFC	8h_LFC	12h_LFC
DVU0504	30S ribosomal protein S15	0.44	-2	2.34	-0.1	-0.08	2.35	-0.15	0.4	2.78
DVU0835	50S ribosomal protein L19	0.22	-0.44	-1.08	0.03	-1.62	-1.77	0.16	-0.67	-0.89
DVU0837	Ribosome maturation factor RimM	0.22	0.57	-0.05	-0.24	1.09	0.51	-0.48	0.86	0.2
DVU0839	30S ribosomal protein S16	0.22	0.08	0.01	-0.3	0.06	-0.56	-0.16	0	0.03
DVU0870	Ribosome-recycling factor (RRF)	0.19	-0.02	0.1	-0.62	0.76	-0.17	-0.2	1	0.46
DVU0874	30S ribosomal protein S2	0.19	-0.25	0.46	0.99	0.32	1.25	0.67	0.08	1.42
DVU0927	50S ribosomal protein L21	0.18	0.98	0.25	0.11	1.12	0.86	0.42	1.11	1.18
DVU0956	30S ribosomal protein S6	0.17	0.15	0.09	-0.43	0.81	0.93	0.75	0.65	1.32
DVU0957	30S ribosomal protein S18	0.17	0.13	-0.3	0.54	1	0.49	0.25	0.83	0.85
DVU0958	50S ribosomal protein L9	0.17	0.51	-0.17	0.07	1.39	0.8	1.08	0.75	0.86
DVU1209	50S ribosomal protein L32	0.12	1.13	0.8	-0.71	2.02	2.33	0.37	1.57	2.42
DVU1211	50S ribosomal protein L28	0.12	0.87	1.05	0.7	0.81	1.04	0.93	0.45	0.72
DVU1298	30S ribosomal protein S12	0.09	-0.17	-0.74	-0.61	-0.41	0.06	0.26	-0.31	-0.29
DVU1299	30S ribosomal protein S7	0.09	-0.35	0.04	0.04	-0.9	0.18	0.36	-0.26	-0.08
DVU1302	30S ribosomal protein S10	0.08	0.17	0.68	0.05	-0.24	0.54	0.14	0.31	0.57
DVU1303	50S ribosomal protein L3	0.08	0.42	0.28	-0.03	0.3	0.67	-0.06	-0.04	0.57
DVU1304	50S ribosomal protein L4	0.08	-0.25	0.78	-0.98	-0.58	0.23	0.39	0.33	1.86
DVU1305	50S ribosomal protein L23	0.08	-0.25	0.6	0.11	-0.73	1.17	1.6	0.24	0.78
DVU1306	50S ribosomal protein L2	0.08	0.28	0.17	0.12	0.23	0.65	0.24	0.28	0.61
DVU1307	30S ribosomal protein S19	0.08	0.15	-0.05	0.09	-0.27	-0.17	0.13	-0.17	-0.27

DVU1308	50S ribosomal protein L22	0.08	1.32	0.26	-0.32	0.35	0.5	-0.19	0.04	1.01
DVU1309	30S ribosomal protein S3	0.07	0.97	0.53	-0.03	1.88	1.33	-2.14	1.28	1.54
DVU1310	50S ribosomal protein L16	0.07	-0.42	-0.36	-1.24	0.35	1.02	-0.07	-0.23	1.94
DVU1312	30S ribosomal protein S17	0.07	0.5	-1.4	-0.08	-1.77	-0.13	0.23	-0.4	-0.05
DVU1313	50S ribosomal protein L14	0.07	0.17	0.3	-0.43	0.37	-0.05	0.47	0.18	0.01
DVU1315	50S ribosomal protein L5	0.07	-0.18	-0.48	-0.94	0.95	0.49	1.69	0.73	1.11
DVU1317	30S ribosomal protein S8	0.07	0.33	0.16	-0.17	0.65	0.82	0.41	0.99	0.67
DVU1318	50S ribosomal protein L6	0.07	0.72	1.71	-0.49	0.29	0.53	0.05	-1.21	0.89
DVU1319	50S ribosomal protein L18	0.06	0.26	0.12	-0.28	0.2	1.1	0.25	0.43	1.05
DVU1320	30S ribosomal protein S5	0.06	-0.31	0.53	-1.02	-0.4	0.03	-0.81	-0.05	0.2
DVU1322	50S ribosomal protein L15	0.06	0.57	0.22	-0.2	0.67	0.75	-0.12	0.45	0.74
DVU1326	30S ribosomal protein S13	0.06	0.22	-0.16	0.16	0.04	0	0.42	0.19	0.08
DVU1327	30S ribosomal protein S11	0.06	0.68	0.73	-0.2	0.02	0.84	0.35	-0.38	0.3
DVU1328	30S ribosomal protein S4	0.06	0.35	0.1	-0.47	0.83	0.98	0.5	0.9	1.07
DVU1330	50S ribosomal protein L17	0.05	0.25	0.13	-0.01	0.34	0.88	0.6	0.4	1.18
DVU1429	Ribosome-binding ATPase YchF	0.03	0.74	0.04	0.08	0.76	0.53	0.37	-0.5	0.22
DVU1469	Ribosomal protein S1, putative	0.02	0.08	-0.03	0.11	-0.19	-0.45	-0.01	-0.17	-0.46
DVU1574	50S ribosomal protein L25	0.01	-0.14	0.21	0	0.28	0.1	0.27	-0.88	0.16
DVU1618	Ribosomal silencing factor RsfS	0	0.13	-0.82	-1.11	-0.08	0.14	-0.72	0.41	0.98
DVU1792	30S ribosomal protein S21	-0.02	1.27	0.19	0.76	1.35	-0.76	1.89	-0.03	1.02
DVU1896	30S ribosomal protein S20	-0.04	0.74	0.96	-0.34	0.51	1.11	-0.1	0.43	1.27
DVU2339	Ribosomal protein L11 methyltransferase, putative	-0.14	-0.29	-0.19	0.69	0.15	0.5	0.35	-0.18	0.59
DVU2519	30S ribosomal protein S9	-0.2	0.11	-0.02	-0.1	-0.07	0.23	0.01	0.07	0.24
DVU2535	50S ribosomal protein L20	-0.21	0.55	-0.2	0.51	-1.12	-1.03	0.27	-1.18	-0.37
DVU2536	50S ribosomal protein L35	-0.21	-0.51	-1	-0.69	-0.62	-0.03	-0.24	-0.2	0.41
DVU2921	50S ribosomal protein L33	-0.31	0.13	-2.32	-1.3	0.33	-0.01	0.77	-0.23	-0.65
DVU2924	50S ribosomal protein L11	-0.32	0.85	-0.63	0.04	0.45	0.71	0.36	0.46	0.56
DVU2925	50S ribosomal protein L1	-0.32	0.63	0.16	-0.48	1.22	1.18	0.5	1.24	0.53
DVU2926	50S ribosomal protein L10	-0.32	-0.11	-0.28	-0.96	-0.61	-0.57	-1.43	-2.16	-1.8

DVU2927	50S ribosomal protein L7/L12	-0.33	0.16	-0.16	-0.01	0.15	0.04	-0.11	0.44	0.06
DVU2981	2-isopropylmalate synthase	-0.37	0.17	0.22	0.04	0.43	0.65	-0.11	0.32	0.33
DVU3150	Ribosomal protein S1	-0.61	0.07	0.07	0.04	0.14	0.1	-0.13	0.16	0.02
DVU3168	Glutamate-1-semialdehyde 2,1-aminomutase	-0.63	0.06	0.01	0.27	0.65	0.65	-0.05	0.63	0.55

Note: LFC of the detected proteins with adjusted q value less than 0.001 is shown in red in which proteins with LFC ≥0.5 or ≤-0.5 are defined as the differential expressed proteins in the presence of FNA, while LFC of the detected proteins with q value value less than 0.05 but larger than 0.001 is shown in blue. All others are the proteins with q value larger than 0.05.

Table 5. Proteins expression dynamics in the presence of different FNA concentrations relevant to oxidative stress

Gene ID	Gene name	1 μg vs Control			4 μg vs Control			8 μg vs Control		
		2h_LFC	8h_LFC	12h_LFC	2h_LFC	8h_LFC	12h_LFC	2h_LFC	8h_LFC	12h_LFC
DVU0019	Nigerythrin	2.32	0.21	0.27	0.21	0.23	0.23	-0.1	-0.26	-0.32
DVU0264	Ferredoxin, 4Fe-4S, putative	0.84	-0.18	-0.19	-0.09	-0.13	-0.27	-0.03	-0.11	-0.32
DVU0273	Uncharacterized protein	0.8	0.03	0.26	-0.41	-1.1	-0.57	-0.39	-0.23	-0.41
DVU0278	Glyoxalase family protein	0.72	0.52	0.53	-0.22	-0.39	-0.34	-0.17	-0.6	-0.55
DVU0305	Ferredoxin II	0.68	-0.05	-0.45	-0.01	-0.71	-0.42	-0.04	-0.31	-0.55
DVU0772	Uncharacterized protein	0.29	-1.27	0.45	0.73	2.91	3.12	0.18	1.67	2.69
DVU0995	ThiJ/PfpI family protein	0.16	0.01	0.2	-0.08	-0.32	-0.34	-0.09	-0.64	-0.72
DVU1228	Probable thiol peroxidase	0.11	-0.25	-0.11	-0.07	-0.71	-0.56	-0.06	-0.81	-0.9
DVU1397	Bacterioferritin	0.04	-0.19	-0.42	-0.01	0.13	-0.02	-0.07	-0.22	-0.42
DVU1457	Thioredoxin reductase, putative	0.02	0.39	0.37	-0.08	0.07	0.12	-0.11	0.04	0.07
DVU1568	Ferritin	0.01	-0.05	0.17	-0.17	-1.03	-0.76	-0.13	-1.16	-0.85
DVU1838	Thioredoxin-disulfide reductase	-0.03	0.2	-0.39	0	-0.04	-0.24	0.06	-0.11	-0.08
DVU1839	Thioredoxin	-0.03	0.08	0.02	0.07	-0.04	0.05	0.13	0.03	0.14
DVU1984	Peptide methionine sulfoxide reductase MsrA	-0.08	-0.53	0.64	-0.52	-0.2	-0.48	0.09	0.75	-0.24
DVU2247	Alkyl hydroperoxide reductase C	-0.12	0.31	0.2	-0.19	0.73	0.85	-0.42	0.59	0.72
DVU2318	Rubrerythrin, putative	-0.13	-0.45	-0.34	-0.25	-0.23	-0.12	-0.32	-0.51	-0.34

DVU2410	Superoxide dismutase, Fe-Mn family	-0.16	-0.48	0.41	0.15	-1.62	-0.29	-0.42	-1.26	-1.01
DVU2680	Flavodoxin	-0.25	0.98	0.71	0.13	0.84	0.52	-0.33	0.26	0.17
DVU3049	Hemerythrin family protein	-0.48	0.24	0.28	-0.24	-0.18	-0.11	-1.2	-0.27	-0.08
DVU3093	Rubredoxin	-0.55	0.05	-0.08	0.67	0.88	-0.26	0	-0.93	0.01
DVU3094	Rubrerythrin (Rr)	-0.55	-0.08	0.01	-0.19	-0.71	-0.51	-0.2	-0.77	-0.83
DVU3183	Desulfoferrodoxin (Dfx)	-0.64	-0.08	0.02	-0.13	-0.26	-0.32	-0.13	-0.41	-0.64
DVU3185	Rubredoxin-oxygen oxidoreductase	-0.64	-0.05	-0.18	-0.02	-0.35	-0.43	-0.04	-0.25	-0.37
DVU3212	Pyridine nucleotide-disulfide oxidoreductase	-0.73	0.25	0.16	0.33	0.63	0.81	0.21	0.82	1.01
DVU3276	Ferredoxin I	-0.98	-0.93	-0.77	0.15	-1.33	-2.01	-0.29	-1.7	-2.2
DVU3282	ADP-ribosylglycohydrolase family protein	-1.04	0.2	0.16	-0.17	0.18	0.06	-0.19	-0.07	-0.27
DVUA0091	Catalase	NA	-0.19	-0.19	-0.18	-0.39	-0.77	0.08	-0.44	-1.15

Note: LFC of the detected proteins with adjusted q value less than 0.001 is shown in red in which proteins with LFC ≥0.5 or ≤-0.5 are defined as the differential expressed proteins in the presence of FNA, while LFC of the detected proteins with q value value less than 0.05 but larger than 0.001 is shown in blue. All others are the proteins with q value larger than 0.05.

Table 6. Proteins expression dynamics differences in the presence of four different FNA concentrations at different treatment time.

Gene ID	**Gene name**	**1 μg vs Control**			**4 μg vs Control**			**8 μg vs Control**		
		2h_LFC	8h_LFC	12h_LFC	2h_LFC	8h_LFC	12h_LFC	2h_LFC	8h_LFC	12h_LFC
1.0 μg N/L										
DVU0004	DNA gyrase subunit A	3.71	0.22	0.19	0.2	0	-0.64	-0.19	-0.52	-0.54
DVU0042	RNA methyltransferase	1.91	0.82	-0.16	0.53	1.29	0.77	-0.12	-0.05	0.55
DVU0419	Carboxynorspermidine/carboxyspermidine decarboxylase	0.54	-0.68	-0.27	-0.2	-0.87	-0.67	-0.49	-1.92	-0.93
DVU3199	Nucleoid-associated protein DVU3199	-0.7	0.45	1.19	0.42	0.58	0.68	0.29	0.63	0.62
DVU3228	Chemotaxis protein CheY	-0.76	-0.16	0.07	-0.14	-0.52	-0.47	0.43	-1.01	-0.24
DVUA0132	CRISPR-associated protein, TM1801 family	4.94	0.04	0.11	-0.35	-0.8	-0.49	0.05	-0.59	-1.19
DVUA0146	Uncharacterized protein	3.96	-1.19	0.08	-0.86	-0.38	0.56	-0.83	-1.96	-1.52
4.0 μg N/L										

DVU0034	DSBA-like thioredoxin domain protein	1.91	-0.39	0.08	-0.1	-1.12	-0.5	0.11	-0.58	-0.41
DVU0060	Efflux transporter, RND family, MFP subunit	1.82	-0.3	-0.16	-0.4	-0.79	-0.61	-0.17	-0.4	-0.54
DVU0417	Arginine decarboxylase	0.54	-0.33	-0.45	-0.38	-0.97	-0.84	-0.14	-0.75	-0.65
DVU0423	Universal stress protein family	0.53	0.21	0.17	0.55	0.42	0.42	0.03	0.18	0.11
DVU0854	NirD protein, putative	0.2	-0.41	-0.17	-0.07	-0.75	-0.65	0.07	-0.57	-0.43
DVU1176	Uncharacterized protein	0.13	-0.08	0	0.02	-0.52	-0.33	-0.08	-0.36	-0.35
DVU2093	ThiH protein	-0.09	-0.18	-0.12	-0.21	-1.88	-1.23	0.17	-0.79	-1.13
DVU3055	Ribonuclease, Rne/Rng family	-0.51	-0.05	-0.33	0.26	-1.77	-0.42	0.44	-0.51	-0.81
8.0 µg N/L										
DVU0319	NAD-dependent epimerase/dehydratase family protein	0.66	-0.19	0.01	0.35	-0.14	-0.34	0.27	-0.59	-0.43
DVU0353	Alcohol dehydrogenase, iron-containing	0.61	0.04	-0.02	-0.08	-0.24	-0.2	-0.08	-0.34	-0.54
DVU0418	Saccharopine dehydrogenase	0.54	-0.18	-0.39	-0.14	-0.47	-0.56	-0.14	-0.76	-1.32
DVU0664	Cysteine desulfurase	0.37	-0.11	-0.15	-0.23	-0.2	-0.27	-0.23	-0.19	-0.52
DVU0811	Chaperone protein DnaK (HSP70)	0.25	0.24	-0.11	-0.14	-0.32	-0.37	-0.13	-0.25	-0.68
DVU0857	Radical SAM domain protein	0.19	-0.21	0	-0.29	-0.31	-0.14	-0.35	-0.64	-0.45
DVU1382	HesB family selenoprotein	0.04	0.14	-0.07	-0.2	-0.18	-0.45	-0.16	-0.13	-0.6
DVU1864	DNA-binding protein HU, beta subunit, putative	-0.04	1.37	1.5	0.17	1.43	1.82	-0.54	1.49	2.56
DVU1878	Threonine aldolase, low-specificity	-0.04	-0.16	-0.08	-0.12	-0.6	-0.61	-0.52	-0.71	-0.68
DVU1937	Phosphonate ABC transporter, periplasmic phosphonate-binding protein, putative	-0.06	-0.07	0.01	0.01	-0.22	-0.38	0.11	-0.29	-0.84
DVU1951	Indolepyruvate oxidoreductase subunit IorA	-0.07	-0.3	-0.29	-0.6	-0.38	-0.12	-0.85	-0.38	-0.23
DVU2105	Uncharacterized protein	-0.09	-0.34	-0.4	-0.56	-1.02	-0.76	-0.89	-1.51	-1.62
DVU2108	MTH1175-like domain family protein	-0.1	-0.28	-0.2	-0.02	-0.6	-1.03	0.07	-0.81	-1.78
DVU2929	DNA-directed RNA polymerase subunit beta	-0.34	-0.18	0.14	-0.42	-0.52	-0.32	-0.58	-0.46	-0.89
DVU3065	AMP-binding enzyme family protein	-0.53	-0.25	-0.26	-0.26	-0.21	-0.27	-0.47	-0.33	-0.53
DVU3181	Phosphoribosylformylglycinamidine synthase subunit PurL	-0.64	0.02	-0.02	-0.06	-0.07	-0.16	-0.2	-0.2	-1.21
4.0 and 8.0 µg N/L										
DVU0007	Asparagine--tRNA ligase	2.98	-0.2	-0.21	-0.13	-0.54	-0.58	0.03	-0.29	-0.53
DVU0261	Universal stress protein family	0.85	-0.27	-0.19	-0.04	-0.62	-0.68	0.14	-0.42	-0.6
DVU0410	Uncharacterized protein	0.55	-0.24	-0.03	-0.18	-0.64	-0.76	-0.27	-0.34	-0.67

DVU0671	Uncharacterized protein	0.36	0.05	0.02	0.09	0.4	0.57	0.11	0.49	0.59
DVU1030	Universal stress protein	0.15	0.2	0.08	0.42	0.75	0.84	0.03	0.57	0.8
DVU1241	Uncharacterized protein	0.11	5.48	4.26	3.63	5.1	4.43	3.28	4.99	4.13
DVU1257	RNA-binding protein	0.1	0.01	-0.15	-0.44	-1.04	-0.95	-0.53	-0.65	-0.74
DVU1260	Outer membrane protein P1, putative	0.1	0.11	0.14	0.16	0.4	0.43	0.01	0.53	0.63
DVU1343	Cation ABC transporter, periplasmc-binding protein	0.05	0.36	0.28	0.21	1.16	1.1	0.15	1.06	0.89
DVU1612	ACT domain protein	0	0.2	0.09	0.28	0.53	0.7	0.23	0.44	0.84
DVU2347	Acetylornithine aminotransferase	-0.14	-0.05	0.03	0.01	-0.85	-1.06	-0.18	-0.99	-1.07
DVU2422	Nitroreductase family protein	-0.16	-0.44	-0.21	-0.03	-0.69	-0.87	0.18	-0.56	-0.88
DVU2427	Uncharacterized protein	-0.16	0.03	-0.03	0.32	0.2	-0.55	0.2	-0.06	-0.62
DVU2441	Heat shock protein, Hsp20 family	-0.17	0.04	-0.1	0.6	0.89	0.8	0.5	1	0.89
DVU2569	Peptidyl-prolyl cis-trans isomerase	-0.23	-0.15	-0.21	-0.28	-0.49	-0.78	-0.4	-0.44	-0.61
DVU2590	Sensory box protein	-0.24	-0.13	-0.12	-0.09	-0.29	-0.67	-0.09	-0.2	-0.51
DVU2770	Response regulator	-0.26	-0.01	-0.11	0.63	-0.11	-0.16	0.7	-0.12	-0.11
DVU3319	Bifunctional protein PutA	-1.22	-0.24	-0.08	-0.07	-0.75	-0.74	0.11	-0.62	-0.88
DVU4006	hypothetical protein	NA	0.34	0.15	0.36	0.8	0.57	0.03	0.65	0.48
DVUA202	hypothetical protein	NA	-0.2	-0.08	-0.08	-0.64	-0.86	0.08	-0.75	-0.99

Note: LFC of the detected proteins with adjusted q value less than 0.001 is shown in red in which proteins with LFC ≥0.5 or ≤-0.5 are defined as the differential expressed proteins in the presence of FNA, while LFC of the detected proteins with q value value less than 0.05 but larger than 0.001 is shown in blue. All others are the proteins with q value larger than 0.05.

3.3.5 Comparison of responses between *P. aeruginosa* PAO1 and *D. vulgaris* Hildenborough to the antimicrobial agent FNA

This thesis describes the antimicrobial effects of FNA on two model microbes (*P. aeruginosa* PAO1 and *D. vulgairs* Hildenborough) using a combination of physiological detections and molecular techniques. In order to successfully observe the responses of microbes to FNA from the transcriptional and translational level, transcriptomics and quantitative proteomics methods were chosen. Using these newly developed techniques combined with physiological and substrate consumption measurements, the mechanism of antimicrobial effect of FNA were revealed.

FNA inhibits carbon utilization, anaerobic respiration and energy production for both *P. aeruginosa* PAO1 and *D. vulgaris* Hildenborough

There is potential for FNA to act as uncoupler and disrupt the cellular proton motive force (Zhou et al. 2011). Such action would decrease respiration and impair the energetics and ATP production. This was indeed detected when *P. aeruginosa* PAO1 and *D. vulgaris* Hildenborough were exposed to FNA and additionally a decrease in intracellular pH was detected as well. These events all support that FNA was acting as an uncoupler of the proton motive force.

P. aeruginosa PAO1 was cultivated in anaerobic denitrifying conditions with nitrate as the electron acceptor and glycerol the electron donor. In the presence of FNA, a number of transcripts coding for enzymes involved in denitrification and glycerol utilization processes were down regulated. This included the genes for nitrate reductase, nitrite reductase, and N_2O reductase. Additionally, genes coding for NADH dehydrogenase and ATP synthase were down regulated in the presence of FNA. In the presence of FNA glycerol utilisation was lowered, and this coincided with genes for glycerol metabolism having decreased expression when exposed to FNA. For example, Genes encoding enzymes involved in the TCA cycle (*sdhABCD, sucABCD, ipdG*) were down regulated, suggesting this cycle was less active during FNA exposure.

In *D, vulgaris* Hildenborough, lactate oxidation provides electrons for dissimilatory sulfate reduction and these processes are coupled to generate the proton motive force for ATP generation inside the cells (Heidelberg et al. 2004). In the presence of FNA, various genes coding for enzymes involved in lactate oxidation and sulfate reduction processes were down regulated. This included

the genes DVU0848-50 for quinone-interacting membrane-bound oxidoreductase (Qmo complex) and DVU1286-87, DVU1289-90 for sulfite reductase (Dsr) complexes. It is proposed that Qmo complexes transfer electrons from lactate oxidation directly to APS reductase while Dsr complexes transfer electrons to the sulfite reductase (Heidelberg et al. 2004). Recently an operon has been described for lactate oxidation genes (*luo*) in *D. vulgaris* (Vita et al. 2015). This includes genes for lactate permease DVU3026, lactate dehydrogenase (ldh) subunits DVU3027-28 and DVU3032-33, pyruvate-ferredoxin oxidoreductase (PFOR) DVU3025, acetate kinase (ackA) DVU3030, and phosphate acetyltransferase DVU3029. Down-regulation of all the *luo* operon genes were detected when exposed to FNA.

Differences in FNA effect on carbon flux pathways for *P. aeruginosa* PAO1 and *D. vulgaris* Hildenborough

In response to FNA, transcripts of genes coding pyruvate dehydrogenase (PA3416 and PA3417) and dihydrolipoamide acetyltransferase (PA3415) displayed the greatest increases in transcription after FNA treatment in *P. aeruginosa* PAO1. These enzymes produce acetyl-CoA, which would normally feed into the TCA cycle when respiration is active. However, in FNA exposure, respiration and the TCA cycle were inhibited. The genes coding the pyruvate fermentation pathway and specifically required stress proteins (aceF, *pta, ackA,* PA1753, PA3017, PA3309, PA4352) all showed increased abundance after FNA exposure (Schreiber et al. 2006). The possible fermentation products or intermediates pyruvic acid, formic acid, ethanol and lactic acid were not detected in the control or FNA-treated cultures. In contrast, in the presence of FNA there was a 37-fold increase in acetic acid levels in comparison to cells not exposed to added FNA. It seems in response to FNA, unable to produce ATP through respiration, *P. aeruginosa* PAO1 converted the produced acetyl-CoA to acetate through pyruvate fermentation to generate ATP. In response to FNA, unlike *P. aeruginosa* PAO1, there is no evidence for other alternative lactate utilisation pathway in *D. vulgaris* Hildenborough.

Differences in cellular redox status in the presence of FNA for *P. aeruginosa* PAO1 and *D. vulgaris* Hildenborough

FNA is reported to cause oxidative stress to bacterial cells (Poole 2005). Thus, the intracellular redox of *P. aeruginosa* PAO1 and *D. vulgaris* Hildenborough was measured in the presence of

FNA. The results demonstrated when exposed to FNA in general the *P. aeruginosa* PAO1 cells became more reduced while *D. vulgaris* Hildenborough cells becomes more oxidised compared with control cultures without FNA addition. It seems that the oxidative stress caused by FNA is genera dependent and the reason for this could possibly be the oxidative stress in *D. vulgaris* is stronger than that in *P. aeruginosa*. This is explainable since *P. aeruginosa* is a facultative bacterium with more capability to deal with oxidative stress than the strict anaerobe *D. vulgaris*. Understanding the details of oxidative response is important to fully uncover the effect of FNA on microbes.

FNA disrupts DNA replication, transcription and translation for both *P. aeruginosa* PAO1 and *D. vulgaris* Hildenborough

In *P. aeruginosa* PAO1, genes coding key enzymes involved in DNA replication (i.e. DNA polymerase, ATP-dependent DNA helicase) and transcription (DNA-directed RNA polymerase) showed decreased transcripts during exposure to FNA. Additionally, genes encoding various molecules in protein synthesis including ribosomal RNA processing proteins, various amino acid transfer RNA synthases, the small and large ribosome structural proteins, translation initiation and elongation factors, ribosome maturation protein Rimp (PA4746), 16s rRNA processing proteins (*rimM*), and ribosome-binding factor A (*rbfA*) were all down regulated. Similar to *P. aeruginosa* PAO1, genes encoding critical enzymes involved in DNA replication (e.g. chromosomal replication initiator protein DnaA, DNA polymerase, DNA gyrase, DNA topoisomerase) and transcription (DNA-directed RNA polymerase) exhibited down regulation after FNA exposure in *D. vulgaris* Hildenborough. As well, the genes coding for 30S and 50S ribosomal structure proteins (e.g. rpsP, rpsB, rpsF, rplS, rplU, rplB, and rplC) and a variety of amino acid transfer RNA synthetases showed significantly decreased transcripts. It was evident that FNA caused decreased activity of protein synthesis, DNA replication, and transcription in both *P. aeruginosa* PAO1 and *D. vulgaris* Hildenbrough. Inhibition of protein synthesis has been detected in previous studies investigating the response to acidified nitrite stress in *Salmonella enterica* (Mühlig et al. 2014).

It is interesting to know whether the inhibitory effects of FNA result from directly targeting metabolic or structural proteins, or whether these result from FNA causing altered gene expression. Genes coding for RMF and HPF were up regulated in response to FNA exposure in P. aeruginosa PAO1. These factors function to preserve active 70S ribosome units into inactive units in stressful conditions. Once the stress disappears, the inactive ribosomes are liberated from the RMF and the

HPF to become active again in translation (Kato et al. 2010; Polikanov et al. 2012). Similarly, the gene *yfi* coding for the ribosomal subunit interface protein in *D. vulgaris* Hildenborough displayed 14.42 fold up regulation during FNA exposure. This factor is demonstrated to stabilize ribosomes and stop translation in stressful conditions (Agafonov et al. 2001). Therefore, it is likely that for coping with FNA stress, microbes select to cease production of ribosomes and conserve the existing ones. This also implies that the ribosome itself is not the direct target of FNA mediated damage, but that ribosome inactivation is caused by altered regulation of its production and by its storage.

Detoxification plays an important role in alleviating the antimicrobial effect of FNA

In the growth conditions, *P. aeruginosa* PAO1 carried out denitrification using glycerol as the electron donor and nitrate and nitrite as electron acceptors. Denitrification activity was detected when the culture growth was temporarily inhibited by FNA at the concentration of 0.1 mg N/L. This denitrification activity would contribute to lower FNA levels and prevent accumulation of other oxidised nitrogen molecules to detoxify the conditions. On top of this, it is known that flavohaemoglobin is an important detoxifying oxidoreductase that converts toxic NO to non-toxic nitrate in the presence of N_2O in P*seudomonas* (Fang 2004). Our transciptome analysis revealed increased expression of the *fhp* gene encoding flavohaemoglobin during FNA addition. Thus, there is evidence here of a strategy by *P. aeruginosa* PAO1 through the increased activities of NO reductase and flavohaemoglobin for the removal of the toxic NO derived from FNA.

In comparison*, D. vulgaris* Hildenborough has NrfA that can reduce nitrite to ammonium, allowing it to survive in environments in the presence of nitrite (Haveman et al. 2004). Nitrite reduction occurred in the presence of FNA (Figure 11 A, B) after FNA addition. Genes coding for NrfA exhibited considerable up regulation in FNA-added cultures. This would imply the detoxifying role of NrfA for removal of nitrite (and proportional removal of FNA) which is the suggested role of the enzyme (Haveman et al. 2004). This observation agrees with the decreasing nitrite levels detected in the batch cultures (Figure 11A). In addition, another gene, DVU2543, which codes for what is known as the HCP that has a proposed hydroxylamine reductase (Wolfe et al. 2002), was the most up-regulated gene and also highly expressed protein detected when exposed to FNA. Possibly the HCP was acting to remove hydroxylamine as part of the detoxification of nitrite (Vine and Cole 2011), thereby protecting the cultures from oxidative stress conferred by FNA. Consequently, removal of nitrite was an important function during the FNA exposure both in *P. aeruginosa* and *D. vulgaris*.

Chapter 4 Conclusions and Future Work

4.1 Main conclusions of the thesis

This thesis describes the antimicrobial effects of FNA on two different bacteria with relevance to wastewater treatment, one is the denitrifier *P. aeruginosa* PAO1 and the other is the sulfate reducer *D. vulgaris* Hildenborough.

The potential concentration-related effects of FNA on *P. aeruginosa* PAO1 under anaerobic conditions were investigated. The main findings are:

- The antimicrobial effect of FNA on denitrifier *P. aeruginosa* PAO1 is concentration-determined. 0.1-0.2 mg N/L FNA exerted temporary inhibitory effect on the growth of *P. aeruginosa* PAO1, while 1.0 mg N/L caused complete inhibition of culture growth. 5.0 mg N/L FNA caused complete cell killing and likely cell lysis.
- The antimicrobial effect of FNA on *P. aeruginosa* PAO1 is population-specific. From low to high FNA levels, cell killing occurred in a subpopulation of *P. aeruginosa* PAO1 cells, while another subpopulation was inhibited in growth but still active in respiration, suggesting a considerable proportion of cells either already possessed or had developed tolerance to this FNA level, indicating possible differential tolerance towards FNA in the *P. aeruginosa* PAO1 cultures.
- A delayed recovery from FNA treatment suggested that FNA caused cell damage which required repair prior to the organism showing cell growth. Such damage may include disruption to the cell membrane as suggest by the LIVE/DEAD staining results.
- This study for the first time clearly shows that the growth of *P. aeruginosa* PAO1 is more sensitive to FNA than its respiratory activity. There is no clear concentration threshold to distinguish the bacteriostatic and bactericidal effects of FNA on the *P. aeruginosa* PAO1 population. Instead, a heterogeneous response was detected between cells. Additionally, a carry-over effect of FNA on the bacterial cells was detected. The results of the study provide insight of the inhibitory and biocidal mechanisms of FNA on this important microorganism.

The inhibitory mechanism of FNA on *P. aeruginosa* PAO1 and the responses of *P. aeruginosa* PAO1 on inhibitory level FNA exposure were determined by coupling gene expression analysis, by RNA sequencing, and with a suite of physiological analyses. The main findings are:

- The antimicrobial effects of FNA on *P. aeruginosa* PAO1 are multi-targeted.
- Respiration was likely inhibited as denitrification activity was severely depleted and decreased transcript levels of most denitrification genes occurred. As a consequence, the TCA cycle was inhibited due to the lowered cellular redox state in the FNA exposed cultures.
- During FNA exposure *P. aeruginosa* PAO1 rerouted its carbon metabolic pathway from the TCA cycle to pyruvate fermentation with acetate as the end product as a possible survival mechanism.
- Conditions within the cells were more reduced.
- Protein synthesis was significantly decreased while ribosome preservation was evident.
- In response to damaged proteins *P. aeruginosa* PAO1 produces new Fe-S clusters and degrades abnormal proteins for recycling of the amino acids.
- These findings improve our understanding of *P. aeruginosa* PAO1 in response to FNA, and contribute towards the potential application for use of FNA as an antimicrobial agent.

The antimicrobial mechanism of FNA on sulfate reducer *D. vulgaris* Hildenborough and the responses of *D. vulgaris* Hildenborough on various FNA levels were determined by determining growth, physiological and gene expression responses to FNA exposure. The main findings are:

- The antimicrobial effects of FNA on *D. vulgaris* Hildenborough are multi-targeted.
- The activities of growth, respiration and ATP generation were inhibited when exposed to FNA. These changes were reflected by the lowered expression of genes coding for lactate oxidation and sulfate reduction during exposure and suggest that *D. vulgaris* Hildenborough switched from a status of prolific growth to a phase of severely inhibited growth status in the presence of FNA.
- Removal of FNA was evident by nitrite reduction that likely involved nitrite reductase and the poorly characterised hybrid cluster protein, and the genes coding for these proteins were highly expressed.
- Lowered ribosome activity and protein production were detected.
- FNA caused more oxidative conditions in *D. vulgaris* Hildenborough and there was transcriptional evidence of attempts to alleviate the oxidative stress.
- These findings provide new insight for understanding the responses of *D. vulgaris* Hildenborough to FNA and will provide the foundation for optimal application of this antimicrobial agent for improved control of sewer corrosion and odor management.

A comprehensive and systematic understanding of the antimicrobial mechanisms of FNA regarding the protein expression dynamics with different FNA levels on *D. vulgaris* Hildenborough was performed by SWATH-MS quantitative method in the presence of four FNA concentrations (0, 1.0,4.0, and 8.0 μg/L) with three incubation periods after FNA addition (2, 8 and 12 h). The main findings are:

- The antimicrobial effects of FNA are multi-targeted as long as the growth inhibition occurred.
- For 1.0 μg N/L FNA, only the proteins involved in nitrite reduction (nitrite reductase and the poorly characterized hybrid cluster protein) showed obvious increased expression levels over incubation.
- In the presence of 4.0 and 8.0 μg N/L FNA, we also observed the evident increase of the protein levels for nitrite reduction over incubation. Proteins involved in sulfate reduction pathway (from sulfite to hydrogen sulfide) and lactate oxidation pathway (from pyruvate to acetate) were firstly inhibited by FNA at 8 h incubation, and then recovered at 12 h incubation.
- Lowered ribosomal protein levels were detected while the cellular protein levels for viable cells seems to be constant in the presence of FNA.
- There was evidence that DVU2543, DVU0772, and DVU3212 play a critical role in defending oxidative stress caused by FNA.
- These findings offer some new insights for understanding the dynamic responses of *D. vulgaris* Hildenborough to FNA and deliver important findings to guide practical applications of FNA-based technologies to better control corrosion in sewers.

4.2 Recommendations for future research

During the whole period of my PhD, many research challenges, in addition to the research objectives investigated so far, have been identified that entail further research. Some of these are summarized below:

- Our study demonstrated the presence of heterogeneous tolerance of the cell population to FNA. Whereas the mechanism of such differential tolerance (also namely heterogeneity) in a bacterial population towards FNA is unclear. This could be achieved by cell sorting using a flow cytometer and research on physiology, genome, transcriptomics, and proteomics responses of the sorted cells to FNA.

- It is worth to mention that the experiments were done at 30ºC which is somewhat warmer than temperatures typical of sewers or wastewater treatment plants, which varies from around 15°C to 25°C due to the regional and seasonal differences. 30ºC was nearer the optimal growth temperature of the organisms, and this would give good growth activities and enable good response to FNA to be observed.

- It is worth noting that a variety of the significantly differentially expressed genes/proteins after FNA exposure were hypothetical/uncharacterised proteins. These genes/proteins are of great interest since they are likely important for bacterial survival during FNA exposure but no obvious function has yet been assigned. Consequently, mutant studies are needed to further understand and reveal certain functions of the genes/proteins.

- Our study demonstrated the different susceptibilities of *P. aeruginosa* PAO1 and *D. vulgaris* Hildenborough to FNA, which may constitute the basis for use of FNA to selectively inactivate bacterial species during wastewater treatment. However, it is not clear how the susceptibility of these two cultures compares to that of other cultures, such as AOB and NOB which are important nitrifiers in wastewater nitrification treatment process due to the fact that they have different metabolism. Therefore, research on other typical organisms in wastewater treatment is required.

- Our study indicates that FNA can possibly cause cell lysis. However, the reasons behind this are still not completely clear. There are possible hints derived from this thesis showing that FNA affected the expression of genes/proteins involved in cell wall/membrane synthesis. More investigations focusing on the cell wall/membrane proteins would be useful to elucidate the reasons for cell lysis. A deeper understanding of the mechanisms involved in cell lysis would further help to provide knowledge on the possible application of FNA in wastewater treatment to control microbes.

- Our results along with many previous studies suggest that the inhibition of FNA to culture growth is reversible and the recovery time is generally correlated to the treated FNA concentrations. However, it is unknown whether the longer recovery time in cultures treated with high FNA concentrations is simply due to the lowered amount of live cells or caused by

FNA carryover damage to the live cells. Therefore, further investigations are required to elucidate this.

- Responses of *P. aeruginosa* biofilm were initially investigated which demonstrated to be too complicate to explain without information of planktonic cells response to FNA stress. Therefore, the response of planktonic cells to FNA exposure was elucidated in this thesis. Besides, biofilm grown cells can tolerant higher FNA levels than planktonic cells. Based on our experience, it would be quite interesting to further perform the experiments investigating the responses of biofilm when exposed to different levels of FNA based on the results of the planktonic cells to FNA stress. In addition, genes coding for cell signaling should be paid special attention since their differential regulation would have a huge effect on biofilm formation.

- For the transcriptomics investigation and gene expression analysis, only one time point was performed to uncover the antimicrobial effect of FNA. Gene expression analysis at multiple time points could in theory provide more information especially for *P. aeruginosa* PAO1 since there is no previous study reporting this. However, we have to make sure all the time points selected should be when changes in the batch conditions would be minimal and provide relevant comparisons of the transcriptomics. Therefore, we can measure changes that report on the primary effect of FNA not any secondary effects that would occur over longer timescales. Alternatively, the longer responses of the cultures to FNA can be measured and achieved in a chemostat reactor where all other conditions are constant.

- Beside, it would be interesting to explore further the protein changes in *D. vulgaris* Hildenborough at 12 h time frame especially at 8 μg N/L with limited live cells by cell sorting. It would possibly offer significant insight on the survival of the "persistent" cells to FNA stress.

- Huge salt (nitrite) intake from the food when nitrite is used as a preservative was demonstrated to increase the risk of developing cancer in human beings and mice (Joossens et al. 1996; Mirvish et al. 2008), e.g. gastric and other cancers. Diets containing high amounts of food preserved by salting and pickling are associated with an increased risk of cancers of the stomach, nose and throat. Therefore, special attention should be paid when

FNA was used in vivo to ascertain its levels lowers the threshold that could cause the adverse effect on health of mammalian cells.

- The thesis aimed to elucidate the antimicrobial effect of FNA on *P. aeruginosa* PAO1 and *D. vulgaris* Hildenborough. Determining the responses of additional SRB such as *Desulfobacter postgatei* which does not have nitrite reductase capabilities would be very useful to compare its responses to FNA to that of *D. vulgaris* Hildenborough.

- It should be highlighted that the aim of this thesis is to reveal the potential mechanisms involved in the superior antimicrobial effect of FNA on microorganisms using *P. aeruginosa* PAO1 and *D. vuglaris* Hildenborough as model organisms. While the study delivered important findings to guide practical applications of FNA-based technologies, it does not directly focus on applications. Therefore, more research work should be undertaken to fully understand the effectiveness of FNA as an antimicrobial agent in comparison with other biocides.

References

1. Abeling U., Seyfried C.F. 1992. Anaerobic-aerobic treatment of high-strength ammonium wastewater-nitrogen removal via nitrite. *Water Science & Technology,* 26, 1007-1015.
2. Agafonov D.E., Kolb V.A., Spirin A.S. 2001. A novel stress-response protein that binds at the ribosomal subunit interface and arrests translation. *Cold Spring Harbor Symposia on Quantitative Biology,* 66, 509-514.
3. Alefounder P.R., Greenfield A.J., McCarthy J.E., Ferguson S.J. 1983. Selection and organisation of denitrifying electron-transfer pathways in *Paracoccus denitrificans*. *Biochimica et Biophysica Acta (BBA)-Bioenergetics,* 724, 20-39.
4. Almeida J.S., Júlio S.M., Reis M.A., Carrondo M.J. 1995. Nitrite inhibition of denitrification by *Pseudomonas fluorescens*. *Biotechnology and Bioengineering,* 46, 194-201.
5. Anthonisen A.C., Loehr R.C., Prakasam T.B., Srinath E.G. 1976. Inhibition of nitrification by ammonia and nitrous acid. *Journal of the Water Pollution Control Federation,* 48, 835-852.
6. Aragao D., Mitchell E.P., Frazao C.F., Carrondo M.A., Lindley P.F. 2008. Structural and functional relationships in the hybrid cluster protein family: structure of the anaerobically purified hybrid cluster protein from *Desulfovibrio vulgaris* at 1.35 angstrom resolution. *Acta Crystallographica Section D-Biological Crystallography,* 64, 665-674.
7. Avery, S.V.2006. Microbial cell individuality and the underlying sources of heterogeneity. Nature Reviews Microbiology, 4, 577-587.
8. Bai X., Naghdi F.G., Ye L., Lant P., Pratt S. 2014. Enhanced lipid extraction from algae using free nitrous acid pretreatment. *Bioresource Technology,* 159, 36-40.
9. Barraud N., Schleheck D., Klebensberger J., Webb J.S., Hassett D.J., Rice S.A., Kjelleberg S. 2009. Nitric oxide signaling in *Pseudomonas aeruginosa* biofilms mediates phosphodiesterase activity, decreased cyclic di-GMP levels, and enhanced dispersal. *Journal of Bacteriology,* 191, 7333-7342.
10. Baumann B., van der Meer J.R., Snozzi M., Zehnder A.J. 1997. Inhibition of denitrification activity but not of mRNA induction in *Paracoccus denitrificans* by nitrite at a suboptimal pH. *Antonie van Leeuwenhoek,* 72, 183-189.

11. Beaumont H.J., Lens S.I., Reijnders W.N., Westerhoff H.V., van Spanning R.J. 2004. Expression of nitrite reductase in *Nitrosomonas europaea* involves NsrR, a novel nitrite-sensitive transcription repressor. *Molecular Microbiology,* 54, 148-158.
12. Benjamin N., O'Driscoll F., Dougall H., Duncan C., Smith L., Golden M., McKenzie H. 1994. Stomach NO synthesis. *Nature,* 368, 502-502.
13. Borisov V.B., Forte E., Konstantinov A.A., Poole R.K., Sarti P., Giuffrè A. 2004. Interaction of the bacterial terminal oxidase cytochrome bd with nitric oxide. *FEBS Letters,* 576, 201-204.
14. Brioukhanov A.L., Durand M.C., Dolla A., Aubert C. 2010. Response of *Desulfovibrio vulgaris* Hildenborough to hydrogen peroxide: enzymatic and transcriptional analyses. *FEMS Microbiology Letters,* 310, 175-181.
15. Buchmeier N.A., Lipps C.J., So M.Y., Heffron F. 1993. Recombination-deficient mutants of *Salmonella typhimurium* are avirulent and sensitive to the oxidative burst of macrophages. *Molecular Microbiology,* 7, 933-936.
16. Butler A.R., Flitney F.W., Williams D.L. 1995. NO, nitrosonium ions, nitroxide ions, nitrosothiols and iron-nitrosyls in biology: a chemist's perspective. *Trends in Pharmacological Sciences,* 16, 18-22.
17. Bykov D., Neese F. 2015. Six-electron reduction of nitrite to ammonia by cytochrome c nitrite reductase: insights from density functional theory studies. *Inorganic Chemistry,* 54, 9303-9316.
18. Casadesús, J., Low, D.A. 2013. Programmed heterogeneity: epigenetic mechanisms in bacteria. The Journal of Biological Chemistry, 288, 13929-13935.
19. Chandler, R., 2007, Microbial control in wastewater systems, *70th Annual Victorian Water Industry Engineers & Operators Conference Exhibition Centre-Bendigo*, 56-62.
20. Chavarría M., Nikel P.I., Pérez-Pantoja D., de Lorenzo V. 2013. The Entner-Doudoroff pathway empowers *Pseudomonas putida* KT2440 with a high tolerance to oxidative stress. *Environmental Microbiology,* 15, 1772-1785.
21. Chen L., Le Gall J., Xavier A.V. 1994. Purification, characterization and properties of an NADH oxidase from *Desulfovibrio vulgaris* (Hildenborough) and its coupling to adenylyl phosphosulfate reductase. *Biochemical and Biophysical Research Communications,* 203, 839-844.

22. Chen L., Xie Q.W., Nathan C. 1998. Alkyl hydroperoxide reductase subunit C (AhpC) protects bacterial and human cells against reactive nitrogen intermediates. *Molecular Cell,* 1, 795-805.
23. Chhabra S.R., He Q., Huang K.H., Gaucher S.P., Alm E.J., He Z., Hadi M.Z., Hazen T.C., Wall J.D., Zhou J., Arkin A.P., Singh A.K. 2006. Global analysis of heat shock response in *Desulfovibrio vulgaris* Hildenborough. *Journal of Bacteriology,* 188, 1817-1828.
24. Chhabra S.R., Joachimiak M.P., Petzold C.J., Zane G.M., Price M.N., Reveco S.A., Fok V., Johanson A.R., Batth T.S., Singer M., Chandonia J.M., Joyner D., Hazen T.C., Arkin A.P., Wall J.D., Singh A.K., Keasling J.D. 2011. Towards a Rigorous Network of Protein-Protein Interactions of the Model Sulfate Reducer *Desulfovibrio vulgaris* Hildenborough. *PloS one,* 6, e21470.
25. Choi M., Chang C.Y., Clough T., Broudy D., Killeen T., MacLean B., Vitek O. 2014. MSstats: an R package for statistical analysis of quantitative mass spectrometry-based proteomic experiments. *Bioinformatics,* 30, 2524-2526.
26. Clark M.E., He Q., He Z., Huang K.H., Alm E.J., Wan X.F., Hazen T.C., Arkin A.P., Wall J.D., Zhou J.Z., Fields M.W. 2006. Temporal transcriptomic analysis as *Desulfovibrio vulgaris* Hildenborough transitions into stationary phase during electron donor depletion. *Applied and Environmental Microbiology,* 72, 5578-5588.
27. Cross R., Lloyd D., Poole R.K., Moir J.W. 2001. Enzymatic removal of nitric oxide catalyzed by cytochrome *c'* in *Rhodobacter capsulatus*. *Journal of Bacteriology,* 183, 3050-3054.
28. D'Autreaux B., Touati D., Bersch B., Latour J.M., Michaud-Soret I. 2002. Direct inhibition by nitric oxide of the transcriptional ferric uptake regulation protein via nitrosylation of the iron. *Proceedings of the National Academy of Sciences of the United States of America,* 99, 16619-16624.
29. Davis R.D., Hall J.E. 1997. Production, treatment and disposal of wastewater sludge in Europe from a UK perspective. *European Water Pollution Control,* 2, 9-17.
30. D B., Holyoak H., Caron G.N.-V., Coote C. 1998. Determination of the intracellular pH (pHi) of growing cells of *Saccharomyces cerevisiae*: the effect of reduced-expression of the membrane H^+-ATPase. *Journal of Microbiological Methods,* 31, 113-125.
31. Drapier J.C., Pellat C., Henry Y. 1991. Generation of EPR-detectable nitrosyl-iron complexes in tumor target cells cocultured with activated macrophages. *Journal of Biological Chemistry,* 266, 10162-10167.

32. Drews A. 2010. Membrane fouling in membrane bioreactors characterisation, contradictions, cause and cures. *Journal of Membrane Science,* 363, 1-28.
33. Elvers K.T., Wu G., Gilberthorpe N.J., Poole R.K., Park S.F. 2004. Role of an inducible single-domain hemoglobin in mediating resistance to nitric oxide and nitrosative stress in *Campylobacter jejuni* and *Campylobacter coli*. *Journal of Bacteriology,* 186, 5332-5341.
34. Fang F.C. 2004. Antimicrobial reactive oxygen and nitrogen species: concepts and controversies. *Nature reviews. Microbiology,* 2, 820-832.
35. Fang F.C. 1997. Perspectives series: host/pathogen interactions. Mechanisms of nitric oxide-related antimicrobial activity. *The Journal of Clinical Investigation,* 99, 2818-2825.
36. Filenko N.A., Browning D.F., Cole J.A. 2005. Transcriptional regulation of a hybrid cluster (prismane) protein. *Biochemical Society Transactions,* 33, 195-197.
37. Filiatrault M.J., Picardo K.F., Ngai H., Passador L., Iglewski B.H. 2006. Identification of *Pseudomonas aeruginosa* genes involved in virulence and anaerobic growth. *Infection and Immunity,* 74, 4237-4245.
38. Filloux E., Wang J., Pidou M., Gernjak W., Yuan Z. 2015. Biofouling and scaling control of reverse osmosis membrane using one-step cleaning-potential of acidified nitrite solution as an agent. *Journal of Membrane Science,* 495, 276-283.
39. Frey A.D., Farrés J., Bollinger C.J., Kallio P.T. 2002. Bacterial hemoglobins and flavohemoglobins for alleviation of nitrosative stress in *Escherichia coli*. *Applied and Environmental Microbiology,* 68, 4835-4840.
40. Fux C., Lange K., Faessler A., Huber P., Grueniger B., Siegrist H. 2003. Nitrogen removal from digester supernatant via nitrite--SBR or SHARON? *Water Science and Technology,* 48, 9-18.
41. Gao S.H., Fan L., Peng L., Guo J., Agulló-Barceló M., Yuan Z., Bond P.L. 2016b. Determining multiple responses of *Pseudomonas aeruginosa* PAO1 to an antimicrobial agent, free nitrous acid. *Environmental Science & Technology,* 50, 5305-5312.
42. Gao S.H., Fan L., Yuan Z., Bond P.L. 2015. The concentration-determined and population-specific antimicrobial effects of free nitrous acid on Pseudomonas aeruginosa PAO1. *Applied Microbiology and Biotechnology,* 99, 2305-2312.
43. Gao S.H., Ho J.Y., Fan L., Richardson D.J., Yuan Z., Bond P.L. 2016a. Antimicrobial effects of free nitrous acid on Desulfovibrio vulgaris: implications for sulfide induced concrete corrosion. *Applied and environmental microbiology*, doi:10.1128/AEM.01655-16.

44. Gardner A.M., Helmick R.A., Gardner P.R. 2002. Flavorubredoxin, an inducible catalyst for nitric oxide reduction and detoxification in *Escherichia coli*. *Journal of Biological Chemistry,* 277, 8172-8177.
45. Gillet L.C., Navarro P., Tate S., Röst H., Selevsek N., Reiter L., Bonner R., Aebersold R. 2012. Targeted data extraction of the MS/MS spectra generated by data-independent acquisition: a new concept for consistent and accurate proteome analysis. *Molecular & Cellular Proteomics,* 11, O111.016717.
46. Glass C., Silverstein J., Oh J. 1997. Inhibition of denitrification in activated sludge by nitrite. *Water Environment Research,* 69, 1086-1093.
47. Glaze W.H., Kang J.W., Chapin D.H. 1987. The chemistry of water treatment processes involving ozone, hydrogen peroxide and ultraviolet radiation. Ozone: Science & Engineering: The Journal of the International Ozone Association, 9, 335-352.
48. Gow A.J., Buerk D.G., Ischiropoulos H. 1997. A novel reaction mechanism for the formation of S-nitrosothiol in vivo. *Journal of Biological Chemistry,* 272, 2841-2845.
49. De Groote M.A., Fang F.C. 1995a. NO inhibitions: antimicrobial properties of nitric oxide. *Clinical Infectious Diseases,* 21 Suppl 2, S162-165.
50. De Groote M.A., Ochsner U.A., Shiloh M.U., Nathan C., McCord J.M., Dinauer M.C., Libby S.J., Vazquez-Torres A., Xu Y., Fang F.C. 1997. Periplasmic superoxide dismutase protects *Salmonella* from products of phagocyte NADPH-oxidase and nitric oxide synthase. *Proceedings of the National Academy of Sciences,* 94, 13997-14001.
51. De Groote M.A., Testerman T., Xu Y., Stauffer G., Fang F.C. 1996. Homocysteine antagonism of nitric oxide-related cytostasis in *Salmonella typhimurium*. *Science,* 272, 414-417.
52. Halliwell B., Hu M.L., Louie S., Duvall T.R., Tarkington B.K., Motchnik P., Cross C.E. 1992. Interaction of nitrogen dioxide with human plasma. Antioxidant depletion and oxidative damage. *FEBS Letters,* 313, 62-66.
53. Hausladen A., Privalle C.T., Keng T., DeAngelo J., Stamler J.S. 1996. Nitrosative stress: activation of the transcription factor OxyR. *Cell,* 86, 719-729.
54. Haveman S.A., Greene E.A., Stilwell C.P., Voordouw J.K., Voordouw G. 2004. Physiological and gene expression analysis of inhibition of *Desulfovibrio vulgaris* Hildenborough by nitrite. *Journal of Bacteriology,* 186, 7944-7950.
55. Heberer T. 2002. Occurrence, fate, and removal of pharmaceutical residues in the aquatic environment: a review of recent research data. *Toxicology Letters,* 131, 5-17.

56. Heidelberg J.F., Seshadri R., Haveman S.A., Hemme C.L., Paulsen I.T., Kolonay J.F., Eisen J.A., Ward N., Methe B., Brinkac L.M., Daugherty S.C., Deboy R.T., Dodson R.J., Durkin A.S., Madupu R., Nelson W.C., Sullivan S.A., Fouts D., Haft D.H., Selengut J., Peterson J.D., Davidsen T.M., Zafar N., Zhou L., Radune D., Dimitrov G., Hance M., Tran K., Khouri H., Gill J., Utterback T.R., Feldblyum T.V., Wall J.D., Voordouw G., Fraser C.M. 2004. The genome sequence of the anaerobic, sulfate-reducing bacterium *Desulfovibrio vulgaris* Hildenborough. *Nature Biotechnology,* 22, 554-559.
57. He Q., Huang K.H., He Z., Alm E.J., Fields M.W., Hazen T.C., Arkin A.P., Wall J.D., Zhou J. 2006. Energetic consequences of nitrite stress in *Desulfovibrio vulgaris* Hildenborough, inferred from global transcriptional analysis. *Applied and Environmental Microbiology,* 72, 4370-4381.
58. He Z., Zhou A., Baidoo E., He Q., Joachimiak M.P., Benke P., Phan R., Mukhopadhyay A., Hemme C.L., Huang K., Alm E.J., Fields M.W., Wall J., Stahl D., Hazen T.C., Keasling J.D., Arkin A.P., Zhou J. 2010. Global transcriptional, physiological, and metabolite analyses of the responses of *Desulfovibrio vulgaris* hildenborough to salt adaptation. *Applied and Environmental Microbiology,* 76, 1574-1586.
59. Hinze H., Holzer H. 1985. Accumulation of nitrite and sulfite in yeast cells and synergistic depletion of the intracellular ATP content. *Zeitschrift für Lebensmittel-Untersuchung und -Forschung,* 180, 117-120.
60. Hinze H., Holzer H. 1986. Analysis of the energy metabolism after incubation of *Saccharomyces cerevisiae* with sulfite or nitrite. *Archives of Microbiology,* 145, 27-31.
61. Hirsch R., Ternes T., Haberer K., Kratz K.L. 1999. Occurrence of antibiotics in the aquatic environment. *Science of the Total Environment,* 225, 109-118.
62. Hwang B.K., Lee W.-N., Yeon K.-M., Park P.-K., Lee C.-H., Chang I.-S., Drews A., Kraume M. 2008. Correlating TMP increases with microbial characteristics in the bio-cake on the membrane surface in a membrane bioreactor. *Environmental Science & Technology,* 42, 3963-3968.
63. Ischiropoulos H., Al-Mehdi A.B. 1995. Peroxynitrite-mediated oxidative protein modifications. *FEBS Letters,* 364, 279-282.
64. Jiang G., Gutierrez O., Sharma K.R., Keller J., Yuan Z. 2011. Optimization of intermittent, simultaneous dosage of nitrite and hydrochloric acid to control sulfide and methane productions in sewers. *Water Research,* 45, 6163-6172.

65. Jiang G., Gutierrez O., Sharma K.R., Yuan Z. 2010. Effects of nitrite concentration and exposure time on sulfide and methane production in sewer systems. *Water Research,* 44, 4241-4251.
66. Jiang G., Gutierrez O., Yuan Z. 2011. The strong biocidal effect of free nitrous acid on anaerobic sewer biofilms. *Water Research,* 45, 3735-3743.
67. Jiang G., Keating A., Corrie S., O'halloran K., Nguyen L., Yuan Z. 2013. Dosing free nitrous acid for sulfide control in sewers: Results of field trials in Australia. *Water Research,* 47, 4331-4339.
68. Jiang G., Yuan Z. 2013. Synergistic inactivation of anaerobic wastewater biofilm by free nitrous acid and hydrogen peroxide. *Journal of Hazardous Materials,* 250-251, 91-98.
69. Jiménez E., Giménez J.B., Seco A., Ferrer J., Serralta J. 2012. Effect of pH, substrate and free nitrous acid concentrations on ammonium oxidation rate. *Bioresource Technology,* 124, 478-484.
70. Joossens, J.V., Hill, M.J., Elliott, P., Stamler, R., Lesaffre, E., Dyer, A., Nichols, R., Kesteloot, H. 1996. Dietary salt, nitrate and stomach cancer mortality in 24 countries. International Journal of Epidemiology, 25, 494-504.
71. Juedes M.J., Wogan G.N. 1996. Peroxynitrite-induced mutation spectra of pSP189 following replication in bacteria and in human cells. *Mutation Research,* 349, 51-61.
72. Kappler U., Nouwens A.S. 2013. The molybdoproteome of *Starkeya novella*--insights into the diversity and functions of molybdenum containing proteins in response to changing growth conditions. *Metallomics,* 5, 325-334.
73. Karp P.D., Paley S.M., Krummenacker M., Latendresse M., Dale J.M., Lee T.J., Kaipa P., Gilham F., Spaulding A., Popescu L., Altman T., Paulsen I., Keseler I.M., Caspi R. 2010. Pathway Tools version 13.0: integrated software for pathway/genome informatics and systems biology. *Briefings in Bioinformatics,* 11, 40-79.
74. Kato T., Yoshida H., Miyata T., Maki Y., Wada A., Namba K. 2010. Structure of the 100S ribosome in the hibernation stage revealed by electron cryomicroscopy. *Structure,* 18, 719-724.
75. Keller-Lehmann B., Corrie S., Ravn R., Yuan Z., and Keller J. 2006. Preservation and simultaneous analysis of relevant soluble sulfur species in sewage samples. Proceedings of the Second International IWA Conference on Sewer Operation and Maintenance, Vienna, Austria.

76. Keren, I., Shah, D., Spoering, A., Kaldalu, N., Lewis, K. 2004. Specialized persister cells and the mechanism of multidrug tolerance in *Escherichia coli*. Journal of Bacteriology, 186, 8172-8180.
77. Kim J.H., Akagi J.M. 1985. Characterization of a trithionate reductase system from *Desulfovibrio vulgaris*. *Journal of Bacteriology,* 163, 472-475.
78. Kim S., Aga D.S. 2007. Potential ecological and human health impacts of antibiotics and antibiotic-resistant bacteria from wastewater treatment plants. *Journal of Toxicology and Environmental Health, Part B Critical Review,* 10, 559-573.
79. Krzywinski M., Schein J., Birol I., Connors J., Gascoyne R., Horsman D., Jones S.J., Marra M.A. 2009. Circos: an information aesthetic for comparative genomics. *Genome Research,* 19, 1639-1645.
80. Kulshrestha P., McKinstry K.C., Fernandez B.O., Feelisch M., Mitch W.A. 2010. Application of an optimized total N-nitrosamine (TONO) assay to pools: placing N-nitrosodimethylamine (NDMA) determinations into perspective. *Environmental Science & Technology,* 44, 3369-3375.
81. Lepoivre M., Fieschi F., Coves J., Thelander L., Fontecave M. 1991. Inactivation of ribonucleotide reductase by nitric oxide. *Biochemical and Biophysical Research Communications,* 179, 442-448.
82. Lijinsky W. 1999. N-Nitroso compounds in the diet. *Mutation Research/Genetic Toxicology and Environmental Mutagenesis,* 443, 129-138.
83. Liu L., Hausladen A., Zeng M., Que L., Heitman J., Stamler J.S. 2001. A metabolic enzyme for S-nitrosothiol conserved from bacteria to humans. *Nature,* 410, 490-494.
84. Lobysheva I.I., Stupakova M.V., Mikoyan V.D., Vasilieva S.V., Vanin A.F. 1999. Induction of the SOS DNA repair response in *Escherichia coli* by nitric oxide donating agents: dinitrosyl iron complexes with thiol-containing ligands and S-nitrosothiols. *FEBS Letters,* 454, 177-180.
85. Maeda S., Okamura M., Kobayashi M., Omata T. 1998. Nitrite-specific active transport system of the cyanobacterium *Synechococcus* sp. strain PCC 7942. *Journal of Bacteriology,* 180, 6761-6763.
86. Ma J., Yang Q., Wang S.Y., Wang L., Takigawa A., Peng Y.Z. 2010. Effect of free nitrous acid as inhibitors on nitrate reduction by a biological nutrient removal sludge. *Journal of Hazardous Materials,* 175, 518-523.

87. Malling H.V. 2004. History of the science of mutagenesis from a personal perspective. *Environmental and Molecular Mutagenesis,* 44, 372-386.
88. Maraj S.R., Khan S., Cui X.Y., Cammack R., Joannou C.L., Hughes M.N. 1995. Interactions of nitric oxide and redox-related species with biological targets. *The Analyst,* 120, 699-703.
89. Master S.S., Springer B., Sander P., Boettger E.C., Deretic V., Timmins G.S. 2002. Oxidative stress response genes in *Mycobacterium tuberculosis*: role of ahpC in resistance to peroxynitrite and stage-specific survival in macrophages. *Microbiology,* 148, 3139-3144.
90. Mayburd A.L., Kassner R.J. 2002. Mechanism and biological role of nitric oxide binding to cytochrome c' *Biochemistry,* 41, 11582-11591.
91. Metcalf and Eddy, 2003. Wastewater Engineering: Treatment and Reuse, Fourth Edition. McGraw Hill Education. ISBN: 0070418780.
92. Mirvish, S.S., Davis, M.E., Lisowyj, M.P., Gaikwad, N.W. 2008. Effect of feeding nitrite, ascorbate, hemin, and omeprazole on excretion of fecal total apparent N-nitroso compounds in mice. Chemical Research in Toxicology, 21, 2344-2351.
93. Moore C.M., Nakano M.M., Wang T., Ye R.W., Helmann J.D. 2004. Response of *Bacillus subtilis* to nitric oxide and the nitrosating agent sodium nitroprusside. *Journal of Bacteriology,* 186, 4655-4664.
94. Morita H., Yoshikawa H., Suzuki T., Hisamatsu S., Kato Y., Sakata R., Nagata Y., Yoshimura T. 2004. Anti-microbial action against verotoxigenic *Escherichia coli* O157:H7 of nitric oxide derived from sodium nitrite. *Bioscience, Biotechnology and Biochemistry,* 68, 1027-1034.
95. Morita Y., Tomida J., Kawamura Y. 2014. Responses of *Pseudomonas aeruginosa* to antimicrobials. *Frontiers in Microbiology,* 4, 422.
96. Mu J.C., Jiang H., Kiani A., Mohiyuddin M., Bani Asadi N., Wong W.H. 2012. Fast and accurate read alignment for resequencing. *Bioinformatics,* 28, 2366-2373.
97. Mukhopadhyay A., Redding A.M., Joachimiak M.P., Arkin A.P., Borglin S.E., Dehal P.S., Chakraborty R., Geller J.T., Hazen T.C., He Q., Joyner D.C., Martin V.J., Wall J.D., Yang Z.K., Zhou J., Keasling J.D. 2007. Cell-wide responses to low-oxygen exposure in *Desulfovibrio vulgaris* Hildenborough. *Journal of Bacteriology,* 189, 5996-6010.
98. Mühlig A., Behr J., Scherer S., Müller-Herbst S. 2014. Stress response of *Salmonella enterica* serovar typhimurium to acidified nitrite. *Applied and Environmental Microbiology,* 80, 6373-6382.

99. Nakaki T., Nakayama M., Kato R. 1990. Inhibition by nitric oxide and nitric oxide-producing vasodilators of DNA synthesis in vascular smooth muscle cells. *European Journal of Pharmacology: Molecular Pharmacology,* 189, 347-353.

100. Nathan C., Shiloh M.U. 2000. Reactive oxygen and nitrogen intermediates in the relationship between mammalian hosts and microbial pathogens. *Proceedings of the National Academy of Sciences of the United States of America,* 97, 8841-8848.

101. Neca A.J., Soares R., Carepo M.S., Pauleta S.R. 2016. Resonance assignment of DVU2108 that is part of the Orange Protein complex in *Desulfovibrio vulgaris* Hildenborough. *Biomolecular NMR Assignments,* 10, 117-120.

102. Nunoshiba T., DeRojas-Walker T., Tannenbaum S.R., Demple B. 1995. Roles of nitric oxide in inducible resistance of *Escherichia coli* to activated murine macrophages. *Infection and Immunity,* 63, 794-798.

103. Oldreive C., Rice-Evans C. 2001. The mechanisms for nitration and nitrotyrosine formation in vitro and in vivo: impact of diet. *Free Radical Research,* 35, 215-231.

104. O'Leary V., Solberg M. 1976. Effect of sodium nitrite inhibition on intracellular thiol groups and on the activity of certain glycolytic enzymes in *Clostridium perfringens*. *Applied and Environmental Microbiology,* 31, 208-212.

105. Ouellet H., Ouellet Y., Richard C., Labarre M., Wittenberg B., Wittenberg J., Guertin M. 2002. Truncated hemoglobin HbN protects *Mycobacterium bovis* from nitric oxide. *Proceedings of the National Academy of Sciences of the United States of America,* 99, 5902-5907.

106. Park J.W. 1993. S-Nitrosylation of sulfhydryl groups in albumin by nitrosating agents. *Archives of Pharmacal Research,* 16, 1-5.

107. Patel R.K., Jain M. 2012. NGS QC Toolkit: a toolkit for quality control of next generation sequencing data. *PloS one,* 7, e30619.

108. Phillips R., Adjei O., Lucas S., Benjamin N., Wansbrough-Jones M. 2004. Pilot randomized double-blind trial of treatment of *Mycobacterium ulcerans* disease (Buruli ulcer) with topical nitrogen oxides. *Antimicrobial Agents and Chemotherapy,* 48, 2866-2870.

109. Pierson M.D., Smoot L.A. 1982. Nitrite, nitrite alternatives, and the control of *Clostridium botulinum* in cured meats. *Critical Reviews in Food Science and Nutrition,* 17, 141-187.

110. Pijuan M., Wang Q.L., Ye L., Yuan Z.G. 2012. Improving secondary sludge biodegradability using free nitrous acid treatment. *Bioresource Technology,* 116, 92-98.

111. Pijuan M., Ye L., Yuan Z.G. 2010. Free nitrous acid inhibition on the aerobic metabolism of poly-phosphate accumulating organisms. *Water Research,* 44, 6063-6072.

112. Pikaar I., Sharma K.R., Hu S., Gernjak W., Keller J., Yuan Z. 2014. Water engineering. Reducing sewer corrosion through integrated urban water management. *Science,* 345, 812-814.

113. Platt M.D., Schurr M.J., Sauer K., Vazquez G., Kukavica-Ibrulj I., Potvin E., Levesque R.C., Fedynak A., Brinkman F.S.L., Schurr J., Hwang S.-H., Lau G.W., Limbach P.A., Rowe J.J., Lieberman M.A., Barraud N., Webb J., Kjelleberg S., Hunt D.F., Hassett D.J. 2008. Proteomic, microarray, and signature-tagged mutagenesis analyses of anaerobic *Pseudomonas aeruginosa* at pH 6.5, likely representing chronic, late-stage cystic fibrosis airway conditions. *Journal of Bacteriology,* 190, 2739-2758.

114. Polikanov Y.S., Blaha G.M., Steitz T.A. 2012. How hibernation factors RMF, HPF, and YfiA turn off protein synthesis. *Science,* 336, 915-918.

115. Poock S.R., Leach E.R., Moir J.W., Cole J.A., Richardson D.J. 2002. Respiratory detoxification of nitric oxide by the cytochromec nitrite reductase of *Escherichia coli Journal of Biological Chemistry,* 277, 23664-23669.

116. Poole R.K. 2005. Nitric oxide and nitrosative stress tolerance in bacteria. *Biochemical Society Transactions,* 33, 176-180.

117. Poole R.K., Hughes M.N. 2000. New functions for the ancient globin family: bacterial responses to nitric oxide and nitrosative stress. *Molecular Microbiology,* 36, 775-783.

118. Rabus, R., Hansen, T. A. & Widdel, F. 2006. The prokaryotes. Fourth Edition. Springer Heidelberg New York Dordrecht London. ISBN: 978-3-642-30137-7.

119. Rao A., Jump R.L., Pultz N.J., Pultz M.J., Donskey C.J. 2006. In vitro killing of nosocomial pathogens by acid and acidified nitrite. *Antimicrobial Agents and Chemotherapy,* 50, 3901-3904.

120. Redding A.M., Mukhopadhyay A., Joyner D.C., Hazen T.C., Keasling J.D. 2006. Study of nitrate stress in *Desulfovibrio vulgaris* Hildenborough using iTRAQ proteomics. *Briefings in Functional Genomics & Proteomics,* 5, 133-143.

121. Reddy D., Lancaster J. R., and Cornforth D. P. 1983. Nitrite inhibition of *Clostridium botulinum*: electron spin resonance detection of iron-nitric oxide complexes. Science. 221, 769-770.

122. Rhoades E.R., Orme I.M. 1997. Susceptibility of a panel of virulent strains of *Mycobacterium tuberculosis* to reactive nitrogen intermediates. *Infection and Immunity,* 65, 1189-1195.

123. Richardson D., Felgate H., Watmough N., Thomson A., Baggs E. 2009. Mitigating release of the potent greenhouse gas N_2O from the nitrogen cycle--could enzymic regulation hold the key? *Trends in Biotechnology,* 27, 388-397.

124. Rogstam A., Larsson J.T., Kjelgaard P., von Wachenfeldt C. 2007. Mechanisms of adaptation to nitrosative stress in *Bacillus subtilis*. *Journal of Bacteriology,* 189, 3063-3071.

125. Rowe J.J., Yarbrough J.M., Rake J.B., Eagon R.G. 1979. Nitrite inhibition of aerobic bacteria. *Current Microbiology,* 2, 51-54.

126. Rubbo H., Radi R., Trujillo M., Telleri R., Kalyanaraman B., Barnes S., Kirk M., Freeman B.A. 1994. Nitric oxide regulation of superoxide and peroxynitrite-dependent lipid peroxidation. Formation of novel nitrogen-containing oxidized lipid derivatives. *Journal of Biological Chemistry,* 269, 26066-26075.

127. Saby S., Djafer M., Chen G.H. 2002. Feasibility of using a chlorination step to reduce excess sludge in activated sludge process. *Water Research,* 36, 656-666.

128. Schapiro J.M., Libby S.J., Fang F.C. 2003. Inhibition of bacterial DNA replication by zinc mobilization during nitrosative stress. *Proceedings of the National Academy of Sciences of the United States of America,* 100, 8496-8501.

129. Schopfer F.J., Baker P.R.S., Freeman B.A. 2003. NO-dependent protein nitration: a cell signaling event or an oxidative inflammatory response? *Trends in Biochemical Sciences,* 28, 646-654.

130. Schreiber K., Boes N., Eschbach M., Jaensch L., Wehland J., Bjarnsholt T., Givskov M., Hentzer M., Schobert M. 2006. Anaerobic survival of *Pseudomonas aeruginosa* by pyruvate fermentation requires an Usp-type stress protein. *Journal of Bacteriology,* 188, 659-668.

131. Schulthess R.V., Gujer W. 1996. Release of nitrous oxide (N_2O) from denitrifying activated sludge: Verification and application of a mathematical model. *Water Research,* 30, 521-530.

132. Schulthess R.V., Kühni M., Gujer W. 1995. Release of nitric and nitrous oxides from denitrifying activated sludge. *Water Research,* 29, 215-226.

133. Schurek, K. N., Breidenstein, E. B. & Hancock, R. E. 2012. Antibiotic Discovery and Development. Springer New York Dordrecht Heidelberg London. ISBN: 978-1-4614-1399-8.

134. Sijbesma W.F., Almeida J.S., Reis M.A., Santos H. 1996. Uncoupling effect of nitrite during denitrification by *Pseudomonas fluorescens*: An in vivo ^{31}P-NMR study. *Biotechnology and Bioengineering,* 52, 176-182.

135. Simpson J.A., Smith S.E., Dean R.T. 1989. Scavenging by alginate of free radicals released by macrophages. *Free Radical Biology & Medicine,* 6, 347-353.

136. Soum E., Drapier J.C. 2003. Nitric oxide and peroxynitrite promote complete disruption of the [4Fe-4S] cluster of recombinant human iron regulatory protein 1. *Journal of Biological Inorganic Chemistry,* 8, 226-232.

137. Spallarossa A., Forlani F., Pagani S., Salvati L., Visca P., Ascenzi P., Bolognesi M., Bordo D. 2003. Inhibition of *Azotobacter vinelandii* rhodanese by NO-donors. *Biochemical and Biophysical Research Communications,* 306, 1002-1007.

138. Stein L.Y., Arp D.J. 1998. Ammonium limitation results in the loss of ammonia-oxidizing activity in *Nitrosomonas europaea*. *Applied and Environmental Microbiology,* 64, 1514-1521.

139. Stolyar S., He Q., Joachimiak M.P., He Z.L., Yang Z.K., Borglin S.E., Joyner D.C., Huang K., Alm E., Hazen T.C., Zhou J.Z., Wall J.D., Arkin A.P., Stahl D.A. 2007. Response of *Desulfovibrio vulgaris* to alkaline stress. *Journal of Bacteriology,* 189, 8944-8952.

140. Stover C.K., Pham X.Q., Erwin A.L., Mizoguchi S.D., Warrener P., Hickey M.J., Brinkman F.S., Hufnagle W.O., Kowalik D.J., Lagrou M., Garber R.L., Goltry L., Tolentino E., Westbrock-Wadman S., Yuan Y., Brody L.L., Coulter S.N., Folger K.R., Kas A., Larbig K., Lim R., Smith K., Spencer D., Wong G.K., Wu Z., Paulsen I.T., Reizer J., Saier M.H., Hancock R.E., Lory S., Olson M.V. 2000. Complete genome sequence of *Pseudomonas aeruginosa* PAO1, an opportunistic pathogen. *Nature,* 406, 959-964.

141. Sun H.W., Bai Y., Peng Y.Z., Xie H.G., Shi X.N. 2013. Achieving nitrogen removal via nitrite pathway from urban landfill leachate using the synergetic inhibition of free ammonia and free nitrous acid on nitrifying bacteria activity. *Water Science and Technology,* 68, 2035-2041.

142. Sun J., Hu S., Sharma K.R., Ni B.J., Yuan Z. 2014. Stratified microbial structure and activity in sulfide- and methane-producing anaerobic sewer biofilms. *Applied and Environmental Microbiology,* 80, 7042-7052.

143. Sun X., Jiang G., Bond P.L., Keller J., Yuan Z. 2015. A novel and simple treatment for control of sulfide induced sewer concrete corrosion using free nitrous acid. *Water Research,* 70, 279-287.

144. Takahama, U. & Hirota, S. 2012. Chapter 13: Transformation of nitrite and nitric oxide produced by oral bacteria to reactive nitrogen oxide species in the oral cavity. Oral Health Care - Prosthodontics, Periodontology, Biology, Research and Systemic Conditions. Intach Open Access Publisher. ISBN 978-953-51-0040-9.

145. Trapnell C., Roberts A., Goff L., Pertea G., Kim D., Kelley D.R., Pimentel H., Salzberg S.L., Rinn J.L., Pachter L. 2012. Differential gene and transcript expression analysis of RNA-seq experiments with TopHat and Cufflinks. *Nature Protocols,* 7, 562-578.

146. Vadivelu V.M., Keller J., Yuan Z. 2007. Free ammonia and free nitrous acid inhibition on the anabolic and catabolic processes of *Nitrosomonas* and *Nitrobacter*. *Water Science and Technology,* 56, 89-97.

147. Vadivelu V.M., Keller J., Yuan Z.G. 2006a. Effect of free ammonia and free nitrous acid concentration on the anabolic and catabolic processes of an enriched *Nitrosomonas* culture. *Biotechnology and Bioengineering,* 95, 830-839.

148. Vadivelu V.M., Yuan Z., Fux C., Keller J. 2006b. The inhibitory effects of free nitrous acid on the energy generation and growth processes of an enriched nitrobacter culture. *Environmental Science & Technology,* 40, 4442-4448.

149. Van Hulle S.W., Volcke E.I., Teruel J.L., Donckels B., van Loosdrecht M., Vanrolleghem P.A. 2007. Influence of temperature and pH on the kinetics of the Sharon nitritation process. *Journal of Chemical Technology and Biotechnology,* 82, 471-480.

150. Vine C.E., Cole J.A. 2011. Unresolved sources, sinks, and pathways for the recovery of enteric bacteria from nitrosative stress. *FEMS Microbiology Letters,* 325, 99-107.

151. Vita N., Valette O., Brasseur G., Lignon S., Denis Y., Ansaldi M., Dolla A., Pieulle L. 2015. The primary pathway for lactate oxidation in *Desulfovibrio vulgaris*. *Frontiers in Microbiology,* 6, 606.

152. Vizcaíno J.A., Côté R.G., Csordas A., Dianes J.A., Fabregat A., Foster J.M., Griss J., Alpi E., Birim M., Contell J., O'Kelly G., Schoenegger A., Ovelleiro D., Pérez-Riverol Y., Reisinger F., Ríos D., Wang R., Hermjakob H. 2013. The PRoteomics IDEntifications (PRIDE) database and associated tools: status in 2013. *Nucleic Acids Research,* 41, D1063-1069.

153. Vowinckel J., Capuano F., Campbell K., Deery M.J., Lilley K.S., Ralser M. 2013. The beauty of being (label)-free: sample preparation methods for SWATH-MS and next-generation targeted proteomics. *F1000Research,* 2, 272.

154. Walian P.J., Allen S., Shatsky M., Zeng L., Szakal E.D., Liu H., Hall S.C., Fisher S.J., Lam B.R., Singer M.E., Geller J.T., Brenner S.E., Chandonia J.M., Hazen T.C., Witkowska H.E., Biggin M.D., Jap B.K. 2012. High-throughput isolation and characterization of untagged membrane protein complexes: outer membrane complexes of *Desulfovibrio vulgaris*. *Journal of Proteome Research,* 11, 5720-5735.

155. Wang Q., Jiang G., Ye L., Yuan Z. 2014a. Enhancing methane production from waste activated sludge using combined free nitrous acid and heat pre-treatment. *Water Research,* 63C, 71-80.

156. Wang Q., Ye L., Jiang G., Hu S., Yuan Z. 2014b. Side-stream sludge treatment using free nitrous acid selectively eliminates nitrite oxidizing bacteria and achieves the nitrite pathway. *Water Research,* 55, 245-255.

157. Wang Q., Ye L., Jiang G., Jensen P., Batstone D., Yuan Z. 2013a. Free Nitrous Acid (FNA)-based pre-treatment enhances methane production from waste activated sludge. *Environmental Science & Technology,* 47, 11897-11904.

158. Wang Q., Ye L., Jiang G., Yuan Z. 2013b. A free nitrous acid (FNA)-based technology for reducing sludge production. *Water Research,* 47, 3663-3672.

159. Wang W., Kinkel T., Martens-Habbena W., Stahl D.A., Fang F.C., Hansen E.J. 2011. The Moraxella catarrhalis nitric oxide reductase is essential for nitric oxide detoxification. *Journal of Bacteriology,* 193, 2804-2813.

160. Wang Z., Gerstein M., Snyder M. 2009. RNA-Seq: a revolutionary tool for transcriptomics. *Nature Reviews. Genetics,* 10, 57-63.

161. Warren J.B., Loi R., Rendell N.B., Taylor G.W. 1990. Nitric oxide is inactivated by the bacterial pigment pyocyanin. *Biochemical Journal,* 266, 921-923.

162. Webb J.S., Thompson L.S., James S., Charlton T., Tolker-Nielsen T., Koch B., Givskov M., Kjelleberg S. 2003. Cell death in *Pseudomonas aeruginosa* biofilm development. *Journal of Bacteriology,* 185, 4585-4592.

163. Wei Y., Van Houten R.T., Borger A.R., Eikelboom D.H., Fan Y. 2003. Minimization of excess sludge production for biological wastewater treatment. *Water Research,* 37, 4453-4467.

164. Weller R., Price R.J., Ormerod A.D., Benjamin N., Leifert C. 2001. Antimicrobial effect of acidified nitrite on dermatophyte fungi, *Candida* and bacterial skin pathogens. *Journal of Applied Microbiology,* 90, 648-652.

165. Wildschut J.D., Lang R.M., Voordouw J.K., Voordouw G. 2006. Rubredoxin:oxygen oxidoreductase enhances survival of *Desulfovibrio vulgaris* hildenborough under microaerophilic conditions. *Journal of Bacteriology,* 188, 6253-6260.

166. Wolfe M.T., Heo J., Garavelli J.S., Ludden P.W. 2002. Hydroxylamine reductase activity of the hybrid cluster protein from *Escherichia coli*. *Journal of Bacteriology,* 184, 5898-5902.

167. Woodmansee A.N., Imlay J.A. 2003. A mechanism by which nitric oxide accelerates the rate of oxidative DNA damage in *Escherichia coli*. *Molecular Microbiology,* 49, 11-22.

168. Woods L.F., Wood J.M. 1982. A note on the effect of nitrite inhibition on the metabolism of *Clostridium botulinum*. *The Journal of Applied Bacteriology,* 52, 109-110.

169. Woods L.F., Wood J.M., Gibbs P.A. 1981. The involvement of nitric oxide in the inhibition of the phosphoroclastic system in *Clostridium sporogenes* by sodium nitrite. *Journal of General Microbiology,* 125, 399-406.

170. Wu Q., Stewart V. 1998. NasFED proteins mediate assimilatory nitrate and nitrite transport in *Klebsiella oxytoca* (*pneumoniae*) M5al. *Journal of Bacteriology,* 180, 1311-1322.

171. Xafenias N., Zhang Y., Banks C. 2013. Enhanced performance of hexavalent chromium reducing cathodes in the presence of *Shewanella oneidensis* MR-1 and lactate. *Environmental Science & Technology,* 47, 4512-4520.

172. Yakimov M.M., Timmis K.N., Golyshin P.N. 2007. Obligate oil-degrading marine bacteria. *Current Opinion in Biotechnology,* 18, 257-266.

173. Ye L., Pijuan M., Yuan Z. 2012. The effect of free nitrous acid on key anaerobic processes in enhanced biological phosphorus removal systems. *Bioresource Technology,* 130C, 382-389.

174. Ye L., Pijuan M., Yuan Z. 2013. The effect of free nitrous acid on key anaerobic processes in enhanced biological phosphorus removal systems. *Bioresource Technology,* 130, 382-389.

175. Ye L., Pijuan M., Yuan Z.G. 2010a. The effect of free nitrous acid on the anabolic and catabolic processes of glycogen accumulating organisms. *Water Research,* 44, 2901-2909.

176. Ye L., Pijuan M., Yuan Z.G. 2010b. The effect of free nitrous acid on the anabolic and catabolic processes of glycogen accumulating organisms. *Water Research,* 44, 2901-2909.

177. Yoon S.S., Coakley R., Lau G.W., Lymar S.V., Gaston B., Karabulut A.C., Hennigan R.F., Hwang S.-H., Buettner G., Schurr M.J., Mortensen J.E., Burns J.L., Speert D., Boucher

R.C., Hassett D.J. 2006. Anaerobic killing of mucoid *Pseudomonas aeruginosa* by acidified nitrite derivatives under cystic fibrosis airway conditions. *The Journal of Clinical Investigation,* 116, 436-446.

178. Zahrt T.C., Deretic V. 2002. Reactive nitrogen and oxygen intermediates and bacterial defenses: unusual adaptations in *Mycobacterium tuberculosis*. *Antioxidants & Redox Signaling,* 4, 141-159.

179. Zaki M.H., Akuta T., Akaike T. 2005. Nitric oxide-induced nitrative stress involved in microbial pathogenesis. *Journal of Pharmacological Sciences,* 98, 117-129.

180. Zhang L., De Schryver P., De Gusseme B., De Muynck W., Boon N., Verstraete W. 2008. Chemical and biological technologies for hydrogen sulfide emission control in sewer systems: a review. *Water Research,* 42, 1-12.

181. Zhao G., Ceci P., Ilari A., Giangiacomo L., Laue T.M., Chiancone E., Chasteen N.D. 2002. Iron and hydrogen peroxide detoxification properties of DNA-binding protein from starved cells. *Journal of Biological Chemistry,* 277, 27689-27696.

182. Zhou A.F., He Z.L., Redding-Johanson A.M., Mukhopadhyay A., Hemme C.L., Joachimiak M.P., Luo F., Deng Y., Bender K.S., He Q., Keasling J.D., Stahl D.A., Fields M.W., Hazen T.C., Arkin A.P., Wall J.D., Zhou J.Z. 2010a. Hydrogen peroxide-induced oxidative stress responses in *Desulfovibrio vulgaris* Hildenborough. *Environmental Microbiology,* 12, 2645-2657.

183. Zhou Y., Ganda L., Lim M., Yuan Z.G., Kjelleberg S., Ng W.J. 2010b. Free nitrous acid (FNA) inhibition on denitrifying poly-phosphate accumulating organisms (DPAOs). *Applied Microbiology and Biotechnology,* 88, 359-369.

184. Zhou Y., Ganda L., Lim M., Yuan Z.G., Ng W.J. 2012. Response of poly-phosphate accumulating organisms to free nitrous acid inhibition under anoxic and aerobic conditions. *Bioresource Technology,* 116, 340-347.

185. Zhou Y., Oehmen A., Lim M., Vadivelu V., Ng W.J. 2011. The role of nitrite and free nitrous acid (FNA) in wastewater treatment plants. *Water Research,* 45, 4672-4682.

186. Zhou Y., Pijuan M., Yuan Z. 2007. Free nitrous acid inhibition on anoxic phosphorus uptake and denitrification by poly-phosphate accumulating organisms. *Biotechnology and Bioengineering,* 98, 903-912.

187. Zhou Y., Pijuan M., Zeng R.J., Yuan Z. 2008. Free nitrous acid inhibition on nitrous oxide reduction by a denitrifying-enhanced biological phosphorus removal sludge. *Environmental Science & Technology,* 42, 8260-8265.

Appendix A

The concentration-determined and population-specific antimicrobial effects of free nitrous acid on *Pseudomonas aeruginosa* PAO1

Shu-Hong Gao, Lu Fan*, Zhiguo Yuan and Philip L Bond*

This paper is published in *Applied Microbiology and Biotechnology*.

Abstract

There is great potential to use free nitrous acid (FNA/HNO_2), the protonated form of nitrite, as an antimicrobial agent due to its bacteriostatic and bactericidal effects on a range of microorganisms. Here we determine the effects of FNA on the opportunistic pathogen *Pseudomonas aeruginosa* PAO1, a well-studied denitrifier capable of nitrate/nitrite reduction in its anaerobic respiration. It was seen that lower FNA concentrations in the range of 0.1 to 0.2 mg N/L exerted a temporary inhibitory effect on the growth of *P. aeruginosa*, while respiratory inhibition was not detected until an FNA concentration of 1.0 mg N/L was applied. The FNA concentration of 5.0 mg N/L caused complete cell killing and likely cell lysis. The results suggest concentration-related and multiple antimicrobial effects of FNA. Differential killing of FNA in the *P. aeruginosa* subpopulations was detected, suggesting intra-strain heterogeneity and does not support the idea of specific concentrations of FNA bringing about bacteriostatic and bactericidal effects on this species. A delayed recovery from FNA treatment suggested that FNA caused cell damage which required repair prior to the organism showing cell growth. The results of the study provide insight of the inhibitory and biocidal mechanisms of FNA on this important microorganism.

Keywords: free nitrous acid, bacteriostatic, bactericidal, *Pseudomonas aeruginosa* PAO1

Introduction

Control and inhibition of microbial growth is an essential undertaking in the food and biotechnology industries and for control of disease and infection. The antimicrobial properties of nitrite have been long known (Cammack et al. 1999; Rowe et al. 1979). However, recently it is demonstrated that the protonated form of nitrite, free nitrous acid (FNA, or HNO_2), is the true metabolic inhibitor (Vadivelu et al. 2006b). Consequently, there is opportunity to use FNA as a bacteriostatic or bactericidal agent to control the growth and activities of microorganisms for various industrial and medical applications (Wang et al. 2013a; Wang et al. 2013b; Weller et al. 2001). For example, in wastewater treatment FNA has been applied to reduce sludge production

and to enhance methane production during the anaerobic sludge digestion (Wang et al. 2013a; Wang et al. 2013b). It has also been experimentally used to reduce pathogen levels involved in gastrointestinal (Rao et al. 2006), periodontal (Allaker et al. 2001), dermal (Weller et al. 2001), and other chronic diseases (Firmani and Riley 2002; Kevil et al. 2011).

The antimicrobial mechanism of FNA is believed to be multi-targeted (Fang 1997) and currently relative studies are inconclusive. FNA per se and possibly the reactive nitrogen species (RNS) derived directly from unstable FNA or by reactions of FNA with other molecules (Dykhuizen et al. 1996) are thought to cause various types of cellular damage. This could be damage to cell enzymes, cellular membranes, cell walls and nuclear acids (Fang 1997). Hypotheses proposed for the antimicrobial effect include proton motive force collapse (Maeda et al. 1998; Wu and Stewart 1998), direct enzyme inhibition (O'Leary and Solberg 1976; Park 1993), nitrosylation of iron-sulphur centers and reduced thiols (Nakaki et al. 1990; Phillips et al. 2004; Woods and Wood 1982; Woods et al. 1981) , DNA mutation and damage (Fang 1997; Juedes and Wogan 1996) , and membrane lipid peroxidation (Halliwell et al. 1992; Rubbo et al. 1994) .

In the recent treatment of activated sludge the antimicrobial effects of FNA are seen to be concentration-related. In general, parts per billion (ppb, equal to μg N/L) levels FNA is bacteriostatic (Pijuan et al. 2010; Vadivelu et al. 2006a; Vadivelu et al. 2006b; Ye et al. 2010; Zhou et al. 2007; Zhou et al. 2008), where as parts per million (ppm, equal to mg N/L) levels exhibit a strong bactericidal effect (Jiang et al. 2011). For instance, Zhou et al. (2008) revealed that 0.004 mg N/L completely inhibited the reduction of nitrous oxide (N_2O) by a denitrifying sludge (Zhou et al. 2008). Vadivelu et al. (2006a&b) reported that the growth of enriched *Nitrobacter* and *Nitrosomonas* cultures stopped at FNA concentrations of 0.023 and 0.4 mg N/L, respectively. These inhibitory effects on respiration and culture growth are generally reversible, as growth resumption is observed immediately or within several hours after the removal of FNA (Vadivelu et al. 2006b; Ye et al. 2010). In contrast, 0.2 mg N/L FNA efficiently disrupted and removed sewer biofilms primarily consisting of sulfate-reducing and methanogenic microorganisms after treatment for 6 to 24 hours (Jiang et al. 2011).

While there are these concentration-related antimicrobial effects of FNA, different microbial populations show differential tolerance to FNA. This is not only observed between bacterial species (Vadivelu et al. 2006a; Vadivelu et al. 2006b) but also in intraspecies strains (Rhoades and Orme 1997). It is currently unknown whether there is a clear concentration threshold that determines the

bacteriostatic or bactericidal effects, in terms of metabolic activity and cell viability, of FNA on microbes.

Pseudomonas aeruginosa is an important model organism with respect to its significant roles both in medicine as an opportunistic pathogen and in the environment as a ubiquitous denitrifier (Morita et al. 2014; Stover et al. 2000). It is a facultative anaerobic bacterium that forms biofilms, which are essential for its persistence and resistance to various antimicrobial agents (Filiatrault et al. 2006; Schurek K.N. et al., 2012) . Presently, there are limited investigations of the antimicrobial effects of FNA or nitrite on *P. aeruginosa*. Rowe et al. (1979) reported that nitrite could exert a bacteriostatic effect through the oxidation of cytochrome ferrous iron to disrupt the aerobic respiratory activity of *P. aeruginosa* (Rowe et al. 1979). In other studies, bacteriophage genes are seen to be activated in *P. aeruginosa* biofilms by nitric oxide (NO) (Barraud et al. 2006; Platt et al. 2008), and this was believed to account for cell lysis and biofilm dispersal.

This study investigates the potential concentration-related effects of FNA on *P. aeruginosa* under anaerobic conditions. Anaerobic respiratory growth conditions were chosen to examine the antimicrobial effects of FNA on *P. aeruginosa*, as these conditions are relevant to the organisms in various natural environments. Culture growth, respiratory activity and cell integrity of *P. aeruginosa* PAO1 planktonic culture was investigated in the presence of various FNA levels. The recovery of growth after the removal of FNA was also determined. The findings provide fundamental insight to the bacteriostatic/bactericidal effects of FNA on *P. aeruginosa* and contribute towards the application of FNA as an antimicrobial agent.

Materials and Methods

Bacterial strain and cultivation condition. *P. aeruginosa* PAO1 (DSM No: 22644) was obtained from the Deutsche Sammlung von Mikroorganismen und Zellkulturen GmbH (DSMZ), Germany. Glycerol modified M9 (GLYM9) medium was established and used to cultivate the bacterium in anaerobic conditions (Webb et al. 2003). This medium contained 0.2 M phosphate buffer, 9 mM NaCl, 38 mM NH_4Cl, 2 mM $MgSO_4 \cdot 3H_2O$, 100 μM $CaCl_2 \cdot 2H_2O$, 10 g/L glycerol, 0.2 g/L yeast extract and 30 mM of $NaNO_3$ with the pH adjusted to 6.3±0.3. *P. aeruginosa* was activated according to the supplier (DSMZ) and grown on tryptic soy agar (TSA) plates at 30 ºC for 26 hours. One colony was then selected and transferred to tryptic soy broth (TSB) medium and incubated shaken at 150 rpm at 30 ºC for another 26 hours. Afterwards, 5 mL of bacterium suspension was transferred into the serum bottles containing 150 mL of sterile anaerobic GLYM9 medium in an anaerobic chamber. The anaerobic GLYM9 medium was made by aerating each serum bottle with

nitrogen gas for 30 minutes before capping with butyl rubber stopper. After 26 hours' incubation, optical density at 600 nm (OD_{600}) was measured and then adjusted to 0.5. 10 mL of this inoculum standard was transferred into 150 mL of sterile anaerobic GLYM9 medium in serum bottles in an anaerobic chamber to finally achieve the anaerobic condition. *P. aeruginosa* cultures were then incubated at 30 ˚C while shaken at 150 rpm for the use of growth inhibition experiments described below.

Culture growth and respiratory activity measurements during FNA treatment. *P. aeruginosa* cultures were prepared in serum bottles and incubated as mentioned above. All culture growth and analyses of the cultures (described below) were performed in triplicate. Eleven hours after the inoculation when the culture was in early log phase of growth, nitrite was added to reach starting FNA concentrations of 0.01, 0.05, 0.1, 0.15, 0.2, 1.0, and 5.0 mg N/L in seven bottles. The FNA concentration is dependent on pH and temperature and was determined from the measured nitrite concentration as HNO_2-N mg/L using Equation 1 (Anthonisen et al. 1976). The cultures were incubated for a further 53 hours (a total of 64 hours incubation). The culture OD_{600} and pH were monitored throughout the entire incubation using a Cary 50 bio UV visible spectrophotometer (Varian, Australia) and a labCHEM-pH Benchtop pH – mV – Temperature Meter, respectively. For all growth experiments the pH was monitored and this ranged from 6.1 to 6.4. The slight pH increases occurring during the incubation time was due to denitrification activity.

Equation 1: $\mathrm{FNA\ (as\ HNO_2 - N)} = \frac{\mathrm{NO_2{-}N}}{\mathrm{K_a \times 10^{pH}}}$

$\mathrm{K_a} = \mathrm{e}^{-2300/(270+\mathrm{T(^{\circ}C)})}$

During the incubation of the cultures the levels of glycerol, nitrate, and nitrite were determined. For nitrite and nitrate analyses culture samples were immediately filtered through 0.22 μm filters (Merck Millipore, USA) and analyzed on a Lachat QuikChem 8000 flow injection analyzer (FIA). Glycerol levels were determined in filtered samples using an external standard by a high performance liquid chromatography (HPLC). This was a Shimadzu LC equipped with a Phenomenex Rezex ROA column (300 nm × 7.8 nm), specialized for organic acid analysis, and a Shimadzu refractive index detector (RID-10A). The mobile phase was 0.008N H_2SO_4 with a flow rate of 0.4 mL/min.

LIVE/DEAD staining. During the growth of *P. aeruginosa* samples were taken to perform Live/Dead staining to determine the viable cell percentage before and after FNA treatment. *P.*

aeruginosa cultures were prepared as described above and nitrite was added to reach FNA starting concentrations of: 0, 0.05, 0.1, 1.0, and 5.0 mg N/L. All experiments were performed in triplicate. 500 µL of *P. aeruginosa* cultures were taken at different stages and treated with the LIVE/DEAD BacLight Bacterial Viability Kit (Molecular Probes, L7012) to differentially stain cells with intact or damaged membranes. The stained cells were then quantified using the FACSArial™ II (BD Biosciences, San Jose, USA) type flow cytometer.

Culture growth recovery after FNA treatment. The recovery growth of *P. aeruginosa* was determined following FNA exposure once the FNA was removed. Triplicated *P. aeruginosa* cultures were prepared and treated with FNA at concentrations of 0, 0.05, 0.1, 1.0 and 5.0 mg N/L as described above. During the incubation when the cultures were still inhibited by FNA, 50 mL of bacterial suspension was taken and centrifuged at 5000 g for 10 minutes at room temperature. Then the wet cell pellet masses were determined immediately after discarding the supernatant and the masses obtained ranged from 0.05g to 0.15g. This was done at the incubation times of 11, 12, and 16 hours for the FNA concentrations of 0, 0.05, and 0.1mg N/L respectively, and also at 48 hours for the FNA concentrations 1.0 and 5.0 mg N/L. The bacterial pellets were washed twice with autoclaved fresh GLYM9 medium in the anaerobic chamber to completely remove the residual FNA and then resuspended into 150 mL of sterile anaerobic GLYM9 medium in serum bottles following by incubation at 30 ºC shaken at 150 rpm for 72 hours.

To estimate the cell biomass concentration of the cultures, samples were taken and after centrifugation the supernatant was discarded and the wet cell mass of the pellets were measured. The live cell amounts within each wet biomass sample were determined from Live/Dead staining that was performed as described above.

Results

Concentration-determined effects of FNA on culture growth, respiratory activity and cell lysis of *P. aeruginosa.* During the 64 hours incubation, similar growth patterns were observed for *P. aeruginosa* in the control cultures (no FNA addition) and in the cultures exposed to low starting FNA concentrations of 0.01 and 0.05 mg N/L (Figure 1). The term 'starting concentration' is used as FNA levels change during the incubation due to denitrification activity of *P. aeruginosa* described below. FNA induced inhibition of growth was evident at FNA concentrations higher than 0.05 mg N/L. The length of the inhibition time period, before the culture regrowth was detected, increased with increasing starting concentrations from 0.05 to 1.0 mg N/L. The higher the starting FNA concentration applied, the longer the inhibition time lasted (Figure 1). After the inhibition

period and within the total 64 hours incubation, cultures treated with 0.15 mg N/L or lower FNA starting concentrations eventually grew to reach cell levels similar to the control cultures (Figure 1).

P. aeruginosa respiration by denitrification was observed through the utilization of glycerol as the electron donor, and nitrate and nitrite as the electron acceptors (Figure 2a, b and c). Denitrification still occurred when the growth of *P. aeruginosa* was inhibited. This was indicated by the consumption of electron donors and acceptor in the cultures with starting FNA concentrations of 0.1, 0.15 and 0.2 mg N/L during the growth inhibitory periods (Figures 1 and 2). Nitrate and nitrite reductase activities seem to be inactivated by FNA concentrations of approximately 0.05 and 0.18 mg N/L, respectively (Figures 2 b and d). Additionally, the nitrite reduction rate seems to be independent of FNA concentrations while the nitrate reduction rate decreased as the FNA concentration increased (Figures 2 b and c). Consequently, the FNA concentrations were lowered to below the growth inhibitory threshold as nitrite reduction occurred (between 0.05 and 0.1 mg N/L) to allow the regrowth of the cultures (Figure 1 and 2d). It was evident that the difference in time it took to recover between 0.15 mg N/L and 0.2 mg N/L FNA was bigger than that of between 0.1 mg N/L and 0.15 mg N/L FNA. It is apparent that at the starting FNA concentration of 0.2 mg N/L there is some additional antimicrobial effect of FNA. Consequently, the cells activities, such as denitrification, were lower than those at the lower FNA concentrations (Figure 2 c and d).

Neither growth recovery nor glycerol utilization was detected for *P. aeruginosa* with starting FNA concentrations of 1.0 and 5.0 mg N/L (Figure 1 and 2a). Although FNA levels cannot be accurately measured at these high levels with the method mentioned above, high levels of FNA remained throughout the incubation time for these cultures. These high levels of FNA likely disrupted bacterial cells and caused cell lysis as OD_{600} depletion was detected after 40 and 17 hours incubation for these two cultures, respectively (Figure 1). Bacteriophage genes were reported to express in *P. aeruginosa* biofilms by nitric oxide (NO) (Barraud et al. 2006; Platt et al. 2008) and phage-induced cell lysis was believed to the cause of biofilm dispersal. However, we did not detect remarkable phage activity in this study (data not shown).

Population differential disruption of cell membrane integrity by FNA. To determine whether there is a clear concentration threshold to distinguish bacteriostatic and bactericidal effects of FNA upon *P. aeruginosa*, we measured cell viability in different FNA levels by LIVE/DEAD staining. Prior to FNA treatment the *P. aeruginosa* cultures consistently contained around 90% viable cells (Figure 3). The control cultures (no FNA addition) maintained this level up to the end of the exponential growth, which was about 30 hours. Following that, in the stationary phase, for both

control and the FNA concentration 0.05 mg N/L, the live cells percentage decreased to around 60% when the incubation time was 64 hour, and this was likely resulting from substrate depletion and low cell energetics. In contrast, there were substantial decreases in the proportion of live cells immediately upon the addition of FNA (Figure 3) and throughout the inhibitory period, even with the lowest FNA addition. For the starting FNA concentrations of 0.05, 0.1 and 1.0 mg N/L the overall cell killing rate (indicated as the rate of decreasing live cell percentages, Figure 3) positively correlated with FNA levels during inhibition periods ($p < 0.01$). In contrast, *P. aeruginosa* cells were almost completely killed within 10 hours of adding an FNA concentration of 5.0 mg N/L (Figure 3). This is consistent with the strong cell lytic effect of FNA at this level as suggested from the growth profile (Figure 1).

This result does not support the previous assumption that there is a clear concentration threshold between the bacteriostatic and bactericidal effects of FNA (Jiang et al. 2011; Pijuan et al. 2010; Vadivelu et al. 2006a; Vadivelu et al. 2006b; Ye et al. 2010; Zhou et al. 2007; Zhou et al. 2008). In contrast, we show here that, from low to high FNA levels, cell killing occurred in a subpopulation of *P. aeruginosa* cells, while another subpopulation was inhibited in growth but still active in respiration (Figure 1, 2 and 3). Interestingly, even at the high FNA level of 1.0 mg N/L when the whole culture's respiratory activity was inhibited, there were still about 30% of the cells with intact membranes. This suggests a considerable proportion of cells either already possessed or had developed tolerance to this FNA level, indicating possible differential tolerance towards FNA in the *P. aeruginosa* cultures.

FNA inhibition on culture growth recoverability. The regrowth of cultures following the removal of FNA was studied to detect the possible carryover of detrimental effects on cell activities. Cultures were exposed to FNA and during growth inhibition periods the FNA was removed and the extent of regrowth was then detected in fresh media. It was seen that with the higher FNA starting concentrations, slower culture regrowth occurred (Figure 4a). At relatively low starting FNA concentrations of 0.05 and 0.1 mg HNO_2- N/L, the regrowth was comparable to that of the control. However, in starting FNA concentration of 1.0 mg N/L, culture regrowth was delayed by 53 hours (Figure 4a) and it took approximately 100 hours to reach stationary phase (not shown in Figure 4a). No recovery was observed for the culture with starting FNA concentration of 5.0 mg N/L, suggesting complete killing of the cells at this high level of FNA (Figure 3).

As different proportions of cells were killed after different levels of FNA treatment (Figure 3), the growth delay of the culture after high levels of FNA treatment could be due to the lower number of

live cells in the biomass rather than lower growth activity of the survived live cells. To examine whether there was a carryover growth-delay effect of FNA on live cells, we compared the growth time needed to achieve an OD_{600} of 0.5 between FNA treated and untreated *P. aeruginosa* cultures that were inoculated with equivalent amounts of live cells (see Materials and Methods for the calculation). It was evident that the recovery times of the cultures with high FNA concentrations were much greater than those of the untreated cells, even though these had equivalent levels of live cells (Figure 4b). These extended recovery times were about 10 hours for a starting FNA concentration of 0.1 mg N/L and about 60 hours for a starting FNA concentration of 1.0 mg N/L (Figure 4b).

Discussion

Concentration-related multi-level effects of FNA. Previous studies suggest there are multiple antimicrobial effects of FNA that include reduced cell growth and respiration, and disruption of cellular components (Fang 1997; Vadivelu et al. 2006a; Vadivelu et al. 2006b; Zhou et al. 2008). However, specific effects are seldom related to specific FNA concentrations. This study shows concentration-related multiple-level effects of FNA on *P. aeruginosa* cultures (Figure 1 and 2). With FNA concentrations of 0.05 mg N/L and lower, growth and respiration occurred as for the culture without FNA addition. Inhibition of growth inhibition occurred at FNA levels from 0.1 to 0.2 mg N/L although cell respiration was still functioning through denitrification (Figure 2). Once denitrification activity had lowered the FNA to below this threshold, culture growth recovered. This respiratory activity was not completely inhibited until FNA had risen to 1.0 mg N/L. At high FNA levels, (i.e. 1.0 and 5.0 mg N/L) both cell growth and respiration had stopped and cell lysis was observed. Therefore, we detected a significantly lower FNA threshold concentration for cell growth (anabolism) inhibition in comparison to catabolic inhibition (i.e. 0.1 versus 1.0 mg N/L). This is consistent with previous studies upon FNA treatment of enriched cultures (Vadivelu et al. 2006a; Vadivelu et al. 2006b) and cultures of *Pseudomonas fluorescens (Almeida et al. 1995)*. For instance, Vadivelu et. al (2006a) reported that FNA initiated inhibition of the anabolic processes of *Nitrobacter* (NOB) at approximately 0.011 mg N/L and completely stopped biomass synthesis at a concentration of approximately 0.023 mg N/L, while up to 0.05 mg N/L did not show any inhibitory effect on the catabolic processes. The selective inhibition of some key steps in the carbon transformation could possibly account for this as suggested by Vadivelu et. al (2006a, b).

Heterogeneous tolerance of the cell population to FNA. Recent studies imply that FNA exerts a bacteriostatic effect at ppb levels and a bactericidal effect at ppm levels (Jiang et al. 2011; Pijuan et al. 2010; Zhou et al. 2010; Zhou et al. 2007; Zhou et al. 2008). While these studies were based on

observation of mixed cultures, various experiments suggest there are organism-specific FNA-tolerant levels (Vadivelu et al. 2006a; Vadivelu et al. 2006b; Ye et al. 2013). Vadivelu et al. (2006a,b) revealed that the anabolic processes (growth) of an enriched *Nitrobacter* and an enriched *Nitrosomonas* culture were stopped by the FNA concentration of 0.023 and 0.4 mg N/L, respectively. Ye et al. (2013) demonstrated that FNA has a detrimental effect on the acetate uptake rate by both polyphosphate accumulating organisms (PAOs) and glycogen accumulating organisms (GAOs), however, this adverse effect was much stronger on PAOs than on GAOs. However, it is not known whether there are particular bacteriostatic specific and bactericidal specific FNA concentrations for a certain bacterial species. Intriguingly, here we detected an immediate bactericidal effect on *P. aeruginosa* cells even at low FNA concentrations. At the FNA concentration of 0.05 mg N/L, the live cell percentage decreased from 90% to about 70% during the inhibitory period (Figure 3). In contrast, 30% of the cells were still alive after 53 hours exposure to 1.0 mg N/L FNA. This not only indicates the high tolerance of *P. aeruginosa* to FNA but this also contradicts the existence of a uniform bactericidal threshold of FNA within a specific bacterial strain.

The mechanism of such differential tolerance (also namely heterogeneity) in a bacterial population towards FNA is unclear. Although currently there is little known regarding details of tolerance to FNA, some mechanisms for FNA and RNSs have been proposed. These include activating expression of genes that encode proteins involved in detoxification (e.g. globins and reductases), repair (e.g. glutathione and homocysteine) and maintenance of homeostasis (e.g. sequestration of iron) (Poole 2005; Rogstam et al. 2007). Population heterogeneity may provide opportunity for development of resistance to antimicrobial agents, such as has occurred in the application of antibiotics (Gefen and Balaban 2009). Various subpopulations of bacteria may form, e.g. “persisters”, that have the potential to better resist antibiotics and other environmental stress (Avery 2006). For example, *Escherichia coli* cells can enter a state in which some of the cells temporarily stop growing and subsequently elude the killing action of ß-lactam antibiotics (Keren et al. 2004). Recently it is discovered that genetic heterogeneity in *P. aeruginosa* enabled diversification and selection within the population in a short period (McElroy et al. 2014). Consequently, population heterogeneity may explain the results observed here, such that resistance to FNA occurred. If this has occurred, this would be significant as resistance to biocidal agents like FNA, that have multiple disrupting effects, are not generally detected (Codling et al. 2003).

The carryover detrimental effects of FNA to survived cells. Our results along with many previous studies suggest that the inhibition of FNA to culture growth is reversible and the recovery

time is generally correlated to the treated FNA concentrations (Zhou et al. 2008). However, it is unknown whether the longer recovery time in cultures treated with high FNA concentrations is simply due to the lower amount of live cells or caused by FNA carryover damage to the live cells. In this study we detected the occurrence of a significantly extended recovery time, and this could be explained by carryover damage. Such damage may include disruption to cell proteins, lipids and DNA (Fang 1997; Zhou et al. 2011). Detrimentally effected cells would likely require more maintenance energy prior to regrowth occurring (Zhou et al. 2008). An alternative possibility is that cells may need to be invoked from a resting or self-protecting state before restoring growth (Harrison et al. 2005; Keren et al. 2004). Additionally, we cannot rule out the possibility that a subpopulation of cells in the FNA treated cultures were actually killed while still maintaining membrane integrity. Inoculums containing these 'pseudo-live' cells may recover slowly simply because of fewer viable cells.

Achieving control of microbial growth is extremely important in many industrial, environmental and medical situations. In this study, we demonstrate that FNA causes bacteriostatic/bactericidal effects to *P. aeruginosa*, an important opportunistic pathogen. These findings are providing a platform of understanding for the potential use of FNA to control the growth and activity of the organism in anaerobic growth conditions. Addtitionally, different effects of FNA were detected in the *P. aeruginosa* population, and such differences would likely be important for the possible development of resistance to this antimicrobial agent. Further studies should be performed to determine the details of the antimicrobial effect and mechanism of FNA.

Acknowledgements

We acknowledge the Australian Research Council for funding support of project DP120102832 **(**Biofilm Control in Wastewater Systems using Free Nitrous Acid - a Renewable Material from Wastewater) and scholarship support for Shu-Hong Gao from the China Scholarship Council. We thank Dr. Beatrice Keller and Jianguang Li, University of Queensland for FIA analysis and Dr. Michael Nefedov, University of Queensland for assistance with the BD FACS AriaII flow cytometer and data analysis.

References

Allaker R.P., Silva Mendez L.S., Hardie J.M., Benjamin N. 2001. Antimicrobial effect of acidified nitrite on periodontal bacteria. *Oral Microbiology and Immunology,* 16, 253-256.

Almeida J.S., Júlio S.M., Reis M.A., Carrondo M.J. 1995. Nitrite inhibition of denitrification by *Pseudomonas fluorescens*. *Biotechnology and Bioengineering,* 46, 194-201.

Anthonisen A.C., Loehr R.C., Prakasam T.B., Srinath E.G. 1976. Inhibition of nitrification by ammonia and nitrous acid. *Water Pollution Control Federation,* 8, 835-852.

Avery S.V. 2006. Microbial cell individuality and the underlying sources of heterogeneity. *Nature Reviews. Microbiology,* 4, 577-587.

Barraud N., Hassett D.J., Hwang S.H., Rice S.A., Kjelleberg S., Webb J.S. 2006. Involvement of nitric oxide in biofilm dispersal of *Pseudomonas aeruginosa*. *Journal of Bacteriology,* 188, 7344-7353.

Cammack R., Joannou C.L., Cui X.Y., Torres Martinez C., Maraj S.R., Hughes M.N. 1999. Nitrite and nitrosyl compounds in food preservation. *Biochimica et biophysica acta,* 1411, 475-488.

Codling C.E., Maillard J.Y., Russell A.D. 2003. Aspects of the antimicrobial mechanisms of action of a polyquaternium and an amidoamine. *The Journal of Antimicrobial Chemotherapy,*51, 1153-1158.

Dykhuizen R.S., Frazer R., Duncan C., Smith C.C., Golden M., Benjamin N., Leifert C. 1996. Antimicrobial effect of acidified nitrite on gut pathogens: importance of dietary nitrate in host defense. *Antimicrobial Agents and Chemotherapy,* 40, 1422-1425.

Fang F.C. 1997. Perspectives series: host/pathogen interactions. Mechanisms of nitric oxide-related antimicrobial activity. *The Journal of Clinical Investigation,* 99, 2818-2825.

Filiatrault M.J., Picardo K.F., Ngai H., Passador L., Iglewski B.H. 2006. Identification of *Pseudomonas aeruginosa* genes involved in virulence and anaerobic growth. *Infection and Immunity,* 74, 4237-4245.

Firmani M.A., Riley L.W. 2002. Reactive nitrogen intermediates have a bacteriostatic effect on *Mycobacterium tuberculosis* in vitro. *Journal of Clinical Microbiology,* 40, 3162-3166.

Gefen O., Balaban N.Q. 2009. The importance of being persistent: heterogeneity of bacterial populations under antibiotic stress. *FEMS Microbiology Reviews,* 33, 704-717.

Halliwell B., Hu M.L., Louie S., Duvall T.R., Tarkington B.K., Motchnik P., Cross C.E. 1992. Interaction of nitrogen dioxide with human plasma. antioxidant depletion and oxidative damage. *FEMS Letters,* 313, 62-66.

Harrison J.J., Turner R.J., Ceri H. 2005. Persister cells, the biofilm matrix and tolerance to metal cations in biofilm and planktonic *Pseudomonas aeruginosa*. *Environmental Microbiology,* 7, 981-994.

Jiang G., Gutierrez O., Yuan Z. 2011. The strong biocidal effect of free nitrous acid on anaerobic sewer biofilms. *Water Research,* 45, 3735-3743.

Juedes M.J., Wogan G.N. 1996. Peroxynitrite-induced mutation spectra of pSP189 following replication in bacteria and in human cells. *Mutation Research,* 349, 51-61.

Keren I., Shah D., Spoering A., Kaldalu N., Lewis K. 2004. Specialized persister cells and the mechanism of multidrug tolerance in *Escherichia coli*. *Journal of Bacteriology,* 186, 8172-8180.

Kevil C.G., Kolluru G.K., Pattillo C.B., Giordano T. 2011. Inorganic nitrite therapy: historical perspective and future directions. *Free Radical Biology & Medicine,* 51, 576-593.

Maeda S., Okamura M., Kobayashi M., Omata T. 1998. Nitrite-specific active transport system of the *Cyanobacterium Synechococcus sp.* strain PCC 7942. *Journal of Bacteriology,* 180, 6761-6763.

McElroy K.E., Hui J.G., Woo J.K., Luk A.W., Webb J.S., Kjelleberg S., Rice S.A., Thomas T. 2014. Strain-specific parallel evolution drives short-term diversification during *Pseudomonas aeruginosa* biofilm formation. *Proceedings of the National Academy of Sciences of the United States of America,* 111, E1419-E1427.

Morita Y., Tomida J., Kawamura Y. 2014. Responses of *Pseudomonas aeruginosa* to antimicrobials. *Frontiers in Microbiology,* 4, 422.

Nakaki T., Nakayama M., Kato R. 1990. Inhibition by nitric oxide and nitric oxide-producing vasodilators of DNA synthesis in vascular smooth muscle cells. *European Journal of Pharmacology,* 189, 347-353.

O'Leary V., Solberg M. 1976. Effect of sodium nitrite inhibition on intracellular thiol groups and on the activity of certain glycolytic enzymes in *Clostridium perfringens*. *Applied and Environmental Microbiology,* 31, 208-212.

Park J.W. 1993. S-Nitrosylation of sulfhydryl groups in albumin by nitrosating agents *Archives of Pharmacal Research,* 16, 1-5.

Phillips R., Adjei O., Lucas S., Benjamin N., Wansbrough-Jones M. 2004. Pilot randomized double-blind trial of treatment of *Mycobacterium ulcerans* disease (Buruli ulcer) with topical nitrogen oxides. *Antimicrobial Agents and Chemotherapy,* 48, 2866-2870.

Pijuan M., Ye L., Yuan Z.G. 2010. Free nitrous acid inhibition on the aerobic metabolism of poly-phosphate accumulating organisms. *Water Research,* 44, 6063-6072.

Platt M.D., Schurr M.J., Sauer K., Vazquez G., Kukavica-Ibrulj I., Potvin E., Levesque R.C., Fedynak A., Brinkman F.S.L., Schurr J., Hwang S.-H., Lau G.W., Limbach P.A., Rowe J.J., Lieberman M.A., Barraud N., Webb J., Kjelleberg S., Hunt D.F., Hassett D.J. 2008. Proteomic, microarray, and signature-tagged mutagenesis analyses of anaerobic *Pseudomonas aeruginosa* at pH 6.5, likely representing chronic, late-stage cystic fibrosis airway conditions. *Journal of Bacteriology,* 190, 2739-2758.

Poole R.K. 2005. Nitric oxide and nitrosative stress tolerance in bacteria. *Biochemical Society Transactions,* 33, 176-180.

Rao A., Jump R.L., Pultz N.J., Pultz M.J., Donskey C.J. 2006. In vitro killing of nosocomial pathogens by acid and acidified nitrite. *Antimicrobial Agents and Chemotherapy,* 50, 3901-3904.

Rhoades E.R., Orme I.M. 1997. Susceptibility of a panel of virulent strains of *Mycobacterium tuberculosis* to reactive nitrogen intermediates. *Infection and Immunity,* 65, 1189-1195.

Rogstam A., Larsson J.T., Kjelgaard P., von Wachenfeldt C. 2007. Mechanisms of adaptation to nitrosative stress in *Bacillus subtilis*. *Journal of Bacteriology,* 189, 3063-3071.

Rowe J.J., Yarbrough J.M., Rake J.B., Eagon R.G. 1979. Nitrite inhibition of aerobic bacteria. *Current Microbiology,* 2, 51-54.

Rubbo H., Radi R., Trujillo M., Telleri R., Kalyanaraman B., Barnes S., Kirk M., Freeman B.A. 1994. Nitric oxide regulation of superoxide and peroxynitrite-dependent lipid peroxidation. Formation of novel nitrogen-containing oxidized lipid derivatives. *Journal of Biological Chemistry,* 269, 26066-26075.

Schurek, K. N., Breidenstein, E. B. & Hancock, R. E. 2012. Antibiotic Discovery and Development. Springer.

Stover C.K., Pham X.Q., Erwin A.L., Mizoguchi S.D., Warrener P., Hickey M.J., Brinkman F.S., Hufnagle W.O., Kowalik D.J., Lagrou M., Garber R.L., Goltry L., Tolentino E., Westbrock-Wadman S., Yuan Y., Brody L.L., Coulter S.N., Folger K.R., Kas A., Larbig K., Lim R., Smith K., Spencer D., Wong G.K., Wu Z., Paulsen I.T., Reizer J., Saier M.H., Hancock R.E., Lory S., Olson M.V. 2000. Complete genome sequence of *Pseudomonas aeruginosa* PAO1, an opportunistic pathogen. *Nature,* 406, 959-964.

Vadivelu V.M., Keller J., Yuan Z.G. 2006a. Effect of free ammonia and free nitrous acid concentration on the anabolic and catabolic processes of an enriched *Nitrosomonas* culture. *Biotechnology and Bioengineering,* 95, 830-839.

Vadivelu V.M., Yuan Z., Fux C., Keller J. 2006b. The inhibitory effects of free nitrous acid on the energy generation and growth processes of an enriched nitrobacter culture. *Environmental Science & Technology,* 40, 4442-4448.

Wang Q., Ye L., Jiang G., Jensen P., Batstone D., Yuan Z. 2013a. Free Nitrous Acid (FNA)-based pre-treatment enhances methane production from waste activated sludge. *Environmental Science & Technology,* 47, 11897-11904.

Wang Q., Ye L., Jiang G., Yuan Z. 2013b. A free nitrous acid (FNA)-based technology for reducing sludge production. *Water Research,* 47, 3663-3672.

Webb J.S., Thompson L.S., James S., Charlton T., Tolker-Nielsen T., Koch B., Givskov M., Kjelleberg S. 2003. Cell death in *Pseudomonas aeruginosa* biofilm development. *Journal of Bacteriology,* 185, 4585-4592.

Weller R., Price R.J., Ormerod A.D., Benjamin N., Leifert C. 2001. Antimicrobial effect of acidified nitrite on dermatophyte fungi, *Candida* and bacterial skin pathogens. *Journal of Applied Microbiology,* 90, 648-652.

Woods L.F., Wood J.M. 1982. A note on the effect of nitrite inhibition on the metabolism of *Clostridium botulinum*. *The Journal of Applied Bacteriology,* 52, 109-110.

Woods L.F., Wood J.M., Gibbs P.A. 1981. The involvement of Nitric Oxide in the inhibition of the phosphoroclastic system in *Clostridium sporogenes* by sodium nitrite. *Journal of General Microbiology,* 125, 399-406.

Wu Q., Stewart V. 1998. NasFED proteins mediate assimilatory nitrate and nitrite transport in *Klebsiella oxytoca* (*pneumoniae*) M5al. *Journal of Bacteriology,* 180, 1311-1322.

Ye L., Pijuan M., Yuan Z. 2013. The effect of free nitrous acid on key anaerobic processes in enhanced biological phosphorus removal systems. *Bioresource Technology,* 130, 382-389.

Ye L., Pijuan M., Yuan Z.G. 2010. The effect of free nitrous acid on the anabolic and catabolic processes of glycogen accumulating organisms. *Water Research,* 44, 2901-2909.

Zhou Y., Ganda L., Lim M., Yuan Z.G., Kjelleberg S., Ng W.J. 2010. Free nitrous acid (FNA) inhibition on denitrifying poly-phosphate accumulating organisms (DPAOs). *Applied Microbiology and Biotechnology,* 88, 359-369.

Zhou Y., Oehmen A., Lim M., Vadivelu V., Ng W.J. 2011. The role of nitrite and free nitrous acid (FNA) in wastewater treatment plants. *Water research,* 45, 4672-4682.

Zhou Y., Pijuan M., Yuan Z. 2007. Free nitrous acid inhibition on anoxic phosphorus uptake and denitrification by poly-phosphate accumulating organisms. *Biotechnology and Bioengineering,* 98, 903-912.

Zhou Y., Pijuan M., Zeng R.J., Yuan Z. 2008. Free Nitrous Acid Inhibition on Nitrous Oxide Reduction by a Denitrifying-Enhanced Biological Phosphorus Removal Sludge. *Environmental Science & Technology,* 42, 8260-8265.

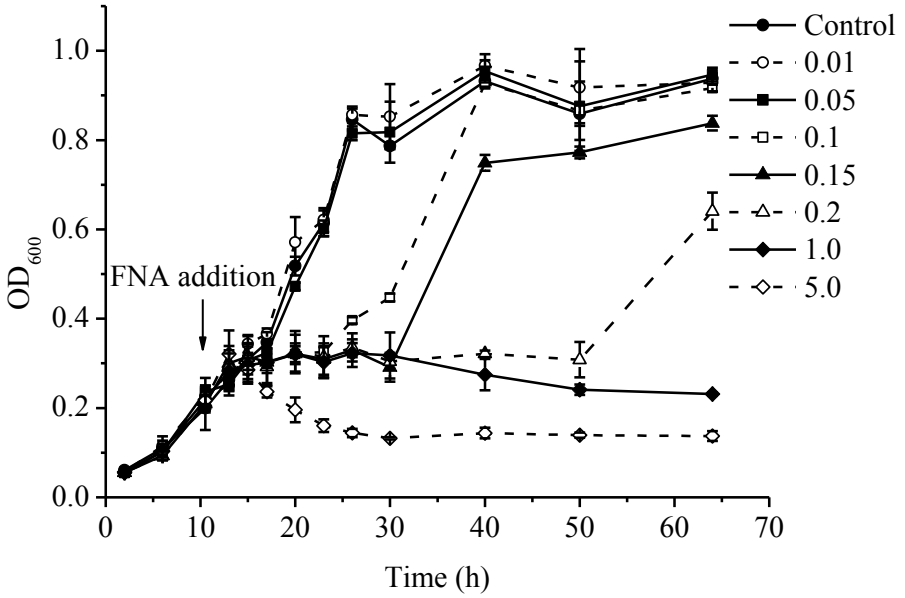

Figure. 1 Growth of *P. aeruginosa* batch cultures treated with different levels of FNA (mg N/L). FNA was added 11 hours into the incubation period. The control culture had no FNA addition. Error bars show the standard deviation of the triplicated control samples. S/C means starting concentration.

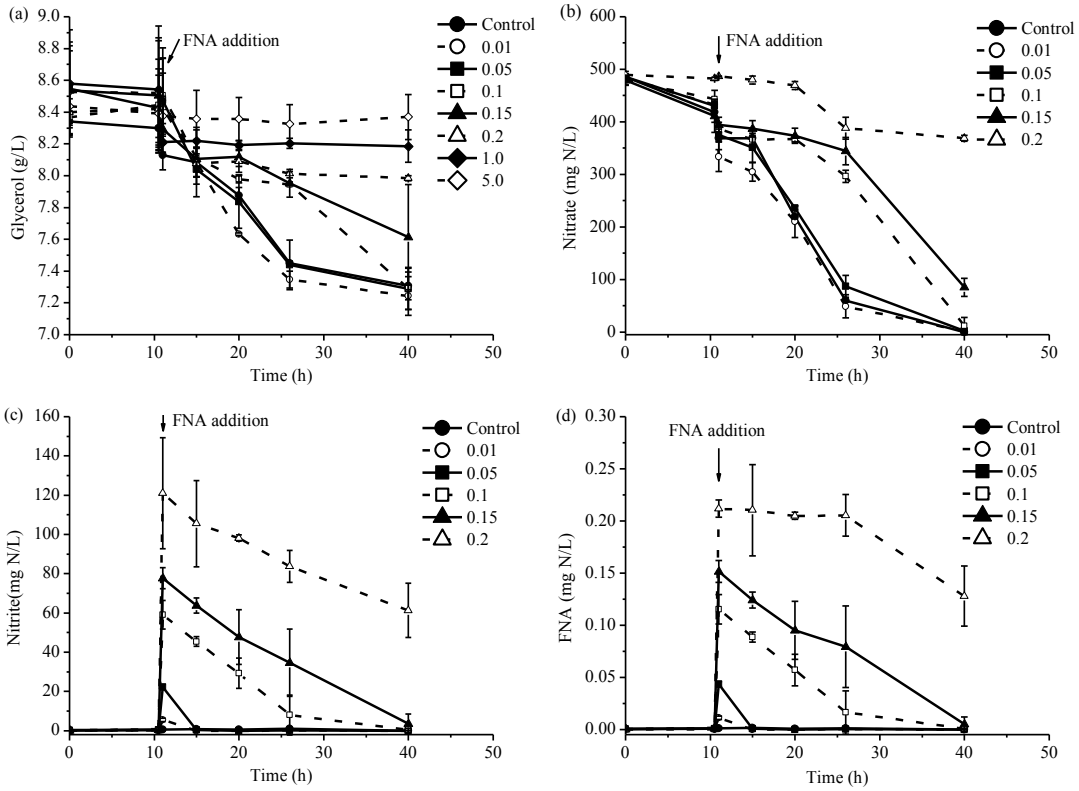

Figure.2 Glycerol (a), nitrate (b), nitrite (c), and FNA (d) levels in *P. aeruginosa* batch cultures during incubation with different FNA starting concentrations. Different levels of FNA starting concentration were added 11 hours into the incubation period. The control culture had no addition of FNA. Error bars show the standard deviation of the triplicated control samples. Nitrate, nitrite and FNA concentrations in the cultures with FNA starting concentrations of 1.0 and 5.0 mg N/L are not shown as such high levels of nitrite cannot be accurately measured using the analytical method in this study. S/C means starting concentration.

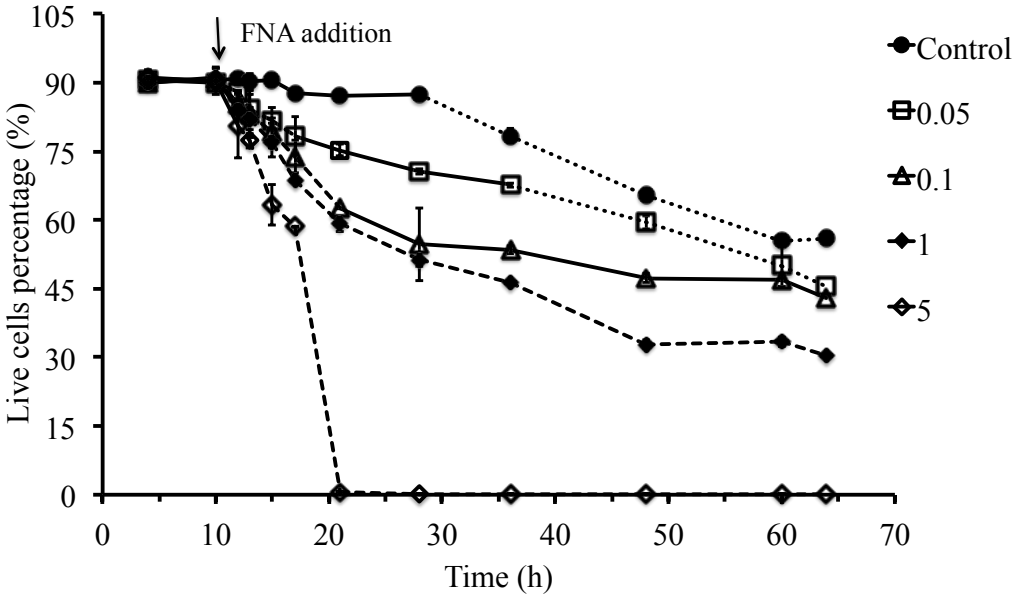

Figure. 3 Cell viability of *P. aeruginosa* cultures treated with different levels of FNA (mg N/L) as determined by the LIVE/DEAD BacLight stain. Dashed lines represent periods when the culture growth was inhibited by FNA. Solid lines after FNA addition represent the period of exponential growth. Dot lines represent the stationary growth phase after adding FNA. Error bars were determined for all samples and show the standard deviation of triplicate analyses. S/C means starting concentration.

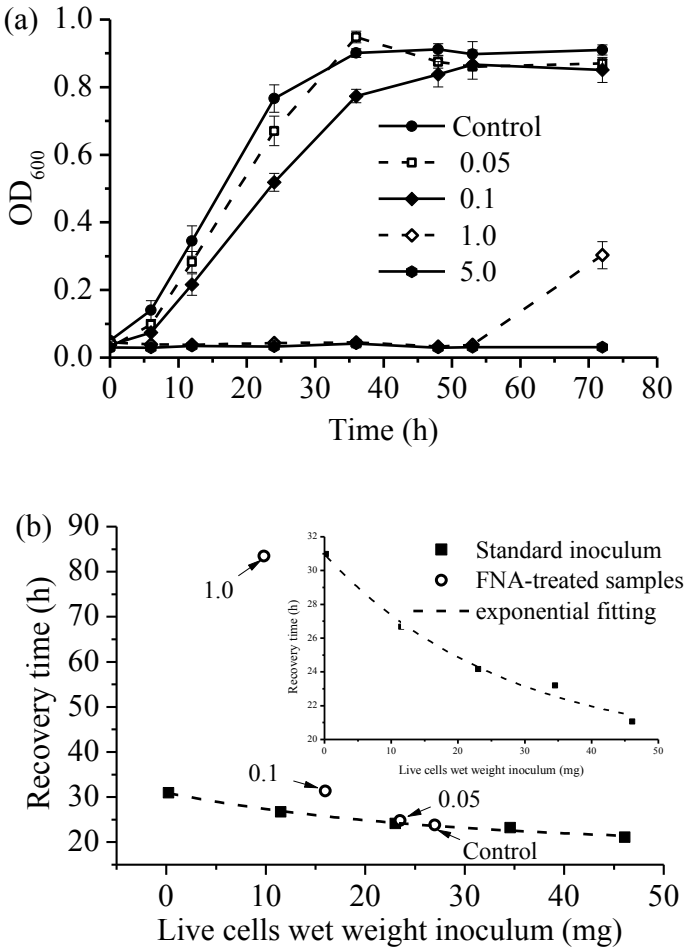

Figure. 4 FNA effects on growth recoverability of *P. aeruginosa* cultures. (a) Growth recovery of cultures after being treated with different FNA starting levels (mg N/L). (b) The carryover effects of FNA on the growth recoverability of live cells. The embedded graph shows the standard inoculum curve over a smaller time scale. Recovery time is the time needed for cultures to achieve OD_{600} 0.5. Error bars indicate the standard deviation of the triplicate samples. S/C means starting concentration.

Appendix B

Determining multiple responses of *Pseudomonas aeruginosa* PAO1 to an antimicrobial agent, free nitrous acid

Shu-Hong Gao, Lu Fan*, Lai Peng, Jianhua Guo, Míriam Agulló-Barceló, Zhiguo Yuan and Philip L Bond*

This paper is published in *Environmental Science & Technology*.

Abstract

Free nitrous acid (FNA) has recently been demonstrated as an antimicrobial agent on a range of microorganisms, especially in wastewater treatment systems. However, the antimicrobial mechanism of FNA is largely unknown. Here we report that the antimicrobial effects of FNA are multi-targeted. The response of a model denitrifier, *Pseudomnas aeruginosa* PAO1 (PAO1), common in wastewater treatment was investigated in the absence and presence of an inhibitory level of FNA (0.1 mg N/L) under anaerobic denitrifying conditions. This was achieved through coupling gene expression analysis, by RNA sequencing, with a suite of physiological analyses. Various transcripts exhibited significant changes in abundance in the presence of FNA. Respiration was likely inhibited as denitrification activity was severely depleted and decreased transcript levels of most denitrification genes occurred. As a consequence, the tricarboxylic acid (TCA) cycle was inhibited due to the lowered cellular redox state in the FNA exposed cultures. Meanwhile, during FNA exposure PAO1 rerouted its carbon metabolic pathway from the TCA cycle to pyruvate fermentation with acetate as the end product as a possible survival mechanism. Additionally, protein synthesis was significantly decreased while ribosome preservation was evident. These findings improve our understanding of PAO1 in response to FNA, and contribute towards the potential application for use of FNA as an antimicrobial agent.

Introduction

There is strong potential to apply free nitrous acid (FNA), the protonated form of nitrite (HNO_2), as an antimicrobial agent. Recently, while using nitrite as an antimicrobial agent, FNA was discovered to be the true metabolic inhibitor (Vadivelu et al. 2006b). Consequently, there is a great potential to use FNA to control the growth and activities of unwanted microbes in various industrial and medical applications (Wang et al. 2013a; Wang et al. 2013b; Weller et al. 2001). It is shown that parts per billion (ppb, equal to 1 μg N/L) levels of FNA are bacteriostatic (Pijuan et al. 2010; Vadivelu et al. 2006b; Zhou et al. 2008). There are a number of findings relating to the inhibitory

effects of FNA in studies of wastewater treatment applications. For example, it is reported that FNA inhibits the anabolic processes of the nitrite oxidizing bacterium (NOB) *Nitrobacter* at approximately 0.01 mg N/L (Vadivelu et al. 2006b). In comparison, inhibition of growth of the ammonium oxidizing bacterium (AOB) *Nitrosomonas* occurs at higher concentrations of approximately 0.1 mg N/L FNA (Vadivelu et al. 2006a). We previously show that denitrifying activities of PAO1 are completely inhibited by FNA levels of 1 mg N/L (Gao et al. 2015). Thus, the low levels of FNA may be used in wastewater treatment to cause the favoured nitritation reactions, and is likely not to effect activities of denitrifiers. These findings highlight tolerance differences among bacteria towards FNA and highlight the need for research on other bacteria relevant to wastewater treatment. Consequently, there is great potential to selectively manipulate these nitrifying bacteria and achieve a more efficient wastewater treatment nitrogen removal process through nitritation (Wang et al. 2014). Typically nitrite and thus FNA is at low levels in conventional wastewater treatment plants. However, within plants that use nitritation for treatment of high ammonia waste streams, high nitrite levels could occur (Nhat et al. 2014) and that may be detrimental to other microbial activities, such as denitrification for nitrogen removal.

More recently, FNA has been shown to cause strong bactericidal effects at parts per million (ppm, equal to 1 mg N/L) levels (Jiang et al. 2011; Wang et al. 2013a). Sewer biofilms consisting of sulfate reducing bacteria (SRB) and methanogenic bacteria were destroyed at a FNA concentration of 0.2 mg N/L (Jiang et al. 2011). This is significant as it greatly reduces the production of sulfide, which will considerably lower sewer corrosion (Jiang et al. 2013). In another application, FNA at 2.13 ppm causes lysis of activated sludge cells and this improves the biodegradability of the sludge and enhances methane production during its anaerobic digestion (Wang et al. 2013a).

As there are many potential applications of FNA for control and manipulation of microbial growth, it is of great necessity and interest to better understand the antimicrobial action of FNA. This includes knowledge of how microorganisms may respond to and tolerate exposure to FNA and whether adapted resistance may occur. Some investigations suggest the antimicrobial effect of FNA is multi-targeted. FNA *per se* and the reactive nitrogen intermediates (RNIs) derived directly from FNA or by reactions of FNA with other cellular molecules are thought to cause oxidative damage in microbial cells (Zahrt and Deretic 2002). This could involve direct damage to cell enzymes, cellular membranes and walls, and nuclear acids (Fang 2004). Other hypotheses proposed for the antimicrobial effect of FNA include the collapse of the proton motive force (Zhou et al. 2011), direct enzyme inhibition, nitrosylation of iron-sulfur centers, the reduction of thiols, DNA mutation, and oxidation of membrane lipids (Fang 2004). Currently, experimental support for these

hypotheses is lacking and there is little understanding of how microorganisms respond to and potentially tolerate exposure to FNA.

Pseudomonas aeruginosa thrives in various environments. It is a ubiquitous denitrifier in wastewater treatment systems where its activities may be desired for nitrogen removal. It is also an opportunistic pathogen frequently found in the hospital environment, and infections can result in significant morbidity and mortality in immunocompromised and cystic fibrosis patients (Rosenfeld et al. 2003). As a ubiquitous and metabolically versatile microbe it can flourish in many environments, *P. aeruginosa* grows under both aerobic and anaerobic conditions, and possesses a number of virulence factors that contribute to its pathogenesis (Morita et al. 2014). Therefore, for the potential application of novel antimicrobial agents, there is great interest to investigate how these may inhibit the growth of environmentally and medically relevant organisms, such as *P. aeruginosa*. Recently we have found the antimicrobial effects of FNA on *Pseudomonas aeruginosa* PAO1 (PAO1) were concentration-determined and population-specific (Gao et al. 2015). However, details of the mechanism of the antimicrobial effects of FNA were not determined in that investigation.

To date, there is only one other genome-wide transcriptional investigation of the antimicrobial effects of nitrite on *P. aeruginosa*, and that was based on microarray analysis and performed on aerobic planktonic cultures (Platt et al. 2008). Anaerobic denitrifying conditions are more relevant to the organism's existence in situations of wastewater treatment and as an infectious biofilm. Consequently, there lacks a clear and systematic understanding of the fundamental mechanisms of microbial tolerance and resistance to exposure of FNA on PAO1 cultures under anaerobic denitrifying conditions. In this study, we focused on the inhibitory mechanisms of FNA towards PAO1 and performed genome-wide RNA sequencing (RNA-Seq) analysis on PAO1 in the absence and presence of a bacteriostatic-level of FNA (0.1 mg N/L) (Gao et al. 2015) in anaerobic denitrifying conditions. By combining gene expression profiles with selected measured physiological responses, we detected the microbial response to FNA exposure and revealed potential multi-targeted mechanisms of FNA on this environmentally and medically important bacterium.

Materials and Methods

Growth and FNA treatment of PAO1

PAO1 was cultured and prepared for experiment in glycerol modified M9 medium (See Materials and Methods in Supporting Information (SI)). When the cultures were in early log phase of growth,

11h after inoculation, FNA was added with starting concentration of 0.1 mg N/L. FNA concentrations were determined from nitrite levels using the following equation (FNA (as $HNO_2 - N$) $= \frac{NO_2-N}{K_a \times 10^{pH}}$, $K_a = e^{-2300/(270+T(°C))}$) and 0.1 mg N/L FNA was previously determined to have a temporary inhibitory effect on PAO1 (Gao et al. 2015). Control cultures (no added FNA) had the same volume of sterilized Milli-Q water added. Experiments of the control and FNA treated cultures were conducted in triplicate.

RNA extraction and sequencing

Samples were taken for RNA extraction from the triplicate FNA treated and the control cultures of PAO1 after 13 h incubation, that is 2 h after FNA addition. This time point was chosen to ensure the organism was under stress from the added FNA (Gao et al. 2015). 5 mL of the bacterial suspension from each serum bottle was centrifuged at 13,000 x g for 2 minutes, the supernatant was discarded and the pellets were immediately frozen in liquid nitrogen before storing at -80ºC for later RNA extraction. Total RNA extraction was performed using the QIAGEN miRNeasy Mini Kit (Catalog number: 217004) according to the manufacturer's instructions, except an extra bead-beating step was added to ensure complete lysis of the bacterial cells. Strand-specific cDNA library construction and Illumina paired-end sequencing (HiSeq 2000, Illumina Inc., San Diego, CA, USA) was performed on the extracted RNA (Macrogen, Seoul, Korea). The raw sequencing data was deposited in NCBI's Gene Expression Omnibus and this is accessible through the GEO series accession number GSE73323.

RNA-Seq data processing and differentially expressed gene analysis

The raw sequence reads were obtained for the triplicate cultures and the sequences were progressively trimmed at the 3'-ends until a quality value ≥ 20 was reached. The ambiguous characters (Ns/Xs) and poly-As/Ts longer than six bases at either end of the reads were then removed. Reads containing at least 85% bases with quality value > 20 were kept. The 3'-end residual adapter and primer sequences were removed and then one base from the 5'-end and three from the 3'-end were trimmed. The NGS QC Toolkit (v2.3.3) (Patel and Jain 2012) was used for all these sequence-modifying processes. The resulting clean reads no shorter than 75 bp were used for downstream analyses.

The cleaned sequence reads for each sample were aligned to the PAO1 reference genome (NC_002516) using SeqAlto (version 0.5) (Mu et al. 2012). Strand-specific coverage for each gene was calculated and differential expression analysis was conducted using the cuffdiff command in

Cufflinks (version 2.2.1) on the triplicated samples (Trapnell et al. 2012). Statistical analyses and visualization were conducted using the cummeRbund package in R (http://compbio.mit.edu/cummeRbund/). Gene expression was calculated as reads per kilobase of a gene per million mapped reads (RPKM), a normalized value derived from the frequency of detection and the length of a given gene (Trapnell et al. 2012). Differences in fold-change values were calculated between control and FNA-treated samples (0.1 mg N/L) by determining the $\log_2$ fold-change (LFC) of the averaged RPKM values determined from the replicate experiments run on two separate occasions. Genes with LFC of ≥2.5 and ≤-2.5 with q value less than 0.01 were defined as the "highly" differentially expressed genes. Genes with LFC of <2.5 but ≥1.0 and ≤-1.0 but >-2.5 with q value less than 0.01 were defined as the "moderately" differentially expressed genes. All other genes are considered as no change in response to FNA. The q value is the allowed false discovery rate (FDR) such that for q<0.01 there is less than one false positive in a total of one hundred significantly expressed gene transcripts. This value is determined by the characteristics of the transcriptional profile of the samples. Annotation of the differentially expressed genes was based on the online-curated pathway tools genome database PseudoCyc (http://www.pseudomonas.com). The program Circos was used to visualize expression and determine the RPKM values for each gene (Krzywinski et al. 2009).

Chemical analyses

During growth from the replicate cultures, samples were taken and filtered (pore size 0.22 μm, Merck Millipore, USA) for analysis of acetate, lactate, formic acid, glucose, 1, 3-propanediol, ethanol and pyruvate. These were measured by applying 1000 μl of filtered sample to a high performance liquid chromatography (HPLC) unit fitted with an Agilent Hi-Plex H 300 mm × 7.8 mm column. High purity helium was used as the carrier gas at a constant pressure of 103 kPa. The mobile phase was 0.008 N H_2SO_4 with a flow rate of 0.4 mL/min.

Physiological assays

Various assays were conducted on samples of PAO1 cultured cells taken at different times of growth in the absence and presence of FNA. LIVE/DEAD staining was conducted on the cells as described in the manufacturers instructions (BacLight Bacterial Viability Kit, Molecular Probes, L7012). The LIVE/DEAD ratio of cells was then quantified by applying 500 μL of the stained samples to a FACSAria™ II (BD Biosciences, San Jose, USA) flow cytometer. To determine the cellular redox status 500 μL samples of cultured cells were stained using the RedoxSensor™ Green reagent provided in the BacLight RedoxSensor Green Vitality Kit (Life Technologies, B34954) as per the manufacturers instructions. The fluorescence signal of the stained cultures was quantified

using the FACSAria™ II type flow cytometer and as described in the manufacturers protocol. Cellular ATP levels were measured in 500 μL samples using the BacTiter-Glo™ Microbial Cell Viability Assay (Promega Corporation, G8231) as described by the manufacturers instructions. Intracellular pH was determined using the fluorescent probes cFSE (Molecular Probes, C1157) as previously described (D et al. 1998). Cellular thiol levels were determined on 200 μL samples using the Thiol and Sulfide Quantitation Kit (Molucular Probes, T-6060) as instructed by the manufacturer.

Results and Discussion

Cell growth and activity of PAO1 detected during exposure to FNA

In this study, PAO1 was cultured utilizing nitrogen oxides (nitrate, nitrite, nitric oxide (NO) and nitrous oxide (N_2O)) as the electron acceptors and glycerol as the electron donor with the production of nitrogen and carbon dioxide. We have previously reported transformations that show the utilization of nitrate, nitrite and glycerol during incubation of PAO1 cultures with different levels of FNA (Gao et al. 2015). Here we report a detailed investigation of the organism's response to an inhibitory level of FNA by monitoring various cellular functions and changes to its transcriptome.

During the early growth phase of PAO1 we added FNA at a starting concentration of 0.1 mg N/L and the observed growth profile (Figure 1A) was similar to that previously reported (Gao et al. 2015). The PAO1 cultures stopped growth after the addition of FNA and this inhibited state lasted for about 10 h before growth reoccurred (Figure 1A). During this period the utilization of nitrate initially stopped and the added nitrite was progressively transformed and reduced. Then when the FNA level was lowered to 0.05 mg N/L growth of PAO1 resumed (Figure 1). Additionally, the utilization of glycerol was delayed in the presence of FNA (Gao et al. 2015). It was apparent that this level of FNA had a bacteriostatic effect on PAO1 that lowered the denitrifying activity of organic carbon oxidation.

It is thought that FNA will diffuse into bacterial cells and function as a protonophore that would disrupt the cellular proton motive force, inhibit ATP synthesis, and lower the intracellular pH (Zhou et al. 2011). Consequently, we found the cellular ATP levels of PAO1 decreased from 0.6 fmol per cell to around 0.4 fmol per cell after 6 h exposure to FNA (Figure 1B). The percentage of live cells after this exposure showed only a slight decrease, from near 90% (no FNA addition) to about 80% (Figure 1C). The intracellular pH of PAO1 decreased from 7.5 to 7.2 at one hour after FNA exposure and dropped further to 6.4 after 6 h exposure (Figure 1D). This drop in intracellular pH is

consistent with other studies of bacteria exposed to nitrite (Mühlig et al. 2014). Protein thiol groups are reported to be altered by FNA exposure, this resulting in an antimicrobial effect (Fang 2004). In the PAO1 culture cellular thiol levels were seen to rise after 2 h of FNA exposure and then return to pre-FNA added levels 6 h after the FNA addition (Figure 1E). FNA is also reported to cause oxidative stress to bacterial cells (Poole 2005). Thus, the intracellular redox of PAO1 was measured and during the 6 h incubation period it was seen that in general the cells became more oxidized over time (Figure 1F). However, in the cultures exposed to FNA the intracellular redox was always lower than the control cells.

Gene expression of PAO1 was compared when the cells were exposed and not exposed to added FNA. Of the RNA sequence reads obtained, more than 96.9% were aligned to the PAO1 reference genome (Table S1 in SI). A total of 591 genes were significantly differentially expressed, in which 167 genes showed increased transcripts and 424 had decreased transcripts in response to FNA exposure. A global overview of gene expression comparison between the control and FNA added cultures also indicates multiple changes occurring in response to FNA exposure (Figures S1 and S2).

FNA inhibited anaerobic respiration and energy production

A number of transcripts coding for the enzymes involved in denitrification processes were highly or moderately down regulated in the presence of FNA. This included the genes for nitrate reductase, nitrite reductase, and N_2O reductase (Figure 3) (Table S2). Additionally, genes coding for NADH dehydrogenase and ATP synthase (Table S2) were down regulated in the presence of FNA. Typically respiratory denitrification would contribute to formation of cellular proton motive force and facilitate ATP generation in *P. aeruginosa* through the membrane-bound ATPase (Richardson et al. 2009). In fact we did detect decreased ATP levels in PAO1 following exposure to FNA (Figure 1B). As well, the exposed cells had a lower intracellular redox potential than the control cells (Figure 1F), and this could be caused by disrupted electron flow in the presence of FNA. Together, these events of decreased utilization of nitrate and glycerol, lowered ATP production, lower intracellular redox potential, and decreased expression of denitrification genes and ATP synthase genes, all strongly support the notion that FNA had an impairing effect on the denitrification pathway and respiration of PAO1.

In contrast to the denitrification genes mentioned above, genes encoding NO reductase and those of the operon *nir*QOP showed relatively moderately higher expression in the presence of FNA. NO reductase activity is reported to be essential for nitric oxide detoxification (Wang et al. 2011). It is likely that while other denitrification steps of PAO1 were inhibited by FNA, NO reductase levels

were raised as a response to reduce toxic levels of NO derived from the added FNA. The *nir*QOP operon also having increased expression, is located between the genes for nitrite reductase and NO reductase, and is reported to play a role in energy conservation during anaerobic growth of *P. aerguinosa* (Arai 2011).

There is potential for FNA to act as uncoupler and disrupt the cellular proton motive force (Zhou et al. 2011). Such action would decrease respiration and impair the energetics and ATP production. This was indeed detected when PAO1 was exposed to FNA and additionally a decrease in intracellular pH was detected. These events all support that FNA was acting as an uncoupler of the proton motive force.

FNA caused altered carbon flux pathways

In the presence of FNA glycerol utilization was lowered, and this coincided with some genes for glycerol metabolism having variation in expression when exposed to FNA. Typically, glycerol would firstly be transformed to glyceraldehyde-3-phosphate and then to pyruvate, via Embden-Meyerhof-Parnas (EMP) pathway, before being utilized in the TCA cycle for energy generation (Figure 2). Most of the genes (*pgk* and *pykA*) coding for enzymes of the EMP had moderately decreased transcript levels and the gene *eno* had highly decreased transcript levels (Table S2) (Figure 2). In contrast a number of genes involved in the Entner-Duoforoff (ED) pathway (PA3181, *zwf*, and *edd*) showed either no change or moderately increased transcript levels in the presence of FNA (Table S2) (Figure 2). The EMP pathway to pyruvate produces NADH, while the ED pathway, an alternative route for pyruvate production, produces NADPH. During exposure to FNA it is possible the ED pathway was favoured, this brought about by intracellular redox (NADH) levels causing altered gene expression (Chavarría et al. 2013). Additionally, production of NADPH may have been favoured in this condition as NADPH related metabolism has been linked to coping with stress in *Pseudomonas* (Chavarría et al. 2013).

Genes encoding enzymes involved in TCA cycle (*sdhABCD, sucABCD, ipdG*) were highly down regulated, suggesting this cycle was less active during FNA exposure (Figure 3). Possibly, these genes were also regulated by cellular redox status. Some of the genes coding for the glyoxylate shunt, were up regulated during FNA exposure (Table S2). Activation of this pathway could enable carbon assimilation from C_2 compounds such as acetate. Such action could be implemented as a means to supplement the lowered pool of TCA cycle intermediates for possible biosynthetic processes (Dunn et al. 2009).

Transcripts of genes coding pyruvate dehydrogenase (PA3416 and PA3417) and dihydrolipoamide acetyltransferase (PA3415) displayed the greatest increases in transcription after FNA treatment (Table S2). These enzymes produce acetyl-CoA, which would normally feed into the TCA cycle when respiration is active. However, in FNA exposure, respiration and the TCA cycle were inhibited. The genes coding the pyruvate fermentation pathway and specifically required stress proteins (aceF, *pta, ackA,* PA1753, PA3017, PA3309, PA4352) all showed either highly or moderately increased abundance after FNA exposure (Schreiber et al. 2006) (Table S2). The possible fermentation products or intermediates pyruvic acid, formic acid, ethanol and lactic acid were not detected in the control or FNA-treated cultures (Table S7). In contrast, in the presence of FNA there was a 37-fold increase in acetic acid levels in comparison to cells not exposed to added FNA. It seems in response to FNA, unable to produce ATP through respiration, PAO1 converted the produced acetyl-CoA to acetate through pyruvate fermentation to generate ATP. Potentially, this could provide a possible survival mechanism for PAO1 in the presence of FNA, and possibly enable the organism faster recovery following the removal of the inhibitor (Schreiber et al. 2006).

In summary, it was apparent that during FNA exposure, the major pathway for carbon metabolism and energy conservation and the TCA cycle were shut down. In this condition the glycerol metabolism was altered from the EMP to the ED pathway for generation of pyruvate. This pyruvate was subsequently fermented to produce acetate and for substrate level production of ATP.

FNA disrupted DNA replication, transcription and translation

Genes coding key enzymes involved in DNA replication (i.e. DNA polymerase, ATP-dependent DNA helicase) and transcription (DNA-directed RNA polymerase) showed either highly or moderately decreased transcripts during exposure to FNA (Table S4). Additionally, genes encoding various molecules in protein synthesis including ribosomal RNA processing proteins, various amino acid transfer RNA synthases (32 tRNA modification genes), the small and large ribosome structural proteins, translation initiation and elongation factors, ribosome maturation protein Rimp (PA4746), 16s rRNA processing proteins (*rimM*), and ribosome-binding factor A (*rbfA*) were all highly or moderately down regulated (Table S3). It was evident that FNA caused decreased activity of protein synthesis, DNA replication, and transcription in PAO1. Inhibition of protein synthesis has been detected in previous studies investigating the response to acidified nitrite stress in *Salmonella enterica* (Mühlig et al. 2014). Decreased DNA replication and protein synthesis is reflected by the decreased cell growth during FNA exposure (Figure 1A). There is the possibility that these decreased activities could be due to a "stringent response" in PAO1 to FNA. For example, in the stringent response to an amino acid starvation the ribosomal protein L11 activates the proteins RelA

and SpoT for production of pppGpp (Hauryliuk et al. 2015). In response to FNA we detected highly decreased expression of L11 (LFC of -3.55) and small decreases in expression of the *relA* and *spoT* genes (Table S3). Consequently, it does not seem that the stringent response was involved with FNA stress.

FNA possibly acts as a multi-targeting antimicrobial agent, which potentially affects various cellular functions (Fang 2004; Gao et al. 2015; Zhou et al. 2010). It is not clear whether these inhibitory effects result from FNA directly targeting metabolic or structural proteins, or whether these result from FNA causing altered gene expression. It was seen that genes coding for the ribosome modulation factor (RMF) and the hibernation-promoting factor (HPF) were up regulated in response to FNA exposure. These factors function to preserve active 70S ribosome units into inactive units in stressful conditions. Once the stress disappears, the inactive ribosomes are liberated from the RMF and the HPF to become active again in translation (Kato et al. 2010; Polikanov et al. 2012). It is likely that for coping with FNA stress, PAO1 ceases production of ribosomes and conserves the existing ones. This implies that the ribosome itself is not the direct target of FNA mediated damage, but that ribosome inactivation is caused by altered regulation of its production and by its storage.

Detoxification of FNA

In the growth conditions of this study PAO1 carried out denitrification using glycerol as the electron donor and nitrate and nitrite as electron acceptors. Denitrification activity was detected when the culture growth was temporarily inhibited by FNA at the concentration of 0.1 mg N/L. This denitrification activity would contribute to lower FNA levels and prevent accumulation of other oxidized nitrogen molecules to detoxify the conditions. Additionally, it is known that flavohaemoglobin is an important detoxifying oxidoreductase that converts toxic NO to non-toxic nitrate in the presence of N_2O in *Pseudomonas* (Fang 2004). The suggested increased activity of NO reductase we detected would also result in removal of NO and produce N_2O, which would facilitate the activity of the flavohaemoglobin. Our transciptome analysis revealed moderately increased expression of the *fhp* gene encoding flavohaemoglobin during FNA addition (Table S6). Thus, there is evidence here of a strategy by PAO1 through the increased activities of NO reductase and flavohaemoglobin for the removal of the toxic NO derived from FNA.

Recovery from possible nitrosative damage to proteins and DNA

During exposure to FNA PAO1 has limited energy and inhibition of transcription and protein synthesis occurs. However, as FNA levels decrease then recovery of cell activities and growth occurs (Gao et al. 2015).

DNA and enzymes can be targets for damage by reactive nitrogen intermediates (RNIs). The genes involved in the SOS response for DNA repair may be expected to change in response to FNA stress. The protein RecA reportedly mediates gap repair as well as DNA replication (Ayora et al. 2011) and importantly RecA is involved in inactivating repression by the regulator LexA on the SOS response genes (Michel 2005). We did detect increased expression of *recA and lexA*, although this was not considered significant, and other SOS genes such as *radC* did not show significant increased expression as well (Table S6). While there are suggestions that FNA and RNIs cause oxidative damage to cells (Zahrt and Deretic 2002), in the PAO1 culture conditions of this study there was no evidence for this.

Iron-sulfur clusters (Fe-S) are important components of many enzymes involved in diverse cellular processes, such as DNA repair, gene regulation, RNA modifications, biosynthetic pathways, aerobic and anaerobic respiration, and nitrogen and carbon metabolism (Romsang et al. 2014). It is reported that FNA or FNA-derived RNIs could directly damage proteins containing Fe-S clusters through nitrosalytion (Fang 2004). In PAO1, the *isc* operon (*iscRSUA, hscBA*, *fdx2*, and PA3808) and the gene *nfuA* code for the synthesis of Fe-S clusters. In this study all these genes showed highly increased transcripts levels (Table S5), suggesting that FNA affected PAO1 was attempting to assemble new Fe-S clusters to replace damaged components. Additionally, the gene PA4615, coding for a ferredoxin oxidoreductase, was highly up regulated (Table S5), and this also functions for Fe-S cluster biogenesis (Romsang et al. 2015). It is likely that FNA and derivatives are damaging Fe-S clusters in PAO1 and the organism is responding to that by repair and assembly of new clusters. Such damage would have an impact on numerous cellular redox dependent reactions.

Interestingly, genes encoding several proteolysis enzymes had increased expression during FNA exposure. This includes an ATP-binding protease component ClpA (PA2620), periplasmic serine protease (PA1832) and an ATP dependent Lon protease (PA1803) (Table S5). It is speculated that ClpA degrades abnormal and damaged proteins and the Lon protease cleaves multiple peptide bonds. Consequently, it appears that FNA and/or the RNIs are causing damage to proteins, and then this induced activity is enabling recycling of peptides and amino acids.

The multifaceted response of PAO1 to FNA exposure

In this study we investigated the effects of FNA on the global transcriptome of the ubiquitous denitrifier *P. aeruginosa* PAO1. The accuracy and precision of RNA-Seq is comparable to quantitative real-time PCR (González-Ballester et al. 2010; Simon et al. 2013). Consequently, we identified critical determinants in the bacteriostatic effects of FNA on this bacterium and the protective responses of PAO1 to the FNA stress. Here we compile a proposed model to describe the effects of FNA and the multiple responses that enable PAO1 to withstand this bacteriostatic level of FNA exposure (Figure 4).

In this model, during exposure to FNA, most of the denitrification pathway is less active. As a result, NADH consumption and ATP generation coupled with denitrification is suppressed leading to energy starvation in PAO1 cultures. In contrast, the respiratory enzyme NO reductase shows increased activity to detoxify the NO that is derived from FNA. The lowered requirement of NADH further restrains the carbon utilization, in which normal glycerol metabolism and TCA cycle activities are impeded. Consequently, PAO1 alters its normal glycerol utilization from the EMP pathway to the ED pathway to generate pyruvate. The pyruvate, no longer utilized through the TCA cycle, is then fermented to acetate for energy generation and to provide a survival mechanism to the stress imposed by FNA. Meanwhile, in response to the lowered cell metabolism, PAO1 shuts down protein synthesis, ceases nucleic acid replication and the ribosome units are preserved in a dormant state. Additionally, in response to damaged proteins PAO1 produces new Fe-S clusters and degrades abnormal proteins for recycling of the amino acids.

Acknowledgements

We acknowledge the Australian Research Council for funding support through project DP120102832 (Biofilm Control in Wastewater Systems using Free Nitrous Acid - a Renewable Material from Wastewater) and we thank scholarship support for Shu-Hong Gao from the China Scholarship Council. We thank Dr. Beatrice Keller, University of Queensland for IC and HPLC analysis and Dr. Michael Nefedov, University of Queensland for assistance with the BD FACSAria™ II flow cytometer and data analysis.

References

Arai H. 2011. Regulation and function of versatile aerobic and anaerobic respiratory metabolism in *Pseudomonas aeruginosa*. *Frontiers in Microbiology,* 2, 103.

Ayora S., Carrasco B., Cárdenas P.P., César C.E., Cañas C., Yadav T., Marchisone C., Alonso J.C. 2011. Double-strand break repair in bacteria: a view from *Bacillus subtilis*. *FEMS Microbiology Reviews,* 35, 1055-1081.

Chavarría M., Nikel P.I., Pérez-Pantoja D., de Lorenzo V. 2013. The Entner-Doudoroff pathway empowers *Pseudomonas putida* KT2440 with a high tolerance to oxidative stress. *Environmental Microbiology,* 15, 1772-1785.

D B., Holyoak H., Caron G.N.-V., Coote C. 1998. Determination of the intracellular pH (pHi) of growing cells of *Saccharomyces cerevisiae*: the effect of reduced expression of the membrane H^+-ATPase. *Journal of Microbiological Methods,* 31, 113 - 125.

Dunn M.F., Ramírez-Trujillo J.A., Hernández-Lucas I. 2009. Major roles of isocitrate lyase and malate synthase in bacterial and fungal pathogenesis. *Microbiology,* 155, 3166-3175.

Fang F.C. 2004. Antimicrobial reactive oxygen and nitrogen species: concepts and controversies. *Nature Reviews. Microbiology,* 2, 820-832.

Gao S.H., Fan L., Yuan Z., Bond P.L. 2015. The concentration-determined and population-specific antimicrobial effects of free nitrous acid on *Pseudomonas aeruginosa* PAO1. *Applied Microbiology and Biotechnology,* 99, 2305-2312.

González-Ballester D., Casero D., Cokus S., Pellegrini M., Merchant S.S., Grossman A.R. 2010. RNA-seq analysis of sulfur-deprived *Chlamydomonas* cells reveals aspects of acclimation critical for cell survival. *The Plant Cell,* 22, 2058-2084.

Hauryliuk V., Atkinson G.C., Murakami K.S., Tenson T., Gerdes K. 2015. Recent functional insights into the role of (p)ppGpp in bacterial physiology. *Nature Reviews. Microbiology,* 13, 298-309.

Jiang G., Gutierrez O., Yuan Z. 2011. The strong biocidal effect of free nitrous acid on anaerobic sewer biofilms. *Water Research,* 45, 3735-3743.

Jiang G., Keating A., Corrie S., O'halloran K., Nguyen L., Yuan Z. 2013. Dosing free nitrous acid for sulfide control in sewers: Results of field trials in Australia. *Water Research,* 47, 4331-4339.

Kato T., Yoshida H., Miyata T., Maki Y., Wada A., Namba K. 2010. Structure of the 100S ribosome in the hibernation stage revealed by electron cryomicroscopy. *Structure,* 18, 719-724.

Krzywinski M., Schein J., Birol I., Connors J., Gascoyne R., Horsman D., Jones S.J., Marra M.A. 2009. Circos: an information aesthetic for comparative genomics *Genome Research,* 19, 1639-1645.

Michel B. 2005. After 30 years of study, the bacterial SOS response still surprises us. *PLoS Biology,* 3, e255.

Morita Y., Tomida J., Kawamura Y. 2014. Responses of *Pseudomonas aeruginosa* to antimicrobials. *Frontiers in Microbiology,* 4, 422.

Mu J.C., Jiang H., Kiani A., Mohiyuddin M., Bani Asadi N., Wong W.H. 2012. Fast and accurate read alignment for resequencing. *Bioinformatics,* 28, 2366-2373.

Mühlig A., Behr J., Scherer S., Müller-Herbst S. 2014. Stress response of *Salmonella enterica serovar* typhimurium to acidified nitrite. *Applied and Environmental Microbiology,* 80, 6373-6382.

Nhat P.T., Biec H.N., Mai N.T.T., Thanh B.X., Dan N.P. 2014. Application of a partial nitritation and anammox system for the old landfill leachate treatment. *International Biodeterioration & Biodegradation,* 95, 144-150.

Patel R.K., Jain M. 2012. NGS QC Toolkit: a toolkit for quality control of next generation sequencing data. *PloS one,* 7, e30619.

Pijuan M., Ye L., Yuan Z.G. 2010. Free nitrous acid inhibition on the aerobic metabolism of poly-phosphate accumulating organisms. *Water Research,* 44, 6063-6072.

Platt M.D., Schurr M.J., Sauer K., Vazquez G., Kukavica-Ibrulj I., Potvin E., Levesque R.C., Fedynak A., Brinkman F.S.L., Schurr J., Hwang S.-H., Lau G.W., Limbach P.A., Rowe J.J., Lieberman M.A., Barraud N., Webb J., Kjelleberg S., Hunt D.F., Hassett D.J. 2008. Proteomic, microarray, and signature-tagged mutagenesis analyses of anaerobic *Pseudomonas aeruginosa* at pH 6.5, likely representing chronic, late-stage cystic fibrosis airway conditions. *Journal of Bacteriology,* 190, 2739-2758.

Polikanov Y.S., Blaha G.M., Steitz T.A. 2012. How hibernation factors RMF, HPF, and YfiA turn off protein synthesis. *Science,* 336, 915-918.

Poole R.K. 2005. Nitric oxide and nitrosative stress tolerance in bacteria. *Biochemical Society Transactions,* 33, 176-180.

Richardson D., Felgate H., Watmough N., Thomson A., Baggs E. 2009. Mitigating release of the potent greenhouse gas N_2O from the nitrogen cycle--could enzymic regulation hold the key? *Trends in Biotechnology,* 27, 388-397.

Romsang A., Duang-Nkern J., Leesukon P., Saninjuk K., Vattanaviboon P., Mongkolsuk S. 2014. The iron-sulphur cluster biosynthesis regulator IscR contributes to iron homeostasis and resistance to oxidants in *Pseudomonas aeruginosa*. *PloS one,* 9, e86763.

Romsang A., Duang-Nkern J., Wirathorn W., Vattanaviboon P., Mongkolsuk S. 2015. *Pseudomonas aeruginosa* IscR-regulated ferredoxin $NADP^+$ reductase gene (fprB) functions in iron-sulfur cluster biogenesis and multiple stress response. *PloS one,* 10, e0134374.

Rosenfeld M., Ramsey B.W., Gibson R.L. 2003. *Pseudomonas* acquisition in young patients with cystic fibrosis: pathophysiology, diagnosis, and management. *Current Opinion in Pulmonary Medicine,* 9, 492-497.

Schreiber K., Boes N., Eschbach M., Jaensch L., Wehland J., Bjarnsholt T., Givskov M., Hentzer M., Schobert M. 2006. Anaerobic survival of *Pseudomonas aeruginosa* by pyruvate fermentation requires an Usp-type stress protein. *Journal of Bacteriology,* 188, 659-668.

Simon D.F., Domingos R.F., Hauser C., Hutchins C.M., Zerges W., Wilkinson K.J. 2013. Transcriptome sequencing (RNA-seq) analysis of the effects of metal nanoparticle exposure on the transcriptome of *Chlamydomonas reinhardtii*. *Applied and Environmental Microbiology,* 79, 4774-4785.

Trapnell C., Roberts A., Goff L., Pertea G., Kim D., Kelley D.R., Pimentel H., Salzberg S.L., Rinn J.L., Pachter L. 2012. Differential gene and transcript expression analysis of RNA-seq experiments with TopHat and Cufflinks. *Nature Protocols,* 7, 562-578.

Vadivelu V.M., Keller J., Yuan Z.G. 2006a. Effect of free ammonia and free nitrous acid concentration on the anabolic and catabolic processes of an enriched *Nitrosomonas* culture. *Biotechnology and Bioengineering,* 95, 830-839.

Vadivelu V.M., Yuan Z., Fux C., Keller J. 2006b. The inhibitory effects of free nitrous acid on the energy generation and growth processes of an enriched *Nitrobacter* culture. *Environmental Science & Technology,* 40, 4442-4448.

Wang Q., Ye L., Jiang G., Hu S., Yuan Z. 2014. Side-stream sludge treatment using free nitrous acid selectively eliminates nitrite oxidizing bacteria and achieves the nitrite pathway. *Water Research,* 55, 245-255.

Wang Q., Ye L., Jiang G., Jensen P., Batstone D., Yuan Z. 2013a. Free Nitrous Acid (FNA)-Based Pre-treatment Enhances Methane Production from Waste Activated Sludge. *Environmental Science & Technology,* 47, 11897-11904.

Wang Q., Ye L., Jiang G., Yuan Z. 2013b. A free nitrous acid (FNA)-based technology for reducing sludge production. *Water Research,* 47, 3663-3672.

Wang W., Kinkel T., Martens-Habbena W., Stahl D.A., Fang F.C., Hansen E.J. 2011. The *Moraxella catarrhalis* nitric oxide reductase is essential for nitric oxide detoxification. *Journal of Bacteriology,* 193, 2804-2813.

Weller R., Price R.J., Ormerod A.D., Benjamin N., Leifert C. 2001. Antimicrobial effect of acidified nitrite on *dermatophyte* fungi, *Candida* and bacterial skin pathogens. *Journal of Applied Microbiology,* 90, 648-652.

Zahrt T.C., Deretic V. 2002. Reactive nitrogen and oxygen intermediates and bacterial defenses: unusual adaptations in *Mycobacterium tuberculosis*. *Antioxidants & Redox Signaling,* 4, 141-159.

Zhou Y., Ganda L., Lim M., Yuan Z.G., Kjelleberg S., Ng W.J. 2010. Free nitrous acid (FNA) inhibition on denitrifying poly-phosphate accumulating organisms (DPAOs). *Applied Microbiology and Biotechnology,* 88, 359-369.

Zhou Y., Oehmen A., Lim M., Vadivelu V., Ng W.J. 2011. The role of nitrite and free nitrous acid (FNA) in wastewater treatment plants. *Water Research,* 45, 4672-4682.

Zhou Y., Pijuan M., Zeng R.J., Yuan Z. 2008. Free Nitrous Acid Inhibition on Nitrous Oxide Reduction by a Denitrifying-Enhanced Biological Phosphorus Removal Sludge. *Environmental Science & Technology,* 42, 8260-8265.

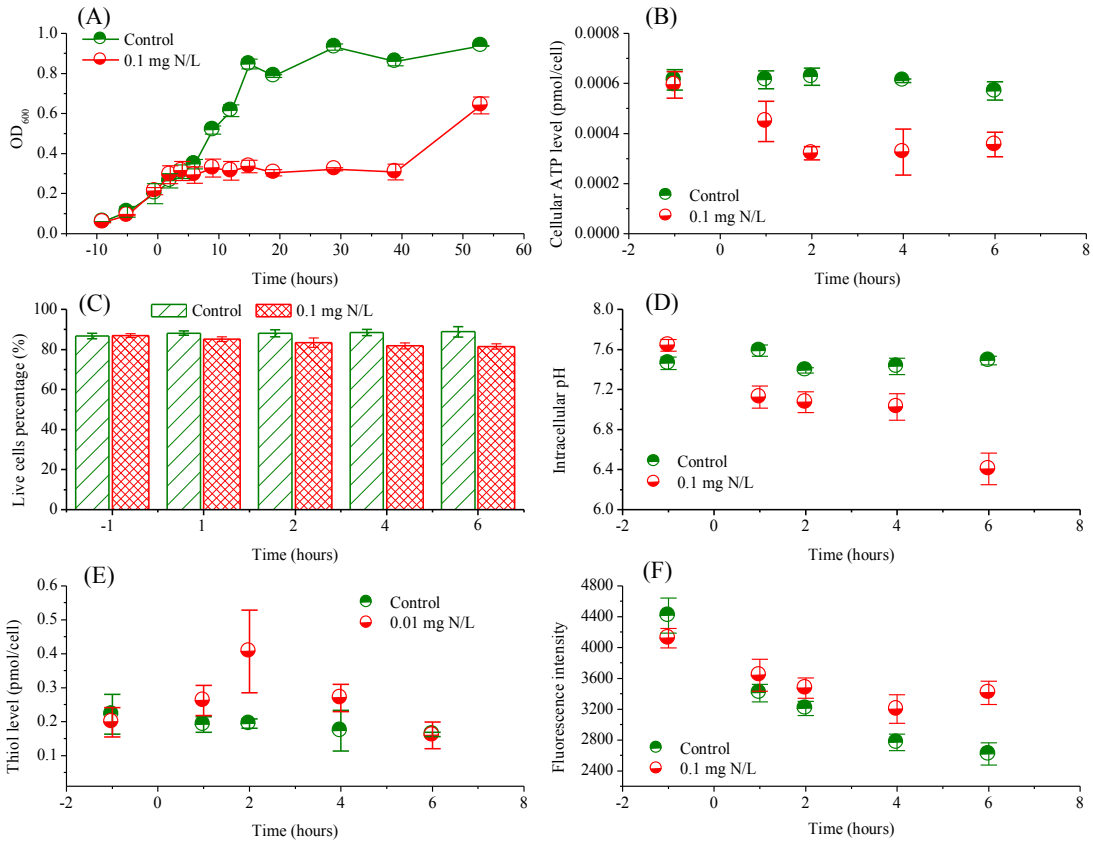

Figure 1. Different physiological features of PAO1 growth measured in the presence and absence (Control) of 0.1 mg N/L FNA. Growth profiles in terms of OD_{600} (A), cellular ATP levels (B), the percentage of live cells (C), intracellular pH (D), cellular thiol levels (E), and intracellular redox levels where higher fluorescence indicates lower redox potential (F). FNA was added at time 0 h. Error bars indicate the standard deviations derived from the analysis of triplicate samples.

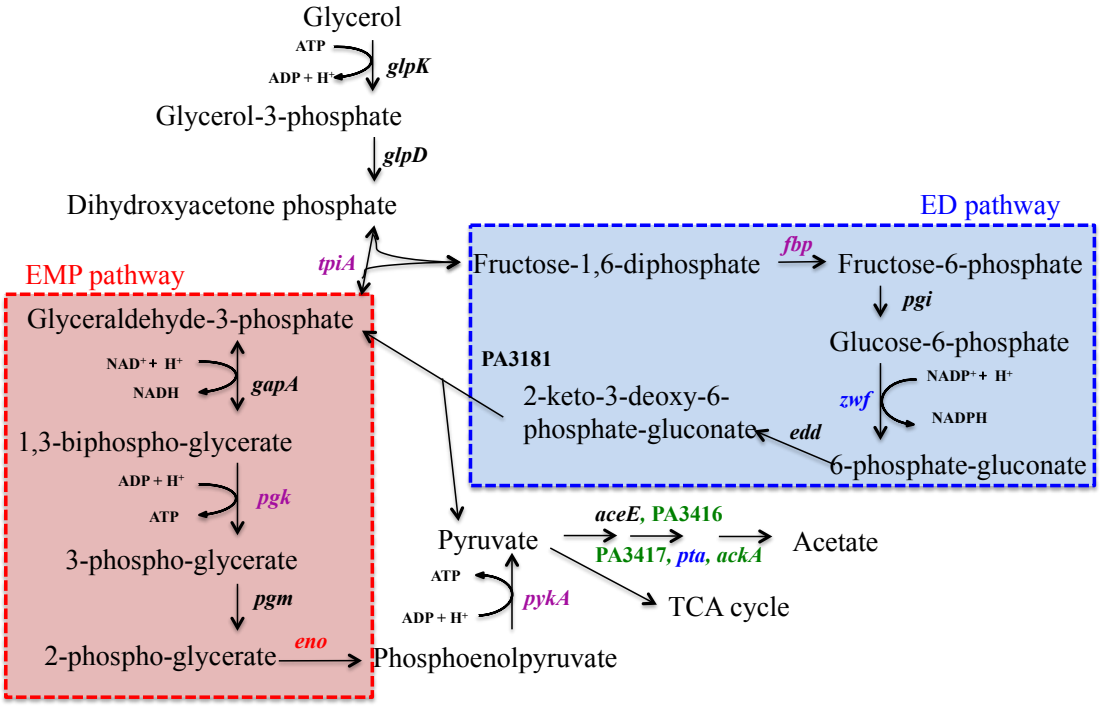

Figure 2. Catabolism of glycerol in PAO1 in the presence of FNA. Genes in green and red represent the "highly" up or down regulated genes respectively, genes in blue and purple represent the "moderately" up or down regulated genes respectively, and genes in black are the genes with no change with FNA treatment. Gene abbreviations in the figure are coding for the respective enzymes: *glpK*, glycerol kinase; *glpD,* glycerol-3-phophate dehydrogenase; *tpiA*, triosephosphate isomerase; *gapA*, glyceraldehyde 3-phosphate dehydrogenase; *pgk*, phosphoglycerate kinase; *pgm*, phosphoglyceromutase; *eno*, phosphopyruvate hydratase; *pykA*, pyruvate kinase; *fbp*, fructose-1,6-biphosphatase; *pgi*, glucose-6-phosphate isomerase; *zwf*, glucose-6-phosphate 1-dehydrogenase; *edd*, phosphogluconate dehydratase; PA3181, keto-hydrooxyglutarate-aldolase; *aceE*, pyruvate dehydrogenase subunit E1; PA3416, pyruvate dehydrogenase E1 component, subunit beta; PA3417, pyruvate dehydrogenase E1 component subunit alpha; *pta*, phosphate acetyltransferase; *ackA*, acetate kinase.

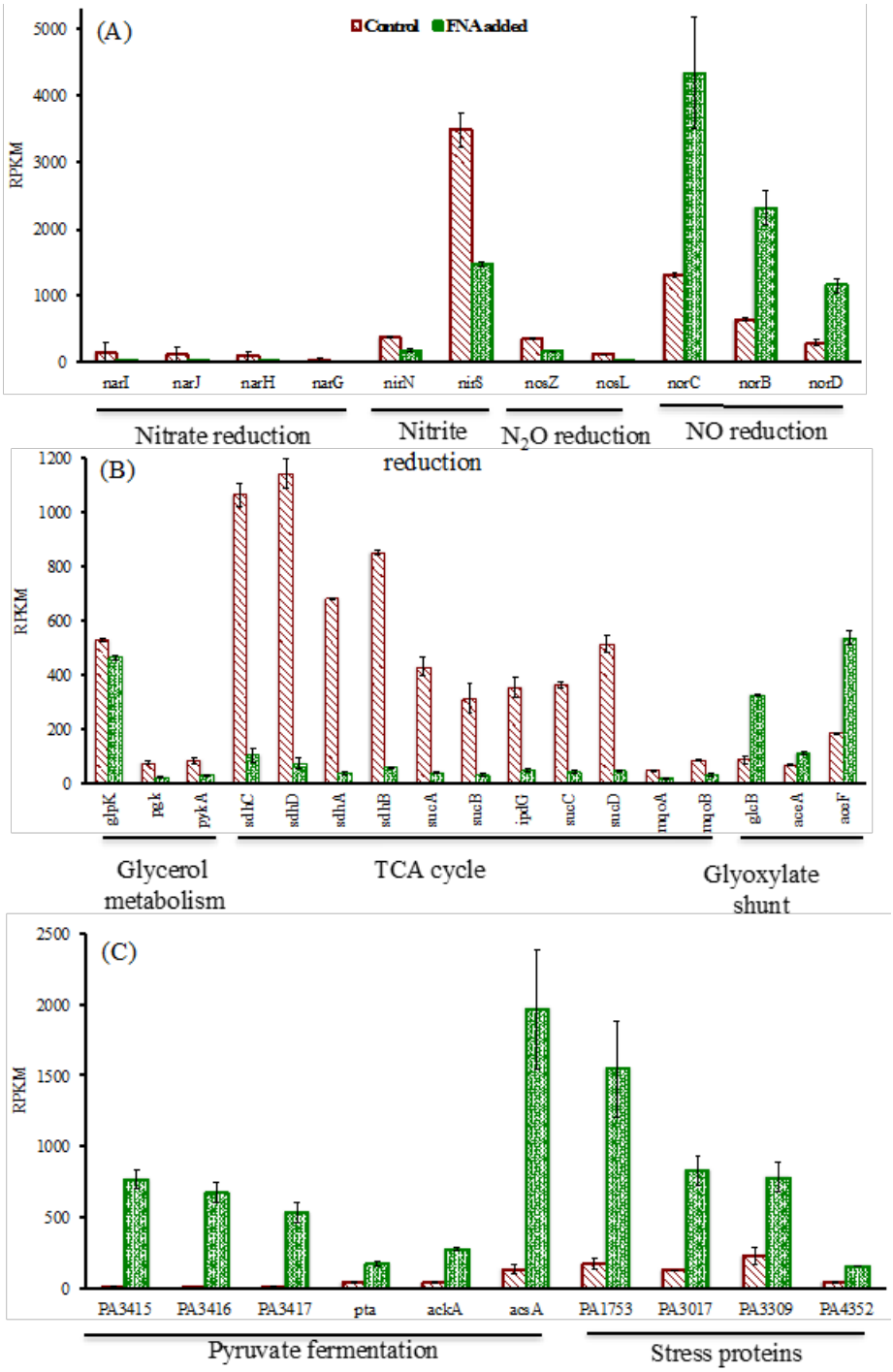

Figure 3. Detailed gene expression involved in (A) denitrification, (B) carbon utilization and (C) pyruvate fermentation of PAO1 with and without FNA treatment. Error bars indicate the standard deviations derived from the analysis of triplicate samples.

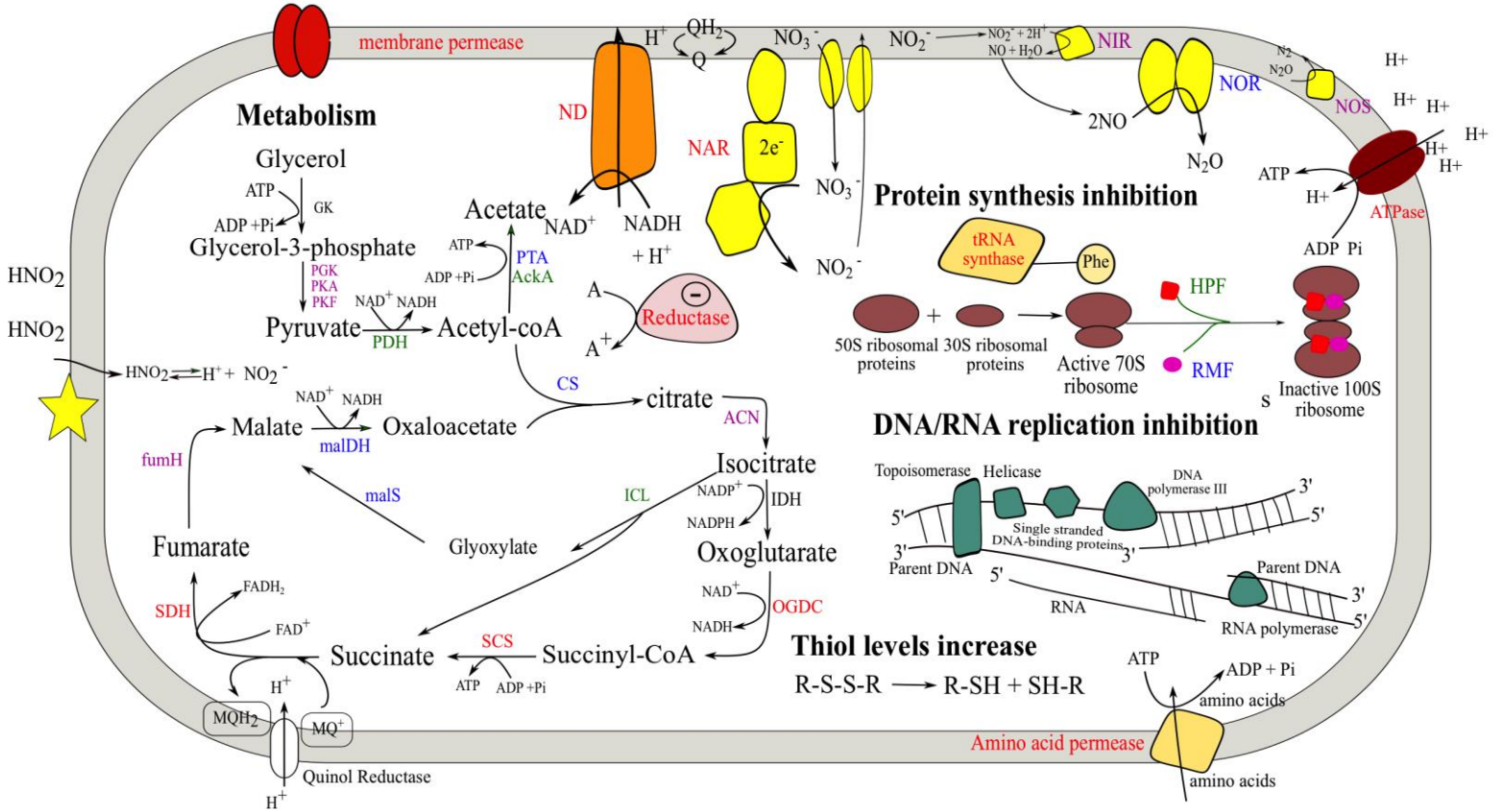

Figure 4. A proposed model for the response of PAO1 to FNA stress and its survival strategies. The enzymes/proteins in red and green represent the encoding genes "highly" up or down regulated respectively, enzymes/proteins in blue and purple represent the encoding genes "moderately" up or down regulated respectively, and enzymes/proteins in black stand for encoding genes with no change with FNA treatment. GK: Glycerol kinase; PGK: phosphoglycerate kinase; PKA: pyruvate kinase II; PKF: pyruvate kinase I; PDH: pyruvate dehydrogenase; PTA: phosphotransacetylase; AckA: acetate kinase; CS: citrate synthase; ACN: aconitase; IDH: isocitrate dehydrogenase; malS: malate synthase; malDH: probable L-malatedehydrogenase; ICL: isocitrate lyase; OGDC: 2-oxoglutarate dehydrogenase; SCS: succinyl-coA decarboxylase; SDH: succinate dehydrogenase; fumH: fumarate hydratase.

Supporting Information

Material and Methods

PAO1 culture preparation. Glycerol modified M9 (GLYM9) medium, which contained 0.2 M phosphate buffer, 9 mM NaCl, 38 mM NH_4Cl, 2 mM $MgSO_4 \cdot 3H_2O$, 100 μM $CaCl_2 \cdot 2H_2O$, 10 g/L glycerol, 0.2 g/L yeast extract and 30 mM $NaNO_3$ with the pH adjusted to 6.3±0.3 was utilized to cultivate PAO1 under anaerobic conditions (Gao et al. 2015). Prior to inoculation the GLYM9 medium was transferred to 150 mL clean serum bottles. Each bottle was bubbled with nitrogen gas for 30 minutes and then was capped using butyl rubber stoppers before autoclave sterilization.

The PAO1 (DSM No: 22644) strain used in this study was obtained from the Deutsche Sammlung von Mikroorganismen und Zellkulturen GmbH, Germany. The strain was activated according to supplier's instructions and grown on tryptic soy agar plates at 30 ºC for 26h. One colony was then transferred to tryptic soy broth medium and incubated shaken at 150 rpm and 30 ºC for another 26 h. Afterwards, 5 mL of the bacterium suspension was transferred into serum bottles containing 150 mL of sterile anaerobic GLYM9 medium in an anaerobic chamber. After 26 hours' incubation the optical density at 600 nm (OD_{600}) of the culture was adjusted to 0.5. Then 10 mL of this culture was transferred into 150 mL of sterile anaerobic GLYM9 medium in serum bottles in an anaerobic chamber and then taken out before incubating at 30 ˚C shaken at 150 rpm (Gao et al. 2015).

Results and Discussion

Global transcript profiles and differential gene expression

The absolute and relative coverage of the genes of PAO1 are shown (Figure S1). Genes that were significantly differentially transcribed between the control and FNA-treated cultures were detected (see the selective criterion in Materials and Methods). The transcription of a total of 591 genes were significantly different, in which 167 genes showed increased transcripts and 424 were down regulated in response to FNA exposure. An overview of gene expression is summarised based on the numbers of genes falling within the categories for the clusters of orthologous groups (COG) that were differentially expressed (Figure S2).

Figure S1 provides a genome overview of gene expression differences between the control and FNA exposed cells. Genes showing large changes of expression in terms of LFC (PA3415-17 and *isc* operon) during FNA exposure encoded enzymes participating in pyruvate fermentation and for the synthesis of iron sulfur clusters. This implies that applied FNA can possibly alter the carbon flux and is having an impact on systems that rely on iron sulfur clusters, such as the cells respiratory mechanism. In addition, the genes *norC* (encoding NO reductase) and *rmf* (encoding ribosome

modulation factor to conserve unused ribosome) were highly expressed, implying stress responses of PAO1 to the FNA exposure.

From Figure S2, a most striking gene expression difference between cultures with and without FNA treatment is the large number of genes in the class of "metabolism" that were down regulated (Figure S2A). The category "Translation, ribosomal structure and biogenesis" contained the largest number of genes that were down regulated in PAO1, this was followed by the numbers of genes assigned to the categories "Energy production and conversion", "Amino acid transport and metabolism", and "Cell wall/membrane/envelope biogenesis" (Figure S2B). Additionally, it is worth noting that a high percentage of the up-regulated genes after FNA exposure were hypothetical proteins (Table S8). These genes are of interest since they are likely important for bacterial survival during FNA exposure but no obvious function has yet been assigned. From this overview it seems that FNA severely affected the protein synthesis process, energy production pathways as well as the synthesis of cell components.

Figure S1. Global transcript profiles of PAO1 samples with and without FNA treatment. The outmost circle represents the full genome of strain PAO1. The red and blue columns on the next two inner circles represent genes more expressed in the FNA treated samples or controls, respectively. Each grid stands for 6.25-fold (log_2 = ±2.5) change. The wave lines in the blue and green innermost circles represent global gene expression level (RPKM) of PAO1 with and without FNA treatment, respectively. Each grid represents an RPKM value of 1000. The outermost circle represents the length of the full genome of PAO1 (6,264,404 bp) and the numbers on the outer ring, from 0.00 to 0.99, represent location points on the whole PAO1 genome.

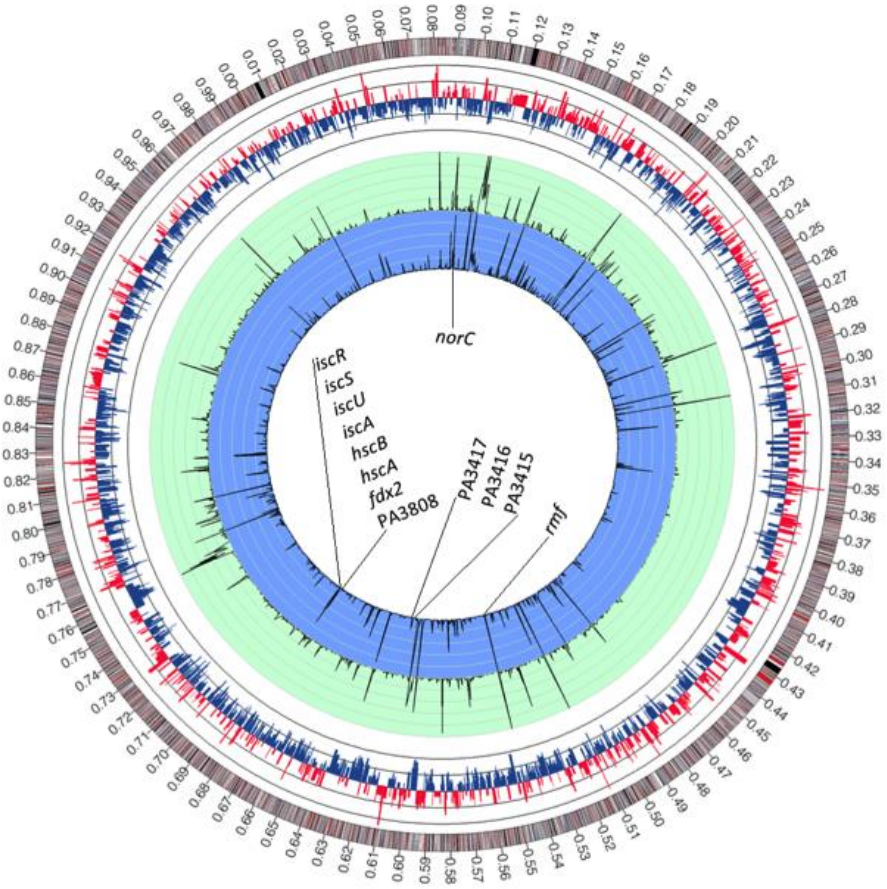

Figure S2. An overview of differentially expressed genes by PAO1 in response to FNA treatment when assigned to COG categories. (A) Percentage of up and down regulated genes falling within COG classes. (B) Numbers of up and down regulated genes belonging to different functional COG categories.

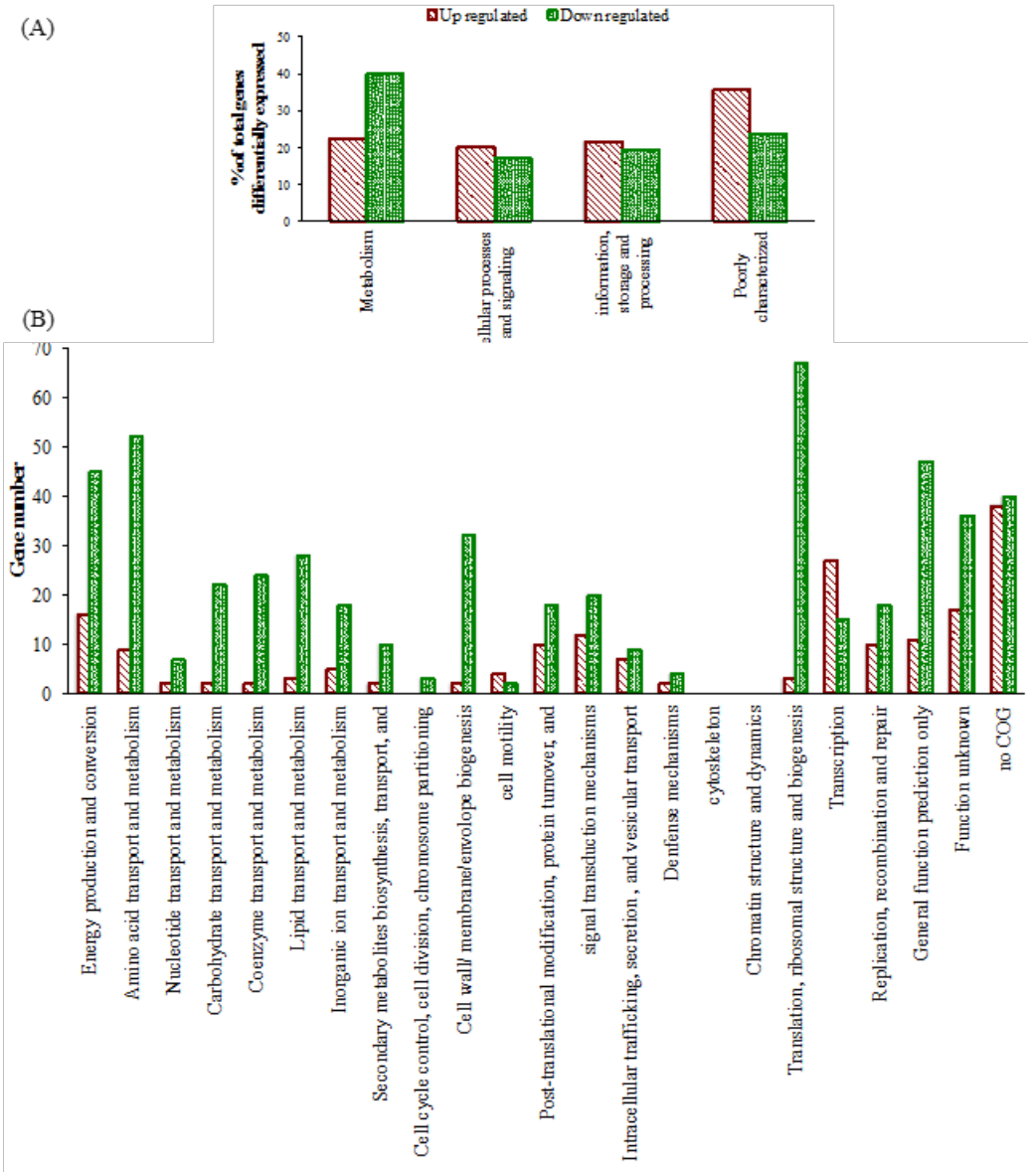

Table S1. Summary of RNA-Seq reads number and mapped rate

Sample	Clean reads	Mapped reads	Mapped rate (%)
Control-A	5,204,651	5,151,013	98.2
Control-B	4,592,299	4,505,710	97.3
FNA-A	5,223,608	5,102,296	96.9
FNA-B	5,127,740	5,025,781	97.3
FNA-C	4,755,988	4,682,029	97.8

Note: For the genes listed in the tables S2, S3, S4, S5 and S7, those with LFC of ⩾2.5 and ⩽-2.5 with q value less than 0.01 were defined as the "highly" differentially expressed genes. Genes with log2 fold changes of <2.5 but ⩾1.0 and ⩽-1.0 but >-2.5 with q value less than 0.01 were defined as the "moderately" differentially expressed genes. All other genes are considered as no change in response to FNA. Some of the genes considered as no change but strongly relevant were also included into the table to better illustrate the FNA affected pathways or its effective mechanisms.

Table S2. Differentially expressed genes involved in metabolism induced by addition of FNA

Gene ID	**Gene name**	**Product**	Fold change	Fold change (Log2)	RPKM Control	RPKM FNA 0.1 mg N/L	q value
Glycerol Metabolism							
PA3581	glpF	glycerol uptake facilitator protein	1.76	0.81	428.78	754.06	0.00046
PA3582	glpK	glycerol kinase	-1.14	-0.19	528.51	463.59	0.00016
PA3584	glpD	glycerol-3-phosphate dehydrogenase	1.67	0.74	1534.97	2566.68	0.00113
PA4748	tpiA	triosephosphate isomerase	-2.78	-1.48	298.23	107.24	0.00016
PA3195	gapA	glyceraldehyde-3-phosphate dehydrogenase	1.69	0.76	831.43	1407.16	0.00016
PA0552	pgk	phosphoglycerate kinase	-3.56	-1.83	76.50	21.48	0.00016
PA5131	pgm	phosphoglycerate mutase	-1.92	-0.94	73.12	38.00	0.00016
PA3635	eno	enolase	-9.49	-3.25	448.80	47.27	0.00016
PA5110	fbp	fructose-1,6-biphosphatase	-2.85	-1.51	320.43	112.35	0.00016
PA4732	pgi	glucose-6-phosphate isomerase	0.00	0.00	63.94	63.90	0.00016
PA3183	zwf	glucose-6-phosphate 1-dehydrogenase	2.28	1.19	631.58	1439.15	0.00016
PA3194	edd	phosphogluconate dehydratase	1.61	0.69	267.91	430.73	0.00250
PA3181		2-keto-3-deoxy-6-phosphogluconate aldolase	1.78	0.83	471.02	840.15	0.00046
Pyruvate fermentation							

PA0836	ackA	acetate kinase	6.63	2.73	41.62	275.85	0.00016
PA5016	aceF	dihydrolipoamide acetyltransferase	2.86	1.51	197.66	563.82	0.00016
PA0835	pta	phosphate acetyltransferase	3.90	1.96	43.89	171.01	0.00016
PA3415		probable dihydrolipoamide acetyltransferase	97.91	6.61	7.74	757.79	0.00016
PA3417		probable pyruvate dehydrogenase E1 component, alpha subunit	55.63	5.80	8.99	500.35	0.00016
PA3416		probable pyruvate dehydrogenase E1 component, beta chain	122.23	6.93	5.30	648.22	0.00016
PA5015	aceE	pyruvate dehydrogenase	2.86	0.77	830.46	1413.66	0.00060
PA1753		Universal stress protein UspA and related nucleotide-binding proteins	9.01	3.17	177.29	1597.32	0.00016
PA3017		Universal stress protein UspA and related nucleotide-binding proteins	6.37	2.67	129.11	821.93	0.00016
PA3309		Universal stress protein UspA and related nucleotide-binding proteins	3.44	1.78	240.68	828.70	0.00016
PA4352		Universal stress protein UspA and related nucleotide-binding proteins	3.33	1.74	45.72	152.20	0.00016
Denitrification							
PA0509	nirN	probable c-type cytochrome	-2.36	-1.24	405.83	171.69	0.00016
PA0519	nirS	nitrite reductase precursor	-2.82	-1.49	4647.52	1648.93	0.00016
PA0520	nirQ	regulatory protein NirQ	3.19	1.67	250.22	798.48	0.00016
PA0521	nirO	probable cytochrome c oxidase subunit	2.44	1.29	61.18	149.35	0.00016
PA0522	nirP	hypothetical protein	3.41	1.77	43.91	149.74	0.00016
PA0523	norC	nitric-oxide reductase subunit C	3.46	1.79	1349.17	4672.41	0.00016
PA0524	norB	nitric-oxide reductase subunit B	3.28	1.71	673.31	2207.90	0.00016
PA0525	norD	probable dinitrification protein NorD (Nitric oxide reductase activation protein)	4.35	2.12	257.47	1119.89	0.00016
PA3392	nosZ	nitrous-oxide reductase precursor	-2.57	-1.36	463.59	180.53	0.00016
PA3396	nosL	NosL protein (Predicted lipoprotein involved in nitrous oxide reduction)	-4.64	-2.22	121.35	26.13	0.00016
PA3872	narI	respiratory nitrate reductase gamma chain	-5.80	-2.54	165.08	28.46	0.00016
PA3873	narJ	respiratory nitrate reductase delta chain	-4.85	-2.28	107.40	22.16	0.00016
PA3874	narH	respiratory nitrate reductase beta chain	-4.37	-2.13	121.63	27.85	0.00016

PA3875	narG	respiratory nitrate reductase alpha chain	-3.08	-1.62	60.62	19.68	0.00016
ATP synthesis							
PA5553	atpC	ATP synthase epsilon chain	-7.34	-2.88	278.58	37.93	0.00016
PA5554	atpD	ATP synthase beta chain	-7.24	-2.86	463.32	64.04	0.00016
PA5555	atpG	ATP synthase gamma chain	-9.15	-3.19	505.52	55.24	0.00016
PA5556	atpA	ATP synthase alpha chain	-5.86	-2.55	468.45	79.94	0.00016
PA5557	atpH	ATP synthase delta chain	-6.71	-2.75	335.88	50.07	0.00016
PA5558	atpF	ATP synthase B chain	-4.86	-2.28	490.96	101.06	0.00016
PA5559	atpE	ATP synthase C chain	-2.60	-1.38	634.21	244.04	0.00016
PA5560	atpB	ATP synthase A chain	-4.81	-2.27	124.58	25.88	0.00016
PA5561	atpI	ATP synthase protein I	-5.67	-2.50	183.87	32.40	0.00016
TCA cycle							
PA1585	sucA	2-oxoglutarate dehydrogenase (E1 subunit)	-11.76	-3.56	473.94	40.30	0.00016
PA1787	acnB	aconitate hydratase 2	-4.54	-2.18	134.97	29.75	0.00016
PA1580	gltA	citrate synthase	-5.99	-2.58	485.69	81.14	0.00016
PA0795	prpC	citrate synthase 2	5.16	2.37	82.00	423.50	0.00016
PA1586	sucB	dihydrolipoamide succinyltransferase (E2 subunit)	-11.43	-3.51	340.40	29.78	0.00016
PA4470	fumC1	fumarate hydratase	5.02	2.33	3.83	19.20	0.00016
PA2624	idh	isocitrate dehydrogenase	-1.60	-0.68	355.76	221.72	0.00285
PA2634	aceA	isocitrate lyase AceA	1.52	0.60	79.26	120.33	0.00999
PA1587	ipdG	lipoamide dehydrogenase-glc	-8.39	-3.07	401.56	47.84	0.00016
PA0482	glcB	malate synthase G	3.39	1.76	103.51	350.67	0.00016
PA3452	mqoA	malate:quinone oxidoreductase	-2.69	-1.43	51.50	19.17	0.00016
PA4640	mqoB	malate:quinone oxidoreductase	-3.16	-1.66	94.30	29.88	0.00016
PA0794		probable aconitate hydratase	8.35	3.06	12.60	105.21	0.00016

PA4333		probable fumarase	-3.01	-1.59	68.82	22.84	0.00016
PA1252		probable L-malate dehydrogenase	2.86	1.79	3.03	10.45	0.00031
PA1583	sdhA	succinate dehydrogenase (A subunit)	-21.37	-4.42	759.27	35.53	0.00016
PA1584	sdhB	succinate dehydrogenase (B subunit)	-16.82	-4.07	919.56	54.66	0.00016
PA1581	sdhC	succinate dehydrogenase (C subunit)	-9.37	-3.23	1075.57	114.83	0.00016
PA1582	sdhD	succinate dehydrogenase (D subunit)	-15.06	-3.91	1162.88	77.24	0.00016
PA1589	sucD	succinyl-CoA synthetase alpha chain	-13.53	-3.76	612.46	45.26	0.00016
PA1588	sucC	succinyl-CoA synthetase beta chain	-9.62	-3.27	435.54	45.29	0.00016
NADH dehydrogenase							
PA2639	nuoD	NADH dehydrogenase I chain C,D	-3.75	-1.91	251.55	67.15	0.00016
PA2640	nuoE	NADH dehydrogenase I chain E	-4.01	-2.00	215.85	53.80	0.00016
PA2641	nuoF	NADH dehydrogenase I chain F	-4.10	-2.04	135.20	32.97	0.00016
PA2642	nuoG	NADH dehydrogenase I chain G	-5.54	-2.47	147.42	26.60	0.00016
PA2643	nuoH	NADH dehydrogenase I chain H	-4.18	-2.06	179.31	42.94	0.00016
PA2644	nuoI	NADH Dehydrogenase I chain I	-4.72	-2.24	211.98	44.88	0.00016
PA2645	nuoJ	NADH dehydrogenase I chain J	-4.72	-2.24	105.19	22.31	0.00016
PA2646	nuoK	NADH dehydrogenase I chain K	-5.18	-2.37	162.23	31.31	0.00706
PA2647	nuoL	NADH dehydrogenase I chain L	-5.86	-2.55	128.37	21.92	0.00016
PA2648	nuoM	NADH dehydrogenase I chain M	-5.06	-2.34	70.76	13.97	0.00016
PA2649	nuoN	NADH dehydrogenase I chain N	-6.96	-2.80	94.60	13.58	0.00016

Table S3. Differentially expressed genes involved in protein biosynthesis induced by addition of FNA

Gene ID	Gene name	Product	Fold change	Fold change (Log2)	RPKM Control	RPKM FNA 0.1 mg N/L	q value
PA3744	rimM	16S rRNA processing protein	-9.85	-3.30	1182.60	120.10	0.00016
PA3162	rpsA	30S ribosomal protein S1	-4.61	-2.20	2552.73	554.13	0.00016
PA4264	rpsJ	30S ribosomal protein S10	-3.78	-1.92	3081.80	814.29	0.00016
PA4240	rpsK	30S ribosomal protein S11	-16.07	-4.01	1748.94	108.86	0.00016
PA4268	rpsL	30S ribosomal protein S12	-5.87	-2.55	1438.20	244.86	0.00016
PA4241	rpsM	30S ribosomal protein S13	-11.88	-3.57	1790.39	150.67	0.00016
PA4250	rpsN	30S ribosomal protein S14	-7.88	-2.98	1606.37	203.80	0.00016
PA4741	rpsO	30S ribosomal protein S15	-2.17	-1.12	1560.82	717.74	0.00016
PA3745	rpsP	30S ribosomal protein S16	-6.57	-2.72	520.57	79.24	0.00016
PA4254	rpsQ	30S ribosomal protein S17	-13.35	-3.74	2504.19	187.56	0.00016
PA4934	rpsR	30S ribosomal protein S18	-4.53	-2.18	1693.19	373.86	0.00016
PA4259	rpsS	30S ribosomal protein S19	-12.64	-3.66	3708.11	293.38	0.00016
PA3656	rpsB	30S ribosomal protein S2	-6.98	-2.80	1398.74	200.53	0.00016
PA4563	rpsT	30S ribosomal protein S20	-9.08	-3.18	998.79	110.05	0.00016
PA0579	rpsU	30S ribosomal protein S21	-6.03	-2.59	1553.39	257.74	0.00016
PA4257	rpsC	30S ribosomal protein S3	-14.75	-3.88	2827.35	191.65	0.00016
PA4239	rpsD	30S ribosomal protein S4	-13.62	-3.77	1747.44	128.26	0.00016
PA4246	rpsE	30S ribosomal protein S5	-9.98	-3.32	2120.13	212.47	0.00016
PA4935	rpsF	30S ribosomal protein S6	-4.22	-2.08	1123.12	266.32	0.00016
PA4267	rpsG	30S ribosomal protein S7	-5.06	-2.34	1517.31	299.98	0.00016
PA4249	rpsH	30S ribosomal protein S8	-4.65	-2.22	1603.59	344.65	0.00016
PA4432	rpsI	30S ribosomal protein S9	-3.99	-2.00	986.64	247.48	0.00016
PA4273	rplA	50S ribosomal protein L1	-6.59	-2.72	1273.23	193.10	0.00016
PA4272	rplJ	50S ribosomal protein L10	-4.88	-2.29	1618.52	331.90	0.00016

PA4274	rplK	50S ribosomal protein L11	-11.67	-3.55	2455.50	210.35	0.00016
PA4433	rplM	50S ribosomal protein L13	-4.58	-2.19	931.27	203.46	0.00016
PA4253	rplN	50S ribosomal protein L14	-11.70	-3.55	2874.80	245.81	0.00016
PA4244	rplO	50S ribosomal protein L15	-10.79	-3.43	3045.92	282.18	0.00016
PA4256	rplP	50S ribosomal protein L16	-14.08	-3.82	4058.17	288.24	0.00016
PA4237	rplQ	50S ribosomal protein L17	-6.86	-2.78	1277.11	186.07	0.00016
PA4247	rplR	50S ribosomal protein L18	-6.89	-2.79	771.55	111.92	0.00016
PA3742	rplS	50S ribosomal protein L19	-1.72	-0.78	777.37	451.60	0.00060
PA4260	rplB	50S ribosomal protein L2	-11.17	-3.48	2143.90	191.88	0.00016
PA4568	rplU	50S ribosomal protein L21	-4.89	-2.29	1514.50	309.97	0.00016
PA4258	rplV	50S ribosomal protein L22	-11.35	-3.50	1697.40	149.59	0.00016
PA4261	rplW	50S ribosomal protein L23	-8.70	-3.12	1541.56	177.27	0.00016
PA4252	rplX	50S ribosomal protein L24	-12.13	-3.60	2656.74	218.98	0.00016
PA4567	rpmA	50S ribosomal protein L27	-3.14	-1.65	2471.60	786.08	0.00016
PA4263	rplC	50S ribosomal protein L3	-6.50	-2.70	2234.71	343.58	0.00016
PA4245	rpmD	50S ribosomal protein L30	-12.12	-3.60	4903.09	404.68	0.00016
PA5049	rpmE	50S ribosomal protein L31	-1.92	-0.94	415.16	216.48	0.00087
PA2970	rpmF	50S ribosomal protein L32	-5.09	-2.35	1453.87	285.63	0.00016
PA5315	rpmG	50S ribosomal protein L33	-1.87	-0.91	2258.36	1204.71	0.00031
PA5570	rpmH	50S ribosomal protein L34	-3.99	-1.99	2381.11	597.45	0.00016
PA4242	rpmJ	50S ribosomal protein L36	-8.81	-3.14	2588.11	293.82	0.00822
PA4262	rplD	50S ribosomal protein L4	-7.91	-2.98	2240.31	283.19	0.00016
PA4251	rplE	50S ribosomal protein L5	-9.11	-3.19	3201.91	351.33	0.00016
PA4248	rplF	50S ribosomal protein L6	-7.79	-2.96	1826.02	234.47	0.00016
PA4271	rplL	50S ribosomal protein L7 / L12	-3.24	-1.70	967.30	298.72	0.00016
PA4932	rplI	50S ribosomal protein L9	-3.54	-1.82	861.67	243.27	0.00016
PA4463		conserved hypothetical protein (ribosome hibernation promoting factor HPF)	6.63	2.73	1780.89	11812.40	0.00016

PA4746		conserved hypothetical protein (ribosome maturation protein RimP)	-7.59	-2.92	569.47	75.00	0.00016
PA2830	htpX	heat shock protein HtpX(Zn-dependent protease with chaperone function)	6.21	2.63	19.39	120.36	0.00016
PA4671		probable ribosomal protein L25	-4.56	-2.19	602.59	132.28	0.00016
PA3049	rmf	ribosome modulation factor	3.39	1.76	9017.38	30566.20	0.00016
PA4743	rbfA	ribosome-binding factor A	-20.80	-4.38	204.87	9.85	0.00016
PA3655	tsf	translation elongation factor Ts	-7.56	-2.92	678.48	89.69	0.00016
PA4744	infB	translation initiation factor IF-2	-9.97	-3.32	565.15	56.66	0.00016
PA0934	relA	GTP pyrophosphokinase	-1.74	-0.80	132.71	76.27	0.00046
PA5338	spoT	guanosine-3',5'-bis(diphosphate) 3'-pyrophosphohydrolase	-3.76	-1.91	109.76	29.21	0.00016

Table S4. Differentially expressed genes involved in nucleic acid replication induced by addition of FNA

Gene ID	Gene name	Product	Fold change	Fold change (Log2)	RPKM Control	RPKM FNA 0.1 mg N/L	q value
PA5345	recG	ATP-dependent DNA helicase RecG	-3.22	-1.69	38.18	11.85	0.00016
PA3344	recQ	ATP-dependent DNA helicase RecQ	-6.68	-2.74	55.13	8.25	0.00016
PA5296	rep	ATP-dependent DNA helicase Rep	-7.93	-2.99	39.49	4.98	0.00016
PA3861	rhl	ATP-dependent RNA helicase RhlB	-6.29	-2.65	92.55	14.71	0.00016
PA0001	dnaA	chromosomal replication initiator protein DnaA	-2.23	-1.16	140.17	62.72	0.00016
PA3168	gyrA	DNA gyrase subunit A	-4.80	-2.26	280.72	58.53	0.00016
PA0004	gyrB	DNA gyrase subunit B	-2.28	-1.19	251.53	110.55	0.00016
PA5443	uvrD	DNA helicase II	-2.04	-1.03	45.68	22.41	0.00016
PA0382	micA	DNA mismatch repair protein MicA	-3.72	-1.89	19.61	5.28	0.00016
PA3620	mutS	DNA mismatch repair protein MutS	-7.20	-2.85	52.44	7.29	0.00016
PA5493	polA	DNA polymerase I	-3.87	-1.95	68.63	17.75	0.00016
PA3640	dnaE	DNA polymerase III, alpha chain	-5.55	-2.47	73.78	13.29	0.00016
PA0002	dnaN	DNA polymerase III, beta chain	-1.84	-0.88	180.54	98.27	0.00016
PA2961	holB	DNA polymerase III, delta prime subunit	-2.51	-1.33	36.43	14.49	0.00738
PA3989	holA	DNA polymerase III, delta subunit	-21.57	-4.43	62.71	2.91	0.00016
PA1816	dnaQ	DNA polymerase III, epsilon chain	-2.04	-1.03	35.64	17.47	0.00031
PA1532	dnaX	DNA polymerase subunits gamma and tau	-3.55	-1.83	37.11	10.45	0.00016
PA0577	dnaG	DNA primase	-4.69	-2.23	43.28	9.23	0.00016
PA4609	radA	DNA repair protein RadA	-2.47	-1.30	22.48	9.11	0.00016
PA4763	recN	DNA repair protein RecN	1.57	0.65	248.97	389.84	0.00262
PA3011	topA	DNA topoisomerase I	-5.75	-2.52	139.39	24.24	0.00016
PA4269	rpoC	DNA-directed RNA polymerase beta* chain	-4.12	-2.04	379.64	92.05	0.00016
PA4238	rpoA	DNA-directed RNA polymerase, alpha subunit/40 kD subunit	-11.60	-3.54	1707.76	147.19	0.00016
PA4761	dnaK	DnaK protein	-2.32	-1.21	297.03	128.21	0.00016

PA4937	rnr	exoribonuclease RNase R	-1.92	-0.94	268.88	140.02	0.00031
PA0967	ruvB	Holliday junction DNA helicase RuvB	-3.13	-1.65	137.42	43.89	0.00016
PA2138		probable ATP-dependent DNA ligase	-2.72	-1.44	13.47	4.95	0.00016
PA0428		probable ATP-dependent RNA helicase	-5.61	-2.49	144.86	25.83	0.00016
PA2840		probable ATP-dependent RNA helicase	-14.17	-3.82	73.95	5.22	0.00016
PA3466		probable ATP-dependent RNA helicase	-6.84	-2.77	48.41	7.07	0.00016
PA3950		probable ATP-dependent RNA helicase	-2.70	-1.43	34.03	12.61	0.00016
PA1678		probable DNA methylase	-1.82	-0.86	40.54	22.31	0.00113
PA4931	dnaB	replicative DNA helicase	-1.89	-0.92	53.59	28.34	0.00016
PA0455	dbpA	RNA helicase DbpA	-2.79	-1.48	71.55	25.64	0.00016
PA3308	hepA	RNA helicase HepA	-7.65	-2.93	22.73	2.97	0.00016
PA4462	rpoN	RNA polymerase sigma-54 factor	-2.19	-1.13	115.14	52.46	0.00016
PA4232	ssb	single-stranded DNA-binding protein	-2.67	-1.42	235.44	88.15	0.00016
PA3725	recJ	single-stranded-DNA-specific exonuclease RecJ	-7.37	-2.88	28.74	3.90	0.00016

Table S5. Differentially expressed genes involved in detoxification, and recovery from possible nitrosative damage induced by addition of FNA

Gene ID	Gene name	Product	Fold change	Fold change (Log2)	RPKM Control	RPKM FNA 0.1 mg N/L	q value
PA3808		conserved hypothetical protein	8.22	3.04	255.22	2097.55	0.00016
PA3809	fdx2	ferredoxin [2Fe-2S]	4.67	2.22	121.04	565.28	0.00016
PA3810	hscA	heat shock protein HscA	4.04	2.02	69.92	282.75	0.00016
PA3811	hscB	heat shock protein HscB	7.12	2.83	267.49	1905.68	0.00016
PA3815	iscR	IscR	9.48	3.25	159.96	1516.63	0.00016
PA3814	iscS	L-cysteine desulfurase (pyridoxal phosphate-dependent)	7.49	2.91	315.61	2365.18	0.00016
PA1847	nfuA	NfuA	11.65	3.54	302.00	3518.74	0.00016
PA3812	iscA	probable iron-binding protein IscA	9.29	3.22	333.68	3098.97	0.00016
PA3813	iscU	probable iron-binding protein IscU	7.12	2.83	500.55	3563.10	0.00016
PA2298		probable oxidoreductase	6.41	2.68	49.82	312.21	0.00016
PA4615		probable oxidoreductase	29.24	4.87	38.40	1121.16	0.00016
PA1803	lon	ATP-dependent Lon protease, bacterial type	1.83	0.87	290.91	531.60	0.00031
PA1832		periplasmic serine proteases (ClpP class)	4.69	2.23	47.28	221.84	0.00016

Table S6. Differentially expressed genes involved in oxidoreductase and DNA repair proteins induced by addition of FNA

Gene ID	Gene name	Product	Fold change	Fold change (Log2)	RPKM Control	RPKM FNA 0.1 mg N/L	q value
PA5319	radC	DNA repair protein RadC	1.57	0.65	59.60	93.30	0.00016
PA2664	fhp	flavohemoprotein	4.17	2.06	549.96	2292.67	0.00016
PA4615		probable oxidoreductase (Ferredoxin-NADP(+) reductase)	29.20	4.87	38.40	1121.16	0.00016
PA2298		probable oxidoreductase (Succinate dehydrogenase/fumarate reductase, flavoprotein subunit)	6.27	2.65	49.82	312.21	0.00016
PA3617	recA	RecA protein	1.96	0.97	818.95	1606.20	0.00016
PA3007	lexA	repressor protein LexA	1.95	0.97	380.06	743.00	0.00016

Table S7. VFAs (mg/L) levels detected in PAO1 cultures during the absence (control) and presence of added FNA

FNA levels (mg N/L)	glucose	pyruvic acid	formic acid	acetic acid (mg/L)	ethanol	lactate acid
Control	0.000 BDL	0.000 BDL	0.000 BDL	0.000 BDL	0.000 BDL	0.000 BDL
Control	0.000 BDL	0.000 BDL	0.000 BDL	0.93	0.000 BDL	0.000 BDL
Control	0.000 BDL	0.000 BDL	0.000 BDL	0.000 BDL	0.000 BDL	0.000 BDL
0.10	0.000 BDL	0.000 BDL	0.000 BDL	12.20	0.000 BDL	0.000 BDL
0.10	0.000 BDL	0.000 BDL	0.000 BDL	10.24	0.000 BDL	0.000 BDL
0.10	0.000 BDL	0.000 BDL	0.000 BDL	11.89	0.000 BDL	0.000 BDL

Table S8. Differentially expressed genes encoding hypothetical proteins induced by addition of FNA

Gene ID	Gene name	Product	Fold change	Fold change (Log2)	RPKM Control	RPKM FNA 0.1 mg N/L	q value
PA0200		hypothetical protein	14.63	3.87	117.92	1724.71	0.00016
PA0269		conserved hypothetical protein	38.47	5.27	22.46	863.94	0.00016
PA0270		hypothetical protein	38.94	5.28	16.47	641.41	0.00016
PA0271		hypothetical protein	28.24	4.82	18.55	523.86	0.00016
PA0276		hypothetical protein	8.29	3.05	12.17	100.95	0.00016
PA0585		hypothetical protein	10.22	3.35	41.88	428.16	0.00016
PA0586		conserved hypothetical protein	10.72	3.42	276.49	2964.17	0.00016
PA0587		conserved hypothetical protein	11.60	3.54	261.95	3038.61	0.00016
PA0713		hypothetical protein	7.84	2.97	9.72	76.22	0.00016
PA0793		hypothetical protein	11.79	3.56	9.42	111.08	0.00016
PA0826		hypothetical protein	6.26	2.65	29.21	182.70	0.00016
PA0874		hypothetical protein	10.92	3.45	19.05	208.12	0.00016
PA0940		hypothetical protein	34.59	5.11	36.73	1270.45	0.00016
PA1029		hypothetical protein	6.98	2.80	56.78	396.24	0.00016
PA1190		conserved hypothetical protein	38.33	5.26	92.09	3529.41	0.00016
PA1333		hypothetical protein	26.47	4.73	84.06	2225.04	0.00016
PA1414		hypothetical protein	11.18	3.48	1246.74	13933.80	0.00016
PA1516		hypothetical protein	6.46	2.69	23.30	150.41	0.00016
PA1545		hypothetical protein	7.13	2.83	187.11	1333.33	0.00016
PA1728		hypothetical protein	14.98	3.91	1032.13	15463.20	0.00016
PA1887		hypothetical protein	8.33	3.06	15.53	129.35	0.00016
PA1888		hypothetical protein	7.95	2.99	24.20	192.31	0.00016
PA2095		hypothetical protein	9.01	3.17	2.92	26.34	0.00016
PA2101		conserved hypothetical protein	5.98	2.58	6.45	38.58	0.00016

PA2120	hypothetical protein	10.66	3.41	3.90	41.59	0.00060
PA2145	hypothetical protein	9.56	3.26	3.79	36.21	0.00201
PA2226	hypothetical protein	6.73	2.75	45.92	309.10	0.00016
PA2288	hypothetical protein	9.79	3.29	99.94	978.17	0.00016
PA2422	hypothetical protein	17.05	4.09	6.97	118.87	0.00016
PA2461	hypothetical protein	5.96	2.58	38.03	226.66	0.00016
PA2753	hypothetical protein	12.68	3.66	14.45	183.21	0.00016
PA2759	hypothetical protein	7.64	2.93	8.82	67.40	0.00016
PA2799	hypothetical protein	5.90	2.56	86.65	510.83	0.00016
PA2883	hypothetical protein	7.68	2.94	485.95	3733.88	0.00016
PA2937	hypothetical protein	6.91	2.79	151.32	1044.92	0.00016
PA3090	hypothetical protein	8.23	3.04	1.54	12.65	0.00113
PA3231	hypothetical protein	5.96	2.58	52.76	314.43	0.00769
PA3362	hypothetical protein	8.03	3.01	8.96	71.94	0.00016
PA3390	hypothetical protein	7.37	2.88	28.89	212.84	0.00016
PA3662	hypothetical protein	13.62	3.77	86.71	1181.13	0.00016
PA3808	conserved hypothetical protein	8.22	3.04	255.22	2097.55	0.00016
PA3835	hypothetical protein	15.13	3.92	14.47	218.97	0.00016
PA4368	hypothetical protein	10.73	3.42	17.71	189.99	0.00016
PA4369	hypothetical protein	7.90	2.98	39.07	308.65	0.00016
PA4523	hypothetical protein	19.77	4.31	100.93	1995.81	0.00016
PA4611	hypothetical protein	8.53	3.09	338.12	2883.21	0.00016
PA4691	hypothetical protein	6.11	2.61	30.84	188.49	0.00016
PA5023	conserved hypothetical protein	5.79	2.53	7.33	42.39	0.00016

Reference

Gao S.H., Fan L., Yuan Z., Bond P.L. 2015. The concentration-determined and population-specific antimicrobial effects of free nitrous acid on *Pseudomonas aeruginosa* PAO1. *Applied Microbiology and Biotechnology,* 99, 2305-2312.

Appendix C

Antimicrobial effects of free nitrous acid on *Desulfovibrio vulgaris*: implications for sulfide induced concrete corrosion

Shu-Hong Gao, Jun Yuan Ho, Lu Fan, David J Richardson, Zhiguo Yuan and Philip L Bond*

This paper is published in *Applied and Environmental Microbiology*.

Abstract

Hydrogen sulfide produced by sulfate reducing bacteria (SRB) in sewers causes odor problems and asset deterioration due to the sulfide induced concrete corrosion. Free nitrous acid (FNA) was recently demonstrated as a promising antimicrobial agent to alleviate hydrogen sulfide production in sewers. However, knowledge of the antimicrobial mechanisms of FNA is largely unknown. Here we report the multiple-targeted antimicrobial effects of FNA on the SRB *Desulfovibrio vulgaris* Hildenborough by determining growth, physiological and gene expression responses to FNA exposure. The activities of growth, respiration and ATP generation were inhibited when exposed to FNA. These changes were reflected in transcript levels detected during exposure. Removal of FNA was evident by nitrite reduction that likely involved nitrite reductase and the poorly characterised hybrid cluster protein, and the genes coding for these proteins were highly expressed. During FNA exposure lowered ribosome activity and protein production were detected. Additionally, conditions within the cells were more oxidising and there was evidence of oxidative stress. Based on interpretation of the measured responses we present a model depicting the antimicrobial effects of FNA on *D. vulgaris*. These findings provide new insight for understanding the responses of *D. vulgaris* to FNA and will provide foundation for optimal application of this antimicrobial agent for improved control of sewer corrosion and odor management.

Keywords: free nitrous acid; antimicrobial agent; inhibitory mechanism; *Desulfovibrio vulgaris* Hildenborough

Importance

Hydrogen sulfide produced by SRB in sewers causes odor problems and results in serious deterioration of sewer assets that requires very costly and demanding rehabilitation. Currently, there is successful application of the antimicrobial agent free nitrous acid (FNA), the protonated form of nitrite, for the control of sulfide levels in sewers (Jiang et al. 2013). However, the details of the

antimicrobial mechanisms of FNA are largely unknown. In this study, we identified the key determinants (inhibiting anaerobic respiration, reducing FNA, causing oxidative stress, and shutting down protein synthesis) for how *Desulfobivrio vulgaris* Hildenborough, a model sewer corrosion bacterium, responds to FNA by examining the growth, physiological and gene expression changes. These findings provide new insight and underpinning knowledge for understanding the responses of *D. vulgaris* to FNA exposure, thereby benefiting the practical application for improved control of sewer corrosion and odor.

Introduction

Sulfate reducing bacteria (SRB) are anaerobic chemoorganotrophic microorganisms that typically use sulfate as the terminal electron acceptor for respiration and generate energy with the production of hydrogen sulfide (Heidelberg et al. 2004). In confined spaces production of hydrogen sulfide can cause odor and corrosion problems. This is particularly the case in sewers and inlet structures of wastewater treatment plants where the oxidation of sulfide produces sulfuric acid which corrodes the concrete surfaces of the sewer. This results in serious deterioration of sewer assets that requires very costly and demanding rehabilitation efforts (Jiang et al. 2011b; Pikaar et al. 2014) . Consequently there is great interest to efficiently control SRB and thereby minimising hydrogen sulfide production in sewers.

Various chemical dosing methods are used to lower hydrogen sulfide production in sewers and four strategies currently used include: sulfide oxidation by injection of chemical oxidants such as air, oxygen, or nitrate (Gutierrez et al. 2008; Mohanakrishnan et al. 2009); sulfide precipitation by addition of iron salts (Zhang et al. 2009b); application of magnesium hydroxide or lime to raise the wastewater pH and prevent the release of hydrogen sulfide (Gutierrez et al. 2009); and to inhibit the activities of SRB to lessen the generation of hydrogen sulfide (Zhang et al. 2009a). However, to obtain the required sulfide control these strategies require continuous chemical consumption and considerable operational costs (Jiang et al. 2011a).

Free nitrous acid (FNA), the protonated form of nitrite, was recently demonstrated to be the true metabolic inhibitor behind the usually observed “nitrite inhibition” (Vadivelu et al. 2006). In recent treatment of sewer biofilms it was seen that application of FNA for 6-24 hours at 0.2-0.3 mg N/L decreased the live cell percentage from about 80% to 5-15% (Jiang et al. 2011b). Since then FNA has been applied in sewer field trials in which an 80% reduction of sulfide production was achieved by intermittent FNA dosing at 0.26 mg N/L for 8-24 hours every four weeks (Jiang et al. 2013).

These investigations support that the application of FNA for control of sulfide levels in sewers is highly feasible.

Therefore, FNA is emerging as an extremely promising antimicrobial agent for the control of SRB, their activities and sulfide production, and there is great interest to understand how SRB respond to and withstand exposure to FNA. Nitrite is reported to cause decreased expression of the genes coding for dissimilatory sulfite reductase (DsrAB) and thereby disrupting respiration of SRB (Haveman et al. 2004; He et al. 2006) . Currently, the antimicrobial effects of FNA on bacteria in general are believed to be multi-targeted (Fang 2004). It is thought that FNA, and perhaps reactive nitrogen species (RNS) derived from FNA, causes oxidative stress resulting in damage to cell enzymes, cellular membranes and walls, and nucleic acids (Zahrt and Deretic 2002). Other hypotheses to explain the antimicrobial effects include FNA causing disruption of the proton motive force (Zhou et al. 2011), nitrosylation of metal centres or thiol groups in enzymes (O'Leary and Solberg 1976), and DNA mutation (Fang 2004). However, these hypotheses are not well verified and it is not clear whether some of these effects are more important than others in different bacteria. Additionally, different bacteria will have different levels of tolerance to FNA (Wang et al. 2014).

Desulfovibrio species can be prevalent SRB in sewers (Sun et al. 2014) and are likely important for hydrogen sulfide production in sewage. *Desulfovibrio vulgaris* Hildenborough is well studied and is demonstrated to have a periplasmic cytochrome c nitrite reductase (NrfA) for the conversion of nitrite to ammonium (Heidelberg et al. 2004). It is largely thought that this nitrite reductase activity is not respiratory or for growth (Pereira et al. 2000), but is a mechanism to remove the toxic nitrite (He et al. 2006). Although, in a recent twist there is suggestion that the nitrite reduction activity can conserve energy for growth (Korte et al. 2015).

To date, there have been some transcriptional investigations, based on macroarray and microarray analyses, to examine the effects of nitrite on *D. vulgaris* (Haveman et al. 2004; He et al. 2006) . These studies implicate that nitrite stress could inhibit sulfate reduction and cause possible oxidative stress, as well as disrupt iron homeostasis. However, all the conclusions and hypotheses drawn from those investigations are based only on the transcriptional responses. A comprehensive and systematic understanding of the antimicrobial mechanisms of FNA on *D. vulgaris* is still lacking. This could be achieved by combining the transcriptional response with detection of cell activities and physiological changes.

In this study, substrate transformations and physiological changes were detected in response to different levels of FNA. In addition, whole genome messenger RNA sequencing (RNA-seq) analysis was also conducted on *D. vuglaris* cultures in the presence and absence of sub-bactericidal level of FNA (4.0 μg N/L). The global transcriptome response was combined with analyses of substrate transformations and physiological responses to test the hypotheses mentioned above. From this a more comprehensive understanding of the effects of FNA was obtained to verify the key determinants of FNA stress in this model sewer hydrogen sulfide producing bacterium.

Material and Methods

Cultivation of *D. vulgaris* Hildenborough

D. vulgaris Hildenborough (ATCC 29579) was provided by Professor Jizhong Zhou and Dr. Aifen Zhou from the Institute for Environmental Genomics, University of Oklahoma. For all experiments, a defined lactate sulfate medium (LS4D medium) (Zhou et al. 2010) was used to cultivate the bacterium. The LS4D medium was prepared and added to serum bottles, gassed with nitrogen gas for 30 min before capping with butyl rubber stoppers for autoclaving. 1.5 ml of a glycerol preserved stock of *D. vulgaris* was used to inoculate the serum bottles containing 140 ml of medium. These were then cultivated at 37°C for 48 h to achieve the early stationary phase of growth (an optical density at 600 nm [OD_{600}] of 0.9 to 1.0). The OD_{600} of the culture was then adjusted to 0.5 and multiple 10 ml aliquots of this was used to inoculate serum bottles containing 140 ml of fresh LS4D medium. The inoculated bottles were then incubated at 30°C without shaking for further use of experiments described below. All experimental procedures of culture growth, physiological assays and RNA-seq analyses were performed on triplicate cultures unless otherwise mentioned.

FNA treatment on cultures of *D. vulgaris*

After 26 h growth at 30°C, when the cultures were in early log phase (OD_{600} of around 0.3), nitrite was added to achieve the starting FNA concentrations of 0, 1.0, 4.0, and 8.0 μg N/L. The term "starting concentration" is used to describe the levels of FNA added in the different experiments, as during the incubations the actual FNA concentrations change, most likely due to the nitrite reduction activity of *D. vulgaris*. For each FNA concentration the culture incubations were performed in triplicate. The FNA concentration is dependent on the level of nitrite, pH and temperature, and this was calculated based on the equation already described (Gao et al. 2015). These concentrations of FNA were chosen based on preliminary studies (not shown) where it was observed that these levels of exposure covered the spectrum of growth responses to FNA, from slight inhibition of growth to near complete killing of the organism. Following the addition of FNA

the cultures were incubated for a further 48 h at 30°C. During exposure to the different FNA levels the concentrations of lactate, acetate, sulfate, sulfite, sulfide, thiosulfate, nitrite and FNA were determined from filtered samples of the inoculated cultures. Additionally, samples from the triplicate controls (no added FNA) and FNA-treated cultures (4.0 μg N/L) were taken for RNA extraction at 1 h after FNA addition. These conditions were chosen for study of the transcriptional response as (i) it has been previously observed in *D. vulgaris* that the peak of the gene expression response to nitrite occurs at 1 h after nitrite exposure (He et al. 2006), and (ii) our preliminary studies showed that at 4.0 μg N/L of FNA exposure there was significant effect on the organisms growth, but complete killing did not occur and eventually the organism could overcome the stress. In preparation for the RNA extraction 5 ml of the bacterial suspension from each serum bottle was centrifuged at 13,000 x g for 2 minutes, the supernatant was discarded and the pellets were immediately frozen in liquid nitrogen before storing at -80ºC. Total RNA extraction was performed from the pellets using the QIAGEN miRNeasy Mini Kit (catalog number 217004) according to the manufacturer's instructions, except for the addition of an extra bead-beating step to ensure the complete lysis of the cells. Strand-specific cDNA libraries were constructed and Illumina paired-end sequencing (HiSeq 2000, Illumina Inc., San Diego, CA, USA) was performed (Macrogen, Seoul, Korea) on the extracted RNA. The raw sequencing data was deposited in NCBI's Gene Expression Omnibus and are accessible through GEO series accession number GSE78834.

Chemical analyses of culture samples

Culture OD_{600} and pH were monitored during the incubations with a Cary 50 bio UV visible spectrophotometer (Varian, Australia) and a labCHEM-pH Benchtop pH - mV - Temperature Meter, respectively. Slight increases in pH occurred during incubation which ranged from 7.15 to 7.4 due to the conversion of nitrite to ammonium. For nitrite detection, culture samples were taken, immediately filtered through 0.22 μm filters (Merck Millipore, USA) and analysed on a Lachat QuikChem 8000 flow injection analyzer (FIA). The concentrations of sulfur species (sulfide, sulfite, thiosulfate, and sulfate) were determined in culture samples by ion chromatography. For this 1.5 ml samples were filtered (0.22 μm, Merck Millipore, USA) into 2 ml vials that contained 0.5 ml of an anti-oxidant preservative buffer (16). Samples were then analysed within 24 h by ion chromatography (Dionex ICS-2000). The culture lactate and acetate levels were determined in 1.0 ml filtered (0.22 μm, Merck Millipore, USA) samples by high performance liquid chromatography as previously described (Gao et al. 2016b).

Physiological assay of *D. vulgaris*

Various assays were conducted during growth of *D. vulgaris* in the absence and presence of different FNA concentrations. LIVE/DEAD staining was conducted on the culture samples as described in the manufacturers instructions (BacLight Bacterial Viability Kit, Molecular Probes, L7012). The LIVE/DEAD ratio of cells was then quantified by applying 500 µL of the stained samples to a FACSAria™ II (BD Biosciences, San Jose, USA) flow cytometer. The cellular redox status of the cultures was determined by staining 500 µL of samples with the RedoxSensor™ Green reagent provided in the BacLight RedoxSensor Green Vitality Kit (Life Technologies, B34954), as per the manufacturers instructions. The fluorescence signal of the stained cultures was quantified using the FACSAria™ II type flow cytometer as suggested in the kit protocol. Cellular ATP levels were determined in 500 µL of culture samples using the BacTiter-Glo™ Microbial Cell Viability Assay (Promega Corporation, G8231). Cellular thiol group levels were determined on 200 µL culture samples using the Thiol and Sulfide Quantitation Kit (Molecular Probes, T-6060). The ATP and thiol group assays were performed as described in the corresponding manufacturers instructions.

RNA-seq data processing and differentially expressed genes analysis

The raw sequence reads were treated using the NGS QC Toolkit (v2.3.3) (Patel and Jain 2012) to trim the 3'-end residual adaptors and primers as well as removing the ambiguous characters in the reads. Then the sequence reads consisting of at least 85% bases with a quality value ≥ 20 were kept. The resulting clean reads no shorter than 75 base pairs were used for downstream analyses. SeqAlto (version 0.5) was used to align the clean reads of each sample to the reference genome (NC_002937) of *D. vulgaris* (Mu et al. 2012). Cufflinks (version 2.2.1) was used to calculate the strand-specific coverage for each gene and to analyse the differential expression on triplicated cultures (Trapnell et al. 2012). CummeRbund package in R (http://compbio.mit.edu/cummeRbund/) was used to conduct the statistic analyses and visualization. Gene expression was calculated as reads per kilobase of a gene per million mapped reads (RPKM), a normalized value generated from the frequency of detection and the length of a given gene (Trapnell et al. 2012). Differences in fold-change values were calculated between control and FNA-treated samples (4.0 µg N/L) by determining the $\log_2$ fold-change (LFC) of the averaged RPKM values of two triplicated experiments. A stringency cut-off of LFC ≥ 1 or ≤ -1 with q value less than 0.05 was used to identify the significantly differentially expressed genes.

Results

Concentration-dependent effects of FNA on culture growth and respiratory activities

In these investigations, *D. vulgaris* utilises sulfate as the electron acceptor and lactate as the electron donor with sulfide and acetate as the respective end products (Heidelberg et al. 2004). Additionally, *D. vulgaris* has NrfA that can reduce nitrite to ammonium, allowing it to survive in environments in the presence of nitrite (Heidelberg et al. 2004). The growth of *D. vulgaris* cultures exposed to the lowest starting FNA concentration of 1.0 μg N/L was slightly inhibited during the 48 h incubation (Figure 1). Inhibition of growth increased with the increasing levels of FNA and growth was almost completely stopped with FNA at 8.0 μg N/L (Figure 1).

In the presence of FNA at 1.0 μg N/L the levels of lactate oxidation and sulfate reduction were slightly less than that of the control culture (no FNA addition) (Figure 2C, E) and this coincided with the observed slight decreased growth (Figure 1), indicating FNA was having only a slight inhibitory effect on the organism at this level. During the incubation 1.0 μg N/L FNA was completely reduced within 8 h after addition (Figure 2A, B). In comparison, much lower lactate oxidation levels were detected in cultures with starting FNA concentrations of 4.0 and 8.0 μg N/L (Figure C). In these cultures there would be limited electrons available for sulfate reduction, which was severely diminished (Figure 2E), and this coincided with the reductions in growth levels detected (Figure 1). In the batch cultures nitrite reduction occurred (Figure 2 A, B) after FNA addition. This was evident at all FNA concentrations and was likely due to nitrite reductase activity of *D. vulgaris*.

The absolute ratios of lactate consumed, sulfate used and acetate produced were calculated from the concentrations detected during the 48 h incubations of *D. vulgaris* at the different FNA levels. The ratios were compared to the theoretical ratio determined when acetate is considered as the product of the lactate oxidation (Table 1). For the control culture not exposed to FNA, these values are reasonably close to the stoichiometric ratios for the lactate oxidation (Table 1). However, the ratios of lactate used and acetate produced were increased, at the higher level of applied FNA. This could be explained if there was increased competition for electrons during FNA exposure, which may likely have resulted from increased nitrite reduction activity.

Sulfite and thiosulfate levels were detected during the batch incubations (Figure 2G, H). There were no obvious differences in the levels of sulfite that correlated with the different FNA levels while thiosulfate was detected only in the cultures that were exposed to FNA levels of 4 and 8 μg N/L (Figure 2H).

Changes in specific cell activities during FNA exposure

LIVE/DEAD staining was performed on the *D. vulgaris* batch cultures to evaluate the effect of FNA on cell viability. At early log phase prior to FNA addition, the viable cell numbers in the cultures were around 85%-90% (Figure 3A). When no FNA was added, the live cell percentage stayed at this level until 24 h incubation before dropping to around 65% at 48 h incubation (Figure 3A). This drop in live cells could have resulted from changes in the culture conditions, such as lactate depletion (Figure 2C). In comparison, the viable cell numbers for the FNA concentration of 1.0 μg N/L decreased quickly to around 60% when the incubation time was 7 h and this remained near that level through the incubation period (Figure 3A). Substantial decreases in the percentage of live cells were detected immediately upon the addition of FNA at 4.0 μg N/L FNA, and at 8.0 μg N/L, such that near 95% killing of the *D. vulgairs* cultures occurred within 12 h incubation (Figure 3A). These results support the suggestion that the bacteriostatic and bactericidal effects of FNA are concentration-determined and population-specific as previously detected in *Pseudomonas aeruginosa* PAO1 (Gao et al. 2015).

Cellular thiol levels of *D. vulgaris* increased with the addition of FNA (Figure 3B). At FNA starting concentrations of 1.0 and 4.0 μg N/L N/L, a small increase in cellular thiol levels was detected at 12 and 24 h incubation (Figure 3B). However, cellular thiol levels increased markedly throughout the incubation period when the cells were exposed to 8.0 μg N/L FNA (Figure 3B). It is thought that FNA could nitrosylate thiol groups, such as those on proteins, which could change the activity or function of those (Fang 2004). There is also hypothesis that FNA imposes oxidative stress on bacterial cells (Poole 2005). Thus in these batch cultures the cell redox status was determined and it was observed that with increasing levels of FNA the cells were more oxidised (Figure 3C). Cellular ATP levels of the *D. vulgaris* batch cultures (normalised to per live cell) decreased with the increase of added FNA concentrations (Figure 3D). This supports the idea that FNA acts as a protonophore, to decouple the proton motive force across cell membranes and thereby inhibiting ATP synthesis (Zhou et al. 2011).

Global transcriptomic analysis of FNA stress

To determine the antimicrobial mechanisms of FNA and the possible response pathways adopted by *D. vulgaris*, gene expression profiles were examined by RNA sequencing. To focus on the direct inhibitory mechanisms of FNA on *D. vulgaris* we sought to measure changes that report on the primary effect of FNA, not any secondary affects that would occur over longer timescales more related to changes in growth rate, substrate, products and batch conditions, rather than the direct

response to FNA. We therefore measured the transcriptional response after only 1 h of the FNA addition. This was performed when the cultures were exposed to 4.0 μg N/L at 1 h after FNA addition and compared to gene expression of control cultures when no FNA was added. A total of 239 genes, 6.6% of the total 3623 genes, were detected as significantly differently expressed (see criterion in Material and Methods). 159 genes showed increased transcripts and 80 genes showed decreased transcript levels in response to FNA stress.

Evidence of oxidative stress and detoxification of FNA by *D. vulgaris*

D. vulgaris possesses NrfA that can catalyse the six-electron reduction of nitrite to ammonium and hydroxylamine is an intermediate of the reduction (Bykov and Neese 2015). In these FNA-added cultures the gene coding for NrfA (DVU0625) exhibited considerable up regulation (Table 2), implying its detoxifying role by the reduction of nitrite (and proportional reduction of FNA). This observation agrees with the decreasing nitrite levels detected in the batch cultures (Figure 2A). Additionally, the gene, DVU2543, which codes for what is known as the hybrid cluster protein (HCP), was the most up-regulated gene detected when exposed to FNA (Table 2). The HCP is proposed to have hydroxylamine reductase activity (Wolfe et al. 2002), and was possibly acting to remove hydroxylamine as part of the detoxification of nitrite.

Various genes coding for response to oxidative stress displayed highly increased transcript levels in the FNA-added cultures (e.g. DVU0772 and *ahpC* (DVU2247), Table 2). This implies that FNA caused oxidising conditions, which is what was detected by the cellular redox measurement in FNA-added cultures (Figure 3C). The genes *msrA* (DVU1984) and *msrB* (DVU0576), coding for reductases, that reduce methionine sulfoxides as an antioxidant response, were observed to have increased transcript levels in FNA-added cultures. Additionally, genes of the Fur regulon, DVU0273, *gdp* (DVU3176), and DVU2574, showed increased transcript levels in response to FNA (Table 2), indicating the possibility that FNA causes a response relating to iron levels change in the cell. Alternatively, this could also be a response to increased oxidative condition, as the genes involved in oxidative stress and iron homeostasis are of the same superfamily of metalloregulatory proteins (He et al. 2006).

FNA inhibited anaerobic respiration and energy generation

In the presence of FNA, various genes coding for enzymes involved in lactate oxidation and sulfate reduction processes were down regulated (Table 3). This included the genes DVU0849-50 and DVU1286-90 that code for the quinone-interacting membrane-bound oxidoreductase complex

(Qmo) and the sulfite reductase complex (DsrAB) respectively (Table 3). It is proposed that Qmo transfers electrons from lactate oxidation directly to adenosine-5'-phosphosulfate reductase while DsrAB transfers electrons to the sulfite reductase (Heidelberg et al. 2004).

Recently an operon has been described for lactate oxidation genes (*luo*) in *D. vulgaris* (Vita et al. 2015). This includes the genes DVU3026 for lactate permease, DVU3027-28 and DVU3032-33 for lactate dehydrogenase subunits, DVU3025 for pyruvate-ferredoxin oxidoreductase, DVU3030 for acetate kinase, and DVU3029 for phosphate acetyltransferase. Down-regulation of all these genes in the *luo* operon, excepting DVU3026, was observed when exposed to FNA (Table 3). Other genes proposed for lactate oxidation such as DVU0600 for lactate dehydrogenase and DVU1569-70 for pyruvate-ferredoxin oxidoreductase, were up regulated or had no change respectively in the presence of FNA. However, DVU0600 and DVU1569-70 had very low expression values (Table 3), and as discussed later, there is some question regarding the involvement of the proteins coded by these genes in lactate oxidation.

Down regulation of these genes, involved in lactate oxidation and transfer of electrons for sulfate reduction, correlated with reductions of lactate and sulfate utilisation (Figure 2C, E) and lowered acetate and sulfide production (Figure 2D, F) when *D. vulgaris* was exposed to FNA. Additionally, the transcripts of genes DVU0774-80, and DVU0918 coding for ATP synthase were all markedly down regulated (Table 3). This coincided with the lowered ATP level detected in the cells. It seems the cells were shutting down the main energy conserving reactions when exposed to FNA.

FNA disrupts DNA replication, transcription and translation

Genes encoding for critical enzymes involved in DNA replication (e.g. chromosomal replication initiator protein DnaA, DNA polymerase, DNA gyrase, DNA topoisomerase) and transcription (DNA-directed RNA polymerase) exhibited down regulation after FNA exposure for 1 h (Table 4). As well, the genes coding for 30S and 50S ribosomal structure proteins (Table 4) and a variety of amino acid transfer RNA synthetases showed significantly decreased transcripts. It is apparent that FNA could be causing decreased cell activities of DNA replication, transcription and protein biosynthesis in *D. vulgaris*. The phenomenon of decreased DNA replication, transcription and protein synthesis coincides with the decreased growth and overall metabolism we detected, such as the decreased ability to utilise sulfate and lactate, during FNA exposure (Figure 1 and 2). The gene *yfi* (DVU1629) coding for the ribosomal subunit interface protein displayed 14.4 fold up regulation (Table 4). This factor is demonstrated to stabilise ribosomes and stop translation in stressful

conditions (Agafonov et al. 2001). Possibly *D. vulgaris* is ceasing translation, and inactivates, and conserves the existing ribosomes in the presence of FNA. Consequently, we measured protein levels per live cell of the control and FNA exposed (4.0 μg N/L) cultures after 2 and 8 h incubation periods (Table 5). Protein levels per cell were less in the FNA- added culture in comparison to the control, suggesting that protein synthesis was markedly arrested when exposed to FNA. This is in agreement with the decreased expression we detected of many genes involved with ribosome function (Table 4).

Additionally, the genes coding for DNA repair proteins MutL and RadC showed increased transcript levels when FNA was applied (Table 4). This was also the case for genes coding for chaperone proteins DnaK and DnaJ (Table 4) that are reported to assist in the re-folding of damaged proteins (Srinivasan et al. 2012). The up regulation of these genes indicates that FNA is likely causing damage to DNA and proteins and *D. vulgaris* was attempting the repair of these molecules.

Discussion

In this study, the antimicrobial effects of FNA were determined in the model SRB *D. vulgaris*. For the first time we used a comprehensive approach by combining substrate consumption, physiological analyses, and whole genome RNA-seq, in the presence and absence of FNA, to discover the antimicrobial mechanisms of FNA on *D. vulgaris* Hildenborough. Our findings of the transcriptome analysis revealed significant multiple responses and detoxification activities of *D. vulgaris* in response to FNA stress, and the resulting observations and hypotheses were supported by the cell activities and physiological changes detected.

Nitrite consumption and increased transcription of genes coding for the nitrite reductase NrfA demonstrated that detoxification of FNA by NrfA was evident in *D. vulgaris* in the presence of FNA even when electron supply was low since lactate oxidation was limited (Figure 2A&C, Table 2). This is a logical response and is in agreement with previous observations of *D. vulgaris* to nitrite exposure (Haveman et al. 2004; He et al. 2006). Additionally, the most up-regulated gene detected, with greater than 1000 fold change in the FNA-added cultures was DVU2543 (Table 2), which encodes a proposed hydroxylamine reductase (Wolfe et al. 2002). High expression of this gene in *D. vulgaris* has been reported previously in response to nitrite exposure (Haveman et al. 2004; He et al. 2006). The enzyme is thought to be either for reduction of RNS (the hydroxylamine reductase activity) or for reduction of reactive oxygen species (Aragao et al. 2008). There is strong possibility here that hydroxylamine or other RNS accumulate during FNA exposure, possibly through

incomplete reduction of nitrite by NrfA (Bykov and Neese 2015). Characterisation of the HCP from *E. coli* shows reduction of hydroxylamine with production of ammonium (Wolfe et al. 2002). While the enzyme has not been characterised in *D. vulgaris*, one suggestion is that the HCP is acting similarly or in conjunction with NrfA to detoxify the high levels of nitrite.

Genes coding for electron transfer proteins for sulfate reduction, the Qmo and DsrAB membrane complexes, were significantly down regulated (Table 3). This down regulated gene expression is observed in previous studies of nitrite exposure to *D. vulgaris* (Haveman et al. 2004; He et al. 2006) , and would be an appropriate action in cells that experienced diminished electron flow from lactate oxidation. Interestingly, thiosulfate, the intermediary product of the sulfate reduction by the trithionate-reducing pathway (Kim and Akagi 1985), was found to accumulate in FNA treated samples while sulfite did not (Fig 2G and H). Previous studies demonstrate two possible pathways of sulfite reduction to sulfide in *D. vulgaris*, one is by direct reduction without intermediates and the other is via the trithionate pathway with thiosulfate and sulfite as the intermediates (Rabus R. et al., 2006). The observed accumulation of thiosulfate supports the inhibitory effect of nitrite on DsrAB and suggests that the trithionate-reducing pathway is the mechanism of sulfite reduction in *D. vulgaris* in these conditions. In summary, the FNA exposure caused the down regulation of these genes which severely inhibited the lactate oxidation and sulfate reduction processes.

From early annotations of the *D. vulgaris* genome the genes associated with lactate oxidation have included DVU0600 for lactate dehydrogenase, and DVU1569-70 for pyruvate-ferredoxin oxidoreductase. In a previous microarray study exposing *D. vulgaris* to nitrite levels (2.5 mM) similar to that used here (2.3 mM), they reported up regulation of these genes (He et al. 2006). We also report up regulation for the gene DVU0600 but no change for the genes DVU1569-70. However, the expression levels (RPKM values) of these genes in the presence of FNA was extremely low (Table 3), thus, this questions the involvement of the respected coded proteins in lactate oxidation. Recently, genes of the *luo* operon are deemed to be responsible for lactate oxidation in *D. vulgaris* rather than DVU0600 and DVU1569-70 (Vita et al. 2015). In this study we detected down regulation of most genes in *luo* operon when exposed to FNA (Table 3) and importantly these genes had high expression values when lactate and sulfate utilisation, and when acetate and sulfide production, were active (Table 3, Figure 2C, D, E, and F). This down regulation of the *luo* operon genes during FNA exposure is logical when the cells respiratory activities were lowered, as we observed. Additionally, these findings further support the involvement of the recently described *luo* operon in lactate oxidation (Vita et al. 2015).

In addition to the down regulation of genes involved in respiration, there is suggestion that FNA directly effected enzymes involved in lactate oxidation. The lack of sulfate utilisation during high levels of FNA exposure can be readily explained by the inhibition of the sulfite reductase activity of DsrAB by nitrite/FNA (Haveman et al. 2004). However, there is the question as to why the lactate oxidation stops during exposure to FNA. Nitrite reductase activity in the periplasm would act to consume the protons and electrons produced by lactate oxidation in the cytoplasm, as described in the model for respiration by *D. vulgaris* (Haveman et al. 2004). Thus, lactate oxidation should continue unless FNA or nitrite was having an effect on the enzymes involved in that process. The periplasmic hydrogenases are involved in the flow of protons and electrons produced by lactate oxidation (Haveman et al. 2004). However, gene expression of the highly expressed periplasmic hydrogenase, detected as the Ni-Fe-Se type (Table 3), was significantly decreased. Additionally, it has been seen that the activity of these hydrogenases of *D. vulgaris* is inhibited by nitrite and other RNS (Tibelius and Knowles 1984). Consequently, this lowered gene expression, and the enzyme inhibition could lower the flow of electrons and protons and explain the lowered lactate oxidation activity in the presence of FNA.

To conserve energy *D. vulgaris* performs incomplete lactate oxidation to produce acetate and uses sulfate as the electron acceptor. In our batch cultures, there is limited utilisation of lactate and sulfate, and production of acetate and sulfide at 24 h exposure of 4.0 µg N/L FNA (Figure 2). However, based on 4 electrons being released per molecule of lactate utilised, and 6 and 8 electrons required for nitrite and sulfate reductions respectively, we calculated the electron balance when the culture was exposed to FNA at 4.0 µg N/L at 48 h incubation. It was deduced that even this low amount of lactate utilisation, 7.12 mmol, would provide 28.5 mmol of electrons, which is essentially nearly enough required for the nitrite and sulfate reduction (32.5 mmol) that was detected.

During FNA exposure the cellular redox state was markedly more oxidised (Figure 3C) and genes coding for response to oxidative stress, and those involved in protein repair, had increased expression (Table 2). Additionally, as elucidated above, another possibility for the highly up-regulated gene DVU2543, is that the HCP is acting to relieve oxidative stress (Aragao et al. 2008). Considering these detected events, oxidative stress is suggested as an important antimicrobial effect caused by FNA in *D. vulgaris*. While it is currently not known, it is possible that oxidative damage to the cell components was caused by RNS (Fang 2004; Gao et al. 2015). Interestingly, when

P*seudomonas aeruginosa* was recently exposed to FNA, a more reduced intracellular condition was caused (Gao et al. 2016b). Therefore, the nature of the oxidative stress caused by FNA is genera-dependent rather than a general mode of action.

FNA exposure caused decreased expression of genes involved in protein synthesis in *D. vulgaris*. This is consistent with previous studies of the effect of FNA on *S. enterica* and *P. aeruginosa* (Gao et al. 2016b; Mühlig et al. 2014). Additionally, we detected increased expression of the gene *yfi* (DVU1629) (Table 4), the coded protein of which functions to stabilise ribosomes and stop translation in stressful conditions. Thus, it seems that FNA stress caused *D. vulgaris* to stop protein synthesis, and to inactivate and stabilise the existing ribosomes. This was supported by the decreased cellular protein levels we measured during FNA exposure (Table 5). The nature of these FNA-caused changes to the gene regulation detected here needs further investigation, possibly it was a response to lowered cell energetics. Irrespective, the decreased ribosome activity would have a major impact on the organism's ability to produce its main components for successful cellular activity and operation.

Achieving control of the growth and activity of SRB in sewers is extremely important to mitigate costly concrete corrosion. Growth was detected in the *D. vulgaris* batch cultures at all the concentrations of FNA applied in this study (Figure 1). Although, the growth was low at the high FNA starting concentration of 8.0 μg N/L, when approximately 5% of cells remained live (Figure 3A). While only low levels of lactate and sulfate were consumed in this condition, it appears that the remaining live cells were able to grow at the high level of FNA. These results suggest that the bactericidal effects of FNA are concentration-determined and higher concentrations of FNA need to be applied to kill *D. vulgaris*. We recently proposed that heterogeneity in P*seudomonas aeruginosa* populations explained differential resistance to FNA (Gao et al. 2015). It is also possible here that differential resistance to FNA is detected in SRB. The occurrence of resistance would be of concern in the application of FNA in the sewers. Recently, in field trials lasting 6 months the sulfide production from actual sewer biofilms was reduced by 80% after dosing the sewage with FNA at 0.26 mg N/L (Jiang et al. 2013). Consequently, good levels of sulfide control were achieved and increased tolerance to the applied FNA was not observed under the dosing regime. Although the laboratory application of FNA is very different to that in the real sewer situation, through the improved understanding gained in this study, there is likely opportunity to improve on real FNA applications. For example, combining FNA with treatments that cause increased oxidative stress is seen to achieve more effective biofilm control (Jiang and Yuan 2013).

In conclusion, several key findings were identified in this study regarding the responses of *D. vulgaris* to FNA stress. A conceptual model was proposed that summarises the antimicrobial effects of FNA on *D. vulgaris* (Figure 4). During exposure to FNA, *D. vulgaris* switched from a status of prolific growth to a phase of severely inhibited growth. When exposed to FNA at 4.0 μg N/L sulfate reduction and lactate oxidation coupled with ATP generation were suppressed, leading to energy starvation in the FNA-added cultures. Expression of genes coding for lactate oxidation and sulfate reduction were subsequently lowered. In response to energy starvation, *D. vulgaris* stabilised its existing ribosomes and ceased translation of proteins. In addition, FNA caused more oxidative conditions in *D. vulgaris* and there was transcriptional evidence of attempts to alleviate the oxidative stress. The findings of this study not only provide insight and fundamental understanding of the antimicrobial mechanism of FNA, but also can assist in the application of FNA in real sewers for control of sulfide production and corrosion,

Acknowledgments

We acknowledge the Australian Research Council for funding support through project DP120102832 (Biofilm Control in Wastewater Systems using Free Nitrous Acid - a Renewable Material from Wastewater) and we thank the China Scholarship Council for scholarship support for Shu-Hong Gao. We thank Dr. Beatrice Keller, Jianguang Li, University of Queensland for IC and HPLC analysis and Dr. Michael Nefedov, University of Queensland for assistance with the BD FACSAria™ II flow cytometer and data analysis.

References

Agafonov D.E., Kolb V.A., Spirin A.S. 2001. A novel stress-response protein that binds at the ribosomal subunit interface and arrests translation. *Cold Spring Harbor Symposia on Quantitative Biology,* 66, 509-514.

Aragao D., Mitchell E.P., Frazao C.F., Carrondo M.A., Lindley P.F. 2008. Structural and functional relationships in the hybrid cluster protein family: structure of the anaerobically purified hybrid cluster protein from *Desulfovibrio vulgaris* at 1.35 angstrom resolution. *Acta Crystallographica Section D-Biological Crystallography,* 64, 665-674.

Bykov D., Neese F. 2015. Six-electron reduction of nitrite to ammonia by cytochrome c nitrite reductase: insights from density functional theory studies. *Inorganic Chemistry,* 54, 9303-9316.

Fang F.C. 2004. Antimicrobial reactive oxygen and nitrogen species: concepts and controversies. *Nature Reviews. Microbiology,* 2, 820-832.

Gao S.H., Fan L., Peng L., Guo J., Agulló-Barceló M., Yuan Z., Bond P.L. 2016b. Determining multiple responses of *Pseudomonas aeruginosa* PAO1 to an antimicrobial agent, free nitrous acid. *Environmental Science & Technology,* 50, 5305-5312.

Gao S.H., Fan L., Yuan Z., Bond P.L. 2015. The concentration-determined and population-specific antimicrobial effects of free nitrous acid on *Pseudomonas aeruginosa* PAO1. *Applied Microbiology and Biotechnology,* 99, 2305-2312.

Gutierrez O., Mohanakrishnan J., Sharma K.R., Meyer R.L., Keller J., Yuan Z. 2008. Evaluation of oxygen injection as a means of controlling sulfide production in a sewer system. *Water Research,* 42, 4549-4561.

Gutierrez O., Park D., Sharma K.R., Yuan Z. 2009. Effects of long-term pH elevation on the sulfate-reducing and methanogenic activities of anaerobic sewer biofilms. *Water Research,* 43, 2549-2557.

Haveman S.A., Greene E.A., Stilwell C.P., Voordouw J.K., Voordouw G. 2004. Physiological and gene expression analysis of inhibition of *Desulfovibrio vulgaris* Hildenborough by nitrite. *Journal of Bacteriology,* 186, 7944-7950.

Heidelberg J.F., Seshadri R., Haveman S.A., Hemme C.L., Paulsen I.T., Kolonay J.F., Eisen J.A., Ward N., Methe B., Brinkac L.M., Daugherty S.C., Deboy R.T., Dodson R.J., Durkin A.S., Madupu R., Nelson W.C., Sullivan S.A., Fouts D., Haft D.H., Selengut J., Peterson J.D., Davidsen T.M., Zafar N., Zhou L., Radune D., Dimitrov G., Hance M., Tran K., Khouri H., Gill J., Utterback T.R., Feldblyum T.V., Wall J.D., Voordouw G., Fraser C.M. 2004. The genome sequence of the anaerobic, sulfate-reducing bacterium *Desulfovibrio vulgaris* Hildenborough. *Nature Biotechnology,* 22, 554-559.

He Q., Huang K.H., He Z., Alm E.J., Fields M.W., Hazen T.C., Arkin A.P., Wall J.D., Zhou J. 2006. Energetic consequences of nitrite stress in *Desulfovibrio vulgaris* Hildenborough, inferred from global transcriptional analysis. *Applied and Environmental Microbiology,* 72, 4370-4381.

Jiang G., Gutierrez O., Sharma K.R., Keller J., Yuan Z. 2011a. Optimization of intermittent, simultaneous dosage of nitrite and hydrochloric acid to control sulfide and methane productions in sewers. *Water Research,* 45, 6163-6172.

Jiang G., Gutierrez O., Yuan Z. 2011b. The strong biocidal effect of free nitrous acid on anaerobic sewer biofilms. *Water Research,* 45, 3735-3743.

Jiang G., Keating A., Corrie S., O'halloran K., Nguyen L., Yuan Z. 2013. Dosing free nitrous acid for sulfide control in sewers: Results of field trials in Australia. *Water Research,* 47, 4331-4339.

Jiang G., Yuan Z. 2013. Synergistic inactivation of anaerobic wastewater biofilm by free nitrous acid and hydrogen peroxide. *Journal of Hazardous Materials,* 250-251, 91-98.

Keller-Lehmann B., Corrie S., Ravn R., Yuan Z., and Keller J. 2006. Preservation and simultaneous analysis of relevant soluble sulfur species in sewage samples. Proceedings of the Second International IWA Conference on Sewer Operation and Maintenance, Vienna, Austria.

Kim J.H., Akagi J.M. 1985. Characterization of a trithionate reductase system from *Desulfovibrio vulgaris*. *Journal of Bacteriology,* 163, 472-475.

Korte H.L., Saini A., Trotter V.V., Butland G.P., Arkin A.P., Wall J.D. 2015. Independence of nitrate and nitrite Inhibition of *Desulfovibrio vulgaris* Hildenborough and use of nitrite as a substrate for growth. *Environmental Science & Technology,* 49, 924-931.

Mohanakrishnan J., Gutierrez O., Sharma K.R., Guisasola A., Werner U., Meyer R.L., Keller J., Yuan Z. 2009. Impact of nitrate addition on biofilm properties and activities in rising main sewers. *Water Research,* 43, 4225-4237.

Moran M.A., Satinsky B., Gifford S.M., Luo H., Rivers A., Chan L.K., Meng J., Durham B.P., Shen C., Varaljay V.A., Smith C.B., Yager P.L., Hopkinson B.M. 2013. Sizing up metatranscriptomics. *The ISME Journal,* 7, 237-243.

Mu J.C., Jiang H., Kiani A., Mohiyuddin M., Bani Asadi N., Wong W.H. 2012. Fast and accurate read alignment for resequencing. *Bioinformatics,* 28, 2366-2373.

Mühlig A., Behr J., Scherer S., Müller-Herbst S. 2014. Stress response of *Salmonella enterica serovar* typhimurium to acidified nitrite. *Applied and Environmental Microbiology,* 80, 6373-6382.

O'Leary V., Solberg M. 1976. Effect of sodium nitrite inhibition on intracellular thiol groups and on the activity of certain glycolytic enzymes in *Clostridium perfringens*. *Applied and Environmental Microbiology,* 31, 208-212.

Patel R.K., Jain M. 2012. NGS QC Toolkit: a toolkit for quality control of next generation sequencing data. *PloS one,* 7, e30619.

Pereira I.A., LeGall J., Xavier A.V., Teixeira M. 2000. Characterization of a heme c nitrite reductase from a non-ammonifying microorganism, *Desulfovibrio vulgaris* Hildenborough. *Biochimica et Biophysica Acta (BBA) - Protein Structure and Molecular Enzymology,* 1481, 119-130.

Pikaar I., Sharma K.R., Hu S., Gernjak W., Keller J., Yuan Z. 2014. Water engineering. Reducing sewer corrosion through integrated urban water management. *Science,* 345, 812-814.

Poole R.K. 2005. Nitric oxide and nitrosative stress tolerance in bacteria. *Biochemical Society Transactions,* 33, 176-180.

Rabus, R., Hansen, T. A. & Widdel, F. 2006. Dissimilatory sulfate-and sulfur-reducing prokaryotes, p 659-660. In R. Rabus, T. A. Hansen and F. Widdel (ed). The prokaryotes. Springer-Verlag, New York, N.Y.

Srinivasan S.R., Gillies A.T., Chang L., Thompson A.D., Gestwicki J.E. 2012. Molecular chaperones DnaK and DnaJ share predicted binding sites on most proteins in the *E. coli* proteome. *Molecular BioSystems,* 8, 2323-2333.

Sun J., Hu S., Sharma K.R., Ni B.J., Yuan Z. 2014. Stratified microbial structure and activity in sulfide- and methane-producing anaerobic sewer biofilms. *Applied and Environmental Microbiology,* 80, 7042-7052.

Tibelius K.H., Knowles R. 1984. Hydrogenase activity in *Azospirillum brasilense* is inhibited by nitrite, nitric oxide, carbon monoxide, and acetylene. *Journal of Bacteriology,* 160, 103-106.

Trapnell C., Roberts A., Goff L., Pertea G., Kim D., Kelley D.R., Pimentel H., Salzberg S.L., Rinn J.L., Pachter L. 2012. Differential gene and transcript expression analysis of RNA-seq experiments with TopHat and Cufflinks. *Nature Protocols,* 7, 562-578.

Vadivelu V.M., Yuan Z., Fux C., Keller J. 2006. The inhibitory effects of free nitrous acid on the energy generation and growth processes of an enriched *Nitrobacter* culture. *Environmental Science and Technology,* 40, 4442-4448.

Vita N., Valette O., Brasseur G., Lignon S., Denis Y., Ansaldi M., Dolla A., Pieulle L. 2015. The primary pathway for lactate oxidation in *Desulfovibrio vulgaris*. *Frontiers in Microbiology,* 6, 606.

Wang Q., Ye L., Jiang G., Hu S., Yuan Z. 2014. Side-stream sludge treatment using free nitrous acid selectively eliminates nitrite oxidizing bacteria and achieves the nitrite pathway. *Water Research,* 55, 245-255.

Wolfe M.T., Heo J., Garavelli J.S., Ludden P.W. 2002. Hydroxylamine reductase activity of the hybrid cluster protein from *Escherichia coli*. *Journal of Bacteriology,* 184, 5898-5902.

Zahrt T.C., Deretic V. 2002. Reactive nitrogen and oxygen intermediates and bacterial defenses: unusual adaptations in *Mycobacterium tuberculosis*. *Antioxidants & Redox Signaling,* 4, 141-159.

Zhang L., B D.G., P D.S., Mendoza L., Marzorati M., Verstraete W. 2009a. Decreasing sulfide generation in sewage by dosing formaldehyde and its derivatives under anaerobic conditions. *Water Science and Technology,* 59, 1248-1254.

Zhang L., Keller J., Yuan Z. 2009b. Inhibition of sulfate-reducing and methanogenic activities of anaerobic sewer biofilms by ferric iron dosing. *Water Research,* 43, 4123-4132.

Zhou A.F., He Z.L., Redding-Johanson A.M., Mukhopadhyay A., Hemme C.L., Joachimiak M.P., Luo F., Deng Y., Bender K.S., He Q., Keasling J.D., Stahl D.A., Fields M.W., Hazen T.C., Arkin A.P., Wall J.D., Zhou J.Z. 2010. Hydrogen peroxide-induced oxidative stress responses in *Desulfovibrio vulgaris* Hildenborough. *Environmental Microbiology,* 12, 2645-2657.

Zhou Y., Oehmen A., Lim M., Vadivelu V., Ng W.J. 2011. The role of nitrite and free nitrous acid (FNA) in wastewater treatment plants. *Water Research,* 45, 4672-4682.

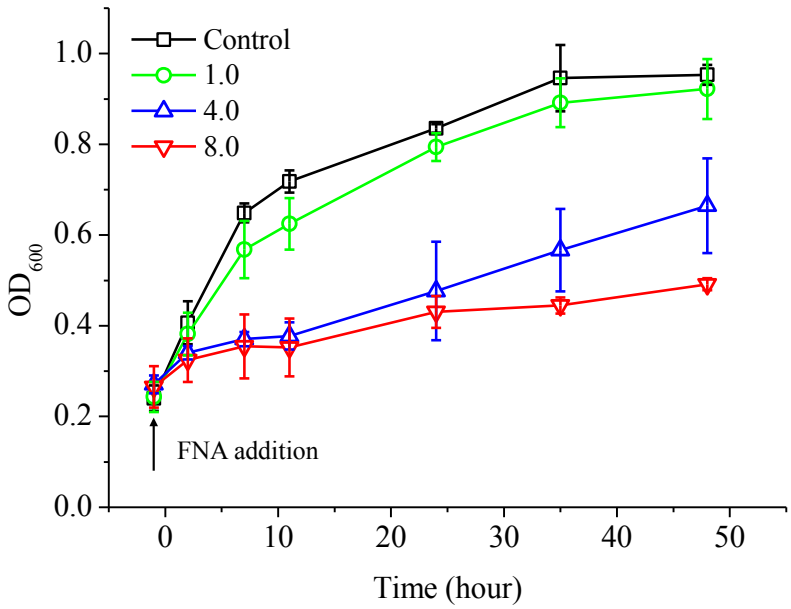

Figure 1. Growth profiles of *D. vulgaris* batch cultures in the presence of different starting FNA concentrations (μg N/L). FNA was added at time 0 h. The control culture has no FNA addition. Error bars show the standard deviation of the triplicated cultures. The figure legend shows the FNA starting concentrations.

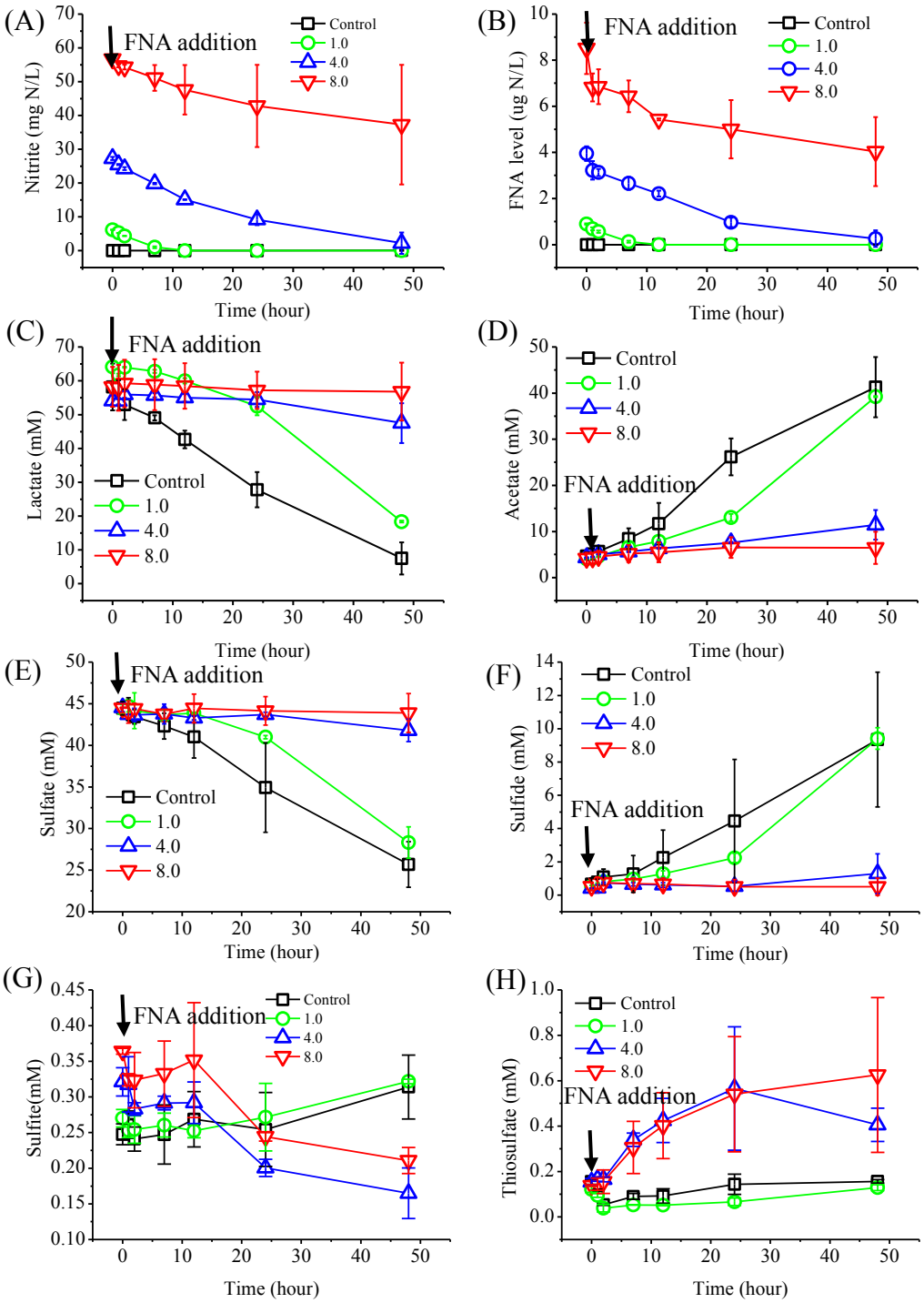

Figure 2. Levels of nitrite (A), FNA (B), lactate (C), acetate (D), sulfate (E), sulfide (F), sulfite (G), and thiosulfate (H) in *D. vulgaris* batch cultures grown on lactate and sulfate. The batch cultures were exposed to different levels of FNA that was added at time 0 h, which was 26 hours after inoculation. No FNA was added to the control cultures. Error bars represent the standard deviation of analyses performed from triplicate batch cultures. The figure legend shows the FNA starting concentrations (μg N/L).

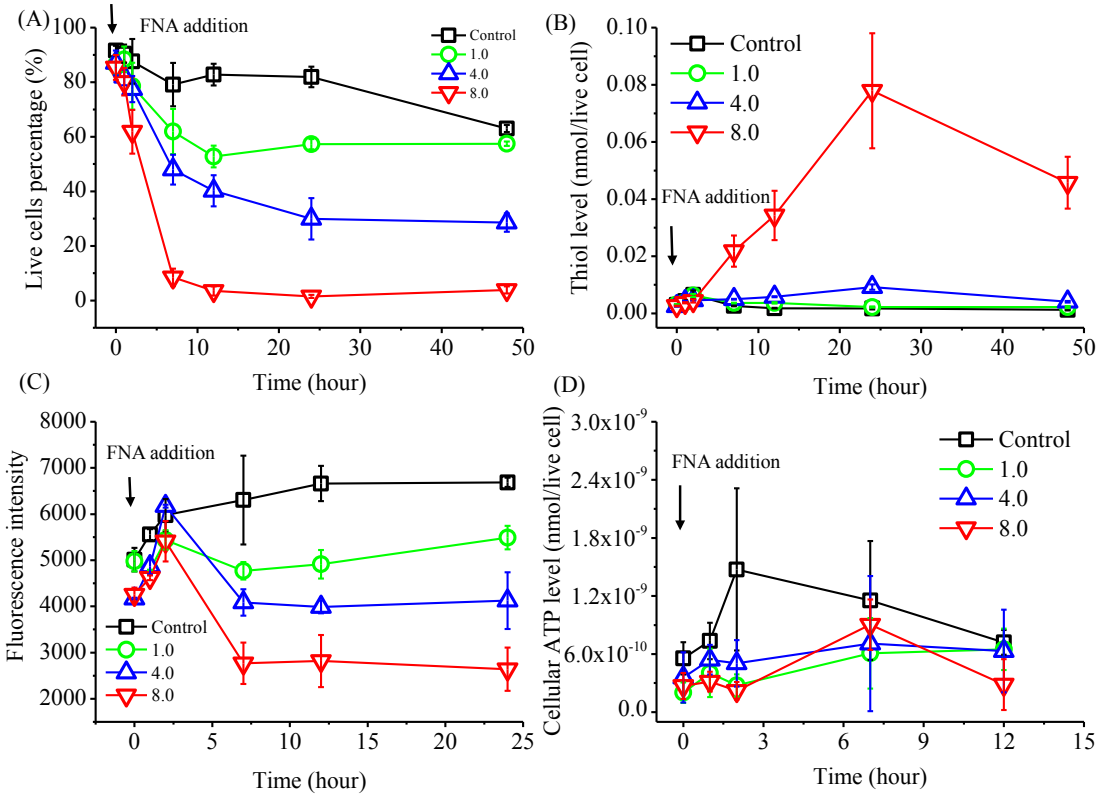

Figure 3. Physiological features of *D. vulgaris* measured during the batch cultures incubations in the presence of different starting FNA levels and when no FNA was added (control). The percentage of live cells (A), cellular thiol levels (B), intracellular redox levels, where higher fluorescence indicates lower redox potential (C), and cellular ATP levels (D). FNA was added at time 0 h. Error bars represent the standard deviation of analyses performed from triplicate batch cultures. The figure legend shows the FNA starting concentrations (µg N/L).

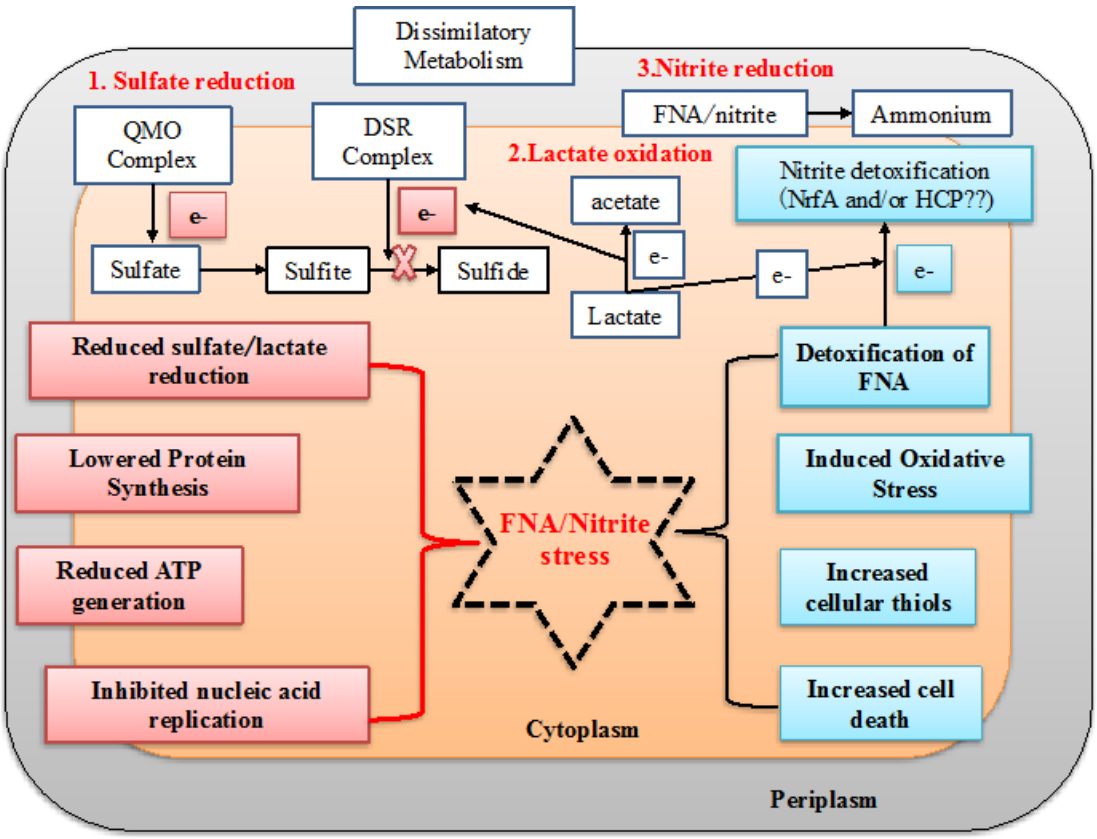

Figure 4. Proposed antimicrobial effects of FNA on *D. vulgaris* based on interpretations of measured physiological activities and the transcriptional responses. The colored boxes indicate activities or events where the associated gene expression was primarily increased (blue) or decreased (pink) in response to FNA exposure.

Table 1. Absolute ratios of lactate and sulfate used and acetate produced during the 48 h incubation of *D. vulgarius* cultures in the presence and absence of added FNA.

Culture condition	Lactate used (mM)	Sulfate used (mM)	Acetate produced (mM)
[a] Theoretical ratio	2	1	2
Control, no FNA	3.00±1.17	1.00±0.31	2.60±1.21
FNA at 1.0 μg N/L	2.83±0.13	1.00±0.08	2.19±0.00
FNA at 4.0 μg N/L	3.00±0.31	1.00±0.27	2.61±0.59
FNA at 8.0 μg N/L	3.51±1.56	1.00±1.17	3.44±1.49

[a] The theoretical ratio based on the stoichiometry if acetate is the product.

Table 2. The transcriptional responses of *D. vulgaris* genes involved in detoxification when exposed to FNA for 1 h with an initial concentration of 4.0 μg N/L.

Gene ID	Gene name	Annotation	RPKM_Control	RPKM_FNA-added	LFC	Fold change	q value
Oxidative stress							
DVU2247	ahpC	anti-oxidant AhpCTSA family protein	643.79	2376.65	1.88	3.68	0.0003
DVU1397	bfr	bacterioferritin	148.13	381.75	1.37	2.58	0.0003
DVU3183	sor	desulfoferrodoxin	1237.40	3966.13	1.68	3.21	0.0003
DVU0772		Hypothetical Protein	1622.19	8374.84	2.37	5.17	0.0003
DVU0576	msrB	methionine sulfoxide reductase B	15.78	649.09	5.36	41.07	0.0003
DVU1984	msrA	peptide methionine sulfoxide reductase MsrA	24.08	181.96	2.92	7.57	0.0003
DVU1457	trxB	thioredoxin reductase	81.88	415.55	2.34	5.08	0.0003
Fur Regulon							
DVU0942	fur	Fur family transcriptional regulator	199.36	340.38	0.77	1.71	0.0241
DVU2574		Ferrous Ion Transport Protein	123.57	708.01	2.52	5.74	0.0003
DVU2680	fld	Flavodoxin, iron-repressed	166.69	1892.42	3.50	11.31	0.0003
DVU0763	gdp	Diguanylate Cyclase	21.37	185.5	3.12	8.69	0.0003
DVU0273		Conserved hypothetical Protein	37.96	244.7	2.69	6.45	0.0003
Nitrite reduction							
DVU0625		Cytochrome c Nitrite Reductase, Catalytic Subunit NfrA	94.88	1874.77	4.30	19.70	0.6357
DVU2543		Hydroxylamine Reductase	8.44	8588.86	9.99	1016.93	0.0003
DVU2544		iron-sulfur cluster-binding protein	4.29	1133.96	8.05	264.58	0.0003

Table 3. FNA effects on the transcriptional responses of *D. vulgaris* genes involved in metabolism when exposed to FNA for 1 h with an initial concentration of 4.0 μg N/L [a].

Gene ID	Gene name	Annotation	RPKM_Control	RPKM_FNA-added	LFC	Fold change	q value
Sulfate reduction							
DVU0847	apsA	adenylylsulfate reductase subunit alpha	6909.68	5078.47	-0.44	-1.36	0.3464
DVU0846	apsB	adenylylsulfate reductase subunit beta	9741.20	7860.48	-0.31	-1.24	0.5378
DVU1288	dsrJ	Cytochrome c family protein (DsrJ)	534.27	61.42	-3.12	-8.70	0.6528
DVU0402	dsrA	dissimilatory sulfite reductase subunit alpha	2089.97	985.96	-1.08	-2.12	0.0128
DVU0403	dsrB	dissimilatory sulfite reductase subunit beta	2141.02	1348.20	-0.67	-1.59	0.1274
DVU0848		Heterodisulfide Reductase (Qmo)	926.97	528.78	-0.81	-1.75	0.0488
DVU0849		Heterodisulfide Reductase, Iron-Sulfur-Binding Subunit (Qmo)	559.5	223.45	-1.32	-2.50	0.0035
DVU0850		Heterodisulfide Reductase, Transmembrane Subunit (Qmo)	705.61	301.39	-1.23	-2.35	0.0042
DVU1290	dsrM	nitrate reductase subunit gamma (DsrM)	812.85	115.61	-2.81	-7.03	0.0003
DVU1289	dsrK	reductase, iron-sulfur binding subunit (DsrK)	344.44	48.62	-2.82	-7.08	0.0003
DVU1287	dsrO	reductase, iron-sulfur binding subunit (DsrO)	366.72	53.15	-2.79	-6.90	0.6170
DVU1286	dsrP	reductase, transmembrane subunit (DsrP)	423.76	69.34	-2.61	-6.11	0.0003
DVU1597	sir	sulfite reductase, assimilatory-type	216.21	113.30	-0.93	-1.91	0.0051
Lactate oxidation							
DVU3030	ackA	acetate kinase	339.10	83.54	-2.02	-4.06	0.0003
DVU3027	glcD	glycolate oxidase subunit GlcD	274.79	125.67	-1.13	-2.19	0.0035
DVU3031		hypothetical protein DVU3031	136.07	17.79	-2.93	-7.65	0.6411
DVU3032		hypothetical protein DVU3032	511.29	42.46	-3.59	-12.04	0.6108
DVU3028		iron-sulfur cluster-binding protein	281.53	136.67	-1.04	-2.06	0.0037
DVU3033		iron-sulfur cluster-binding protein	273.18	30.99	-3.14	-8.82	0.0003

DVU0600		L-lactate Dehydrogenase	5.29	25.03	2.24	4.72	0.0003
DVU2110		L-lactate permease	5.39	5.63	0.06	1.04	0.9109
DVU2285		L-lactate permease	111.29	27.81	-2.00	-4.00	0.0003
DVU2451		L-lactate permease	281.30	156.81	-0.84	-1.79	0.0229
DVU2683		L-lactate permease	118.96	20.57	-2.53	-5.78	0.0003
DVU3026		L-lactate permease	121.11	77.86	-0.64	-1.56	0.0639
DVU3029	pta	phosphate acetyltransferase	236.08	75.62	-1.64	-3.12	0.0003
DVU1569	porA	pyruvate ferredoxin oxidoreductase subunit alpha	40.03	20.68	-0.95	-1.94	0.7719
DVU1570	porB	pyruvate ferredoxin oxidoreductase subunit beta	42.03	26.86	-0.65	-1.56	0.8398
DVU3025	poR	pyruvate-ferredoxin oxidoreductase	821.96	337.59	-1.28	-2.43	0.7256
DVU0577		formate dehydrogenase formation protein FdhE	22.78	53.38	1.23	2.35	0.0012
DVU0587	fdnG-1	formate dehydrogenase subunit alpha	48.25	203.16	2.07	4.20	0.0003
DVU0588		formate dehydrogenase subunit beta	77.04	318.11	2.05	4.14	0.0003
ATP synthesis							
DVU0918	atpB	ATP synthase F0 subunit A	938.08	160.96	-2.54	-5.83	0.0003
DVU0779	atpF	ATP synthase F0 subunit B	1224.30	266.04	-2.20	-4.60	0.6435
DVU0780		ATP synthase F0 subunit B\'	730.80	226.18	-1.69	-3.23	0.0003
DVU0920	atpI	ATP synthase I	956.69	313.18	-1.61	-3.05	0.6970
DVU0777	atpA	F0F1 ATP synthase subunit alpha	1156.37	198.62	-2.54	-5.82	0.0003
DVU0775	atpD	F0F1 ATP synthase subunit beta	1069.12	186.45	-2.52	-5.73	0.0003
DVU0778	atpH	F0F1 ATP synthase subunit delta	1589.63	295.74	-2.43	-5.38	0.6396
DVU0774	atpC	F0F1 ATP synthase subunit epsilon	1510.29	345.95	-2.13	-4.37	0.0003
DVU0776	atpG	F0F1 ATP synthase subunit gamma	1369.15	214.02	-2.68	-6.40	0.0003
Electron transfer							
DVU2524		cytochrome c3, putative	2.70	3.15	0.22	1.17	1

DVU0434		ech hydrogenase subunit EchA	12.66	3.28	-1.95	-3.86	0.6701
DVU0433		ech hydrogenase subunit EchB	11.18	2.20	-2.34	-5.07	0.5587
DVU0432		ech hydrogenase subunit EchC	15.72	5.16	-1.61	-3.05	0.0431
DVU0431		ech hydrogenase subunit EchD	22.67	6.16	-1.88	-3.68	0.0163
DVU0430		ech hydrogenase subunit EchE	13.88	5.16	-1.43	-2.69	0.0066
DVU0429		ech hydrogenase subunit EchF	13.21	5.81	-1.19	-2.28	0.1921
DVU2796		electron transport complex protein RnfA	46.78	33.47	-0.48	-1.40	0.2438
DVU2792		electron transport complex protein RnfC	45.12	43.07	-0.07	-1.05	0.8732
DVU2793		electron transport complex protein RnfD	20.48	18.30	-0.16	-1.12	0.7781
DVU2794		electron transport complex protein RnfG	32.95	30.79	-0.10	-1.07	0.8453
DVU0535		Hmc Operon Protein 2	15.05	38.37	1.35	2.55	0.0003
DVU0534		Hmc Operon Protein 3	12.24	37.62	1.62	3.07	0.0003
DVU0532		Hmc Operon Protein 5	10.58	32.98	1.64	3.12	0.0003
DVU0531		Hmc Operon Protein 6	14.61	45.6	1.64	3.12	0.0003
Hydrogenases							
DVU1769	hydA	Periplasmic [FeFe] Hydrogenase, Large Subunit	17.53	8.14	-1.11	-2.16	0.009
DVU1770	hydB	periplasmic [FeFe] hydrogenase, small subunit	12.08	8.55	-0.50	-1.41	0.6281
DVU2526	hynA-2	periplasmic [NiFe] hydrogenase, large unit, isozyme 2	3.36	4.67	0.47	1.39	0.3684
DVU2525	hynB-2	periplasmic [NiFe] hydrogenase, small unit, isozyme 2	2.26	3.00	0.41	1.33	1
DVU1918	hysA	Periplasmic [NiFeSe] hydrogenase, Large Subunit	575.74	265.41	-1.12	-2.17	0.0062
DVU1917	hysB	Periplasmic [NiFeSe] Hydrogenase, Small Subunit	706.06	236.22	-1.58	-2.99	0.0003

[a] Note: Some genes included in the table were not differentially expressed according to the applied criteria of LFC (see materials and methods section) but were included here to aid illustration of an FNA affected pathway or mechanism.

Table 4. FNA effects on the transcriptional responses of *D. vulgaris* genes involved in DNA replication, transcription and translation when exposed to FNA for 1 h with an initial concentration of 4.0 μg N/L.

Gene ID	Gene name	Annotation	RPKM_Control	RPKM_FNA-added	LFC	Fold change	q value
DVU1469	rpsA	30S ribosomal protein S1	66.08	31.43	-1.07	-2.10	0.0012
DVU1302	rpsJ	30S ribosomal protein S10	2247.95	749.15	-1.59	-3.00	0.0003
DVU1327	rpsK	30S ribosomal protein S11	1785.05	802.95	-1.15	-2.22	0.0022
DVU1298	rpsL	30S ribosomal protein S12	1605.02	539.75	-1.57	-2.97	0.0003
DVU1326	rpsM	30S ribosomal protein S13	1579.22	661.60	-1.26	-2.39	0.0008
DVU1316	rpsN	30S ribosomal protein S14	2500.39	558.05	-2.16	-4.48	0.0003
DVU0839	rpsP	30S ribosomal protein S16	1897.36	902.76	-1.07	-2.10	0.0024
DVU0874	rpsB	30S ribosomal protein S2	568.75	187.39	-1.60	-3.04	0.0003
DVU1896	rpsT	30S ribosomal protein S20	1074.90	347.59	-1.63	-3.09	0.0003
DVU1309	rpsC	30S ribosomal protein S3	1612.99	373.63	-2.11	-4.32	0.0003
DVU1328	rpsD	30S ribosomal protein S4	1832.03	702.74	-1.38	-2.61	0.0010
DVU1320	rpsE	30S ribosomal protein S5	1254.60	345.84	-1.86	-3.63	0.0003
DVU0956	rpsF	30S ribosomal protein S6	846.18	368.63	-1.20	-2.30	0.0003
DVU1299	rpsG	30S ribosomal protein S7	1661.83	516.48	-1.69	-3.22	0.0003
DVU1317	rpsH	30S ribosomal protein S8	1628.86	350.60	-2.22	-4.65	0.0003
DVU2925	rplA	50S ribosomal protein L1	1207.01	322.34	-1.90	-3.74	0.0003
DVU2926	rplJ	50S ribosomal protein L10	2811.97	704.14	-2.00	-3.99	0.0003
DVU2924	rplK	50S ribosomal protein L11	2152.09	479.63	-2.17	-4.49	0.0003
DVU2518	rplM	50S ribosomal protein L13	2740.46	1358.38	-1.01	-2.02	0.0135
DVU1313	rplN	50S ribosomal protein L14	2360.35	587.04	-2.01	-4.02	0.0003
DVU1310	rplP	50S ribosomal protein L16	2220.49	487.73	-2.19	-4.55	0.0003
DVU1319	rplR	50S ribosomal protein L18	1455.69	380.51	-1.94	-3.83	0.0003
DVU0835	rplS	50S ribosomal protein L19	2049.36	953.53	-1.10	-2.15	0.0037

DVU1306	rplB	50S ribosomal protein L2	1281.60	385.53	-1.73	-3.32	0.0003
DVU2535	rplT	50S ribosomal protein L20	1552.62	508.75	-1.61	-3.05	0.0003
DVU0927	rplU	50S ribosomal protein L21	1418.19	648.20	-1.13	-2.19	0.0020
DVU1308	rplV	50S ribosomal protein L22	2353.89	499.49	-2.24	-4.71	0.0003
DVU1574	rplY	50S ribosomal protein L25	2580.36	657.59	-1.97	-3.92	0.0003
DVU0928	rpmA	50S ribosomal protein L27	2170.58	787.25	-1.46	-2.76	0.0003
DVU1303	rplC	50S ribosomal protein L3	2546.31	731.53	-1.80	-3.48	0.0003
DVU1315	rplE	50S ribosomal protein L5	3189.91	604.46	-2.40	-5.28	0.0003
DVU1318	rplF	50S ribosomal protein L6	2154.53	518.55	-2.05	-4.15	0.0003
DVU2927	rplL	50S ribosomal protein L7/L12	4245.40	1100.25	-1.95	-3.86	0.0003
DVU1089	alaS	alanyl-tRNA synthetase	69.54	16.30	-2.09	-4.27	0.0003
DVU3166		alanyl-tRNA synthetase	18.77	2.35	-2.99	-7.97	0.0096
DVU1248	argS	arginyl-tRNA synthetase	108.21	39.12	-1.47	-2.77	0.0003
DVU3367	aspS	aspartyl-tRNA synthetase	87.97	24.05	-1.87	-3.66	0.0003
DVU0808	gatA	aspartyl/glutamyl-tRNA amidotransferase subunit A	31.75	6.67	-2.25	-4.76	0.0003
DVU1885	gatB	aspartyl/glutamyl-tRNA amidotransferase subunit B	72.54	27.09	-1.42	-2.68	0.0003
DVU0001	dnaA-1	chromosomal replication initiator protein DnaA	42.34	14.96	-1.50	-2.83	0.0003
DVU2252	dnaA-2	chromosomal replication initiator protein DnaA	108.04	45.84	-1.24	-2.36	0.0005
DVU0004	gyrA	DNA gyrase subunit A	71.66	10.01	-2.84	-7.16	0.0003
DVU0003	gyrB	DNA gyrase subunit B	76.62	12.47	-2.62	-6.14	0.0003
DVU0483	mutL	DNA mismatch repair protein MutL	10.08	34.23	1.76	3.40	0.0003
DVU0002	dnaN	DNA polymerase III subunit beta	190.12	35.75	-2.41	-5.32	0.0003
DVU1193	radC	DNA repair protein RadC	38.21	109.95	1.52	2.88	0.0003
DVU1899		DNA repair protein RecO	17.57	3.75	-2.23	-4.68	0.0090
DVU3389	topA	DNA topoisomerase I	81.00	25.61	-1.66	-3.16	0.0003
DVU2316	topB	DNA topoisomerase III	11.52	5.40	-1.09	-2.13	0.0037
DVU1730		DNA-binding protein	18.40	122.18	2.73	6.64	0.0003

DVU3193		DNA-binding protein	11.67	31.95	1.45	2.74	0.0003
DVU0396	hup-1	DNA-binding protein HU	665.69	1768.32	1.41	2.66	0.0008
DVU0764	hup-2	DNA-binding protein HU	985.51	449.55	-1.13	-2.19	0.0010
DVU0749		DNA-binding response regulator	4.76	17.72	1.90	3.73	0.0003
DVU0596	lytR	DNA-binding response regulator LytR	26.69	82.99	1.64	3.11	0.0003
DVU2928	rpoB	DNA-directed RNA polymerase subunit beta	253.21	86.11	-1.56	-2.94	0.0003
DVU2929	rpoC	DNA-directed RNA polymerase subunit beta\'	246.76	74.92	-1.72	-3.29	0.0003
DVU1876	dnaJ	dnaJ protein	10.84	123.72	3.51	11.41	0.0003
DVU2150	dnaK	dnaK suppressor protein	429.45	203.48	-1.08	-2.11	0.0012
DVU3256	mutM	formamidopyrimidine-DNA glycosylase	8.23	1.51	-2.45	-5.45	0.0208
DVU2552	gltX	glutamyl-tRNA synthetase	52.07	24.23	-1.10	-2.15	0.0018
DVU0809	gatC	glutamyl-tRNA(Gln) amidotransferase subunit C	56.08	25.83	-1.12	-2.17	0.0381
DVU1898	glyQ	glycyl-tRNA synthetase subunit alpha	124.89	42.47	-1.56	-2.94	0.0003
DVU1897	glyS	glycyl-tRNA synthetase subunit beta	56.85	16.48	-1.79	-3.45	0.0003
DVU1927	ileS	isoleucyl-tRNA synthetase	108.88	40.69	-1.42	-2.68	0.0003
DVU2376	lysS	lysyl-tRNA synthetase	194.54	65.27	-1.58	-2.98	0.0003
DVU0811	dnaK	molecular chaperone DnaK	205.16	1065.21	2.38	5.19	0.0003
DVU1608	ligA	NAD-dependent DNA ligase	21.23	4.26	-2.32	-4.99	0.0003
DVU1573	pth	peptidyl-tRNA hydrolase	152.40	46.24	-1.72	-3.30	0.0003
DVU2534	pheS	phenylalanyl-tRNA synthetase subunit alpha	145.09	29.67	-2.29	-4.89	0.0003
DVU2533	pheT	phenylalanyl-tRNA synthetase subunit beta	68.78	13.54	-2.34	-5.08	0.0003
DVU2904		ribosomal RNA large subunit methyltransferase N	21.51	7.33	-1.55	-2.93	0.0008
DVU1629	yfiA	ribosomal subunit interface protein	564.32	8136.85	3.85	14.42	0.0003
DVU0897		RNA modification protein	10.62	3.19	-1.74	-3.33	0.0072
DVU1257		RNA-binding protein	1913.15	793.62	-1.27	-2.41	0.0003
DVU2246		S1 RNA-binding domain-containing protein	7.47	2.84	-1.39	-2.63	0.0058
DVU0904	recJ	single-stranded-DNA-specific exonuclease RecJ	13.58	5.17	-1.39	-2.63	0.0024

DVU2538	thrS	threonyl-tRNA synthetase	340.59	138.11	-1.30	-2.47	0.0012
DVU0807	trmU	tRNA (5-methylaminomethyl-2-thiouridylate)-methyltransferase	29.96	2.81	-3.41	-10.64	0.0003
DVU1079	trmE	tRNA modification GTPase TrmE	7.35	2.51	-1.55	-2.93	0.0196
DVU1828	gidA	tRNA uridine 5-carboxymethylaminomethyl modification protein GidA	56.17	17.69	-1.67	-3.18	0.0003
DVU0142	trpS	tryptophanyl-tRNA synthetase	137.87	41.34	-1.74	-3.33	0.0003
DVU2842		type II DNA modification methyltransferase	119.70	57.17	-1.07	-2.09	0.0018
DVU0953	tyrS	tyrosyl-tRNA synthetase	207.39	57.07	-1.86	-3.63	0.0003
DVU0732	valS	valyl-tRNA synthetase	76.91	30.16	-1.35	-2.55	0.0003

Table 5. Protein levels measured (pg/cell) per cell in control and FNA treated cells after 2 and 8 h incubation. Protein change detected during the 6 h incubation and the protein change predicted (given average protein half life of 20 h (Moran et al. 2013)).

	2 h	8 h	Amount of protein change over 6 h incubation	Protein change expected due to half life
	Protein levels per cell (pg/cell)			
Control cultures	2.33±0.35	1.97±0.29	-0.36	-0.35
FNA-added cultures (4.0 μg N/L)	2.11±0.18	1.55±0.10	-0.56	-0.32

Appendix D

Comparative proteomic analysis of *Desulfovibrio vulgaris* Hildenborough in response to the antimicrobial agent, free nitrous acid

Shu-Hong Gao, Jun Yuan Ho, Lu Fan, Amanda Nouwens, Robert Hoelzle, Benjamin Schulz, Zhiguo Yuan and Philip L Bond*

This manuscript is to be submitted to *Journal of Proteomics*.

Abstract

Sulfate reducing bacteria (SRB), which can produce hydrogen sulfide in sewers, can lead to severe odor problems and asset deterioration due to the sulfide induced concrete corrosion. Recently, free nitrous acid (FNA) has been discovered as a promising antimicrobial agent to inhibit SRB activities thereby limiting hydrogen sulfide production in sewers. However, knowledge of bacteria response dynamics to the increasing levels of the antimicrobial agent FNA is largely unknown. Here we report the protein expression dynamics of *D. vulgaris* and reveal the antimicrobial effects of FNA is multi-targeted and dependent on the FNA levels. This is achieved by determining differential protein expressions in *D. vulgaris* cultures when exposed to different FNA concentrations using SWATH-MS analysis. During exposure to 1.0 μg N/L FNA, only the proteins involved in nitrite reduction (nitrite reductase and the poorly characterized hybrid cluster protein) showed obvious increased expression levels. In the presence of 4.0 and 8.0 μg N/L FNA, increased levels of proteins for nitrite reduction were detected. Proteins involved in sulfate reduction pathway (from sulfite to hydrogen sulfide) and lactate oxidation pathway (from pyruvate to acetate) were firstly inhibited by FNA at 8 h incubation, and then recovered at 12 h incubation. During FNA exposure, lowered ribosomal protein levels in the culture were detected while the total cellular protein levels (per live cell) were mostly constant in the presence of FNA. Additionally, there was evidence that the genes DVU2543, DVU0772, and DVU3212 coded for proteins that play a critical role in defending oxidative stress caused by FNA. Based on the interpretation of the measured protein changes we determined the responses of *D. vulgaris* to different FNA levels over incubation time. These findings offer some new insights for understanding the dynamic responses of *D. vulgaris* to FNA and deliver important findings to guide practical applications of FNA-based technologies to better control corrosion in sewers.

Introduction

The antimicrobial properties of nitrite have been known for a long time. However, recently, free nitrous acid (FNA), the protonated form of nitrite, is recently discovered as the true metabolic inhibitor behind "nitrite inhibition" (Vadivelu et al. 2006). FNA addition at 0.2-0.3 mg N/L for 6-24 h resulted in the decrease of live cell proportions from about 80% to 5-15% in a recent lab-scale treatment of sewers biofilms (Jiang et al. 2011). Moving toward real world application, FNA has been applied in real sewers for the control of sulfate reducing bacteria (SRB) in which an 80% reduction of hydrogen sulfide production occurred by intermittent FNA dosing at 0.26 mg N/L for 8-24 h every four weeks (Jiang et al. 2013). These investigations demonstrate that FNA is highly applicable for the control of SRB activities to limit sulfide levels that lead to sewer corrosion.

Consequently, FNA is emerging as an extremely promising antimicrobial agent sulfide production control via inhibiting activities of SRB in sewers, and there is great interest to know how FNA inhibits or kills the bacteria and how SRB may survive with FNA stress. Currently, the antimicrobial effects of FNA on bacteria in general are believed to be multi-targeted (Fang 2004; Gao et al. 2016a). It is seen that genes coding for dissimilatory sulfite reductase (DsrAB) were down regulated in the presence of nitrite by disrupting SRB respiration (Gao et al. 2016a; Haveman et al. 2004; He et al. 2006). FNA, and perhaps reactive nitrogen species (RNS) derived from FNA, are thought to cause oxidative stress resulting in damage to cell enzymes, cellular membranes and walls, and nucleic acids (Zahrt and Deretic 2002). There are other hypotheses to explain its antimicrobial effects, suggesting that FNA could result in disrupting the proton motive force (Zhou et al. 2011), nitrosylating metal centres or thiol groups in enzymes (O'Leary and Solberg 1976), and mutating DNA (Fang 2004). Nevertheless, these hypotheses are not well verified and it is unknown whether some of these effects are more important than others in different bacteria and conditions.

SRB are prevalent in sewers and typically use sulfate as the terminal electron acceptor for respiration and generate energy with the production of hydrogen sulfide (Heidelberg et al. 2004). The sulfide diffuses to aerobic parts of the sewers where it can be oxidised by sulfate oxidising bacteria to produce sulfuric acid which corrodes the concrete surfaces of the sewers. This corrosion results in severe deterioration of sewer assets that requires very costly and demanding rehabilitation efforts (Jiang et al. 2011; Pikaar et al. 2014) . Therefore there is great interest to efficiently control SRB and minimise hydrogen sulfide production in sewers. *Desulfovibrio* species are likely important for hydrogen sulfide production in sewage (Sun et al. 2014). *Desulfovibrio vulgaris* Hildenborough is a well-studied bacterium which is demonstrated to have a periplasmic cytochrome c nitrite reductase (NrfA) for the conversion of nitrite to ammonium as a detoxifying mechanism

(Heidelberg et al. 2004). Recently, we have found that the antimicrobial effects of FNA on *D. vulgaris* is concentration-dependent by performing metabolic and physiological measurements and demonstrated that the antimicrobial effect of FNA is multi-targeted by applying whole genome RNA sequencing analysis. However, in that study, only one FNA concentration (4.0 μg N/L) at one time point after FNA addition was selected to perform the RNA sequencing analysis. Additionally, details of whether genes showing differential expression in the presence of FNA translated to the corresponding proteins or not and the protein expression dynamics with increasing FNA levels over incubation were not determined in that investigation.

To date, there have been some transcriptional investigations, based on macroarray and microarray analyses, to examine the effects of nitrite on *D. vulgaris* (Gao et al. 2016a; Haveman et al. 2004; He et al. 2006). These studies suggest that nitrite stress inhibits sulfate reduction and cause possible oxidative stress, as well as disrupting iron homeostasis in a short time after FNA/nitrite addition. However, all the conclusions and hypotheses drawn from those investigations are based only on either physiological responses and/or the transcriptional responses (Gao et al. 2016a; Haveman et al. 2004; He et al. 2006). A comprehensive and systematic understanding of the antimicrobial mechanisms of FNA regarding the protein expression dynamics with different FNA levels on *D. vulgaris* is still lacking. SWATH-MS is a recently developed approach that provides extensive label-free quantitation of the measurable peptide ions in a sample (Vowinckel et al. 2013). Currently a proteomic response to bacterial FNA stress exposure has not been conducted.

In this study, we detected the whole cell protein production and protein expression dynamics of *D. vulgaris* by SWATH-MS in the presence of four FNA concentrations (0, 1.0, 4.0, and 8.0 μg/L) with three incubation periods after FNA addition (2, 8, and 12 h). To test the hypotheses of FNA toxicity and its duration to *D. vulgaris* cultures, differentially expression proteins of FNA treated cultures at different treatment period were compared to control cultures. From this a more comprehensive understanding of the FNA effects on *D. vulgaris* was obtained and the key determinants for withstanding FNA over incubation periods were verified in this sewer corrosion relevant strain.

Material and Methods

Culture cultivation

D. vulgaris Hildenborough (ATCC 29579) was provided by Professor Jizhong Zhou and Dr Aifen Zhou from Institute for Environmental Genomics, University of Oklahoma. A defined lactate

sulfate medium (LS4D medium) was used to cultivate the culture for all the performed experiments (Zhou et al. 2013; Zhou et al. 2012). Each serum bottle containing 140 mL LS4D medium was flushed with nitrogen gas for 30 min before capping with butyl rubber stopper for autoclave sterilization. 1.5 mL culture glycerol stock was inoculated to one serum bottle before cultivating at 37°C for 48 h to achieve the early stationary phase of growth (optical density at 600 nm [OD_{600}] 0.9 to 1.0). OD_{600} of the culture was adjusted to 0.5 and 10 mL of this culture (standard inoculum) was transferred into 140 mL of autoclaved anaerobic LS4D medium in serum bottles inside the anaerobic chamber. The cultures were further incubated at 30°C without shaking for further use of experiments described below.

FNA treatment on *D. vulgaris*

After 26 h incubation when the culture was in early log phase (OD_{600} around 0.3) at 30°C, different amounts of nitrite was added to achieve the starting FNA concentration of 0, 1.0, 4.0, and 8.0 μg N/L. Each FNA concentration was conducted in triplicate. FNA levels are determined by measured nitrite concentration, pH and temperature and was calculated based on the equation described before (Anthonisen et al. 1976; Gao et al. 2015). The cultures were incubated for a further 12 h (a total of 38 h incubation) to conduct proteomics study. Samples from triplicated controls (without FNA addition) and FNA-treated cultures (1.0, 4.0, and 8.0 μg N/L) were taken for total protein extraction at 2, 8, and 12 h after FNA addition.

For total protein extraction, 10 mL of the bacteria suspension was centrifuged at 12,000 rpm for 5 minutes, the supernatant was discarded and the pellets were immediately frozen in liquid nitrogen before storing at -80ºC. Protein extractions were performed on these cell pellets. Each pellet was dissolved in 1 mL extraction buffer (77 mg dithiothreitol & 1 tablet of complete Protease Inhibitor (Roche) into 10 ml B-PER II Bacterial Protein Extraction Reagent (Thermo Scientific, 78260)) and subjected to three freeze/thaw cycles by placing into liquid nitrogen and thawing at 4 ˚C. Cell debris was removed by centrifugation at 14,000 rpm for 15 min at 4 ˚C. From the supernatant, proteins were precipitated by adding trichloroacetic acid (13% v/v final concentration) and incubated overnight at 4 ˚C. Precipitated proteins were collected by centrifugation at 14,000 rpm for 15 min at 4 ˚C before washing in cold 80% acetone twice, dried for no more than 5 minutes and resuspended in buffer (8 mM Urea, 50mM ammonium bicarbonate). Total resuspended protein was quantified by the 2D Quant kit (GE Healthcare).

The protein samples were then reduced and alkylated by adding dithiothreitol (5 mM final concentration) for 30 min at 56 ˚C, cooled to room temperature, then treated with iodoacetamide (25 mM final concentration) and incubated at room temperate in the dark for 30 min. The same volume of dithiolthreitol was added twice to quench the excess iodoacetamide. Protein samples were diluted with 50 mM ammonium bicarbonate buffer to reduce urea concentration to less than 2 M, and digested for 6 hours with trypsin (Promega) at an enzyme to protein ratio of 1:100 at 37˚C. Following this, the protein samples were digested overnight again with additional trypsin using the same enzyme to protein ratio at 37˚C. C18 Zip-tip (Millipore) clean-up was performed on the digested proteins (Kappler and Nouwens 2013). For each sample 1 μg of the digested protein was used for subsequent SWATH-MS analysis in triplicate. In addition, 5 μg aliquots of each triplicate samples were taken and pooled for mass spectrometry analysis and information dependent analysis (IDA) library construction, which was performed in duplicate.

Mass spectrometry analysis

Peptides were directly analysed on a Triple-Tof 5600 instrument (ABSciex) equipped with a Nanospray III interface. Gas 1 was set to 10 psi, curtain gas to 30 psi, ion spray floating voltage 2700 V. Samples were scanned across m/z 350-1800 for 0.5 sec followed by the information dependent acquisition (IDA) on high sensitivity mode of 20 peptides with intensity greater than 100 counts across m/z 40-1800 for 0.05 sec. Collision energy was set to 40 +/- 15 V. SWATH analyses were scanned across m/z 350-1800 for 0.5 sec followed by high sensitivity IDA mode, using 26 Da (1 Da for window overlap) isolation windows for 0.1 sec, across m/z 400-1250. Collision energy for SWATH samples was automatically assigned based on m/z mass windows by Analyst software. Mass spectrometry (MS) data from IDA were combined and searched using ProteinPilot software (ABSciex, Forster City CA). The search setting for enzyme digestion was set to Trypsin and alkylation was set to iodoacetamide. The searched databases were *D. vugaris* (received from NCBI on the 28th of January 2016) with the search effort set to “thorough” and a cut off applied > 0.05 (10%). The false detection rate was determined using proteomics system performance evaluation pipeline software (PSPEP), an add-on to ProteinPilot, which uses a decoy database constructed by reversing all the protein sequences in the searched database.

SWATH-MS data analysis

The IDA library and SWATH-MS data were loaded into PeakView v 1.2 software for processing using the SWATH micro processing script. This used a confidence level of 99, the number of peptides set at 5 and the number of transitions used set at 3. A minimum of 2 peptide and 3

transitions was used for quantitative analysis. The R- based program MSstats (Choi et al. 2014) was used for statistical analysis of the spectral data. Pathway Tools (Karp et al. 2010) was used for metabolic pathway reconstruction of the identified proteins. A stringency cut-off of log2 fold change (LFC) ≥ 1 or ≤ -1 with q value less than 0.001 was used to identify the significantly differentially expressed proteins. The mass spectrometry proteomics data has been deposited to the ProteomeXchange Consortium (http://proteomecentral.proteomexchange.org) via the PRIDE partner repository (Vizcaíno et al. 2013) with the dataset identifier (PXD004475).

Results

FNA effect on protein levels of *D. vulgaris*

In this study, *D. vulgaris* was cultured using sulfate as the electron acceptor and lactate as the electron donor with the generation of hydrogen sulfide and acetate. The inhibitory and bactericidal effects of FNA have been previously reported (Gao et al. 2016a). The growth of *D. vulgaris* with different levels of FNA was similar to that previously reported (Gao et al. 2016a). Inhibition of the growth increased with the increased levels of FNA and the growth was completely stopped with a FNA level of 8 μg/L. Additionally, 8.0 μg N/L was reported to almost completely kill *D. vulgaris* cultures within 12 h incubation.

The amount of protein produced by *D. vulgaris* was detected during incubation (Figure 1). Similar protein levels (g/mL) were observed for *D. vulgaris* in the control cultures (no FNA addition) and in the cultures exposed to FNA at 1 μg N/L. These were higher than the protein levels measured in the presence of FNA at 4 and 8 μg N/L (Figure 1A). The protein levels at 8 and 12 h after FNA addition decreased with the increased levels of FNA except for FNA level of 8 μg/L (Figure 1A). In comparison, there is a slight increase of protein production with 1 μg N/L FNA exposure in terms of cellular protein levels, suggesting the cultures were active and experienced protein synthesis to cope with FNA stress (Figure 1B). This is also coincided with the fact that this level of FNA only slightly inhibited the growth of *D. vulgaris* (Gao et al. 2016a). Meanwhile, cellular protein levels in the presence of 4 μg N/L FNA were lower than that of control cultures due to the inhibition of culture growth (Figure 1B). However, an unexpected high cellular protein level (4 pg/cell) was detected when exposed to a FNA level of 8 μg N/L for 8 h and this protein level decreased to about 2 pg/cell at 12 h (Figure 1B). Extremely low levels of live cells and characteristics of protein stability could account for these outlier cellular protein values at 8 h and 12 h treatment with 8 μg N/L. Otherwise, indications are that the total protein levels per live cell was relatively stable in the viable cells regardless of the FNA level (Figure 1B).

The proteome response of *D. vulgaris* to different levels of FNA exposure

To assess response dynamics of *D. vulgaris* grown in different levels of FNA, whole cell quantitative proteome analyses were conducted at three different treatment periods of 2, 8 and 12 h. A total of 863 unique proteins were identified within the IDA library with a false detection rate of 0.01. The number of significantly different (adjust p value < 0.001) expressed proteins was determined between pairwise comparisons of the *D. vulgaris* cultures treatment with different FNA levels (1.0, 4.0 and 8.0 μg N/L) at different treatment time (2, 8, and 12 h) (Table 1).

Differentially expressed proteins relevant to metabolism

Proteins differentially expressed relevant to metabolism in the presence of FNA were determined (Table 2). In the presence of 1.0 μg N/L FNA at all incubation time points and 2 h after different FNA concentrations applied, all of the proteins detected relevant to lactate oxidation and sulfate reduction showed no change. In contrast, Proteins involved in nitrite reduction showed increased expression levels at all three incubation periods in the presence of all FNA concentrations (Table 2). These include cytochrome c nitrite reductase (DVU0625), the hybrid cluster protein (HCP) (DVU2543), and an iron-sulfur cluster-binding protein (DVU2544) (Table 2). HCP was one of the highest expressed proteins in the FNA-treated cultures. This strongly coincides with a transcriptome investigation of *D. vulgaris* exposed to FNA (Gao et al. 2016a) and implicates the important role played by HCP in defense to FNA stress. Additionally, proteins involved in sulfate reduction and lactate oxidation pathways (Table 2) showed no change compared to control cultures, implying that 1.0 μg N/L FNA had little effect on sulfate reduction and lactate oxidation pathways. This is reflected from the fact that this level of FNA caused no obvious inhibition effect on cell growth, sulfate reduction, and lactate oxidation as previously reported (Gao et al. 2016a).

In comparison, many proteins involved in metabolism including sulfate reduction and lactate oxidation were also differentially expressed with FNA concentrations of 4.0 and 8.0 μg N/L. Adenylyl-sulfate reductase (DVU0846) and sulfate adenylyltransferase (DVU1295) for sulfate reduction (Table 2) showed stable increased expression at either 8 h and/or 12 h incubations with FNA levels 4.0 and 8.0 μg N/L when the sulfate reduction activity was still very low as previously reported (a et al. 2016). This can be explained by the fact that the culture growth started to recover respiration at 8 h incubation at 4.0 μg N/L starting FNA when measured FNA level lowered to around 2.0 μg N/L (Gao et al. 2016a). For starting FNA concentration of 8.0 μg N/L, it is possibly because DVU0846 and DVU1295 were expressed by the remaining viable cultures to perform the

sulfate reduction at 12 h incubation after FNA addition. In comparison, with a starting FNA level at 4.0 μg N/L the heterodisulfide reductase (DVU0850) that performs sulfite reduction had reduced expression at 8 h and no change was observed at 12 h, when FNA concentrations had reduced to around 2.0 μg N/L (Table 2) (Gao et al. 2016a). This demonstrates that heterodisulfide reductase (DVU0850) expression was inhibited by FNA and the approximate inhibition threshold is around 2.0 μg N/L. These observations also indicate that FNA inhibit the expression of DVU0850 rather than DVU0846 and DVU1295 in *D.vulgaris*, and the energy generation by sulfate reduction was down regulated as long as 12 h incubation in the presence of 4 and 8 μg/L.

In agreement with sulfate reduction, several proteins involved in lactate oxidation in the presence of 4.0 and 8.0 μg N/L showed different expression. These proteins include pyruvate ferredoxin oxidoreductase (DVU1569), alcohol dehydrogenase (DVU2201), formate dehydrogenase (DVU2482), and a *luo* operon uncharacterized protein (DVU3032) and an iron-sulfur cluster-binding protein (DVU3033) (Table 2). DVU1569 and DVU2201 showed decreased expression at 8 h incubation while DVU3032 and DVU3033 increased their expression at 8 h and 12h after FNA addition. Elements of the *luo* (for lactate utilization operon) operon are reported to function in lactate oxidation in *D. vulgaris* (Vita et al. 2015), and DVU3032 and DVU3033 are part of *luo* operon. Additionally, ATP synthesis protein (DVU0775) and electron transfer protein HMC (DVU0535) (Table 2) also showed increased expression level at 8 h and/or 12 h with FNA level 4.0 and/or 8.0 μg N/L, indicating the possible metabolic activity recovery of *D. vulgaris* cultures which coincided with the protein expression dynamics in sulfate reduction and lactate oxidation. However, except with the occurrence of nitrite reduction, sulfate reduction and lactate oxidation activity were quite limited at 12 h after adding starting FNA concentrations of 4.0 and 8.0 μg N/L (Gao et al. 2016a). For starting FNA concentration of 4.0 μg N/L, at 12 h incubation after FNA addition, the measured FNA level decreased to approximately 2.0 μg N/L when the inhibition effect on sulfate reduction and lactate oxidation is limited. Therefore, it seems that by then *D. vulgaris* cultures were starting to recover their growth. However, for starting FNA concentration of 8.0 μg N/L at 12 h incubation, albeit on FNA level higher than 4.0 μg N/L, higher expression of proteins involved in sulfate reduction and lactate oxidation still occurred. This could be explained by the possible occurrence of “persister” cells which are going to develop or have developed the resistance in response to this high level of FNA. The about 5% live cells when exposed to starting FNA level of 8.0 μg N/L detected by LIVE/DEAD staining also support this (Gao et al. 2016a). In comparison, transcriptomics results described previously demonstrated the down regulation of all the genes

involved in sulfate and lactate reduction. This could be explained in that the transcriptome was only examined at 1 h after 4.0 μg N/L FNA addition (Gao et al. 2016a).

In addition, more proteins involved in carbon metabolism, including glyceroldehyde-3-phosphate dehydrogenase (DVU0565), sugar dehydratase (DVU0448), 2-oxoglutarate oxidoreductase (DVU3348), and pyruvate flavodoxin-ferredoxin oxidoreductase (DVU3349) (Table 2) exhibited decreased protein abundance in the presence of 4.0 μg N/L at 8 h incubation. This suggests that the carbon metabolism was severely inhibited by 4.0 μg N/L after FNA addition. Moreover, the expression of protein DVU0263 for acidic cytochrome c3 and DVU0266 for uncharacterized protein which is proposed as a respiratory complex in the cell membrane of *D. vulgaris* (Walian et al. 2012), was down regulated in the presence of 4.0 and 8.0 μg N/L FNA over incubation, further supporting that FNA inhibited the respiration activity of *D. vulgaris*.

Proteins differentially expressed relevant to protein synthesis

As is the same case we observed in proteins relevant to metabolism, the levels of proteins involved in protein synthesis showed no significant changes in the presence of 1.0 μg N/L FNA and at 2 h incubation for all the other FNA concentrations (4.0 and 8.0 μg N/L) (Table 3). Of total 53 proteins identified, 5 of them showed increased expression at 8 h and/or 12 h incubation in the presence of 4.0 and 8.0 μg N/L. These proteins include 50S ribosomal protein L15 (DVU1322), 50S protein ribosomal protein L17 (DVU1330), 50S ribosomal protein L32 (DVU1209), 30S ribosomal protein S2, and 30S ribosomal protein S6 (Table 3). Increased expression in these proteins coincided with the increased protein abundance in sulfate reduction and lactate oxidation in the presence of 4.0 and 8.0 μg N/L FNA at 8 and 12 h treatment.

Several proteins (e.g. DVU2981 for 2-isopropylmalate synthase and DVU3168 for Glutamate-1-semialdehyde 2,1-aminomutase) involved in amino acid biosynthesis started to show increased protein abundance in the presence of 4.0 and 8.0 μg N/L at 8 h and 12 h incubation. This observation is consistent with the protein synthesis protein at which the increased protein expression occurred (Table 3).

Evidence of oxidative stress in response to FNA exposure

FNA is proposed to exert the oxidative stress to *D. vulgaris* and this was confirmed by cellular redox measurement in the presence of different FNA levels compared to control cultures (no FNA addition) (Gao et al. 2016a). Surprisingly, this study revealed that in the presence of FNA, only two proteins that are proposed to be involved in oxidative stress were more expressed than control

cultures with FNA concentrations 4.0 and 8.0 μg N/L (Table 4). These two proteins are DVU0772 annotated as uncharacterised protein which is part of the PerR regulon and DVU3212 for pyridine nucleotide-disulfide oxidoreductase. The PerR regulon is predicted to be involved in oxidative stress (Mukhopadhyay et al. 2007). Of the 5 PerR regulon members we detected by SWATH-MS quantitative analysis (DVU0772 for conserved hypothetical protein, DVU2247 for alkyl hydroperoxide reductase subunit C-like protein, DVU3094 for rubrerythrin, DVU3093 for rubredoxin-type Fe(Cys)4 protein, and DVU2318 for rubrerythrin), only protein DVU0772 had significantly increased expression in the presence of high levels of FNA at 8 h and 12 h incubation while other proteins either showed decreased expression or no change. This indicates that DVU0772 plays a critical role in resisting oxidative stress caused by FNA.

In addition to PerR regulon members, rubredoxin including DVU3183 for desulfoferrodoxin, DVU3184 for rubredoxin, DVU3185 for rubredoxin-oxygen oxidoreductase, and DVU3212 for pyridine nucleotide-disulfide oxidoreductase have been suggested to be involved in the oxygen defence mechanism of *D. vulgaris* (Chhabra et al. 2011). It was recently demonstrated that DVU3183 and DVU3185 play important roles under aerobic and anaerobic conditions respectively (Wildschut et al. 2006). DVU3212 is suggested to have a flavin monoculeotide (FMN) cofactor that reduces oxygen to hydrogen peroxide and transfers electrons to adenylylphophosulfate (APS) reductase from NADH, indicating DVU3212 plays a role in both oxygen defence and sulfate reduction (Chen et al. 1994). However, under normal conditions DVU3212 is not found to interact with energy metabolism proteins to a significant degree although it is isolated from the energy metabolism network of *D. vulgaris* (Chhabra et al. 2011). The evidence infers that the primary function of DVU3212 is for defending oxidative stress in *D. vulgaris* (Chhabra et al. 2011). In our study, protein DVU3184 was not detected by SWATH-MS analysis. We observed increased protein levels for DVU3212 in the presence of 4.0 and 8.0 μg N/L at 8 h and 12 h incubation while decreased protein levels/no change for DVU3183 and DVU3185 in the presence of FNA. These results suggest that it is DVU3212 is critical to resist the oxidative stress caused by FNA/RNS rather than DVU3183 and DVU3185.

It should be noted that DVU1228 for thiol peroxidase which accounts for the peroxidase activity in vivo (Brioukhanov et al. 2010; Redding et al. 2006) showed decreased protein levels in the presence of FNA, in agreement with the fact that FNA increased the cellular thiol levels with FNA stress as previously described in *Pseduomonas aeruginosa* PAO1 and *D. vulgaris* (Gao et al. 2016a; Gao et al. 2016b).

Other protein expression dynamics resulting from the FNA exposure

Apart from the proteins aforementioned in three main aspects (metabolism, protein synthesis and oxidative stress), many other proteins showed different expression levels in the presence of different FNA levels. In the presence of 1.0 μg N/L DVU0004 for DNA gyrase subunit A, DVU0042 for RNA methyltransferase, DVU3199 for nucleoid-associated protein, DVU0132 for CRISPR-associated protein, and DVU0146 for uncharacterized protein were observed to have significant higher expression during early exposure to FNA (Table 5). The increased expression of proteins DVU0004, DVU0042 and DVU3199 involved in the DNA and RNA biosynthesis, indicates that *D. vulgaris* enhanced its DNA and RNA replication at low FNA exposure levels. DVU2929 for DNA-directed RNA polymerase subunit beta displayed decreased expression levels with 4.0 μg N/L FNA, suggesting the inhibition of RNA biosynthesis at higher levels of FNA, which coincided with results from previous studies in *P. aeruginosa* and *D. vulgaris* when exposed to FNA (Gao et al. 2016a; Gao et al. 2016b).

DVU2108 belongs to the Orange Protein family (ORP) (Neca et al. 2016)and DVU2105 for uncharacterized protein in *D. vulgaris* exhibited declined protein levels only in the presence of 8.0 μg N/L at 12 h incubation. This complex is proposed to be involved in cell division of this organism. In *D. vuglaris*, there are two *orp* gene clusters including DVU2103-DVU2104-DVU2105 (*orp2*) and DVU2107-DVU2108-DVU2109 (*orp1*) which encode for a protein complex, the absence of which induces aberrant cellular morphology. Down regulation of protein DVU2108 and DVU2105 implies that high FNA levels cause cell morphology change. However, there is no experimental evidence until now to support this. Protein DVU2569 for peptidyl-prolyl cis-trans isomerase, involved in cell wall biosynthesis (Stolyar et al. 2007), was found to be down regulated in the presence of 4.0 and 8.0 μg N/L FNA at 8 h and 12 h incubation. This implicates a pause in cell wall synthesis in response to the stress, which is also reported in the observation of *D. vulgaris* with alkaline stress (Stolyar et al. 2007). Up regulation of several proteins involved in periplasmic binding, transport, and excretion such as DVU1260 for outer membrane protein P1, DVU1343 for cation ABC transporter, and DVU1612 for ACT domain protein occurred in cultures when exposed to 4.0 and 8.0 μg N/L FNA.

Several universal stress proteins (DVU0261, DVU0423, and DVU1030) in *D. vulgaris* had different expression levels with FNA exposure. DVU0261 showed decreased expression levels with the increased FNA concentration and incubation time, concurrently DVU0423 showed almost no

change while DVU1030 exhibited increased expression levels (Table 5). There is a study reporting that DVU1030 is a stasis induced protein (Clark et al. 2006), indicating FNA changed the cultures from active status to stationary phase. It can be inferred that DVU0423 and DVU1030 contribute to dealing with the FNA stress in *D. vulgaris*. DVU2441 codes for a heat shock protein and had increased protein levels in the presence of 4.0 and 8.0 μg N/L FNA. The response to heat shock represents a protective and homeostatic response which assists folding nascent proteins and repairing damaged proteins (Chhabra et al. 2006). This indicates protein damage to the cultures occurred in the presence of FNA. In comparison, another heat shock protein DVU0811 for chaperone protein DnaK (Chhabra et al. 2006) showed decreased abundance at 12 h in the presence of 8.0 μg N/L FNA with no change at other FNA concentrations and incubation time.

In addition, many uncharacterized and hypothetical proteins (DVU0410, DVU0671, DVU1176, DVU1241, DVU2105, DVU2427, DVU4006, and DVUA202) displayed changed expression levels when exposed to FNA (Table 5). However, the detailed function of these proteins in response to FNA stress is not clear and needs further investigations, especially DVU1241 possibly encoding the homology cupin family protein which exhibited the highest increased protein expression levels in all FNA concentrations.

Discussion

FNA is a promising antimicrobial agent in wastewater treatment and there is increasing investigations focusing on its application to inhibit/kill SRB in sewers thereby avoiding sewer corrosion (Jiang et al. 2011; Jiang et al. 2013). However, the underlining mechanism of how SRB responds to FNA over time is one of the important factors to be considered to better the FNA application in wastewater treatment. In this study, the protein dynamics in the presence of different levels of the antimicrobial agent FNA was determined in the model SRB *D. vulgaris*. For the first time we applied a quantitative SWATH-MS whole genome proteome approach to detect and compare the protein dynamics in the presence of different levels of FNA. Our findings of the proteomics analysis for the first time unravelled the significant differences in proteins level changes with different FNA levels and revealed the multiple responses and detoxification mechanisms of *D. vulgaris* in response to FNA stress. Additionally, SWATH-MS analysis is quantitative and enabled a relative comparison of protein abundance between our samples in the presence of different FNA levels. Using this technique we determined the protein dynamics with different FNA levels and these responses were largely in agreement with the growth profiles and physiological responses as previously described (Gao et al. 2016a). Consequently, the aforementioned protein extraction and

SWATH-MS for quantitative proteomic analysis were useful for detection of bacterial responses to environmental change.

High expression of gene DVU2543 for the HCP in *D. vulgaris* has been reported previously in response to nitrite/FNA exposure (Gao et al. 2016a; Haveman et al. 2004; He et al. 2006) HCP isolated from *E. coli* demonstrated its capability for the reduction of hydroxylamine with production of ammonium (Wolfe et al. 2002). In other studies, HCP and rebredoxin oxygen oxidoreductases (ROO1 and ROO2) in *D. vulgaris* were demonstrated to play a role in NO protection and contributed to the survival of *D. vulgaris* during macrophage infection (Figueiredo et al. 2013). Therefore, the enzyme is thought to be functioning for either reduction of RNS (the hydroxylamine reductase activity) or for reduction of reactive oxygen species (Aragao et al. 2008). HCP protein (DVU2543) was one of the most highly expressed proteins in this proteomics study at all treatment times with all FNA concentrations. This agrees with transcriptomics results conducted at no more than 2.5 h after FNA addition as previously reported (Gao et al. 2016a; Haveman et al. 2004; He et al. 2006). This all supports that DVU2543 is critical for either responding to oxidative stress or/and nitrite reduction when exposed to FNA thereby contributing to release FNA stress in *D. vulgaris*. It is previously reported that the cellular redox of *D. vulgaris* became more oxidised during FNA exposure and DVU2543 is the most regulated gene with FNA stress (Gao et al. 2016a). While the enzyme has not been characterised in *D. vulgaris*, one suggestion is that the HCP is acting similarly or in conjunction with NrfA to detoxify the high levels of nitrite.

In addition, in this proteomics study most of the typical proteins responsible for oxygen-related oxidative stress in *D. vulgaris* over incubation such as rubredoxin oxygen oxidoreductases (DVU3093 and DVU3094) showed either no change or reduced expression when exposed to FNA except DVU0772 (part of PerR regulon) and DVU3212 (Table 4). Examination of the responses of *D. vulgaris* to other stress conditions reveals that the up regulation of the PerR regulon takes place not only under oxygen stress, but also under nitrate (He et al. 2010), nitrite (He et al. 2006), salt (Mukhopadhyay et al. 2006; Zhou et al. 2013), and heat stress (Chhabra et al. 2006), suggesting that the response of the PerR regulon may not be specifically linked to oxidative stress. Although there is suggestion that DVU2543 is responsible for nitrosative and/or oxidative stress in *D. vuglaris* (Aragao et al. 2008), the specific function of DVU2543 remains unknown and needs further investigation.

The energetic consequences caused by FNA stress could be considered as the potential mechanisms contributing to the growth inhibition and killing effect of *D. vulgaris* by FNA. Indeed, our results imply that some of the key proteins with functions in energy metabolism exhibited decreased expression when exposed to FNA. These proteins include heterodisulfide reductase (DVU0850) which catalyses the reduction of sulfite to sulfide, formate dehydrogenase (DVU2482) which is involved in carbon metabolism, electron transport complex protein RnfC (DVU2792) which plays a part in electron transfer for respiration, pyruvate ferredoxin oxidoreductase (DVU1569), and alcohol dehydrogenase (DVU2201). These events implicate an inhibition in sulfate reduction, lactate oxidation and electron transfer pathway, especially in the presence of 4.0 μg N/L FNA at 8 h incubation. Interestingly, several proteins consisting of adenylyl-sulfate reductase (DVU0846), sulfate adenylyltransferase (DVU1295), part of the *luo* operon uncharacterized protein (DVU3032) and iron-sulfur cluster-binding protein (DVU3033) had increased expression after exposure to 4.0 and 8.0 μg N/L FNA for 8 h. This suggests that the sulfate reduction pathway (from sulfite to hydrogen sulfide) and the lactate oxidation pathway (from pyruvate to acetate) were inhibited by FNA possibly contributing to the growth inhibition and cell death, in agreement with the lowered actual activities determined (Gao et al. 2016a). Given the known toxicity of FNA on SRB, growth inhibition and cell death caused by FNA could be further confined to inhibition of sulfite reduction.

In addition to the protein expression changes involved in respiration, several proteins which are responsible for protein synthesis showed no change at 2 h incubation and increased abundance at 8 h and 12 h incubation when exposed to 4.0 and 8.0 μg N/L FNA. In comparison, the severe down regulation of the genes involved in protein synthesis was observed in the previous transcriptomics study (Gao et al. 2016a). This discrepancy between transcriptomics and proteomics could possibly be explained by the fact that the ribosomes are probably preserved in an inactive state as suggested by the transcriptomics data, and these inactive state ribosomes are still being detected by the proteomic analyses. There is also a possibility that the initial down regulation of the protein synthesis genes was alleviated over incubation time with the occurrence of nitrite reduction which resulted in FNA levels lowered to around 2.0 μg N/L for starting FNA level 4.0 μg N/L, especially at 8 and 12 h when the culture regrowth was observed (Gao et al. 2016a). There is one possibility that the changes of proteins relevant to protein synthesis could be the corresponding response to decreased activities in lactate oxidation and sulfate reduction (Gao et al. 2016a) rather than the direct effect of FNA. This result is consistent with what we observed in previous studies in *Pseudomonas aeruginosa* PAO1 and *D. vulgaris* by using whole genome transcriptome analysis suggesting that proteins involved in protein synthesis are not the direct targets of FNA (Gao et al.

2016a; Gao et al. 2016b). There is also another possibility here that *D. vulgaris* are developing adaption to FNA exposure since the continued protein synthesis at low ATP levels was documented to enable cell adaption during energy limitation (Jewett et al. 2009), which matched the situation in this study where exposed FNA caused the lowered ATP generation in *D. vulgaris* cultures (Gao et al. 2016a).

In summary, the proteomics results reveal that *D. vulgaris* cells initiate a coordination of differential protein expression allowing the alleviation of nitrite stress by nitrite reduction. The proteomics response dynamics to increasing FNA levels seems logical. Firstly, proteins involved in nitrite reduction especially the HCP (DVU2543) were highly expressed with all FNA concentrations at all treatment times; secondly, FNA exposures at 4.0 and 8.0 μg N/L initially led to inhibition of sulfate reduction (from sulfite to hydrogen sulfide) and lactate oxidation (from pyruvate to acetate). Subsequently, these inhibition effects seem to diminished which can be deduced from the increased protein levels involved in sulfate reduction and lactate oxidation at increased exposure times at high FNA levels. Lastly, the levels of proteins involved in protein synthesis do not change much and could possibly be explained by the preservation of ribosomes as suggested by the previous transcriptomic data. In this study, we further emphasized the importance of the HCP protein in resisting FNA stress, however, further mutant studies and physiological assays are strongly required to elucidate the role HCP played in *D. vulgaris* during nitrite stress.

Acknowledgment

We acknowledge the Australian Research Council for funding support through project DP120102832 (Biofilm Control in Wastewater Systems using Free Nitrous Acid - a Renewable Material from Wastewater) and we thank scholarship support for Shu-Hong Gao from the China Scholarship Council.

References

Anthonisen A.C., Loehr R.C., Prakasam T.B., Srinath E.G. 1976. Inhibition of nitrification by ammonia and nitrous acid. *Journal of the Water Pollution Control Federation,* 48, 835-852.

Aragao D., Mitchell E.P., Frazao C.F., Carrondo M.A., Lindley P.F. 2008. Structural and functional relationships in the hybrid cluster protein family: structure of the anaerobically purified hybrid cluster protein from *Desulfovibrio vulgaris* at 1.35 angstrom resolution. *Acta Crystallographica Section D-Biological Crystallography,* 64, 665-674.

Brioukhanov A.L., Durand M.C., Dolla A., Aubert C. 2010. Response of *Desulfovibrio vulgaris* Hildenborough to hydrogen peroxide: enzymatic and transcriptional analyses. *FEMS Microbiology Letters,* 310, 175-181.

Chen L., Le Gall J., Xavier A.V. 1994. Purification, characterization and properties of an NADH oxidase from *Desulfovibrio vulgaris* (Hildenborough) and its coupling to adenylyl phosphosulfate reductase. *Biochemical and Biophysical Research Communications,* 203, 839-844.

Chhabra S.R., He Q., Huang K.H., Gaucher S.P., Alm E.J., He Z., Hadi M.Z., Hazen T.C., Wall J.D., Zhou J., Arkin A.P., Singh A.K. 2006. Global analysis of heat shock response in *Desulfovibrio vulgaris Hildenborough*. *Journal of Bacteriology,* 188, 1817-1828.

Chhabra S.R., Joachimiak M.P., Petzold C.J., Zane G.M., Price M.N., Reveco S.A., Fok V., Johanson A.R., Batth T.S., Singer M., Chandonia J.M., Joyner D., Hazen T.C., Arkin A.P., Wall J.D., Singh A.K., Keasling J.D. 2011. Towards a Rigorous Network of Protein-Protein Interactions of the Model Sulfate Reducer *Desulfovibrio vulgaris* Hildenborough. *PloS one,* 6, e21470.

Choi M., Chang C.-Y., Clough T., Broudy D., Killeen T., MacLean B., Vitek O. 2014. MSstats: an R package for statistical analysis of quantitative mass spectrometry-based proteomic experiments *Bioinformatics,* 30, 2524-2526.

Clark M.E., He Q., He Z., Huang K.H., Alm E.J., Wan X.F., Hazen T.C., Arkin A.P., Wall J.D., Zhou J.Z., Fields M.W. 2006. Temporal transcriptomic analysis as *Desulfovibrio vulgaris* Hildenborough transitions into stationary phase during electron donor depletion. *Applied and Environmental Microbiology,* 72, 5578-5588.

Fang F.C. 2004. Antimicrobial reactive oxygen and nitrogen species: concepts and controversies. *Nature reviews. Microbiology,* 2, 820-832.

Figueiredo M.C., Lobo S.A., Sousa S.H., Pereira F.P., Wall J.D., Nobre L.S., Saraiva L.M. 2013. Hybrid cluster proteins and flavodiiron proteins afford protection to *Desulfovibrio vulgaris* upon macrophage infection. *Journal of Bacteriology,* 195, 2684-90.

Gao S.H., Fan L., Peng L., Guo J., Agulló-Barceló M., Yuan Z., Bond P.L. 2016b. Determining multiple responses of *Pseudomonas aeruginosa* PAO1 to an antimicrobial agent, free nitrous acid. *Environmental science & technology,* 50, 5305-5312.

Gao S.H., Fan L., Yuan Z., Bond P.L. 2015. The concentration-determined and population-specific antimicrobial effects of free nitrous acid on *Pseudomonas aeruginosa* PAO1. *Applied Microbiology and Biotechnology,* 99, 2305-2312.

Gao S.H., Ho J.Y., Fan L., Richardson D.J., Yuan Z., Bond P.L. 2016a. Antimicrobial effects of free nitrous acid on *Desulfovibrio vulgaris*: implications for sulfide induced concrete corrosion *Applied and Environmental Microbiology,* DOI AEM.01655-16.

Haveman S.A., Greene E.A., Stilwell C.P., Voordouw J.K., Voordouw G. 2004. Physiological and gene expression analysis of inhibition of *Desulfovibrio vulgaris* Hildenborough by nitrite. *Journal of Bacteriology,* 186, 7944-7950.

Heidelberg J.F., Seshadri R., Haveman S.A., Hemme C.L., Paulsen I.T., Kolonay J.F., Eisen J.A., Ward N., Methe B., Brinkac L.M., Daugherty S.C., Deboy R.T., Dodson R.J., Durkin A.S., Madupu R., Nelson W.C., Sullivan S.A., Fouts D., Haft D.H., Selengut J., Peterson J.D., Davidsen T.M., Zafar N., Zhou L., Radune D., Dimitrov G., Hance M., Tran K., Khouri H., Gill J., Utterback T.R., Feldblyum T.V., Wall J.D., Voordouw G., Fraser C.M. 2004. The genome sequence of the anaerobic, sulfate-reducing bacterium *Desulfovibrio vulgaris* Hildenborough. *Nature Biotechnology,* 22, 554-559.

He Q., He Z.L., Joyner D.C., Joachimiak M., Price M.N., Yang Z.K., Yen H.C.B., Hemme C.L., Chen W.Q., Fields M.W., Stahl D.A., Keasling J.D., Keller M., Arkin A.P., Hazen T.C., Wall J.D., Zhou J.Z. 2010. Impact of elevated nitrate on sulfate-reducing bacteria: a comparative Study of *Desulfovibrio vulgaris*. *ISME Journal,* 4, 1386-1397.

He Q., Huang K.H., He Z., Alm E.J., Fields M.W., Hazen T.C., Arkin A.P., Wall J.D., Zhou J. 2006. Energetic consequences of nitrite stress in *Desulfovibrio vulgaris* Hildenborough, inferred from global transcriptional analysis. *Applied and Environmental Microbiology,* 72, 4370-4381.

Jewett M.C., Miller M.L., Chen Y., Swartz J.R. 2009. Continued protein synthesis at low [ATP] and [GTP] enables cell adaptation during energy limitation. *Journal of Bacteriology,* 191, 1083-1091.

Jiang G., Gutierrez O., Yuan Z. 2011. The strong biocidal effect of free nitrous acid on anaerobic sewer biofilms. *Water Research,* 45, 3735-3743.

Jiang G., Keating A., Corrie S., O'halloran K., Nguyen L., Yuan Z. 2013. Dosing free nitrous acid for sulfide control in sewers: Results of field trials in Australia. *Water Research,* 47, 4331-4339.

Kappler U., Nouwens A.S. 2013. The molybdoproteome of *Starkeya novella*--insights into the diversity and functions of molybdenum containing proteins in response to changing growth conditions. *Metallomics,* 5, 325-334.

Karp P.D., Paley S.M., Krummenacker M., Latendresse M., Dale J.M., Lee T.J., Kaipa P., Gilham F., Spaulding A., Popescu L., Altman T., Paulsen I., Keseler I.M., Caspi R. 2010. Pathway

Tools version 13.0: integrated software for pathway/genome informatics and systems biology. *Briefings in Bioinformatics,* 11, 40-79.

Mukhopadhyay A., He Z., Alm E.J., Arkin A.P., Baidoo E.E., Borglin S.C., Chen W., Hazen T.C., He Q., Holman H.Y., Huang K., Huang R., Joyner D.C., Katz N., Keller M., Oeller P., Redding A., Sun J., Wall J., Wei J., Yang Z., Yen H.C., Zhou J., Keasling J.D. 2006. Salt stress in *Desulfovibrio vulgaris* Hildenborough: an integrated genomics approach. *Journal of Bacteriology,* 188, 4068-4078.

Mukhopadhyay A., Redding A.M., Joachimiak M.P., Arkin A.P., Borglin S.E., Dehal P.S., Chakraborty R., Geller J.T., Hazen T.C., He Q., Joyner D.C., Martin V.J., Wall J.D., Yang Z.K., Zhou J., Keasling J.D. 2007. Cell-wide responses to low-oxygen exposure in *Desulfovibrio vulgaris* Hildenborough. *Journal of Bacteriology,* 189, 5996-6010.

Neca A.J., Soares R., Carepo M.S., Pauleta S.R. 2016. Resonance assignment of DVU2108 that is part of the Orange Protein complex in *Desulfovibrio vulgaris* Hildenborough. *Biomolecular NMR Assignments,* 10, 117-120.

O'Leary V., Solberg M. 1976. Effect of sodium nitrite inhibition on intracellular thiol groups and on the activity of certain glycolytic enzymes in *Clostridium perfringens*. *Applied and Environmental Microbiology,* 31, 208-212.

Pikaar I., Sharma K.R., Hu S., Gernjak W., Keller J., Yuan Z. 2014. Water engineering. Reducing sewer corrosion through integrated urban water management. *Science,* 345, 812-814.

Redding A.M., Mukhopadhyay A., Joyner D.C., Hazen T.C., Keasling J.D. 2006. Study of nitrate stress in *Desulfovibrio vulgaris* Hildenborough using iTRAQ proteomics. *Briefings in Functional Genomics & Proteomics,* 5, 133-143.

Stolyar S., He Q., Joachimiak M.P., He Z.L., Yang Z.K., Borglin S.E., Joyner D.C., Huang K., Alm E., Hazen T.C., Zhou J.Z., Wall J.D., Arkin A.P., Stahl D.A. 2007. Response of *Desulfovibrio vulgaris* to alkaline stress. *Journal of Bacteriology,* 189, 8944-8952.

Sun J., Hu S., Sharma K.R., Ni B.J., Yuan Z. 2014. Stratified microbial structure and activity in sulfide- and methane-producing anaerobic sewer biofilms. *Applied and Environmental Microbiology,* 80, 7042-7052.

Vadivelu V.M., Yuan Z., Fux C., Keller J. 2006. The inhibitory effects of free nitrous acid on the energy generation and growth processes of an enriched *Nitrobacter* culture. *Environ Sci Technol,* 40, 4442-4448.

Vita N., Valette O., Brasseur G., Lignon S., Denis Y., Ansaldi M., Dolla A., Pieulle L. 2015. The primary pathway for lactate oxidation in *Desulfovibrio vulgaris*. *Frontiers in Microbiology,* 6, 606.

Vizcaíno J.A., Côté R.G., Csordas A., Dianes J.A., Fabregat A., Foster J.M., Griss J., Alpi E., Birim M., Contell J., O'Kelly G., Schoenegger A., Ovelleiro D., Pérez-Riverol Y., Reisinger F., Ríos D., Wang R., Hermjakob H. 2013. The PRoteomics IDEntifications (PRIDE) database and associated tools: status in 2013. *Nucleic Acids Research,* 41, D1063-1069.

Vowinckel J., Capuano F., Campbell K., Deery M.J., Lilley K.S., Ralser M. 2013. The beauty of being (label)-free: sample preparation methods for SWATH-MS and next-generation targeted proteomics. *F1000Research,* 2, 272.

Walian P.J., Allen S., Shatsky M., Zeng L., Szakal E.D., Liu H., Hall S.C., Fisher S.J., Lam B.R., Singer M.E., Geller J.T., Brenner S.E., Chandonia J.M., Hazen T.C., Witkowska H.E., Biggin M.D., Jap B.K. 2012. High-throughput isolation and characterization of untagged membrane protein complexes: outer membrane complexes of *Desulfovibrio vulgaris*. *Journal of Proteome Research,* 11, 5720-5735.

Wildschut J.D., Lang R.M., Voordouw J.K., Voordouw G. 2006. Rubredoxin:oxygen oxidoreductase enhances survival of *Desulfovibrio vulgaris* Hildenborough under microaerophilic conditions. *Journal of Bacteriology,* 188, 6253-60.

Wolfe M.T., Heo J., Garavelli J.S., Ludden P.W. 2002. Hydroxylamine reductase activity of the hybrid cluster protein from *Escherichia coli*. *Journal of Bacteriology,* 184, 5898-5902.

Zahrt T.C., Deretic V. 2002. Reactive nitrogen and oxygen intermediates and bacterial defenses: unusual adaptations in *Mycobacterium tuberculosis*. *Antioxidants & redox signaling,* 4, 141-59.

Zhou A., Baidoo E., He Z., Mukhopadhyay A., Baumohl J.K., Benke P., Joachimiak M.P., Xie M., Song R., Arkin A.P., Hazen T.C., Keasling J.D., Wall J.D., Stahl D.A., Zhou J. 2013. Characterization of NaCl tolerance in *Desulfovibrio vulgaris* Hildenborough through experimental evolution. *The ISME Journal,* 7, 1790-1802.

Zhou A.F., Chen Y.Y.I., Zane G.M., He Z.L., Hemme C.L., Joachimiak M.P., Baumohl J.K., He Q., Fields M.W., Arkin A.P., Wall J.D., Hazen T.C., Zhou J.Z. 2012. Functional Characterization of Crp/Fnr-Type Global Transcriptional Regulators in *Desulfovibrio vulgaris* Hildenborough. *Applied and Environmental Microbiology,* 78, 1168-1177.

Zhou Y., Oehmen A., Lim M., Vadivelu V., Ng W.J. 2011. The role of nitrite and free nitrous acid (FNA) in wastewater treatment plants. *Water Research,* 45, 4672-4682.

Figure 1. Total protein levels per microliter of *D. vulgaris* culture in the presence of different FNA levels (control, 1.0, 4.0 and 8.0 µg/L) at different incubation time period (2, 8 and 12h) (A), and cellular protein levels per live cells of *D. vulgaris* when exposed to different levels of FNA (control, 1.0, 4.0 and 8.0 µg/L) with different treatment time period (2, 8 and 12h) (B).

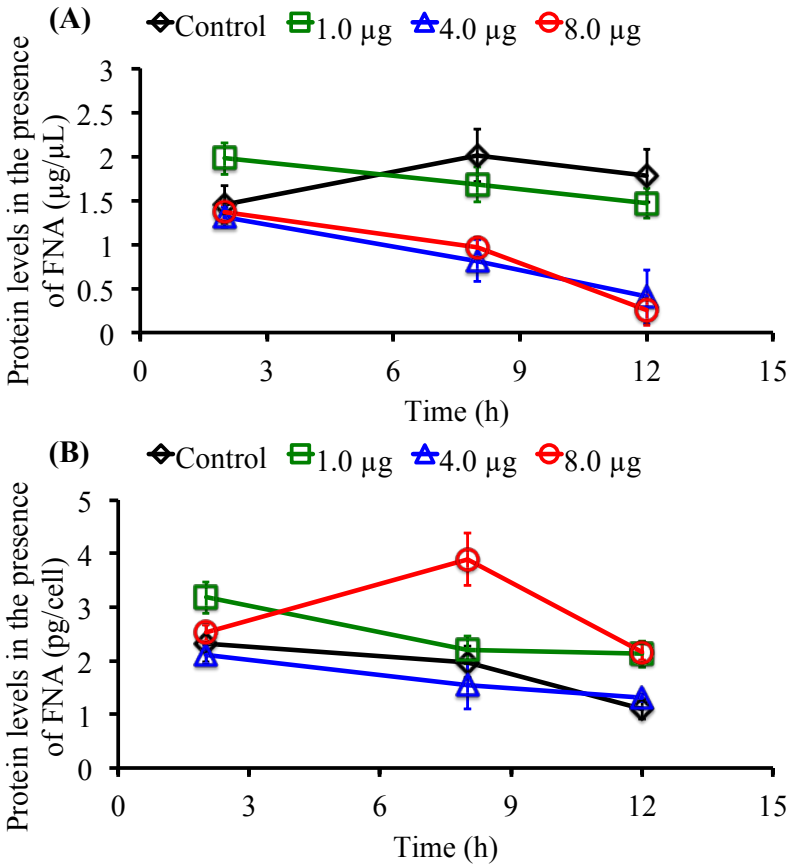

Table 1. Number of differentially expressed proteins between FNA-treated cultures (1.0, 4.0 and 8.0 μg N/L) and control cultures (no FNA addition) at different treatment period.

	FNA treatment time (hour)		
FNA levels (μg N/L)	2 h	8 h	12 h
1	7	4	4
4	4	43	43
8	4	21	64

Table 2. Proteins expression dynamics in the presence of different FNA concentrations relevant to metabolism

Gene ID	Gene name	1 μg vs Control			4 μg vs Control			8 μg vs Control		
		2h_LFC	8h_LFC	12h_LFC	2h_LFC	8h_LFC	12h_LFC	2h_LFC	8h_LFC	12h_LFC
Nitrite reduction										
DVU0625	**Cytochrome c-552 nitrite reductase**	0.39	0.99	0.68	0.09	-0.22	-0.37	0.14	-0.14	-0.29
DVU2543	**Hybrid cluster protein**	-0.22	5.37	4.05	2.94	4.51	3.81	1.73	3.72	3.09
DVU2544	**Iron-sulfur cluster-binding protein**	-0.23	4.6	3.93	2.43	3.2	3.66	1.35	1.93	2.61
Sulfate reduction										
DVU0263	Acidic cytochrome c3	0.84	0.58	0.28	-0.03	0.23	-0.45	0.23	-0.14	-0.9
DVU0266	Uncharacterized protein	0.81	-0.21	-0.3	-0.03	-0.5	-0.68	0.07	-0.38	-0.7
DVU0402	Sulfite reductase, dissimilatory-type subunit alpha	0.56	0.27	0.04	-0.04	0.19	0.14	-0.08	0.07	0.16
DVU0403	Sulfite reductase, dissimilatory-type subunit beta	0.56	0.02	0.03	0.05	-0.11	0.01	0.02	-0.05	-0.16
DVU0847	Adenylylsulphate reductase beta-subunit	0.21	0.27	-0.03	0.31	0.89	0.41	0.27	0.58	0.46
DVU0846	Adenylyl-sulphate reductase, alpha subunit	0.21	0.17	0.15	0	0.55	0.5	-0.05	0.39	0.49
DVU0848	Heterodisulfide reductase, putative	0.21	-0.09	0.01	-0.12	0.13	0.22	0.01	0.13	0.2
DVU0849	Heterodisulfide reductase, iron-sulfur-binding subunit, putative	0.21	-0.13	0.04	0.25	0.24	0.51	0.11	-0.06	0.55
DVU0850	**Heterodisulfide reductase, transmembrane subunit, putative**	0.2	-0.35	0.1	-0.36	-1.65	-0.54	0.34	-0.8	-0.98
DVU1287	Reductase, iron-sulfur binding subunit, putative	0.09	0.22	-1.61	-0.56	NA	0.31	-0.73	-0.21	0.78
DVU1295	Sulfate adenylyltransferase	0.09	0.2	0.11	-0.09	0.44	0.63	-0.23	0.38	0.55
DVU1597	Sulfite reductase, assimilatory-type	0	0.12	-0.05	-0.19	0	0.06	0.1	-0.14	-0.28
Lactate oxidation										
DVU0448	GDP-mannose 4,6-dehydratase	0.53	-0.25	-0.09	-0.2	-0.62	-0.41	-0.37	-0.31	-0.08
DVU0565	Glyceraldehyde-3-phosphate dehydrogenase	0.43	-0.27	-0.22	0.14	-0.78	-1.06	0.34	-0.55	-0.73
DVU0587	Formate dehydrogenase, alpha subunit, selenocysteine-containing	0.42	-0.13	0.27	0.21	-0.26	-0.08	0.47	0.05	0.22
DVU0588	Formate dehydrogenase, beta subunit, putative	0.41	0.08	0.25	0.19	-0.19	-0.09	0.32	-0.08	-0.07
DVU0589	Molybdopterin-guanine dinucleotide biosynthesis protein B, putative	0.41	-0.41	-0.19	-0.66	-1.62	-0.96	-0.14	-1.1	-1.24
DVU1569	**Pyruvate ferredoxin oxidoreductase, alpha subunit**	0.01	-0.28	0.03	0.15	-1.34	-0.53	0.34	-0.57	-0.67
DVU1570	Pyruvate ferredoxin oxidoreductase, beta subunit	0.01	0.11	0.08	0.15	-0.79	-0.89	0.22	-0.63	-0.77
DVU2201	Alcohol dehydrogenase, iron-containing	-0.1	-0.18	-0.21	0.3	-0.53	-0.67	0.51	-0.44	-0.78
DVU2451	L-lactate permease family protein	-0.17	0.05	-0.67	-0.01	0.02	-0.63	-0.06	-0.01	-0.45

DVU2482	Formate dehydrogenase, alpha subunit, selenocysteine-containing	-0.18	-0.06	-0.11	0.34	-0.52	-0.64	0.44	-0.31	-0.43
DVU3026	L-lactate permease family protein	-0.4	0.45	-0.1	-0.03	0.18	0.36	0.24	-0.26	0.26
DVU3028	Glycolate oxidase iron-sulfur subunit	-0.41	-0.43	-0.24	0.43	-0.42	-0.17	1.21	-0.49	-0.23
DVU3027	Glycolate oxidase, subunit GlcD	-0.41	-0.03	-0.1	0.24	-0.04	-0.05	-0.76	-0.43	-0.22
DVU3025	Pyruvate-ferredoxin oxidoreductase	-0.4	0.06	-0.11	0.11	0.12	-0.16	0.17	0.17	-0.18
DVU3029	Phosphate acetyltransferase	-0.41	0.22	-0.67	0.35	0.34	0.02	0.69	0.49	1.16
DVU3030	Acetate kinase	-0.42	-0.01	-0.13	-0.03	0.09	0.13	-0.15	0.1	0.26
DVU3032	Uncharacterized protein	-0.42	0.24	0.07	0.24	0.64	0.46	0.19	0.64	0.7
DVU3033	Iron-sulfur cluster-binding protein	-0.46	0.21	0.14	0.64	0.87	0.86	0.79	0.75	0.8
DVU3348	2-oxoglutarate/2-oxoacid ferredoxin oxidoreductase, subunit beta	-1.37	-0.24	-0.23	-0.18	-2.14	-0.72	-0.08	-0.74	-0.38
DVU3349	Pyruvate flavodoxin/ferredoxin oxidoreductase, thiamine diP-binding domain protein	-1.46	-0.26	-0.25	-0.34	-0.57	-0.3	-0.23	-0.43	-0.2
ATP synthesis										
DVU0777	ATP synthase subunit alpha	0.27	0.1	0.13	0.16	0.37	0.44	0.01	0.41	0.46
DVU0774	ATP synthase epsilon chain	0.28	-0.75	-1.38	-1.06	-0.4	-1.22	-0.65	-0.01	0.46
DVU0775	ATP synthase subunit beta	0.28	0.14	0.13	0.37	0.5	0.51	0.2	0.5	0.57
DVU0776	ATP synthase gamma chain	0.28	-0.14	0.14	0.28	-0.41	-0.18	0.37	-0.21	0.01
Electron transfer										
DVU0431	Ech hydrogenase, subunit EchD, putative	0.53	-0.37	-0.57	0.06	-0.87	NA	-0.27	-0.03	0.14
DVU0535	Protein DVU0535 (HMC operon ORF 2)	0.43	0.31	-0.2	0.93	0.85	1.68	0.22	0.97	2.3
DVU0536	High-molecular-weight cytochrome c	0.43	0.27	0.3	-0.42	-0.4	0.04	-0.8	-0.93	-0.99
DVU2792	Electron transport complex protein RnfC, putative	-0.27	-0.68	-0.23	-0.16	-1.02	-1.1	-0.61	-1.25	-0.7
Hydrogenases										
DVU1769	Periplasmic [Fe] hydrogenase large subunit	-0.02	0.09	-0.05	0.11	0.71	-0.01	0.28	-0.43	0.11
DVU1917	Periplasmic [NiFeSe] hydrogenase, small subunit	-0.05	0.13	-0.05	0.11	-0.08	-0.16	0.04	0.07	-0.11
DVU1918	Periplasmic [NiFeSe] hydrogenase, large subunit, selenocysteine-containing	-0.05	0.23	0.29	-0.01	0.05	0.19	0	0.06	0.03
DVU1921	Periplasmic [NiFe] hydrogenase small subunit 1	-0.06	0.08	-0.62	NA	0.27	-0.16	NA	NA	NA
DUV1922	Periplasmic [NiFe] hydrogenase, large subunit, isozyme 1	-0.06	0.43	0.05	-0.53	0.28	-0.4	-1.54	-1.49	-1.58
DVU2329	Hydrogenase accessory protein HypB	-0.13	-0.3	-0.3	-0.22	-0.4	-0.57	-0.64	-0.28	-0.34

Note: LFC of the detected proteins with adjusted q value less than 0.001 is shown in red in which proteins with LFC ≥0.5 or ≤-0.5 are defined as the differential expressed proteins in the presence of FNA, while LFC of the detected proteins with q value value less than 0.05 but larger than 0.001 is shown in blue. All others are the proteins with q value larger than 0.05.

Table 3. Proteins expression dynamics in the presence of different FNA concentrations relevant to protein synthesis and amino acid metabolism

Gene ID	Gene name	1 μg vs Control			4 μg vs Control			8 μg vs Control		
		2h_LFC	8h_LFC	12h_LFC	2h_LFC	8h_LFC	12h_LFC	2h_LFC	8h_LFC	12h_LFC
DVU0504	30S ribosomal protein S15	0.44	-2	2.34	-0.1	-0.08	2.35	-0.15	0.4	2.78
DVU0835	50S ribosomal protein L19	0.22	-0.44	-1.08	0.03	-1.62	-1.77	0.16	-0.67	-0.89
DVU0837	Ribosome maturation factor RimM	0.22	0.57	-0.05	-0.24	1.09	0.51	-0.48	0.86	0.2
DVU0839	30S ribosomal protein S16	0.22	0.08	0.01	-0.3	0.06	-0.56	-0.16	0.00	0.03
DVU0870	Ribosome-recycling factor (RRF)	0.19	-0.02	0.1	-0.62	0.76	-0.17	-0.2	1.00	0.46
DVU0874	30S ribosomal protein S2	0.19	-0.25	0.46	0.99	0.32	1.25	0.67	0.08	1.42
DVU0927	50S ribosomal protein L21	0.18	0.98	0.25	0.11	1.12	0.86	0.42	1.11	1.18
DVU0956	30S ribosomal protein S6	0.17	0.15	0.09	-0.43	0.81	0.93	0.75	0.65	1.32
DVU0957	30S ribosomal protein S18	0.17	0.13	-0.3	0.54	1.00	0.49	0.25	0.83	0.85
DVU0958	50S ribosomal protein L9	0.17	0.51	-0.17	0.07	1.39	0.8	1.08	0.75	0.86
DVU1209	**50S ribosomal protein L32**	0.12	1.13	0.8	-0.71	2.02	2.33	0.37	1.57	2.42
DVU1211	50S ribosomal protein L28	0.12	0.87	1.05	0.7	0.81	1.04	0.93	0.45	0.72
DVU1298	30S ribosomal protein S12	0.09	-0.17	-0.74	-0.61	-0.41	0.06	0.26	-0.31	-0.29
DVU1299	30S ribosomal protein S7	0.09	-0.35	0.04	0.04	-0.9	0.18	0.36	-0.26	-0.08
DVU1302	30S ribosomal protein S10	0.08	0.17	0.68	0.05	-0.24	0.54	0.14	0.31	0.57
DVU1303	50S ribosomal protein L3	0.08	0.42	0.28	-0.03	0.30	0.67	-0.06	-0.04	0.57
DVU1304	50S ribosomal protein L4	0.08	-0.25	0.78	-0.98	-0.58	0.23	0.39	0.33	1.86
DVU1305	50S ribosomal protein L23	0.08	-0.25	0.6	0.11	-0.73	1.17	1.6	0.24	0.78
DVU1306	50S ribosomal protein L2	0.08	0.28	0.17	0.12	0.23	0.65	0.24	0.28	0.61
DVU1307	30S ribosomal protein S19	0.08	0.15	-0.05	0.09	-0.27	-0.17	0.13	-0.17	-0.27
DVU1308	50S ribosomal protein L22	0.08	1.32	0.26	-0.32	0.35	0.50	-0.19	0.04	1.01
DVU1309	30S ribosomal protein S3	0.07	0.97	0.53	-0.03	1.88	1.33	-2.14	1.28	1.54
DVU1310	50S ribosomal protein L16	0.07	-0.42	-0.36	-1.24	0.35	1.02	-0.07	-0.23	1.94
DVU1312	30S ribosomal protein S17	0.07	0.5	-1.4	-0.08	-1.77	-0.13	0.23	-0.4	-0.05
DVU1313	50S ribosomal protein L14	0.07	0.17	0.3	-0.43	0.37	-0.05	0.47	0.18	0.01
DVU1315	50S ribosomal protein L5	0.07	-0.18	-0.48	-0.94	0.95	0.49	1.69	0.73	1.11

DVU1317	30S ribosomal protein S8	0.07	0.33	0.16	-0.17	0.65	0.82	0.41	0.99	0.67
DVU1318	50S ribosomal protein L6	0.07	0.72	1.71	-0.49	0.29	0.53	0.05	-1.21	0.89
DVU1319	50S ribosomal protein L18	0.06	0.26	0.12	-0.28	0.2	1.1	0.25	0.43	1.05
DVU1320	30S ribosomal protein S5	0.06	-0.31	0.53	-1.02	-0.4	0.03	-0.81	-0.05	0.2
DVU1322	50S ribosomal protein L15	0.06	0.57	0.22	-0.2	0.67	0.75	-0.12	0.45	0.74
DVU1326	30S ribosomal protein S13	0.06	0.22	-0.16	0.16	0.04	0	0.42	0.19	0.08
DVU1327	30S ribosomal protein S11	0.06	0.68	0.73	-0.2	0.02	0.84	0.35	-0.38	0.3
DVU1328	30S ribosomal protein S4	0.06	0.35	0.1	-0.47	0.83	0.98	0.5	0.9	1.07
DVU1330	50S ribosomal protein L17	0.05	0.25	0.13	-0.01	0.34	0.88	0.6	0.4	1.18
DVU1429	Ribosome-binding ATPase YchF	0.03	0.74	0.04	0.08	0.76	0.53	0.37	-0.5	0.22
DVU1469	Ribosomal protein S1, putative	0.02	0.08	-0.03	0.11	-0.19	-0.45	-0.01	-0.17	-0.46
DVU1574	50S ribosomal protein L25	0.01	-0.14	0.21	0	0.28	0.1	0.27	-0.88	0.16
DVU1618	Ribosomal silencing factor RsfS	0	0.13	-0.82	-1.11	-0.08	0.14	-0.72	0.41	0.98
DVU1792	30S ribosomal protein S21	-0.02	1.27	0.19	0.76	1.35	-0.76	1.89	-0.03	1.02
DVU1896	30S ribosomal protein S20	-0.04	0.74	0.96	-0.34	0.51	1.11	-0.1	0.43	1.27
DVU2339	Ribosomal protein L11 methyltransferase, putative	-0.14	-0.29	-0.19	0.69	0.15	0.5	0.35	-0.18	0.59
DVU2512	Ribosomal RNA small subunit methyltransferase H	-0.2	NA	-0.37	2.53	NA	0.41	1.8	NA	0.03
DVU2518	50S ribosomal protein L13	-0.2	1.43	0.32	-0.27	1.17	0.59	0.51	1.61	0.81
DVU2519	30S ribosomal protein S9	-0.2	0.11	-0.02	-0.1	-0.07	0.23	0.01	0.07	0.24
DVU2535	50S ribosomal protein L20	-0.21	0.55	-0.2	0.51	-1.12	-1.03	0.27	-1.18	-0.37
DVU2536	50S ribosomal protein L35	-0.21	-0.51	-1	-0.69	-0.62	-0.03	-0.24	-0.2	0.41
DVU2921	50S ribosomal protein L33	-0.31	0.13	-2.32	-1.3	0.33	-0.01	0.77	-0.23	-0.65
DVU2924	50S ribosomal protein L11	-0.32	0.85	-0.63	0.04	0.45	0.71	0.36	0.46	0.56
DVU2925	50S ribosomal protein L1	-0.32	0.63	0.16	-0.48	1.22	1.18	0.5	1.24	0.53
DVU2926	50S ribosomal protein L10	-0.32	-0.11	-0.28	-0.96	-0.61	-0.57	-1.43	-2.16	-1.8
DVU2927	50S ribosomal protein L7/L12	-0.33	0.16	-0.16	-0.01	0.15	0.04	-0.11	0.44	0.06
DVU2981	2-isopropylmalate synthase	-0.37	0.17	0.22	0.04	0.43	0.65	-0.11	0.32	0.33
DVU3150	Ribosomal protein S1	-0.61	0.07	0.07	0.04	0.14	0.1	-0.13	0.16	0.02
DVU3168	Glutamate-1-semialdehyde 2,1-aminomutase	-0.63	0.06	0.01	0.27	0.65	0.65	-0.05	0.63	0.55

Note: LFC of the detected proteins with adjusted q value less than 0.001 is shown in red in which proteins with LFC ≥0.5 or ≤-0.5 are defined as the differential expressed proteins in the presence of FNA, while LFC of the detected proteins with q value value less than 0.05 but larger than 0.001 is shown in blue. All others are the proteins with q value larger than 0.05.

Table 4. Proteins expression dynamics in the presence of different FNA concentrations relevant to oxidative stress

Gene ID	Gene name	1 μg vs Control			4 μg vs Control			8 μg vs Control		
		2h_LFC	8h_LFC	12h_LFC	2h_LFC	8h_LFC	12h_LFC	2h_LFC	8h_LFC	12h_LFC
DVU0019	Nigerythrin	2.32	0.21	0.27	0.21	0.23	0.23	-0.1	-0.26	-0.32
DVU0264	Ferredoxin, 4Fe-4S, putative	0.84	-0.18	-0.19	-0.09	-0.13	-0.27	-0.03	-0.11	-0.32
DVU0273	Uncharacterized protein	0.8	0.03	0.26	-0.41	-1.1	-0.57	-0.39	-0.23	-0.41
DVU0278	Glyoxalase family protein	0.72	0.52	0.53	-0.22	-0.39	-0.34	-0.17	-0.6	-0.55
DVU0305	Ferredoxin II	0.68	-0.05	-0.45	-0.01	-0.71	-0.42	-0.04	-0.31	-0.55
DVU0772	Uncharacterized protein	0.29	-1.27	0.45	0.73	2.91	3.12	0.18	1.67	2.69
DVU0995	ThiJ/PfpI family protein	0.16	0.01	0.2	-0.08	-0.32	-0.34	-0.09	-0.64	-0.72
DVU1228	Probable thiol peroxidase	0.11	-0.25	-0.11	-0.07	-0.71	-0.56	-0.06	-0.81	-0.9
DVU1397	Bacterioferritin	0.04	-0.19	-0.42	-0.01	0.13	-0.02	-0.07	-0.22	-0.42
DVU1457	Thioredoxin reductase, putative	0.02	0.39	0.37	-0.08	0.07	0.12	-0.11	0.04	0.07
DVU1568	Ferritin	0.01	-0.05	0.17	-0.17	-1.03	-0.76	-0.13	-1.16	-0.85
DVU1838	Thioredoxin-disulfide reductase	-0.03	0.2	-0.39	0	-0.04	-0.24	0.06	-0.11	-0.08
DVU1839	Thioredoxin	-0.03	0.08	0.02	0.07	-0.04	0.05	0.13	0.03	0.14
DVU1984	Peptide methionine sulfoxide reductase MsrA	-0.08	-0.53	0.64	-0.52	-0.2	-0.48	0.09	0.75	-0.24
DVU2247	Alkyl hydroperoxide reductase C	-0.12	0.31	0.2	-0.19	0.73	0.85	-0.42	0.59	0.72
DVU2318	Rubrerythrin, putative	-0.13	-0.45	-0.34	-0.25	-0.23	-0.12	-0.32	-0.51	-0.34
DVU2410	Superoxide dismutase, Fe-Mn family	-0.16	-0.48	0.41	0.15	-1.62	-0.29	-0.42	-1.26	-1.01
DVU2680	Flavodoxin	-0.25	0.98	0.71	0.13	0.84	0.52	-0.33	0.26	0.17
DVU3049	Hemerythrin family protein	-0.48	0.24	0.28	-0.24	-0.18	-0.11	-1.2	-0.27	-0.08
DVU3093	Rubredoxin	-0.55	0.05	-0.08	0.67	0.88	-0.26	0	-0.93	0.01
DVU3094	Rubrerythrin (Rr)	-0.55	-0.08	0.01	-0.19	-0.71	-0.51	-0.2	-0.77	-0.83
DVU3183	Desulfoferrodoxin (Dfx)	-0.64	-0.08	0.02	-0.13	-0.26	-0.32	-0.13	-0.41	-0.64
DVU3185	Rubredoxin-oxygen oxidoreductase	-0.64	-0.05	-0.18	-0.02	-0.35	-0.43	-0.04	-0.25	-0.37
DVU3212	Pyridine nucleotide-disulfide oxidoreductase	-0.73	0.25	0.16	0.33	0.63	0.81	0.21	0.82	1.01
DVU3276	Ferredoxin I	-0.98	-0.93	-0.77	0.15	-1.33	-2.01	-0.29	-1.7	-2.2
DVU3282	ADP-ribosylglycohydrolase family protein	-1.04	0.2	0.16	-0.17	0.18	0.06	-0.19	-0.07	-0.27
DVUA0091	Catalase	NA	-0.19	-0.19	-0.18	-0.39	-0.77	0.08	-0.44	-1.15

Note: LFC of the detected proteins with adjusted q value less than 0.001 is shown in red in which proteins with LFC ≥0.5 or ≤-0.5 are defined as the differential expressed proteins in the presence of FNA, while LFC of the detected proteins with q value value less than 0.05 but larger than 0.001 is shown in blue. All others are the proteins with q value larger than 0.05.

Table 5. Proteins expression dynamics in the presence of different FNA concentrations relevant to others

Gene ID	Gene name	1 µg vs Control			4 µg vs Control			8 µg vs Control		
		2h_LFC	8h_LFC	12h_LFC	2h_LFC	8h_LFC	12h_LFC	2h_LFC	8h_LFC	12h_LFC
1.0 µg N/L										
DVU0004	DNA gyrase subunit A	3.71	0.22	0.19	0.2	0	-0.64	-0.19	-0.52	-0.54
DVU0042	RNA methyltransferase	1.91	0.82	-0.16	0.53	1.29	0.77	-0.12	-0.05	0.55
DVU0419	Carboxynorspermidine/carboxyspermidine decarboxylase	0.54	-0.68	-0.27	-0.2	-0.87	-0.67	-0.49	-1.92	-0.93
DVU3199	Nucleoid-associated protein DVU3199	-0.7	0.45	1.19	0.42	0.58	0.68	0.29	0.63	0.62
DVU3228	Chemotaxis protein CheY	-0.76	-0.16	0.07	-0.14	-0.52	-0.47	0.43	-1.01	-0.24
DVUA0132	CRISPR-associated protein, TM1801 family	4.94	0.04	0.11	-0.35	-0.8	-0.49	0.05	-0.59	-1.19
DVUA0146	Uncharacterized protein	3.96	-1.19	0.08	-0.86	-0.38	0.56	-0.83	-1.96	-1.52
4.0 µg N/L										
DVU0034	DSBA-like thioredoxin domain protein	1.91	-0.39	0.08	-0.1	-1.12	-0.5	0.11	-0.58	-0.41
DVU0060	Efflux transporter, RND family, MFP subunit	1.82	-0.3	-0.16	-0.4	-0.79	-0.61	-0.17	-0.4	-0.54
DVU0417	Arginine decarboxylase	0.54	-0.33	-0.45	-0.38	-0.97	-0.84	-0.14	-0.75	-0.65
DVU0423	Universal stress protein family	0.53	0.21	0.17	0.55	0.42	0.42	0.03	0.18	0.11
DVU0854	NirD protein, putative	0.2	-0.41	-0.17	-0.07	-0.75	-0.65	0.07	-0.57	-0.43
DVU1176	Uncharacterized protein	0.13	-0.08	0	0.02	-0.52	-0.33	-0.08	-0.36	-0.35
DVU2093	ThiH protein	-0.09	-0.18	-0.12	-0.21	-1.88	-1.23	0.17	-0.79	-1.13
DVU3055	Ribonuclease, Rne/Rng family	-0.51	-0.05	-0.33	0.26	-1.77	-0.42	0.44	-0.51	-0.81
8.0 µg N/L										
DVU0319	NAD-dependent epimerase/dehydratase family protein	0.66	-0.19	0.01	0.35	-0.14	-0.34	0.27	-0.59	-0.43
DVU0353	Alcohol dehydrogenase, iron-containing	0.61	0.04	-0.02	-0.08	-0.24	-0.2	-0.08	-0.34	-0.54
DVU0418	Saccharopine dehydrogenase	0.54	-0.18	-0.39	-0.14	-0.47	-0.56	-0.14	-0.76	-1.32
DVU0664	Cysteine desulfurase	0.37	-0.11	-0.15	-0.23	-0.2	-0.27	-0.23	-0.19	-0.52
DVU0811	Chaperone protein DnaK (HSP70)	0.25	0.24	-0.11	-0.14	-0.32	-0.37	-0.13	-0.25	-0.68

DVU0857	Radical SAM domain protein	0.19	-0.21	0	-0.29	-0.31	-0.14	-0.35	-0.64	-0.45
DVU1382	HesB family selenoprotein	0.04	0.14	-0.07	-0.2	-0.18	-0.45	-0.16	-0.13	-0.6
DVU1864	DNA-binding protein HU, beta subunit, putative	-0.04	1.37	1.5	0.17	1.43	1.82	-0.54	1.49	2.56
DVU1878	Threonine aldolase, low-specificity	-0.04	-0.16	-0.08	-0.12	-0.6	-0.61	-0.52	-0.71	-0.68
DVU1937	Phosphonate ABC transporter, periplasmic phosphonate-binding protein, putative	-0.06	-0.07	0.01	0.01	-0.22	-0.38	0.11	-0.29	-0.84
DVU1951	Indolepyruvate oxidoreductase subunit IorA	-0.07	-0.3	-0.29	-0.6	-0.38	-0.12	-0.85	-0.38	-0.23
DVU2105	Uncharacterized protein	-0.09	-0.34	-0.4	-0.56	-1.02	-0.76	-0.89	-1.51	-1.62
DVU2108	MTH1175-like domain family protein	-0.1	-0.28	-0.2	-0.02	-0.6	-1.03	0.07	-0.81	-1.78
DVU2929	DNA-directed RNA polymerase subunit beta	-0.34	-0.18	0.14	-0.42	-0.52	-0.32	-0.58	-0.46	-0.89
DVU3065	AMP-binding enzyme family protein	-0.53	-0.25	-0.26	-0.26	-0.21	-0.27	-0.47	-0.33	-0.53
DVU3181	Phosphoribosylformylglycinamidine synthase subunit PurL	-0.64	0.02	-0.02	-0.06	-0.07	-0.16	-0.2	-0.2	-1.21
4.0 and 8.0 µg N/L										
DVU0007	Asparagine--tRNA ligase	2.98	-0.2	-0.21	-0.13	-0.54	-0.58	0.03	-0.29	-0.53
DVU0261	Universal stress protein family	0.85	-0.27	-0.19	-0.04	-0.62	-0.68	0.14	-0.42	-0.6
DVU0410	Uncharacterized protein	0.55	-0.24	-0.03	-0.18	-0.64	-0.76	-0.27	-0.34	-0.67
DVU0671	Uncharacterized protein	0.36	0.05	0.02	0.09	0.4	0.57	0.11	0.49	0.59
DVU1030	Universal stress protein	0.15	0.2	0.08	0.42	0.75	0.84	0.03	0.57	0.8
DVU1241	Uncharacterized protein	0.11	5.48	4.26	3.63	5.1	4.43	3.28	4.99	4.13
DVU1257	RNA-binding protein	0.1	0.01	-0.15	-0.44	-1.04	-0.95	-0.53	-0.65	-0.74
DVU1260	Outer membrane protein P1, putative	0.1	0.11	0.14	0.16	0.4	0.43	0.01	0.53	0.63
DVU1343	Cation ABC transporter, periplasmc-binding protein	0.05	0.36	0.28	0.21	1.16	1.1	0.15	1.06	0.89
DVU1612	ACT domain protein	0	0.2	0.09	0.28	0.53	0.7	0.23	0.44	0.84
DVU2347	Acetylornithine aminotransferase	-0.14	-0.05	0.03	0.01	-0.85	-1.06	-0.18	-0.99	-1.07
DVU2422	Nitroreductase family protein	-0.16	-0.44	-0.21	-0.03	-0.69	-0.87	0.18	-0.56	-0.88
DVU2427	Uncharacterized protein	-0.16	0.03	-0.03	0.32	0.2	-0.55	0.2	-0.06	-0.62
DVU2441	Heat shock protein, Hsp20 family	-0.17	0.04	-0.1	0.6	0.89	0.8	0.5	1	0.89
DVU2569	Peptidyl-prolyl cis-trans isomerase	-0.23	-0.15	-0.21	-0.28	-0.49	-0.78	-0.4	-0.44	-0.61
DVU2590	Sensory box protein	-0.24	-0.13	-0.12	-0.09	-0.29	-0.67	-0.09	-0.2	-0.51
DVU2770	Response regulator	-0.26	-0.01	-0.11	0.63	-0.11	-0.16	0.7	-0.12	-0.11
DVU3319	Bifunctional protein PutA	-1.22	-0.24	-0.08	-0.07	-0.75	-0.74	0.11	-0.62	-0.88

DVU4006	hypothetical protein	NA	0.34	0.15	0.36	0.8	0.57	0.03	0.65	0.48
DVUA202	hypothetical protein	NA	-0.2	-0.08	-0.08	-0.64	-0.86	0.08	-0.75	-0.99

Note: LFC of the detected proteins with adjusted q value less than 0.001 is shown in red in which proteins with LFC ≥0.5 or ≤-0.5 are defined as the differential expressed proteins in the presence of FNA, while LFC of the detected proteins with q value value less than 0.05 but larger than 0.001 is shown in blue. All others are the proteins with q value larger than 0.05.